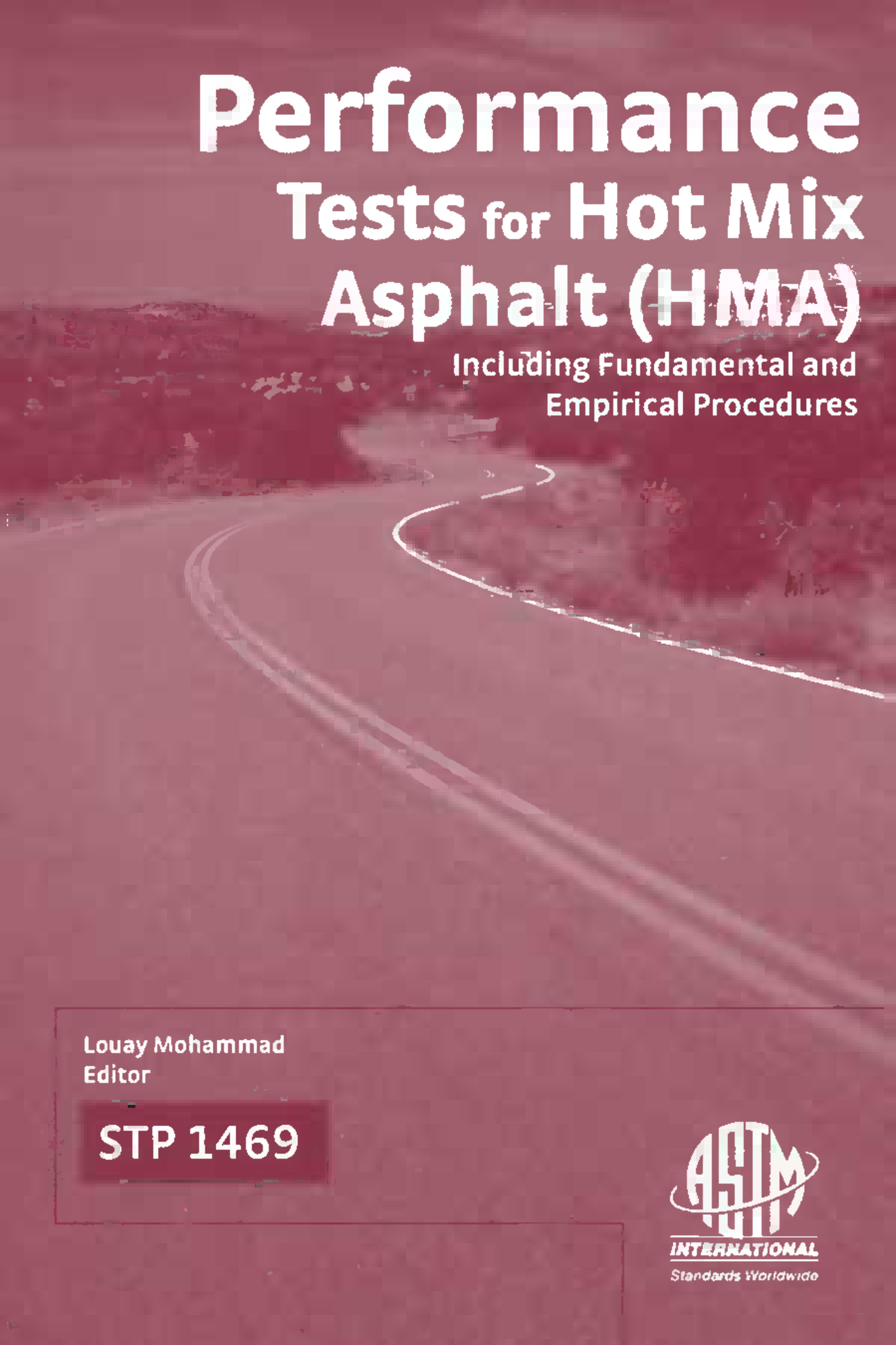

Performance Tests for Hot Mix Asphalt (HMA)

Including Fundamental and Empirical Procedures

Louay Mohammad
Editor

STP 1469

ASTM INTERNATIONAL
Standards Worldwide

STP 1469

Performance Tests for Hot Mix Asphalt (HMA) Including Fundamental and Empirical Procedures

Louay Mohammad, editor

ASTM Stock Number: STP1469

ASTM
100 Barr Harbor Drive
PO Box C700
West Conshohocken, PA 19428-2959

Printed in the U.S.A.

Library of Congress Cataloging-in-Publication Data

Performance tests for hot mix asphalt (HMA) including fundamental and empirical procedures / Louay Mohammad, editor.
p. cm. — (STP ; 1469)
Papers presented at the ASTM symposium held Dec. 9-10, 2003, in Tampa, Florida.
ISBN 0-8031-3495-9 ISBN 978-0-8031-3495-9
1. Pavements, Asphalt—Testing—Congresses. I. Mohammad, Louay N. (Louay Nadhim), 1957– II. ASTM International. III. Series: ASTM special technical publication ; 1469. ISBN: 0-8031-3495-9
TE270.P386 2006
625.8'5—dc22

2006016414

Peer Review Policy

Each paper published in this volume was evaluated by two peer reviewers and at least one editor. The authors addressed all of the reviewers' comments to the satisfaction of both the technical editor(s) and the ASTM International Committee on Publications.

The quality of the papers in this publication reflects not only the obvious efforts of the authors and the technical editor(s), but also the work of the peer reviewers. In keeping with long-standing publication practices, ASTM International maintains the anonymity of the peer reviewers. The ASTM International Committee on Publications acknowledges with appreciation their dedication and contribution of time and effort on behalf of ASTM International.

Printed in Mayfield, PA
August 2006

Foreword

This publication, Performance Tests for Hot Mix Asphalt (HMA), including Fundamental and Empirical Procedures, includes peer reviewed papers presented at the ASTM D04 symposium by this same name in December of 2003. The symposium, held in Tampa, FL, on December 9-10, 2003, focused on this critical topic, chosen to provide practitioners with a forum to discuss the development, application, and field experience of both empirically mechanistically based performance test procedures for use in HMA mixture and quality control.

Contents

Overview

Background

ASTM Committee D04 on Road and Paving Materials is active in sponsoring symposia and the publication of technical papers related to the standardization work of the Committee. This STP, Performance Tests for Hot Mix Asphalt (HMA), Including Fundamental and Empirical Procedures, resulted from the Committee D04 Symposium held on December 9, 2003, at the ASTM Standards Development Meeting in Tampa, Florida. This critical topic was chosen to provide practitioners with a forum to discuss the development, application, and field experience of both empirically and mechanistically based performance test procedures for use in HMA mixture design and quality control. The call for papers brought in 37 abstracts from authors all over the world who wished to present papers at the symposium. Of the 13 papers included in the STP, thirteen were accepted for presentation at the symposium. In addition, xx papers have been published in the Journal of ASTM International (JAI), Vol. 2, No.3, March 2005 (online publication).

SHRP and Other Performance Test Research

The Strategic Highway Research Program (SHRP) concluded with the introduction of the Superpave (Superior Performing Asphalt Pavements) mix design and analysis system. Many state departments of transportation have either implemented or are currently implementing the Superpave system. This system includes the performance graded binder specifications and mixture design methodology. The mixture design method is based on mix volumetric properties of the mixture and has no strength test to complement the designed mixtures similar to traditional Marshall and Hveem mix design methods. However, the original Superpave mix design protocol required mix verification for intermediate and high volume traffic through advanced materials characterizations tests utilizing the Superpave Shear Tester test protocols. It was quickly recognized the complexity of those test protocols for routine mix design application and that a simple performance test is needed to complement the Superpave volumetric mix design procedure. At present, both empirically based test procedures (wheel tracking such as Hamburg, French tester, APA, etc) and engineering based (mechanistic) procedures are being used as proof tests to provide a comfort level in Superpave mix design for rutting. In the past few years, major research was conducted under the National Cooperative Highway Research Program (NCHRP) Project 9-19 "Superpave Support and Performance Models Management", which was aimed to recommend a "Simple Performance Test (SPT)" to complement the Superpave volumetric mixture design method. The results from the NCHRP 9-19 project recommended three candidate SPT tests: dynamic modulus $|E^*|$, static creep (flow time), and triaxial repeated load permanent deformation (flow number) to be used with the Superpave volumetric mix design procedures. However, it will take several years more before these tests are field-validated and standardized for routine use.

This volume provides a collection of research and practical papers from an international as well as state agency research and technology activities on the use of performance tests for HMA mixture design and filed control.

The papers are arranged in four groups designed to aid the reader in locating papers of interest and to compare and contrast the range of work and opinions presented:

(1) Mixture Simulative Performance Tests – The first section relates to the practical use of some simulative loaded-wheel testers used in identifying rut-prone HMA mixtures.
(2) Mechanistic Test for Quality Control – The next grouping includes papers in that the mechanistic tests were used in field Quality Control of HMA mixtures.
(3) Mechanistic Tests for Mixture Design – This group contains several papers relating to the need for mechanistic tests in HMA mixture design.
(4) Application of New Mechanistic Test Methods in HMA Mixture Performance Evaluation – The last group of papers concerns the use of newly developed mechanistic test methods, which have potentials to be used in HMA mixture performance evaluation.

While many of the papers might have been placed in several groups, it is hoped that this organization will help the reader understand and use the technology presented and to help Committee D04 in developing the new standards and tests needed to advance the performance evaluation of HMA materials in the asphalt pavement community.

Importance of Mixture Performance Tests

User experience with the HMA mix design and performance evaluation, combined with the longstanding problems associated with the original SHRP Superpave performance models supporting what was then termed "Level 2 and 3" analyses, demonstrated the need for developing new performance tests used in complementing the current Superpave mixture design system. In the long run, it is important to field-validated and standardized for routine use of those developed test methods. The key is the development of evaluation procedures that will provide an accurate indication of the long-term performance of a mixture when produced, placed, and compacted properly. In advance of standards development, this STP volume provides a cross section of research and practice on the development, application, and field experience of both empirically based and mechanistic based performance test procedures for use in a HMA mixture performance evaluation.

Acknowledgments

I wish to thank the other members of the Committee D04 who all helped in the review of abstracts and papers for the 2003 Symposium on Performance Tests for Hot Mix Asphalt (HMA), Including Fundamental and Empirical Procedures. I am also very appreciative of the professional and friendly help that was received from the ASTM symposium and publication staff.

Louay N. Mohammad
Louisiana State University
Louisiana Transportation Research Center
Baton Rouge, LA

Journal of ASTM International, May 2005, Vol. 2, No. 5
Paper ID JAI12254
Available online at www.astm.org

Jingna Zhang,[1] E. Ray Brown,[2] Prithvi S. Kandhal,[3] and Randy West[4]

An Overview of Fundamental and Simulative Performance Tests for Hot Mix Asphalt

ABSTRACT: Numerous fundamental and simulative test methods are being used to evaluate the performance of Hot Mix Asphalt (HMA). Permanent deformation, fatigue cracking, thermal cracking, loss of surface friction, and stripping are the five main distress types for HMA pavements. All of these distresses can result in loss of performance, but rutting is the one distress that is most likely to be a sudden failure as a result of unsatisfactory HMA. Other distresses are typically long term and show up after a few years of traffic.

This paper provides a general overview of the fundamental, empirical, and simulative tests for HMA corresponding to each of these five distresses. All test methods have been evaluated in terms of advantages and disadvantages. However, major emphasis has been placed on tests for evaluating permanent deformation.

KEYWORDS: Hot Mix Asphalt, performance test, permanent deformation, fundamental, empirical, simulative

Introduction

Numerous test methods are being used to evaluate the performance of Hot Mix Asphalt (HMA). Permanent deformation, fatigue cracking, thermal cracking, loss of surface friction, and stripping are the five main distress types for HMA pavements. All of these distresses can result in loss of performance, but rutting is the one distress that is most likely to be a sudden failure as a result of unsatisfactory HMA. Other distresses are typically long term and show up after a few years of traffic.

Test methods used to characterize the permanent deformation response of asphalt pavement material can generally be categorized as fundamental tests, empirical tests, and simulative tests.

- Fundamental Tests:
    1. Uniaxial and Triaxial Tests: unconfined and confined cylindrical specimens in creep, repeated loading, and strength tests
    2. Diametral Tests: cylindrical specimens in creep or repeated loading test, strength test
    3. Shear Loading Tests: Superpave Shear Tester - Repeated Shear at Constant Height, Frequency Sweep at Constant Height, Field Shear Test, direct shear test

Manuscript received 1 December 2003; accepted for publication 5 October 2004; published May 2005. Presented at ASTM Symposium on Performance of Hot Mix Asphalt (HMA), including Fundamental and Empirical Procedures on 9 December 2003 in Tampa, FL.
[1] Research Engineer, National Center for Asphalt Technology, Auburn, AL 36830.
[2] Director, National Center for Asphalt Technology, Auburn, AL 36830.
[3] Associate Director, Emeritus, National Center for Asphalt Technology, Auburn, AL 36830.
[4] Assistant Director, National Center for Asphalt Technology, Auburn, AL 36830.

- Empirical Tests
  1. Marshall Test
  2. Hveem Test
  3. Corps of Engineering Gyratory Testing Machine
  4. Lateral Pressure Indicator
- Simulative Tests
  1. Asphalt Pavement Analyzer
  2. Hamburg Wheel-Tracking Device
  3. French Rutting Tester
  4. Purdue University Laboratory Wheel Tracking Device
  5. Model Mobile Load Simulator
  6. Dry Wheel Tracker
  7. Rotary Loaded Wheel Tester

Uniaxial and Triaxial Tests

Creep tests, repeated load tests, and dynamic modulus tests can be conducted both in unconfined and confined modes.

Uniaxial and Triaxial Creep Tests

A creep test is conducted by applying a static load to an HMA specimen and measuring the resulting permanent deformation. Extensive studies using the unconfined creep test as a basis of predicting permanent deformation in HMA have been conducted [1–3]. It has been found that the creep test must be performed at relatively low stress levels; otherwise the sample fails prematurely. Test conditions (applying 100 kPa load at 40°C for 1 h) were standardized following a seminar in Zurich in 1977 [4]. This test is inexpensive and easy to conduct, but the ability of the test to predict performance is questionable because the conditions of this test do not closely simulate in-place conditions [5].

The confined creep test, which more closely relates to field conditions, is also relatively simple and easy to perform. By applying a confining pressure (usually approximately 138 kPa (20 psi)), the sample can be tested at a vertical pressure up to 828 kPa (120 psi) or higher and at a temperature up to 60°C. These test conditions are more closely related to actual field conditions than those for unconfined [6].

The creep test has been widely used for determining material properties for predictive analysis because of its simplicity and the fact that many laboratories have the necessary equipment and expertise. Test procedures for both the unconfined and confined creep tests are available. The confined creep test appears to be much more feasible for use since some confinement is needed for some mixes to ensure that early failure of the samples does not occur.

Uniaxial and Triaxial Repeated Load Tests

Uniaxial or triaxial repeated load tests are approaches to measure the permanent deformation characteristics of HMA mixtures typically using several thousand repetitions. During the test, the cumulative permanent deformation as a function of the number of load cycles is recorded. Similar to the comparison between unconfined and confined creep tests, the confined repeated load test has the advantage that both vertical and horizontal stresses can be applied at the levels observed in the pavement structure and at a temperature representative of that experienced in-place.

Triaxial and uniaxial repeated load tests appear to be more sensitive than the creep test to HMA mix variables. On the basis of extensive testing, Barksdale [5] reported that triaxial repeated load tests appear to provide a better measure of rutting characteristics than the creep tests. The triaxial repeated load test, conducted on 100-mm diameter by 150-mm height specimens, is being studied by NCHRP 9-19 as one of their top selected simple performance tests for rutting prediction.

Mallick, Ahlrich, and Brown [8] and Kandhal and Cooley [9] have successfully used other specimen dimensions, which are easy to prepare in the lab, to study the potential of using triaxial repeated load tests to predict rutting. Gabrielson [10] and Brown and Cross [11,12] provided information to show that 13 % strain was a good pass/fail criterion for triaxial repeated load tests.

Uniaxial and Triaxial Dynamic Modulus Tests

The uniaxial dynamic modulus test was standardized in 1979 as ASTM D 3479, "Standard Test for Dynamic Modulus of Asphalt Concrete Mixtures." The test consists of applying a uniaxial sinusoidal compressive stress to an unconfined HMA cylindrical test specimen.

The triaxial dynamic modulus test was used by Francken [13] in the determination of dynamic properties of cylindrical HMA specimens. A constant lateral pressure was used, and sinusoidal vertical pressure was varied over a range of frequencies. Triaxial dynamic tests also permit the determination of additional fundamental properties, such as the phase angle as functions of the frequency of loading, the number of load cycles, and temperature. The dynamic modulus as measured from the triaxial compression test is being evaluated as a simple performance test by NCHRP Project 9-19.

The dynamic modulus test is more difficult to perform than the repeated load test, since a much more accurate deformation measuring system is necessary. The specified height/diameter ratio of the specimen and the complex equipment increase the difficulty of conducting dynamic modulus test as a routine QC/QA test for contractors and agencies.

Diametral Tests

Since the indirect tension device was originally described by Schmidt [14], several versions of this device have been used recently. Sousa et al. [15] have suggested that the diametral test is more suitable for the repeated load testing associated with modulus measurements compared with diametral creep measurements, which take longer time periods for testing. The repeated-load indirect tension test for determining resilient modulus of HMA is conducted by applying diametral loads with a haversine or other suitable waveform.

Diametral testing has been deemed inappropriate for permanent deformation characteristics for two critical reasons [16]:

1. The state of stress is non-uniform and strongly dependent on the shape of the specimen. At high temperature or load, permanent deformation produces changes in the specimen shape that significantly affect both the state of stress and the test measurements.
2. During the test, the only relatively uniform state of stress is tension along the vertical diameter of the specimen. All other states of stress are distinctly non-uniform.

Khosla and Komer [16] found that use of mechanical properties determined by diametral testing almost always resulted in overestimates of pavement rutting. Christienson and Bonaquist [17,18] found a strong relationship between indirect tensile strength and permanent shear strain measured from the repeated shear at constant height test. They reasoned that this relationship was expected since indirect tensile strength is a good predicator of mixture cohesion and binder stiffness. However, it was insensitive to the angle of internal friction component of shear strength and therefore would not relate to rutting resistance by itself. They recommended the use of IDT strength along with the compaction slope from the Superpave gyratory compactor to develop a Mohr-Coulomb type model of asphalt mixture shear strength.

Shear Loading Tests

The Superpave Shear Tester (SST) was developed under SHRP as a way to measure the shear characteristics of HMA. Six SST tests can be performed with the SST for measuring the mix performance characteristics. The Simple Shear, Frequency Sweep, Uniaxial Strain, Volumetric Shear, Repeated Shear at Constant Stress Ratio, and Repeated Shear at Constant Height tests measure properties that may be useful in calculating the resistance to permanent deformation and fatigue cracking. The two tests most often used to evaluate permanent deformation are discussed below.

SST Repeated Shear at Constant Height Test (RSCH)

The Superpave RSCH test was developed to evaluate the rutting resistance of HMA mixtures. As outlined in the AASHTO TP7-01, test procedure C, the RSCH test consists of applying a repeated haversine shear stress of 68 kPa (0.1-s load and 0.6-s rest) to a compacted HMA (150 mm diameter by 50 mm height) specimen while supplying necessary axial stress to maintain a constant height. The test is performed either to 5000 load cycles or until 5 % permanent strain is incurred by the sample. Permanent strain is measured as the response variable at certain interval load cycles throughout the test and recorded using LVDTs and a computerized data acquisition system.

Results from the RSCH tests have been shown to correlate with rutting performance [19–22]. The Asphalt Institute set up criteria for interpreting RSCH maximum permanent shear strain [23]. Unfortunately, even under the most controlled circumstances and operated by experienced users, the data from the RSCH have been shown to have high variability [19–22]. To remedy the high variations, Romero and Anderson [24] recommended that five specimens be tested and the two extremes be discarded from further analysis. The remaining three should be averaged to provide an effective way to reduce the coefficient of variation.

Shear Frequency Sweep Test at Constant Height (FSCH)

FSCH test consists of applying a sinusoidal shear strain of 0.0001 mm/mm at each of the following frequencies (10, 5, 2, 1, 0.5, 0.2, 0.1, 0.05, 0.02, and 0.01 Hz). During the loading cycles, the specimen height is held constant by applying sufficient axial stress. This is accomplished by controlling the vertical actuator using close-up feedback from the axial LVDT.

The shear dynamic modulus (G*) is the output from this test. The master curve can be developed for each mixture using the G* data at all temperatures/frequencies. Specification temperature can also be derived from the master curve.

The SST device is expensive, and availability is limited (at the time this report was prepared there were ten SST devices in the world, eight of them in the United States). It is complex to run, and usually special training is needed to perform the shear tests using SST.

Other Shear Tests

The Field Shear Tester (FST) was developed through NCHRP 9-7 to control Superpave designed HMA mixtures [25]. The device was designed to perform tests comparable to two of the Superpave load related mixture tests: the frequency sweep test at constant height and the simple shear test at constant height (AASHTO TP7-01). The control software is very similar to the software for the SST and can be used to measure the dynamic modulus in shear.

The shear strength test was originally developed to determine the shear strength of bonded concrete. It has also been used to determine the shear strength of Hot Mix Asphalt. Molenaar, Heerkens, and Verhoeven [26] have used the shear test to evaluate the shear resistance of several pavement structures. The direct shear strength test has been used to a much lesser extent than the dynamic modulus and repeated load test in evaluating an HMA mixture's susceptibility to permanent deformation. Insufficient data are available to consider this test for use in predicting performance of HMA.

Empirical Tests

The Marshall Test

The concepts of the Marshall test were developed by Bruce Marshall, formerly Bituminous Engineer with the Mississippi State Highway Department. In 1948, the U.S. Corps of Engineers improved and added certain features to the Marshall test procedure and ultimately developed mix design criteria [27]. The purpose of the test was to measure the strength of an asphalt mixture that had been compacted to a standard laboratory compactive effort. This test is also used as part of the Marshall mix design procedure for optimizing the design asphalt content, and it is used in the quality control of asphalt mixtures. There is much information concerning this test since the Marshall mix design procedure was widely used for more than 50 years.

The Marshall flow indicates when a mixture is over-asphalted – high flow values indicate excessive binder content. The Marshall test conditions may affect the test's values in predicting rutting performance. The effects of the specimen edges are amplified, and the assumption that the Marshall breaking head is applying a uniform load across the specimen is not valid. The effective load on the specimen is higher for mixture with larger nominal maximum aggregate size [28]. The Marshall Method has had its shortcomings despite the overall success. Research at the University of Nottingham [29] showed that the Marshall test is a poor measure of resistance to permanent deformation and may not be able to rank mixes in order of their rut resistance, compared with more realistic repeated load triaxial tests.

The Hveem Test

The concepts of the Hveem method of designing paving mixtures were developed under the direction of Francis N. Hveem, a former Materials and Research Engineer for the California Department of Transportation. It is an HMA mixture design tool that was used primarily in the

Western United States. The basic philosophy of the Hveem method of mix design was summarized by Vallerga and Lovering [30] as containing the following elements:

1. It should provide sufficient asphalt cement to absorb aggregate and to produce an optimum film of asphalt cement on the aggregate as determined by the surface area method.
2. It should produce a compacted aggregate-asphalt cement mixture with sufficient stability to resist traffic.
3. It should contain enough asphalt cement for durability from weathering, including effects of oxidation and moisture susceptibility.

The Hveem stabilometer is a triaxial testing device consisting essentially of a rubber sleeve within a metallic cylinder containing a liquid which registers the horizontal pressure developed by a compacted test specimen as a vertical load is applied. The stabilometer values are measurements of internal friction, which are more a reflection of the properties of the aggregate and the asphalt content than of the binder grade [28]. Stabilometer values are relatively insensitive to asphalt cement characteristics but are indicative of aggregate characteristics. Similar to the Marshall flow values, the Hveem stability does provide an indication when a mixture is over-asphalted – low stability values indicate excessive binder content. Similar to the Marshall mix design method, the Hveem method has a large amount of research data available.

The stabilometer values are measurements of internal friction, which are more a reflection of the properties of the aggregate and the asphalt content than of the binder grade [28]. Stabilometer values are relatively insensitive to asphalt cement characteristics but are indicative of aggregate characteristics. Similar to the Marshall flow values, the Hveem stability does provide an indication when a mixture is over-asphalted – low stability values indicate excessive binder content. Different agencies have modified the Hveem procedure and related equation slightly. Since this test has been replaced with Superpave and there is no significant amount of data to correlate this test with performance, it should not be considered for performance testing.

Gyratory Testing Machine (GTM)

The GTM developed by the Corps of Engineers has been shown to be an effective tool in the evaluation of HMA mixture quality. This machine has the capability to compact HMA mixtures using a kneading process that simulates the action of rollers during construction. The GTM has the flexibility of varying the vertical pressure, gyration angle, and number of gyrations to simulate field compaction equipment and subsequent traffic.

During compaction of a specimen in the GTM, several mixture properties are determined. The gyratory shear index (GSI) is a measure of mixture stability and is related to permanent deformation. GSI values close to 1.0 have been shown to be typical for stable mixtures, and values significantly above 1.1 usually indicate unstable mixtures [5]. However, results have indicted that this does not provide a good relationship with performance [12].

The GTM also has the capability of measuring the shear resistance of the mixture during compaction. Shear resistance, which is measured during compaction at high temperature, is primarily a measure of aggregate properties, since the viscosity of the asphalt is low, resulting in little cohesion.

Lateral Pressure Indicator (LPI)

The lateral pressure indicator gives an indication of the lateral confinement pressure that builds up during compaction of an HMA sample in the mold of a Superpave Gyratory Compactor. The basic premise is that aggregates and asphalt in the gyratory mold, during compaction, behave much like an unsaturatured soil. The mix needs a certain degree of confinement to generate enough confining stress to develop adequate shear strength. Generally, as a mix is compacted, the pressure in the asphalt binder builds up, and at some point this pressure can become excessive, resulting in loss of strength. The LPI provides a method to measure pore pressure on the walls of the molds. In a mix with crushed aggregate particles and good interlocking gradation, the mix aggregates will begin forming a stable interlocking structure with an increase in lateral confinement stress. The mix will show good performance in the field, provided it is designed and constructed properly. It is also believed that use of more rounded aggregate will result in an increase in lateral pressure.

The LPI test can be conducted as a part of the compaction process so testing and time are minimized. Early indications show that this test has potential, but more results are needed before it can be recommended for use in mix design or QC/QA.

Simulative Tests

The stress conditions in a pavement as a loaded wheel passes over it are extremely complex and cannot be precisely calculated nor replicated in a laboratory test on a HMA sample. Hence, it is very difficult to predict performance accurately using a purely mechanistic approach. Recently, advances have been made in mechanistic methods for predicting HMA performance. However, much work is still needed. Simulative tests where the actual traffic loads are modeled have been used to compare the performance of a wide range of materials including HMA. With these tests, conditions similar to that on the roadway are applied to the test specimen, and the performance is monitored. It is difficult to closely simulate the stress conditions observed in the field, but these tests attempt to do that [31].

Several simulative test methods have been used in the past and are currently being used to evaluate rutting performance. Some of these methods include the Asphalt Pavement Analyzer (Georgia Loaded Wheel Tester), Hamburg Wheel-Tracking Device, French Rutting Tester (LCPC Wheel tracker), Purdue University Laboratory Wheel Tracking Device, Model Mobile Load Simulator, Dry Wheel Tracker (Wessex Engineering), and Rotary Loaded Wheel Tester (Rutmeter).

Asphalt Pavement Analyzer

The APA is a modification of the Georgia Loaded Wheel Tester (GLWT) and was first manufactured in 1996 by Pavement Technology, Inc. The APA has been used in an attempt to evaluate rutting, fatigue, and moisture resistance of HMA mixtures.

A loaded wheel is placed on a pressurized linear hose, which sits on the test specimens and is then tracked back and forth to induce rutting. Most testing in the APA is carried out to 8000 cycles. Unlike the GLWT, samples also can be tested dry or while submerged in water. Test specimens for the APA can be either beam or cylindrical. Beams are most often compacted to 7 % air voids; cylindrical samples have been fabricated to both 4 and 7 % air voids [32]. Test temperatures for the APA have ranged from 40.6–64°C. The most recent work has been conducted at or near expected maximum pavement temperatures [33,34]. Wheel load and hose pressure have basically stayed the same as for the GLWT, 445 N, and 690 kPa, respectively. One recent research study [34] did use a wheel load of 533 N and hose pressure of 830 kPa with good success.

Results from the WesTrack Forensic Team study [35] and the NCHRP 9-17 [11] project show that use of the APA may help ensure that a satisfactory mix is designed and produced.

WesTrack Forensic Team study [35] indicates that a laboratory rut depth of 6-mm results in a field rut depth of 12.5 mm. Criteria have also been developed in the past for some other test conditions. Georgia and other states have long specified a maximum rut depth of 5 mm for HMA mixtures as the pass/fail criteria at a temperature of 50°C [36]. A recent study conducted at the National Center for Asphalt Technology [37] provided a criterion of 8.2-mm for the APA rut test at standard PG temperature for the location in which the HMA will be used. This higher value for pass/fail criteria is associated with the higher PG temperature used.

Hamburg Wheel-Tracking Device (HWTD)

The Hamburg Wheel-Tracking Device was developed by Helmut-Wind Incorporated of Hamburg, Germany [38]. It is used as a specification requirement for some of the most traveled roadways in Germany to evaluate rutting and stripping. Test slabs are normally compacted to 7 ± 1 % air voids using a linear kneading compactor. Testing also has been done using Superpave gyratory compacted samples. Results obtained from the HWTD consist of rut depth, creep slope, stripping inflection point, and stripping slopes. The stripping inflection point is used to estimate the relative resistance of the HMA sample to moisture-induced damage [39].

WesTrack Forensic Team study [35] indicated that a laboratory rut depth of 14 mm would be expected to result in a field rut depth of 12.5 mm. A rut depth of less than 10 mm after 20 000 passes has been recommended by the city of Hamburg to be more reasonable [38].

French Rutting Tester (LCPC Wheel Tracker)

The Laboratoire Central des Ponts et Chaussées (LCPC) wheel tracker (also known as the French Rutting Tester (FRT)) has been used in France for over 20 years to successfully prevent rutting in HMA pavement [40]. In recent years, the FRT has been used in the United States, most notably in the state of Colorado and FHWA's Turner Fairbank Highway Research Center.

The FRT is capable of simultaneously testing two HMA slabs. Samples are generally compacted with an LCPC laboratory rubber-tired compactor [41].

In France, an acceptable HMA mix typically will have a rutting depth ≤ 10 % of the test slab thickness after 30 000 cycles. The Colorado Department of Transportation and the FHWA's Turner Fairbank Highway Research Center participated in a research study to evaluate the FRT and the actual field performance [42].

WesTrack Forensic Team [35] members suggested that the FRT provided useful data when experience is available with similar materials (aggregates and asphalts). Similar to that for the HWTD and APA, potential FRT user agencies should develop their own evaluation of test results using local conditions [35]. The data indicated that a laboratory rut depth of 10 mm (10 % of 100 mm thickness) results in an in-place rut depth of 12.5 mm.

Purdue University Laboratory Wheel Tracking Device (PURWheel)

The PURWheel was developed at Purdue University [43]. PURWheel tests slab specimens that can either be cut from roadway or compacted in the laboratory. Laboratory samples are compacted using a linear compactor also developed by Purdue University [44]. PURWheel was designed to evaluate rutting potential and/or moisture sensitivity of HMA. A 12.7-mm rut depth is used to differentiate between good and bad performing mixes with respect to rutting [44].

WesTrack Forensic Team study [35] data indicated that 4500 cycles resulted in a laboratory rut depth of 6.35 mm. This was equivalent to a field rut depth of 12.5 mm.

Model Mobile Load Simulator (MMLS3)

The one-third scale MMLS3 was developed recently in South Africa for testing HMA in either the laboratory or field. This prototype device is similar to the full-scale Texas Mobile Load Simulator (TxMLS) but scaled in size and load. The scaled load of 2.1 KN is approximately one-ninth (the scaling factor squared) of the load on a single tire of an equivalent single axle load carried on dual tires [45].

The MMLS3 can be used for testing samples in dry or wet conditions. Performance monitoring during MMLS3 testing includes measuring rut depth from transverse profiles and determining Seismic Analysis of Surface Waves moduli to evaluate rutting potential and damage due to cracking or moisture, respectively. Rut depth criteria for acceptable performance are currently being developed [46].

Wessex Dry Wheel Tracker

In the Dry Wheel Tracker, a loaded wheel is run over an asphalt sample in a sealed and insulated cabinet for 45 min. The device applies a 710 N vertical force through a 150 mm wide steel wheel with a 12.5 mm thick rubber contact surface. The rate of loading is 26 cycles per minute, which corresponds to 52 wheel passes per min. It has a dual wheel assembly that accommodates testing two specimens simultaneously.

A specially designed computer program controls the operation of the machine and records rut depth, temperature, and elapsed time during the test. The Wheel Tracker test offers a simple and inexpensive method of predicting rutting. An Immersion Wheel Tracker and a Slab Compactor are also available at Wessex. However, there are not any field data available to validate its accuracy in predicting performance.

Rotary Loaded Wheel Tester

Rotary Loaded Wheel Tester (or Rutmeter) was developed by CPN International, Inc. The RLWT automatically measures the plastic deformation of HMA samples as a function of repetitive wheel loadings.

The RLWT utilizes a unidirectional rotary load wheel, and most testing is carried out to 16 000 individual wheel loadings [47]. The RLWT is capable of applying 125 N loads to each spinning single wheel in the load application assembly. The load is provided by static weight such that no external load calibration is required, and it is designed to approximate a contact pressure of 690 kPa. The device utilizes an integrated temperature controller to heat samples. Limited work has shown that there is a general correlation between the APA and the Rotary

Loaded Wheel Tester [47], however there is no correlation that has been developed between the Rotary Loaded Wheel Tester and field performance.

A summary of the advantages and disadvantages of each of the tests considered for permanent deformation is provided in Table 1 [48].

TABLE 1—*Comparative assessment of test methods.*

Test Method		Sample Dimension	Advantages	Disadvantages
Fundamental: Diametral Tests	Diametral Static (creep)	4 in. diameter × 2.5 in. height	• Test is easy to perform • Equipment is generally available in most labs • Specimen is easy to fabricate	• State of stress is nonuniform and strongly dependent on the shape of the specimen • Maybe inappropriate for estimating permanent deformation • High temperature (load) changes in the specimen shape affect the state of stress and the test measurement significantly • Were found to overestimate rutting • For the dynamic test, the equipment is complex
	Diametral Repeated Load	4 in. diameter × 2.5 in. height	• Test is easy to perform • Specimen is easy to fabricate	
	Diametral Dynamic Modulus	4 in. diameter × 2.5 in. height	• Specimen is easy to fabricate • Non destructive test	
	Diametral Strength Test	4 in. diameter × 2.5 in. height	• Test is easy to perform • Equipment is generally available in most labs • Specimen is easy to fabricate • Minimum test time	
Fundamental: Uniaxial Tests	Uniaxial Static (Creep)	4 in. diameter × 8 in. height & others	• Easy to perform • Test equipment is simple and generally available • Wide spread, well known • More technical information	• Ability to predict performance is questionable • Restricted test temperature and load levels does not simulate field conditions • Does not simulate field dynamic phenomena • Difficult to obtain 2:1 ratio specimens in lab
	Uniaxial repeated Load	4 in. diameter × 8 in. height & others	• Better simulates traffic conditions	• Equipment is more complex • Restricted test temperature and load levels does not simulate field conditions • Difficult to obtain 2:1 ratio specimens in lab
	Uniaxial Dynamic Modulus	4 in. diameter × 8 in. height & others	• Non destructive tests	• Equipment is more complex • Difficult to obtain 2:1 ratio specimens in lab
	Uniaxial Strength Test	4 in. diameter × 8 in. height & others	• Easy to perform • Test equipment is simple and generally available • Minimum test time	• Questionable ability to predict permanent deformation
Fundamental: Triaxial Tests	Triaxial Static (creep confined)	4 in. diameter × 8 in. height & others	• Relatively simple test and equipment • Test temperature and load levels better simulate field conditions than unconfined • Potentially inexpensive	• Requires a triaxial chamber • Confinement increases complexity of the test
	Triaxial Repeated Load	4 in. diameter × 8 in. height & others	• Test temperature and load levels better simulate field conditions than unconfined • Better expresses traffic conditions • Can accommodate varied specimen sizes • Criteria available	• Equipment is relatively complex and expensive • Requires a triaxial chamber
	Triaxial Dynamic Modulus	4 in. diameter × 8 in. height & others	• Provides necessary input for structural analysis • Non destructive test	• At high temperature it is a complex test system (small deformation measurement sensitivity is needed at high temperature) • Some possible minor problem due to stud, LVDT arrangement. • Equipment is more complex and expensive • Requires a triaxial chamber
	Triaxial Strength	4 or 6 in. diameter × 8 in. height & others	• Relative simple test and equipment • Minimum test time	• Ability to predict permanent deformation is questionable • Requires a triaxial chamber

Fundamental: Shear Tests	SST Frequency Sweep Test – Shear Dynamic Modulus	6 in. diameter × 2 in. height	• The applied shear strain simulate the effect of road traffic • AASHTO standardized procedure available • Specimen is prepared with SGC samples • Master curve could be drawn from different temperatures and frequencies • Non destructive test	• Equipment is extremely expensive and rarely available • Test is complex and difficult to run, usually need special training • SGC samples need to be cut and glued before testing
	SST Repeated Shear at Constant Height	6 in. diameter × 2 in. height	• The applied shear strains simulate the effect of road traffic • AASHTO procedure available • Specimen available from SGC samples	• Equipment is extremely expensive and rarely available • Test is complex and difficult to run, usually need special training • SGC samples need to be cut and glued before testing • High COV of test results • More than three replicates are needed
	Triaxial Shear Strength Test	6 in. diameter × 2 in. height	Short test time	• Much less used • Confined specimen requirements add complexity
Empirical Tests	Marshall Test	4 in. diameter × 2.5 in. height or 6 in. diameter × 3.75 in. height	• Wide spread, well known, standardized for mix design • Test procedure standardized • Easiest to implement and short test time • Equipment available in all labs.	• Not able to correctly rank mixes for permanent deformation • Little data to indicate it is related to performance
	Hveem Test	4 in. diameter × 2.5 in. height	• Developed with a good basic philosophy • Short test time • Triaxial load applied	• Not used as widely as Marshall in the past • California kneading compacter needed • Not able to correctly rank mixes for permanent deformation
	GTM	Loose HMA	• Simulate the action of rollers during construction • Parameters are generated during compaction • Criteria available	• Equipment not widely available • Not able to correctly rank mixes for permanent deformation
	Lateral Pressure Indicator	Loose HMA	• Test during compaction	• Problems to interpret test results • Not much data available
Simulative Tests	Asphalt Pavement Analyzer	Cylindrical 6 in. × 3.5 or 4.5 in. or beam	• Simulates field traffic and temperature conditions •Modified and improved from GLWT • Simple to perform • 3-6 samples can be tested at the same time • Most widely used LWT in the US • Guidelines (criteria) are available • Cylindrical specimens use SGC	• Relatively expensive except for new table top version
	Hamburg Wheel-Tracking Device	10.2 in. × 12.6 in. × 1.6 in.	• Widely used in Germany • Capable of evaluating moisture-induced damage • 2 samples tested at same time	• Less potential to be accepted widely in the United States
	French Rutting Tester	7.1 in. × 19.7 in. × 0.8 to 3.9 in.	• Successfully used in France • Two HMA slabs can be tested at one time	• Not widely available in U.S.
	PURWheel	11.4 in. × 12.2 in.× 1.3, 2, 3 in.	• Specimen can be from field as well as lab-prepared	• Linear compactor needed • Not widely available
	Model Mobile Load Simulator	47 in. × 9.5 in.× thickness	• Specimen is scaled to full-scaled load simulator	• Extra materials needed • Not suitable for routine use • Standard for lab specimen fabrication needs to be developed
	RLWT	6 in. diameter × 4.5 in. height	• Use SGC sample • Some relationship with APA rut depth	• Not widely used in the United States • Very little data available
	Wessex Device	6 in. diameter × 4.5 in. height	• Two specimens could be tested at one time • Use SGC samples	• Not widely used or well known • Very little data available

Other Distresses [48]

Fatigue Cracking

There has been much research done on the effects of HMA properties on fatigue. Certainly the HMA properties have an effect on fatigue, but the most important factor to help control fatigue is to ensure that the pavement is structurally sound. Since the classical bottom-up fatigue is controlled primarily by the pavement structure, there is no way that a mix test can be used alone to predict fatigue accurately. However, steps can be taken to minimize fatigue problems, such as: use as much asphalt in the mix as allowable without rutting problems, select the proper grade of asphalt, do not overheat the asphalt during construction, keep the filler to asphalt ratio lower, and compact the mix to a relatively low void level. This is a general guidance, but it is the approach that is generally used to ensure good fatigue resistance.

Thermal Cracking

Thermal cracking is a problem in cold climates, and guidance is needed to minimize this problem. At the present time, the best guidance to minimize thermal cracking is to select the proper low temperature grade of the PG asphalt binder for the project location. Other steps during construction can be helpful. For example, do not overheat the HMA. This will result in premature aging of the binder and lead to problems thermal cracking. It is also important to compact the HMA to a relatively low air void level to reduce the rate of oxidation.

Moisture Susceptibility

Moisture susceptibility is typically a problem that can cause the asphalt binder to strip from the aggregate, leading to raveling and disintegration of the mixture. AASHTO T-283 has been used for several years to help control stripping. This test does not appear to be a very accurate indicator of stripping, but it does help to minimize the problem. The Hamburg test has also been shown to identify mixes that tend to strip. There are things during the construction process that can help to minimize stripping potential. Of course liquid anti strip agents or hydrated lime can be used. Other important steps include good compaction and complete drying of aggregate.

Friction Properties

Friction is one of the most important properties of a HMA mixture. There are good methods to measure the in-place friction, but there are not good methods to evaluate mixes in the lab for friction. Several state DOTs have methods that they use, but these have not been adopted nationally. More work is needed to evaluate these local procedures for national adoption. There are several things that can be done in design and construction to improve friction. The primary concern is friction during wet weather. Use of a mix such as open-graded friction course (OGFC) has been shown to be effective in increasing friction in wet weather. Other methods that can be used are to use aggregate that does not tend to polish, use mixes that are not over asphalted, use crushed aggregates, etc. Coarse textured mixes such as SMA have been shown to provide good friction in wet weather. At the present time, past experience with local materials is the best information available for providing good friction.

Summary

Predicting performance of HMA is very difficult due to the complexity of HMA, the complexity of the underlying unbound layers, and varying environmental conditions.

This paper discusses fundamental, empirical, and simulative procedures for evaluating permanent deformation in the laboratory. Advantages and disadvantages of each of the tests are presented. Some general discussions were given for the fatigue cracking, thermal cracking, moisture susceptibility, and friction properties.

References

[1] Hills, J. F., "The Creep of Asphalt Concrete Mixes," *Journal of The Institute of Petroleum*, November 1973.

[2] Van de Loo, P. J., "Creep Testing, a Simple Tool to Judge Asphalt Mix Stability," *Proceeding of the Association of Asphalt Paving Technologists*, Vol. 43, 1974.

[3] Van de Loo, P. J., "Practical Approach to the Predication of Rutting in Asphalt Pavements: the Steel Method," Transportation Research Board, Transportation Research Record 616, 1976.

[4] "Recommendation for the Performance of Unconfined Static Creep Test in Asphalt Specimens," *Proceedings of the International Symposium on Plastic Deformability of Bituminous Mixes*, Zurich, 1977, pp. 335–359.

[5] Roberts, F. L., Prithvi, S., Kandhal, E., Brown, R., Lee, D-Y, and Kennedy, T. W., "Hot Mix Asphalt Materials, Mixture Design, and Construction," NAPA Education Foundation, 2^{nd} ed., 1996.

[6] Foo, K. Y., "Predicting Rutting in Hot Mix Asphalt," Ph.D. Dissertation, Auburn University, 1994.

[7] Barksdale, R. D., "Laboratory Evaluation of Rutting in Base Course Materials," *Proceedings, Third International Conference on the Structural Design of Asphalt Pavements*, Vol. 1, London, 1972, pp. 161–174.

[8] Basu, M. R., Ahlrich, R., and Brown, E. R., "Potential of Dynamic Creep to Predict Rutting," *ASTM STP 1256*, ASTM International, West Conshohocken, PA, 1995.

[9] Kandhal, P. S. and Cooley, Jr., L. A., "Investigation of the Restricted Zone in the Superpave Aggregate Gradation Specification," NCHRP Report 464, 2001.9.

[10] Gabrielson, J. R., "Evaluation of Hot Mix Asphalt (HMA) Static Creep and Repeated Load Tests," Ph.D. Dissertation, Auburn University, December 1992.

[11] Brown, E. R. and Cross, S. A., "A National Study of Rutting in Hot Mix Asphalt (HMA) Pavements," NCAT Report No. 92-5, February 1992.

[12] Brown, E. R. and Cross, S. A., "A National Study of Rutting in Hot Mix Asphalt (HMA) Pavements," *Proceeding of the Association of Asphalt Paving Technologists*, Vol. 61, 1992.

[13] Francken, L., "Permanent Deformation Law of Bituminous Road Mixes in Repeated Triaxial Compression," *Proceedings, Fourth International Conference on the Structural Design of Asphalt Pavements*, Vol. 1, Ann Arbor, 1977, pp. 483-496.

[14] Schmidt, R. J., "A Practical Method for Measuring the Resilient Modulus of Asphalt Treated Mixed," Highway Research Board, Highway Research Record 404, 1972, pp. 22–32.

[15] Sousa, J. B., Craus, J., and Monismith, C. L., "Summary Report on Permanent Deformation in Asphalt Concrete," SHRP-A-318, SHRP National Research Council,. Washington, D.C, 1991.

[16] Khosla, N. P. and Omer, M. S., "Characterization of Asphaltic Mixtures for Prediction of Permanent Deformation," Transportation Research Board, Transportation Research Record 1034, 1985.

[17] Christensen, D. W., Bonaquist, R., and Jack, D. P., "Evaluation of Triaxial Strength as a

Simple Test for Asphalt Concrete Rut Resistance," The Pennsylvania Transportation Institute, August 31, 2000.

[18] Anderson, R. M., Christensen, D. W., and Bonaquist, R., "Estimating the Rutting Potential of Asphalt Mixtures Using the Superpave Gyratory Compaction Properties and Indirect Tensile Strength," *Proceeding of the Association of Asphalt Paving Technologists*, Vol. 72, 2003.

[19] Romero, P. and Mogawer, W., "Evaluating Superpave Shear Tester Using 19-mm Mixtures from the Federal Highway Administration's Accelerated Loading Facility," *Proceeding of the Association of Asphalt Paving Technologists*, Vol. 67, 1998.

[20] Wiliams, R. C., Romero, P., and Stuart, K., "Comparison of Superpave Shear Test Results to Westrack Performance," *Symposium on Highway and Runway Technology*, The 1998 International Conference of Computational Science (ICES 98), 1998.

[21] Tayebali, A. A., Khosla, N., Malpass, G., and Waller, F., "Evaluation of Superapve Repeated Shear at Constant Height Test to Predict Rutting Potential of Mixtures – Performance of Three Pavement Sections in North Carolina," Transportation Research Board, Transportation Research Record 1681, 1999.

[22] Anderson, R. M., Bukowski, J. R., and Turner, P. A., "Using Superpave Performance Tests to Evaluate Asphalt Mixtures," Transportation Research Board, Transportation Research Record 1681, 1999.

[23] Bukowski, J. R. and T. Harman, "Minutes of the Superpave Mixture Report Task Group," Meeting, September 1997.

[24] Romero, P. and Anderson., R. M., "Variability of Asphalt Mixtures Tests Using the Superpave Shear Tester Repeated Shear at Constant Height Test," Transportation Research Board, Transportation Research Record 1767, 2001.

[25] Anderson, R. M., Cominsky, R. J., and Killingsworth, B. M., "Sensitivity Of Superpave Mixture Tests To Changes In Mixture Components," *Proceeding of the Association of Asphalt Paving Technologists*, Vol. 67, 1998.

[26] Molenaar, A. A. A., Heerkens, J. C. P., and Verhoeven, J. H. M., "Effect of Stress Absorbing Membrane Interlayers," *Proceeding of the Association of Asphalt Paving Technologists*, Vol. 55, 1986.

[27] Mix Design Methods, MS-2 Asphalt Institute.

[28] WesTrack Forensic Team Consensus Report, "Superpave Mixture Design Guide," Report No. FHWA-RD-01-052, Federal Highway Administration, Washington, D.C., February 2001.

[29] Brown, S. F., Cooper, K. E., and Pooly, G. R.,"Mechanical Properties of Bituminous Materials for Pavement Design," *Proceedings of the Second Eurobitume Symposium*, Cannes, October 1981, pp. 143–147, reprinted in a special issue of *Asphalt Technology*, January 1982.

[30] Vallerga, B. A. and Lovering, W. R., "Evolution of the Hveem Stabilometer Method of Designing Asphalt Paving Mixtures," *Proceeding of the Association of Asphalt Paving Technologists*, Vol. 54, 1985.

[31] Cooley Jr., L. A., Kandhal, P. S., Buchanan, S., et al. "Loaded Wheel Testers in the United States: State of the Practice," Transportation Research E-Circular, Number E-C016, July 2000.

[32] Neiderhauser, S., "Presentation at the Asphalt Pavement Analyzer User Group Meeting," Auburn, AL, September 28 and 29, 1999.

[33] Kandhal, P. S. and Mallick, R. B., "Evaluation of Asphalt Pavement Analyzer for HMA Mix Design," National Center for Asphalt Technology, Report No. 99-4, June 1999.

[34] Williams, C. R. and Prowell, B. D., "Comparison of Laboratory Wheel-Tracking Test Results to WesTrack Performance," Transportation Research Board, Transportation Research Record 1681, 1999.

[35] WesTrack Forensic Team, "Performance of Coarse-Graded Mixes at WesTrack – Premature Rutting," Final Report, June 1998.

[36] Shami, H. I., Jame, S. L., D'Angelo, J. A., and Harman, R. T. P., "Development of

Temperature-Effect Model for Predicting Rutting of Asphalt Mixtures Using Georgia Loaded Wheel Tester," Transportation Research Board, Transportation Research Record 1590, 1997.
[37] Zhang, J., Cooley, Jr., L. A., and Kandhal, P. S., "Comparison of Fundamental and Simulative Test Methods for Evaluating Permanent Deformation of Hot Mix Asphalt," Transportation Research Board, Transportation Research Record 1789, 2002.
[38] Aschenbrener, T. "Evaluation of Hamburg Wheel-Tracking Device to Predict Moisture Damage in Hot Mix Asphalt," Transportation Research Board, Transportation Research Record 1492, 1995.
[39] Buchanan, M. S., "An Evaluation of Laboratory Wheel-Tracking Devices," Report Prepared for National Asphalt Pavement Association, National Center for Asphalt Technology, August 1997.
[40] Brousseaud, Y., "Assessment of the Use of the LCPC Rutting Tester," Section des Materiaux de Chaussées. Laboratorie Central des Ponts et Chaussées, Nantes, France, 1992.
[41] Bonnot, J., "Asphalt Aggregate Mixtures," Transportation Research Board, Transportation Research Record 1096, 1986.
[42] Aschenbrener, T., "Comparison of Results Obtained From the French Rutting Tester With Pavements Of Known Field Performance," Colorado Department of Transportation, Report No. CDOT-DTD-R-92-11, October 1992.
[43] Lee, C., White, T. D., and West, T. R., "Effect of Fine Aggregate Angularity on Asphalt Mixture Performance," Report No. FHWA/IN/JTRP - 98/20, Joint Transportation Research Project, Purdue University, West Lafayette, IN, July 1999.
[44] Pan, C. and White, T. D., "Conditions for Stripping Using Accelerated Testing," Report No. FHWA/IN/JTRP-97/13, Joint Transportation Research Program, Purdue University, West Lafayette, IN, February 1999.
[45] Epps, A., Little, D. C., Mikhail, M., and Hugo, F., "Comparison of Rut Depth Analysis Methods Using MMLS3 Data," Paper Presented at the 80th Annual Meeting of the Transportation Research Board, Washington, DC, January 2001.
[46] Epps, A., Ahmed, T., Mikhail, M., and Hugo, F., "Performance Prediction with the MMLS3 WesTrack," *Journal of the Association of Asphalt Paving Technologist*, Clearwater, FL, March 19–21, 2001.
[47] Edgar, C., "Rotary Loaded Wheel Testing for Hot-Mix Asphalt Quality Control," A paper prepared for Transportation Research Board, Washington, DC, 2002.
[48] Brown, E. R., Kandhalm P. S., and Zhang, J., "Performance Testing for Hot Mix Asphalt," National Center for Asphalt Technology Report No. 01-05, November 2001.

Journal of ASTM International, April 2005, Vol. 2, No. 4
Paper ID JAI12268
Available online at www.astm.org

R. Chris Williams, Ph.D.,[1] *Daniel W. Hill, M.Sc.,*[1] *and Matthew P. Rottermond, M.Sc.*[1]

Utilization of an Asphalt Pavement Analyzer for Hot Mix Asphalt Laboratory Mix Design

ABSTRACT: The Superpave volumetric mix design system, developed by SHRP in the 1990s, has continued to gain widespread acceptance across the United States. Although it is widely believed to be an improvement over past mix design systems, it does have an inherent flaw. It does not include a performance test to assess HMA's resistance to rutting, fatigue, or low temperature cracking. With the development and implementation of newer performance test specifications, it is an appropriate time to work on integrating a performance based test for construction specifications. Rather than being based on material properties or construction practices, the payment for an HMA pavement could then be based primarily on the performance based specification. The results of this study indicate that although the APA works well as the pass/fail criterion used by state agencies, the variability of APA cycles to failure make it impractical to base a rut prediction model on data obtained from it.

KEYWORDS: asphalt pavement analyzer, Superpave, WesTrack

Introduction

The Superpave volumetric mix design system, as developed by SHRP in the 1990s, has continued to gain widespread acceptance across the United States. The Superpave mix design system originally consisted of three separate design levels. The Level 1, or the Superpave volumetric mix design, was developed for lower volume (ESAL < 10^6) roads. Levels 2 and 3, intended for higher volume roads, included the Level 1 design but had additional performance models based upon performance tests to further aid in the HMA mixture design. Levels 2 and 3 were never implemented because the performance models did not accurately predict actual pavement performance [1]. The Superpave volumetric mix design has gained widespread use and is widely believed to be an improvement over past mix design systems. However, it does have an inherent flaw: it does not include a performance test to assess HMA's resistance to rutting, fatigue, or low temperature cracking.

Design-build and warranty specifications are gaining acceptance at the same time that implementation of newer HMA performance test specifications are being developed. Thus, it is an opportune time to work on integrating a performance-based test for use in newer construction specifications. The philosophy of a Performance Based Specification (PBS) is to design and construct an HMA pavement that will provide a required level of performance [2]. The level of performance may include all or any combination of the following distresses: permanent deformation, fatigue, thermal cracking, or moisture damage. Rather than being based on material properties or construction practices, payment for an HMA pavement is based primarily on the level of performance the as-constructed HMA pavement provides.

Manuscript received 1 December 2003; accepted for publication 23 September 2004; published April 2005.
Presented at ASTM Symposium on Performance of Hot Mix Asphalt (HMA), including Fundamental and Empirical Procedures on 9 December 2003 in Tampa, FL.
[1] Assistant Professor and Research Assistants, respectively, Department of Civil and Environmental Engineering, Michigan Technological University, Houghton, MI 49931.

Mechanisms that Cause HMA Pavement Rutting

Monismith et al. [3] found that well-designed HMA pavement consolidates to 3–5 % air voids after trafficking when pavements were initially compacted to 6–8 % air voids. Eisenmann and Hilmer [4] further described rutting as having two components: first consolidation and then permanent shear deformation. Eisenmann and Hilmer concluded that shear deformation is the result of shear flow of the HMA at constant volume. The decrease in volume of the HMA beneath the wheel loadings is approximately the same as the increase of volume of the upheavals at the edges of the rut. Rutting due to shear flow is the type of rutting that occurs during the majority of the pavement life. The Asphalt Institute [5] states that rutting caused by permanent shear deformation is the result of weak HMA that cannot resist the permanent shear deformations caused by heavy truck loadings.

The three constituents of HMA are aggregate, asphalt binder, and air. All three of the constituents have an effect on the rut resistance of HMA. Perhaps the most important material, in terms of rut resistance, is aggregate since in densely graded HMA, mineral aggregate is approximately 90 % of the mixture by volume. The primary cause of rutting is small permanent shear deformations that accumulate under each passing wheel load. Rough aggregate surface texture and cubical particles tend to lock together and provide more aggregate interlock than do rounded, smooth aggregate [5]. Aggregate properties are increasingly important at high temperatures when binder viscosity decreases. When binder viscosity becomes sufficiently low, the internal friction resultant of aggregate interlock is the primary resistance to permanent shear deformation.

The asphalt binder also contributes to the rut resistance of HMA. Mahboub and Little [6] concluded through the use of uniaxial creep tests that less viscous asphalt makes the HMA less stiff and consequently more susceptible to rutting. Also, the amount of asphalt in HMA can affect the rut resistance. Monismith, Epps, and Finn [7] concluded that a mixture should have an asphalt content such that the air void content after densification by traffic be 4 % but never lower than 3 %. HMA that consolidates to less than 3 % air voids has too much asphalt. This causes a decrease in rut resistance because the additional asphalt provides lubrication between aggregate particles otherwise separated by a very tight network of air voids.

The amount of air in HMA is a function of the compactive effort applied to the HMA layer. High air voids (less compaction) result in excess rutting because they allow for additional densification under traffic. On the other hand, very low air voids (less than 2 or 3 %) can result in a phenomenon known as tertiary flow [5] where the mixture exhibits extreme plastic flow with relatively few wheel loadings.

Loading can also significantly affect HMA rutting and include the following load characteristics [8]:

- truck speed
- tire contact pressure
- HMA layer thickness
- truck wheel wander

Because of the viscoelastic nature of asphalt binders, the speed of truck traffic, the contact pressure of truck wheels, and the pavement temperature all contribute to pavement rutting. As the speed of truck traffic decreases, the duration of the loading on the HMA increases [9]. Because of the time temperature superposition principle of asphalt binders, the increased duration of the loading results in more permanent shear deformation during each truck loading at a given temperature. Increased contact pressure between truck wheels and the HMA pavement surface results in higher stress within the upper portion of the pavement and more permanent shear deformation. Asphalt binders become less viscous when pavement temperatures increase and results in decreased shear resistance in HMA.

Asphalt Pavement Analyzer Background

The Asphalt Pavement Analyzer (APA) became commercially available in 1996 based upon the Georgia Loaded Wheel Tester (GLWT). The GLWT was developed in the mid-1980s through a collaborative effort of the Georgia Department of Transportation and the Georgia Institute of Technology. The basis of its development was to perform efficient, effective, and routine laboratory rut proof testing and field production quality control of HMA [10]. A rut proof tester is a machine used to distinguish between rut resistant and rut prone HMA, but it is not necessarily used to predict actual pavement performance. An APA User Meeting in Jackson, MS reviewed how governmental agencies are using APAs, and this is summarized in Table 1. A photo of the APA is shown in Fig. 1. The APA User's Manual describes the operation of the APA in detail [11].

Some of the advantages and drawbacks of GLWT (the predecessor to the APA) were stated by West et al. in 1991 [12]. The GLWT is advantageous because:

- The principles of the test are straightforward (i.e., it is unnecessary to be familiar with engineering properties).
- The GLWT realistically models a moving wheel load.
- The GLWT is easy to operate.
- The GLWT appears to correlate well with actual field performance.
- The GLWT is versatile (i.e., it can test at a variety of temperatures and loadings).

The disadvantage, as stated by West et al., is that the relationship between field and GWLT results is empirical.

Williams and Prowell [13] found the APA to correlate well with field rut depths. It was concluded that a mix design specification for a PBS could be established for the APA using test temperatures that reflect the in-situ temperature of the pavement.

In studies performed in Georgia and Florida, the GLWT was able to rank mixtures similarly to their actual field performance [12,14]. In another Florida study, the APA ranked three pavements similarly to their known field performance, and the author concluded that the APA had the capability to rank mixes according to their rutting potential [15]. Miller et al. [16] reported an increased correlation between lab rut depths and field rut depths with an increase in testing temperature from 40.6ºC and 46.1ºC. Lai [17] indicated that GLWT rut depths are very sensitive to beam density, and as a result, variability of measured rut depths between labs was quite high.

The objective of NCAT Report No. 99-4, "Evaluation of Asphalt Pavement Analyzer for HMA Mix Design," [18] was to demonstrate the APA's sensitivity to gradation and binder type and to determine a pass/fail rut depth criterion. Kandhal and Mallick found that the APA was sensitive to aggregate gradation and binder grade, and that the APA has the potential to predict relative rutting potential of HMA. They established a tentative pass/fail rut criterion, which was determined to be between 4.5–5 mm at 8000 load cycles.

In a study conducted to determine whether or not the GLWT could differentiate between HMA with different asphalt binders, Stuart and Izzo [19] found that the GLWT ranked mixtures with constant aggregate gradations but differing asphalt binders correctly. Specimens with seven different binders were tested. The GLWT rut depth increased with a decrease in G*/sin δ, as it should. The correlation between G*/sin δ and GLWT rut depth was found to be 0.84 for HMA surface mixtures.

TABLE 1—*A review of APA test methods and settings throughout the United States [28].*

State (see footnotes)	Test Temp (C) and Reliability	Air Voids (target/ range)	Compactor Type(s)	Seating Cycles	# of Test Cycles	Test used in specs?	Criteria
AL, 1a	67 P98	4/1	SGC	25	8000	Y	< 4.5 mm TRZ
AR, 1a	64 P98	4/1	SGC	25	8000	Y	< 3 mm (>10E6), < 5 mm for others
DE, 2a	67	7/0.5	AVC	25	8000	N	< 3 mm (>10E6)
FL, 1ab	64 P98	7/0.5	AVC	25	8000	N	none
GA, 1ab	49	6/1	SGC	50	8000	Y	< 5 mm for all mixes
IL, 2ab	64 P98	7/1	SGC	25	8000	N	none yet
KS, 1ab	(<PG)	7/1	SGC	25	8000	N	developing, temps 52–58°C
KY, 2a	64 P98	7/1	SGC	25	8000	N	rule of thumb < 5 mm
LA, 2ab	64 P98	7/1	SGC	25	8000	N	< 6 mm (research only)
MI	Under development, expect a tiered specification based on trafficking level and level of reliability						
MS, 1a	64 P98	7/1	SGC	50	8000	N	< 10 mm for all mixes
MO, 2a	64 P98	7/1	SGC	25	8000	N	evaluating
NJ, 1a	60	4 & 7/1	SGC	25	8000	N	evaluating
NC, 2ab	64 P98	7/1	SGC/AVC	25	8000	N	evaluating
OK, 2a	64 P98	7/1	SGC	25	8000	N	< 5 mm (> 3E6), < 6 mm (0.3E6+), < 7 mm (<0.3E6)
SC, 2a	64 P98	7/1	AVC	25	8000	Y	< 5 mm for all Superpave
TN, 1ab	64 P98	7/1	SGC	0	8000	N	Rule of Thumb, < 5–6 mm
TX, 2ab	64 P98	7/1	SGC	50	8000	N	Evaluating
UT, 2ab	64 P98	7/1	LKC	50	8000	Y	< 5 mm for all mixes
WV, 1ab	60	7/1	SGC	0	8000	N	evaluating, < 6 mm typical
WY, 2ab	52 P50	7/1	AVC	25	8000	N	evaluating

1 Report manual measurements; use automatic measurements if available.
2 Use automatic measurements to report; check with manual measurements.
a Mix design.
b Plant produced mixture.
SGC = Superpave Gyratory Compactor.
AVC = Pavement Technology, Inc. Asphalt Vibratory Compactor.

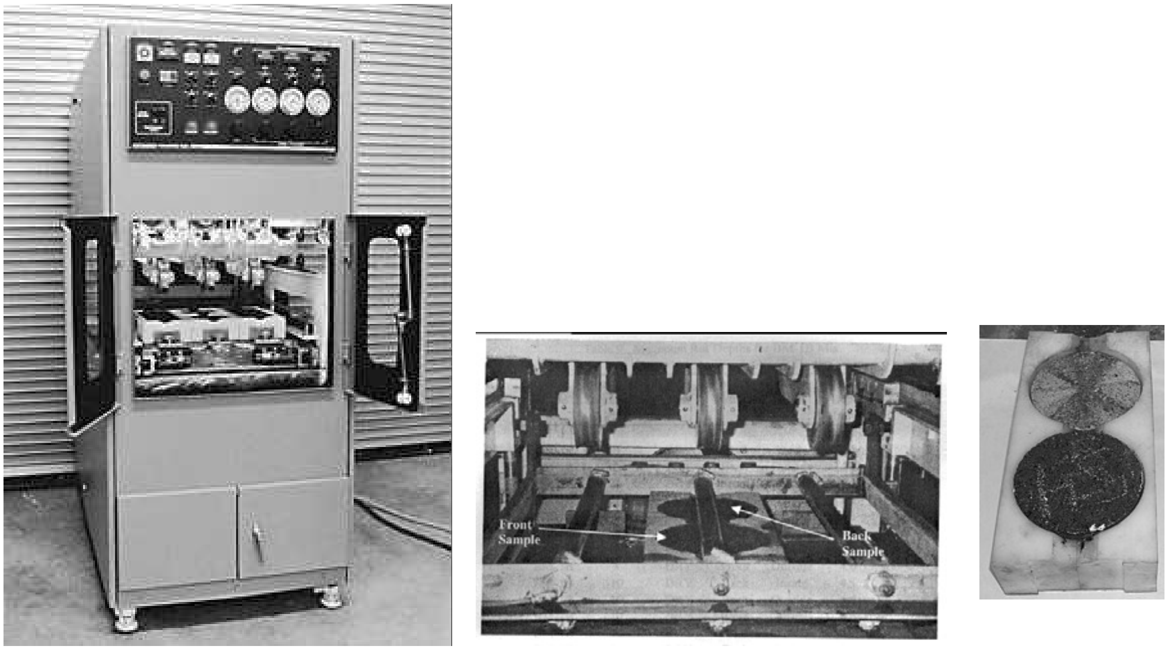

FIG. 1—*The Asphalt Pavement Analyzer.*

APA Specimen Preparation

A Superpave Gryratory Compactor (SGC) was used to compact specimens for APA testing. Field verified mix designs from ten different projects were used in the study. A tolerance of +/– 0.5 % air voids was used for all specimens. Once the SGC specimens are prepared, they are trimmed to a height of 75 mm, the depth of the APA molds. Trimming of the specimens is done using a rock saw. Care is taken to cut the specimens so that the top and bottom of the specimens are parallel. The target air voids and asphalt binder contents for each project are summarized in Table 2. Triplicate samples were procured and tested at each air void and asphalt binder content combination.

TABLE 2—*Test matrix used for testing each HMA project.*

	Air Voids (% of Total Volume)		
	4 %	8 %	12 %
Low Asphalt Content (Opt. AC – 0.5 %)	N/A	XXX	XXX
Optimum Asphalt Content	XXX	XXX	XXX
High Asphalt Content (Opt. AC – 0.5 %)	XXX	XXX	N/A

Preliminary APA Test Method

One of the national goals is to develop a performance criterion for testing HMA mixtures in the APA. Here the development of performance criteria using an APA is examined.

The previous literature revealed that test temperatures should be selected to produce results that would correlate well with field conditions. The APA test settings and methods used in this study are summarized in Table 3.

TABLE 3—*APA machine settings and test methods.*

Parameter	Specification
Test Temperature, (°C)*	Upper Performance Grade of HMA Being Tested
Environmental Condition	Dry
Superpave Specimen Size, mm	Cylindrical Specimens, 150 mm dia., 75 mm height
Load, N (lb)	445 (100)
Hose Pressure, kPa (psi)	689 (100)
Wheel Speed, m/sec	0.61
Number of Test Wheel Load Cycles	8000 (with 50 seating cycles)
Laboratory Compaction Device	Superpave Gyratory Compactor
Pretest Specimen Conditioning	4 h at Test Temperature

*This does not include grade bumping for high volume facilities or slower moving traffic.

The SGC specimens are placed into APA molds so that they are flush with the top of the molds. Plaster of Paris is used to level and confine specimens in the molds whenever specimens and molds are not a snug fit. After preparing the test specimens, the APA molds with the specimens are conditioned at the test temperature for four hours to allow the specimens to come to test temperature prior to testing.

Normally each APA mold contains two specimens for testing. The average rut depth of both specimens is then recorded as the APA rut depth. In this study the standard deviation of three specimens at each asphalt content/air void level was of great importance. The APA does not record each specimen's rut depth independently but rather records the average of the two specimens in each APA mold. Thus, another method had to be used so that the rut depth of each individual specimen was recorded and the standard deviation could be calculated. To do this, a dummy specimen (concrete spacer) was placed into one of the specimen holes, and only one asphalt specimen was tested in each mold during APA testing (Fig. 1). The recorded rut depths were just for the HMA specimens located in the front of the molds.

Development of an Empirical Rut Prediction Model

The APA is a test device which applies a loaded wheel at a prescribed "tire" pressure and a frequency at a programmed temperature. The value measured, the rut depth, cannot be used as a basis for a mechanistic model. In the past, the APA rut depth at 8000 cycles has been used to identify rutprone HMA mixtures before they are used in the field. This is done by establishing a pass/fail rut depth. For example, based upon past experience some state highway agencies have established a rut depth of 5-mm as the dividing point between rut prone and rut resistant HMA mixtures. Hence, no HMA mixtures with an APA rut depth of 5 mm or greater would be constructed in the field. No attempts have been identified in the literature review to use the APA to predict how many 80-kN Equivalent Single Axle Loadings (ESALs) an HMA pavement can be loaded with until failure. The following will be presented:

- A methodology of converting APA rut depth to field rut depth and APA cycles to 80-kN ESALs
- The development of an empirical rut prediction model for local conditions
- A preliminary Performance Based APA Specification

Relating APA Test Performance to Field Performance

The wheel loading in the APA is used to simulate a wheel loading on an in-service pavement, while the rut created is supposed to be similar to the rut created by trafficking on in-service pavements. In this section, a method of converting the APA rut depth and the number of APA load cycles to actual pavement rut depth and ESALs will be presented.

Determination of an APA Rut Depth that is Equivalent to Rutting Failure On an In-Service HMA Pavement—To determine an APA rut depth that is equal to failure on an in-service pavement, a pavement failure rut depth must first be determined. Barksdale [20] found that for pavements with a 2 % crown (typical for the United States), rut depths of 0.5 in. (12.5 mm) are sufficiently deep to hold enough water to cause a car traveling 50 mph to hydroplane. The rut depth referred to by Barksdale is the total rut depth, not the downward rut depth. According to pavement rut depth measurements taken from WesTrack [21], a 12.5 mm total rut depth (consolidation and shear deformation) is approximately equivalent to a downward rut depth (consolidation and shear deformation, less the uplift due to shear flow) of 10 mm. From APA data also taken from WesTrack pavements it can be determined that a 10 mm downward rut depth on an in-service pavement correlates well with a 7 mm rut depth. These correlations can be seen in Figs. 2 and 3, respectively. Based upon these correlations, an APA failure rut depth of 7 mm will be used in establishing an empirical model.

Determination of How Many 80-kN ESALs Are Equal to One APA Cycle—The WesTrack experiment provided a unique opportunity to compare APA results with a full-size pavement testing facility where both the loading and temperature were known. APA test specimens were taken directly from the wheel paths of the test track before truck loading and were tested at 60°C - nearly the same as the average high pavement temperature of 57.53°C at 12.7 mm depth [13]. As can be seen in Fig. 3, the WesTrack pavement rut depths correlated very well with the APA test specimens taken from WesTrack.

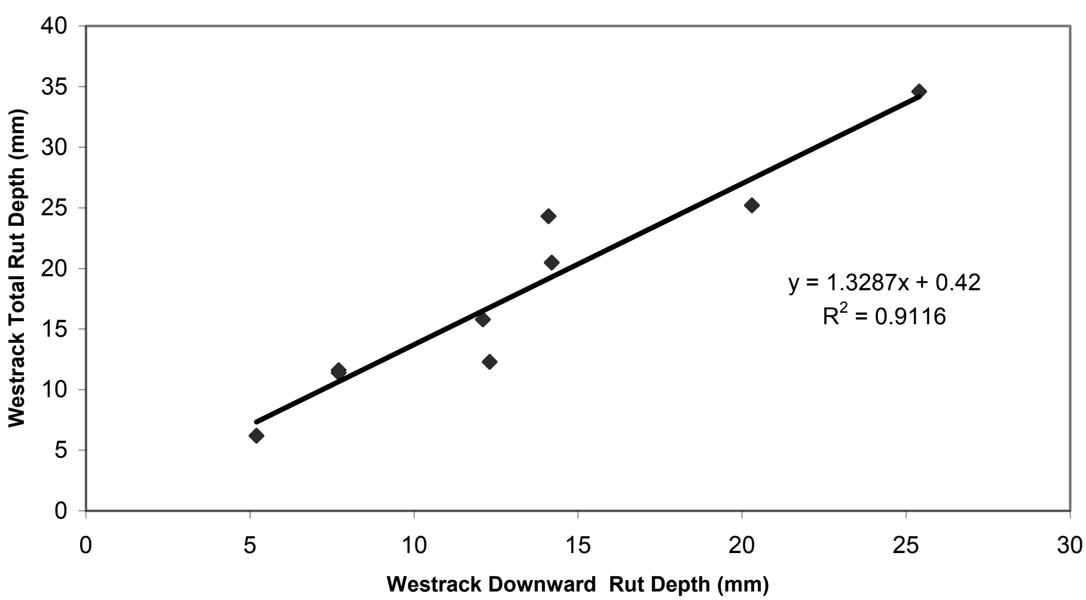

FIG. 2—*WesTrack total rut depth versus WesTrack downward rut depth [13].*

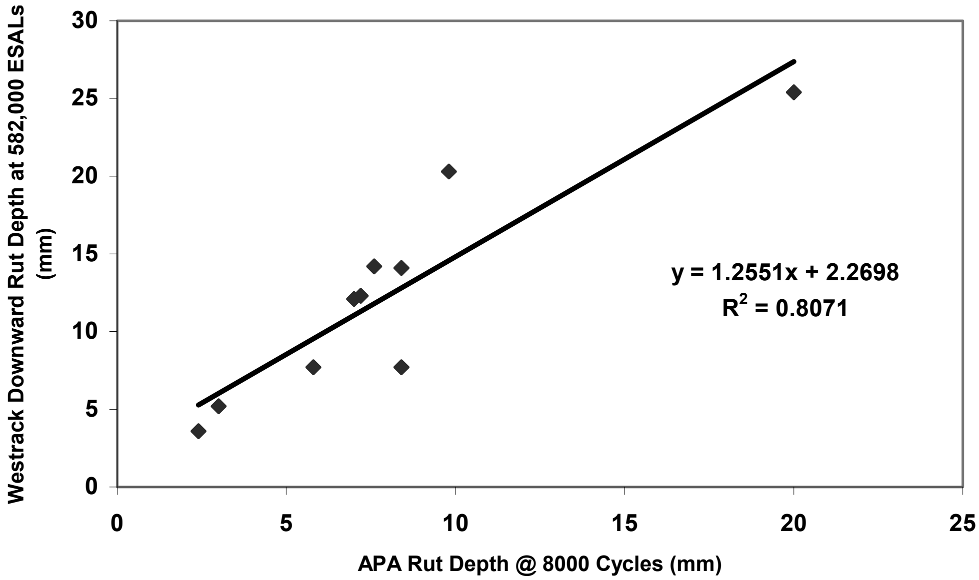

FIG. 3—*WesTrack downward rut depth versus APA rut depth [13].*

Although the WesTrack and APA test temperatures are nearly the same, the number of ESALs per APA cycle cannot be found simply by dividing 582 000 ESALs by 8000 cycles. This is because the trucks that loaded WesTrack traveled slower than ordinary trucks on highways, and the wheel wander of the WesTrack trucks was tighter than ordinary truck traffic. Both truck speed and wheel wander have to be corrected as follows before the amount of rutting ESALs per APA cycles can be determined.

First, the WesTrack trucks traveled at 65 kph, which is slower than ordinary truck traffic, which travels approximately 100 kph at highway speeds. Because of the viscoelastic nature of asphalt cement, the longer loading time caused by slow moving trucks causes increased HMA pavement damage. Haddock et al. [8], in a study by Purdue University conducted in the Indiana Department of Transportation's (INDOT) accelerated pavement testing (APT) facility, developed a relationship between rut depth and truck speed. According to Haddock et al. [8], for an HMA pavement of high density, a truck traveling at 65 kph does approximately 12 % more pavement damage than a truck traveling 100 kph does.

Secondly, the WesTrack trucks, because of their guidance system, wandered less than ordinary trucks on standard 12-ft lanes. Wheel wander refers to the fact that trucks tend to "wander" about the traffic lane rather than staying exactly in the center of the lane. This wheel wander tends to distribute the truck loadings over a wider pavement area and consequently reduces the depth of ruts that single wheel path traffic would create. From past experience, it has been shown that trucks tend to wander over a width of 460 mm when traveling on a 12-ft traffic lane [22]. The WesTrack Trucks wandered over a width of 127 mm. A decrease in wheel wander causes the truck loads to be distributed over a smaller pavement area and consequently causes more pavement damage. Haddock et al [8] developed a relationship between wheel wander and rut depth using the INDOT APT, which had a transverse mechanism to include wheel wander, and can be used to estimate the increased amount of rutting caused by the WesTrack trucks:

$$Increased\ \ Damage = \frac{Rut\ Damage\ at\ 127\ mm\ Wander - Rut\ Damage\ at\ 460\ mm\ Wander}{Rut\ Damage\ at\ 460\ mm\ Wander} \qquad (Eq.1)$$

$$= \frac{8.2422e^{(-0.0014*127mm)} - 8.2422e^{(-0.0014*460mm)}}{8.2422e^{(-0.0014*460mm)}}$$

$$= 0.594$$

The WesTrack loaded trucks did 59.4 % more damage than ordinary trucks as a result of differences in wheel wander.

The previous calculations demonstrate that the WesTrack trucks did more damage per loading than ordinary trucks. The following equation shows how many ordinary truck ESALs the WesTrack Truck ESALs were actually equal because of decreased truck speed and wheel wander:

$$Ordinary\ Truck\ ESALs = (582{,}000\ \ ESALs)*(Wander\ Adjustment)*(Speed\ Adjustment) \qquad (Eq.2)$$

$$= (582{,}000\ \ ESALs)\ \ *\ \ (1.594)\ \ *\ \ (1.12)$$

$$= 1{,}039{,}033\ \ ESALs$$

The amount of 80-kN ESALs per APA cycle is calculated as follows:

$$ESALs\ per\ APA\ Cycle\ = (1{,}039{,}033\ \ ESALs)/(8{,}000\ APA\ Cycles) \qquad (Eq.3)$$

$$= 129.9\ ESALs\ per\ APA\ Cycle$$

Based on the previous equation it is estimated that one APA cycle is approximately 129.9 80-kN ESALs. APA testing is typically done at the temperature of the high Performance Grade (PG) of the binder in the HMA, or approximately the highest pavement temperature the HMA mixture will see in-service. Because of this fact, one APA cycle is equal to 129.9 rutting ESALs and does not include the number of ESALs for all seasons. Since not all truck loadings occur during times when HMA pavements experience rutting (i.e., when pavement temperatures approach the upper PG), any PBS utilizing an APA has to be adjusted to include only rutting ESALs. This is done in the following section.

The Development of an Empirical Rut Prediction Model for Local Conditions

Since asphalt binder viscosity decreases with increasing temperature, HMA rutting occurs when pavement temperatures are above average in the summer months. More specifically, work done by Mahboub and Little [6] stated the following assumptions could be made:

- Permanent deformation occurs daily over the time interval from 7:30 a.m. to 5:30 p.m.
- Permanent deformation occurs only in the period from April to October, inclusive.
- Measurable permanent deformation does not occur at air temperatures below 50°F (10°C).

The Superpave 20-year design life includes all ESAL loadings during the entire 20-year design life. Based on the above assumptions, the number of ESALs in the 20-year design life needs to be adjusted to only the ESALs when rutting occurs, or "rutting ESALs," if a PBS using the APA is to be developed. Hill [23] established a process of making this conversion, which is summarized in Fig. 4.

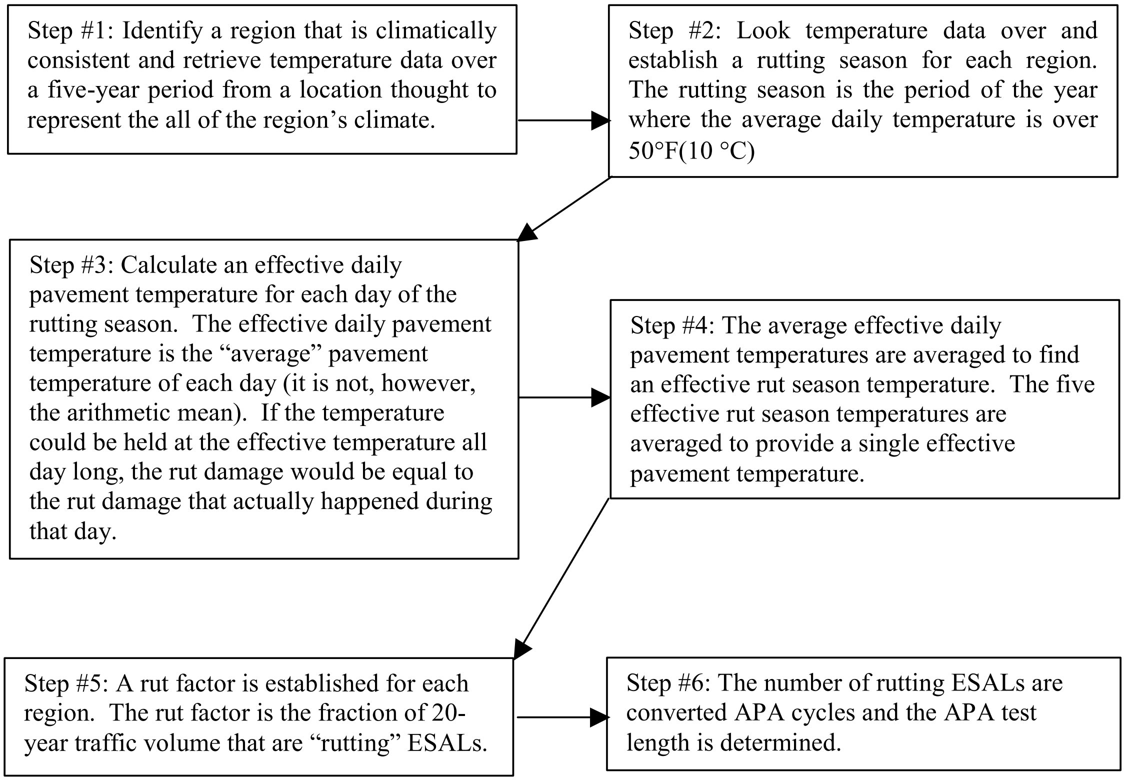

FIG. 4—*A summary of the steps taken to find the amount of rutting ESALs during a Superpave 20-year design life [23].*

A Preliminary PBS

As stated previously, a PBS based upon APA data must include an APA rut depth failure criterion as well as the test length representing the HMA pavements design life, in terms of ESALs. Here a method of finding the amount of rutting ESALs that occurs in the Superpave 20-year design life is presented. As an example, Performance Based APA Specifications were created for six Michigan regions in Fig. 5. As mentioned, a PBS based on APA data must include both a test length (in terms of APA cycles) and a failure rut depth criterion. The rut depth criterion is summarized first, followed by the test length.

The failure criterion for an APA specimen was set at 7 mm based upon data gathered at WesTrack, but this criterion should be adjusted to consider APA testing variability. This rut criterion adjustment is based upon the following factors [13]:

- The level of confidence
- The variance or standard deviation
- The sample size
- The specification limit

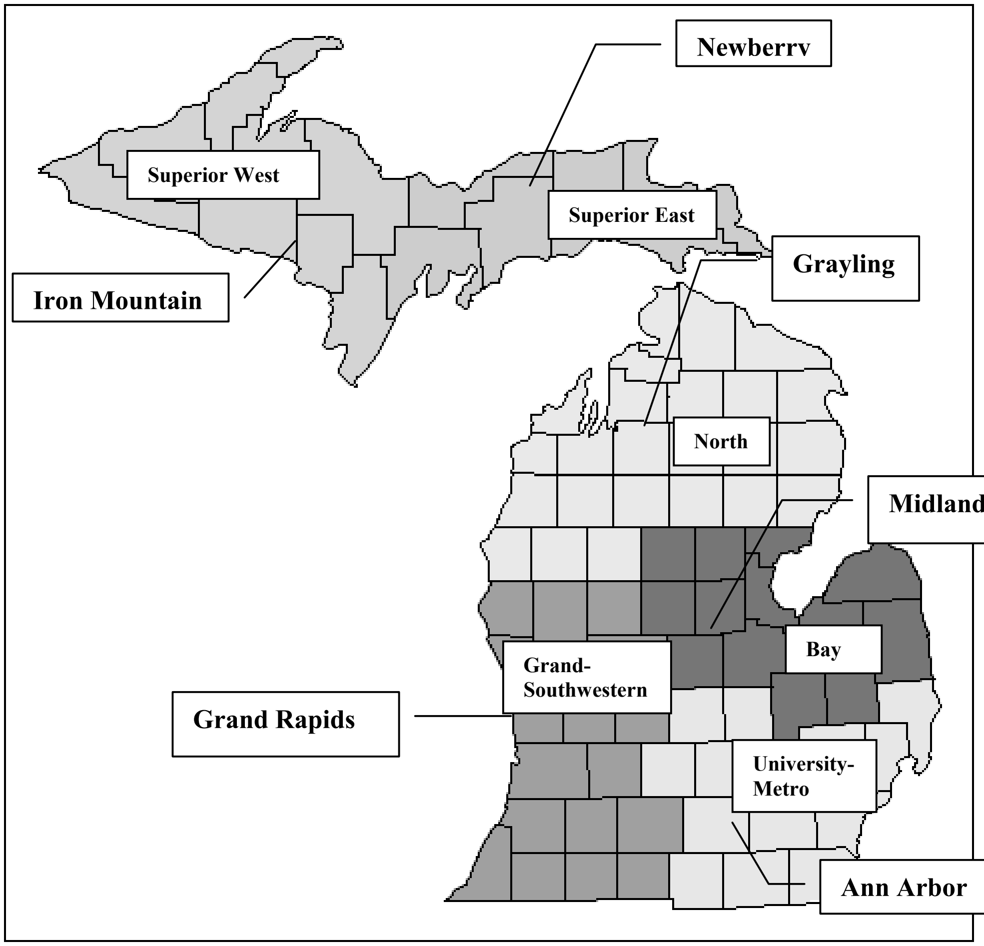

FIG. 5—*Locations where weather data were collected for each region.*

A method was established by Williams and Prowell [13] to develop an APA pass/fail rut depth criteria taking the preceding factors into account. The rut depth criterion is set using the small-sample confidence for a one-tail test [24] as follows:

$$Maximum\ Rut\ Depth = y + t_{Alpha}\left(\frac{S}{\sqrt{n}}\right) \qquad (Eq.4)$$

where:

y = mean APA rut depth at 8000 cycles (mm)

t_{alpha} = confidence limit

S = sample standard deviation (mm)

n = number of APA Specimens in sample

A maximum APA mean rut depth of three APA specimens can be calculated by rearranging Equation 4 and substituting values into the equation as follows:

$$y = Maximum\ Rut\ Depth - t_{alpha}\left(\frac{S}{\sqrt{n}}\right) \qquad (Eq.5)$$

$$= 7\ mm - 2.353\left(\frac{1mm}{\sqrt{3}}\right)$$

$$= 5.64\ mm$$

where:

7mm = maximum allowable APA rut depth based on Figure 3

2.353 = $t_{0.05}$ (Mendenhall and Sincich, 1989)

1 mm = standard deviation based on 7 mm rut depth (Figure 4)

3 = sample sized proposed to be used in an APA specification

An APA average rut depth of 5.64 mm ensures with 95 % confidence that the HMA being tested does not rut more than 7 mm in the APA. This is based on a sample size of three APA specimens. The 95 % confidence limit can be changed according to the level of risk an owner/agency is comfortable accepting.

The test length for a PBS is calculated using the temperature versus mix stiffness and then determining a rut factor based upon mix stiffness. This utilizes an approach developed by Shell [9], and more detail is provided by Hill [23]. Thus, the annual design ESALs are multiplied by the number of rutting days as a percent of a year (365 days) and the rutting factor. Table 4 summarizes the number of rutting days for each Michigan region. A preliminary Performance Based APA specification for Michigan HMA pavements is presented in Table 5 as an example.

Asphalt Pavement Analyzer Test Results

Ten separate 9.5-mm nominal maximum aggregate wearing course mixtures were sampled during the 2000 construction season. The HMA samples included three Superpave traffic levels (i.e. E3, E10, and E30). This project's mix designs were verified and used for testing in APA to determine the following:

- The usefulness of the empirical model.
- The effect that asphalt content and air voids has on APA performance.
- A regression model to predict APA rut depth.
- Perhaps most importantly, the APA data presented will be correlated with future in-service pavement performance to assess the APA's usefulness in predicting the performance of HMA pavements.

TABLE 4—*Length of rutting seasons in each region.*

Region	Dates of Rutting Season	Length of Rutting Season, Days
Superior West	April 1–October 31	214
Superior East	April 1–October 31	214
North	April 1–October 31	214
Bay	March 15–November 15	246
Grand-Southwestern	April 1–October 31	214
University-Metro	March 1–November 30	275

TABLE 5—*A preliminary performance based APA specification.*

Region	Traffic Level	Rutting Days per Year	Rutting Factor	18-Kip ESALs on Rutting Days	Rutting ESALs	APA Test Length (APA Cycles)	APA Failure Criteria (mm)*
Superior West	E3	214	0.084	1 783 333	149 800	1 158	5.64
	E10			5 944 444	499 333	3 859	5.64
	E30			17 833 333	1 498 000	11 577	5.64
Superior East	E3	214	0.071	1 783 333	126 617	978	5.64
	E10			5 944 444	422 056	3 262	5.64
	E30			17 833 333	1 266 167	9 785	5.64
North	E3	214	0.067	1 783 333	119 483	923	5.64
	E10			5 944 444	398 278	3 078	5.64
	E30			17 833 333	1 194 833	9 234	5.64
Bay	E3	246	0.167	2 050 000	342 350	2 646	5.64
	E10			6 833 333	1 141 167	8 819	5.64
	E30			20 500 000	3 423 500	26 457	5.64
Grand-Southwest	E3	214	0.201	1 783 333	358 450	2 770	5.64
	E10			5 944 444	1 194 833	9 234	5.64
	E30			17 833 333	3 584 500	27 701	5.64
University-Metro	E3	275	0.147	2 291 667	336 875	2 603	5.64
	E10			7 638 889	1 122 917	8 678	5.64
	E30			22 916 667	3 368 750	26 034	5.64

* The APA Failure Criterion is Based on the Mean APA Rut Depth of Three APA Specimens.

Two types of APA data can be analyzed. An experimental plan for each mix was executed as shown previously in Table 2. The first, APA rut depth at 8000 cycles, is used industry-wide as an indication of whether or not an HMA mixture will perform in the field. The second is the amount of APA cycles needed to achieve a rut depth of 7 mm. As shown previously, a 7 mm APA rut depth correlated with an in-service HMA rutting failure. The previous section presented a method of converting APA cycles to 80-kN ESALs. Based on this, it is thought that the number of APA cycles needed to achieve a 7 mm rut depth can be converted to how many ESALs an in-service pavement could withstand before failure.

APA Test Results

This section summarizes the APA results from HMA specimens created using materials from ten HMA paving projects. Two performance measures are presented: 1) the APA rut depths at 8000 cycles, a pass/fail criterion used throughout the United States to identify rut prone HMA, and 2) a performance measure that has not been documented in the past. The APA cycles are needed to create a 7 mm rut (or APA cycles to failure). This is the criterion used in the Performance Based Specification (PBS) presented earlier. The APA cycles to failure results can be used to access the feasibility of the developed PBS.

APA Rut Depths at 8000 Cycles Results—Most State Highway Agencies that utilize the APA set a pass/fail criterion for the APA rut depth at 8000 cycles (Table 1). The data from each traffic level were averaged and are presented in Table 6. The standard deviation of the averages was calculated and is shown in parentheses beneath the mean rut depth. This was done so the mean APA rut depth and standard deviation at different traffic levels can be analyzed, and trends in the data can be identified. Each mixture's average and standard deviation of three specimens were determined for examining a performance based specification and are reported in detail by Hill [23].

TABLE 6—*Average APA mean rut depths for all mix types.*

Project Name	Average of All Projects	Air Voids		
Traffic Level	5 E 3	4 %	8 %	12 %
Asphalt Content	Opt. AC -0.5 %	N/A	5.91	7.69
			(1.65)	(1.26)
	Opt. AC	4.51	6.77	8.6
		(1.06)	(0.66)	(1.63)
	Opt. AC +0.5 %	6.18	8.41	N/A
		(1.74)	(1.39)	
Project Name	Average of All Projects	Air Voids		
Traffic Level	5 E 10	4 %	8 %	12 %
Asphalt Content	Opt. AC -0.5 %	N/A	5.67	8.01
			(1.08)	(1.08)
	Opt. AC	4.96	7.03	9.44
		(0.70)	(1.53)	(1.33)
	Opt. AC +0.5 %	6.3	8.47	N/A
		(0.49)	(1.04)	
Project Name	Average of All Projects	Air Voids		
Traffic Level	5 E 30	4 %	8 %	12 %
Asphalt Content	Opt. AC -0.5 %	N/A	5.67	9.37
			(1.87)	(0.45)
	Opt. AC	5.09	7.8	11.87
		(1.45)	(1.83)	(1.08)
	Opt. AC +0.5 %	5.57	9.06	N/A
		(1.55)	(1.28)	

The Amount of APA Cycles to Reach the Failure Rut Depth in the Asphalt Pavement Analyzer—The number of cycles in the APA to achieve a rut depth of 7 mm (or APA cycles to failure) is important to test the effectiveness of an empirical pavement prediction model previously proposed. Recording the APA cycles until failure was done in two different ways. First, if the specimen rutted more than 7 mm in the 8000 cycle test, the number of APA cycles where the specimen rutted 7 mm was determined and is illustrated as Case 1 in Fig. 6. Case 2 in Fig. 6 is where the APA specimen did not rut 7 mm, and thus the APA curve was extrapolated out to a 7 mm rut depth. This extrapolation was done by extending the creep curve outward to 7 mm. The creep portion of the APA curve is assumed to be where permanent shear deformation is taking place. The initial part of the curve is the consolidation curve, and this is assumed to be where the specimen rutting due to densification beneath the loaded wheel. The average APA cycles to failure of the three APA specimens and the standard deviation are presented. The data from each traffic level were averaged together and are presented in Table 7.

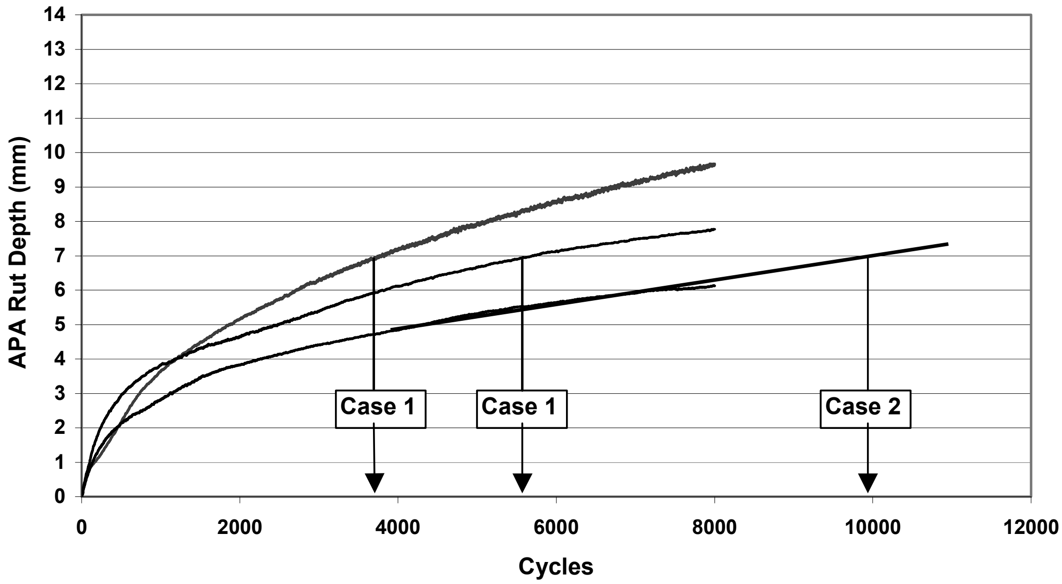

FIG. 6—*Method used to find the number of APA cycles until failure.*

TABLE 7—*Average APA cycles to failure for all mixes.*

Project Name	Average of All Projects	Air Voids		
Traffic Level	5 E 3	4 %	8 %	12 %
Asphalt Content	Opt. AC –0.5 %	N/A	11 133 (6 150)	11 052 (3 410)
	Opt. AC	18 289 (7 379)	11 354 (3 450)	5 638 (2 949)
	Opt. AC +0.5 %	11 264 (4 791)	5 718 (1 479)	N/A
Project Name	Average of All Projects	Air Voids		
Traffic Level	5 E 10	4 %	8 %	12 %
Asphalt Content	Opt. AC -0.5 %	N/A	15 999 (3 666)	7 472 (2 808)
	Opt. AC	20 498 (4 445)	14 388 (9 287)	5 055 (2 056)
	Opt. AC +0.5 %	16 086 (5 329)	10 043 (5 182)	N/A
Project Name	Average of All Projects	Air Voids		
Traffic Level	5 E 30	4 %	8 %	12 %
Asphalt Content	Opt. AC –0.5 %	N/A	15 283 (11 801)	5 208 (1 522)
	Opt. AC	16 068 (7 529)	7 051 (2 996)	2 725 (571)
	Opt. AC +0.5 %	13 308 (6 972)	5 237 (1 928)	N/A

Predicted HMA Rutting Performance

An empirical rut prediction model was developed based upon APA data. Based on the model, a performance based APA specification was developed for Michigan HMA pavements (Table 4). To help determine the usefulness of this PBS, the APA data from ten Michigan projects was used to predict the amount of ESALs the in-service pavements could withstand before failure, which is taken as a 10 mm downward rut depth for in-service pavements. The following equation was used to convert the APA cycles to failure data into ESALs to failure. The equation is simply Eq 6 solved for the total amount of ESALs.

$$ESALs_{Failure} = \frac{\left(APA\ Cycles\ to\ 7mm\ Rut\right) * \left(129.9 \dfrac{Rutting\ ESALs}{Cycle}\right)}{\left(\dfrac{\mathrm{RS} * \mathrm{RF}}{365}\right)} \qquad (Eq.6)$$

where:

$ESALs_{Failure}$ = Amount of ESALs Until Rutting Failure

$APA\ Cycles\ to\ 7mm\ Rut$ = From Data in Section 6.2.2

RS = Length of Rutting Season in Days

RF = The Fraction of the Total ESALs where Rutting Takes Place

The rutting factor and length of rutting season are the values as previously presented. The average predicted amount of ESALs to pavement rutting failure for each traffic level follows in Table 8. These results can be compared to PBS specification in Table 4. Also, these results can be compared with the actual future pavement performance of the ten projects to access the accuracy of the rut prediction model presented in this paper.

Analysis of APA Test Results

The previous section summarized results of APA testing of ten Michigan Hot-Mix Asphalt (HMA) paving projects. Three separate types of results were summarized:

1. The APA rut depth at 8000 cycles
2. The APA cycles until failure (failure being a 7 mm APA rut)
3. The ESALs that the pavement is predicted to withstand until rutting failure, based upon the empirical rut prediction model presented previously

The results are statistically analyzed in the following manner:

1. The results will be analyzed to determine whether changes in asphalt content and air voids result in statistically different APA rut depths at 8000 cycles and APA cycles until failure. Past experience has shown that changing asphalt content and air void content does change rutting performance of in-service pavements. Because of this, it would be beneficial to know if the APA test conditions are sensitive to changes in these properties.
2. The average APA rut depths and standard deviations for each Superpave design level will be analyzed. It is of interest to know if HMA mixtures designed at different Superpave levels perform differently in the APA.

TABLE 8—*The average number of ESALs to pavement rutting failure for all mixes.*

Project Name	Average of All Projects	Air Voids		
Traffic Level	5 E 3	4 %	8 %	12 %
Asphalt Content	Opt. AC -0.5 %	N/A	11 067 821	13 021 599
			(4 420 323)	(2 947 885)
	Opt. AC	19 315 330	11 282 162	6 942 126
		(6 066 580)	(3 461 276)	(1 332 802)
	Opt. AC +0.5 %	11 632 854	4 860 918	N/A
		(2 043 865)	(1 058 882)	
Project Name	Average of All Projects	Air Voids		
Traffic Level	5 E 10	4 %	8 %	12 %
Asphalt Content	Opt. AC –0.5 %	N/A	14 040 336	4 985 121
			(1 214 716)	(870 274)
	Opt. AC	14 607 611	6 770 369	3 179 798
		(2 376 856)	(1 954 084)	(761 774)
	Opt. AC +0.5 %	12 047 727	6 158 502	N/A
		(2 777 235)	(2 212 336)	
Project Name	Average of All Projects	Air Voids		
Traffic Level	5 E 30	4 %	8 %	12 %
Asphalt Content	Opt. AC -0.5 %	N/A	20 164 465	6 165 732
			(12 356 806)	(1 503 606)
	Opt. AC	18 090 574	7 795 201	3 268 938
		(4 952 765)	(2 058 026)	(441 661)
	Opt. AC +0.5 %	15 522 283	5 997 044	N/A
		(6 051 532)	(2 072 878)	

Statistical Analysis of the APA Rut Depth at 8000 Cycles Results

It is of interest to know whether or not the APA is sensitive to changes in asphalt content and air voids. To determine this, a test matrix was developed to analyze APA test results while varying HMA properties. These variations in HMA properties are similar to the variations that may occur in the field.

The goal of the statistical analysis was to determine if the changes in air voids and asphalt content resulted in statistically different APA performance. Two statistical methods were used to evaluate the effects of changes in the HMA properties to determine whether or not statistical differences exist. The two methods used were the Tukey's and Duncan's Multiple Range (DMR) Tests. These tests were used because they are effective when a factorial design is unbalanced. The test matrix in Table 2 is a 3^2 factorial design. It is an unbalanced design because the top left and bottom right cells of the test matrix contain no data. Both types of tests were conducted at the 95 % (100-alpha) level of confidence.

The statistical analysis was performed using SAS statistical software. Using SAS, an analysis of variance (ANOVA) table was developed. The two treatments used in this model were asphalt content and air voids (i.e., rut depth = f(asphalt content, air voids)) where the properties were entered as categorical data (i.e., low, optimum, and high asphalt contents were entered into the program as 1, 2, and 3, respectively, while 4, 8, and 12 % air voids were entered 1, 2, and 3). The ANOVA table includes the mean square error (MSE), an estimator of the sample variance, which is needed for both Tukey and DMR testing. SAS was used to conduct the Tukey and DMR tests.

Carmer and Swanson [25] reported that the DMR test is a very effective test at detecting true differences in means. Montgomery [26] reports that the Duncan procedure is quite powerful and is very effective at detecting differences between means when real differences exist. Tukey's test is a more conservative test. The DMR test will be emphasized in the following statistical analysis for these reasons.

The results of this statistical analysis are shown in Tables 9 and 10. In the Tables, HMA mixture types with the same letter performed the same, while HMA mixtures with different letters performed statistically different.

TABLE 9—*Analysis of the effect of asphalt content on APA rut depth at 8000 cycles (α = 0.05).*

Superpave HMA Mixture Design Level	Project Location	Asphalt Content (% by Mass)	Tukey 95 % Grouping	Duncan 95 % Grouping
E1	Brimley, M-28	Low	A	A
		Optimum	A	A
		High	A	A
E3	Elk Rapids, US-31	Low	A	A
		Optimum	A	A
		High	A	A
	Monroe, US-24	Low	A	A
		Optimum	A	A
		High	B	B
	Brooklyn, M-50	Low	A	A
		Optimum	A	A
		High	A	A
E10	Lansing, M-43	Low	A B	A B
		Optimum	A	A
		High	B	B
	Indian River, I-75	Low	A	A
		Optimum	A	A
		High	B	B
	Grayling, US-27	Low	A	A
		Optimum	A	A
		High	A	A
E30	Auburn Hills, I-75	Low	A	A
		Optimum	B	B
		High	A B	A B
	Clarkston, I-75	Low	A	A
		Optimum	A	A
		High	A	A
	Saginaw, I-75	Low	A	A
		Optimum	A	A B
		High	A	B

TABLE 10—*Analysis of the effect of air voids on APA rut depth at 8000 cycles (α = 0.05).*

Superpave HMA Mixture Design Level	Project Location	Air Voids (% by Volume)	Tukey 95 % Grouping	Duncan 95 % Grouping
E1	Brimley, M-28	4	A	A
		8	B	B
		12	B	B
E3	Elk Rapids, US-31	4	A	A
		8	A	A
		12	B	B
	Monroe, US-24	4	A	A
		8	A	A
		12	A	A
	Brooklyn, M-50	4	A	A
		8	B	A B
		12	A B	B
E10	Lansing, M-43	4	A	A
		8	A	B
		12	B	C
	Indian River, I-75	4	A	A
		8	A	A
		12	A	B
	Grayling, US-27	4	A	A
		8	A	A
		12	B	B
E30	Auburn Hills, I-75	4	A	A
		8	A B	B
		12	B	B
	Clarkston, I-75	4	A	A
		8	B	B
		12	C	C
	Saginaw, I-75	4	A	A
		8	B	B
		12	C	C

Analysis of the Effect of Asphalt Content on APA Rut Depth at 8000 Cycles—It can be seen that the DMR test detected five projects exhibiting sensitivity to changing asphalt content in Table 9. Two of these projects, Lansing M-43 and Auburn Hills I-75, did not rank the specimens correctly (i.e., rut depth did not increase with increasing air voids), and this is probably the result of error. After considering this, only three projects were sensitive to asphalt content. These three projects did not occur within any particular Superpave design level, so the effects of asphalt content on APA performance does not increase or decrease with an increase in the mixture design level. All three of these projects show a statistically greater rut depth when the asphalt content was high (Optimum AC + 0.5 %). This does lend credibility to the APA since high asphalt contents decrease stability in HMA mixtures. But since it only occurred for three out of ten projects, it is concluded, in general, that the APA rut depth at 8000 cycles is not statistically affected by changing asphalt content. This conclusion is based on differing the asphalt content by ±0.5 % from optimum asphalt content. On the other hand, it could be possible that the APA is sensitive to changes in asphalt content. In this case, the seven HMA mixtures did not demonstrate sensitivity to changes in asphalt content because they were in fact not sensitive to changes in asphalt content (i.e., they exhibit the same rut performance at all three of the asphalt contents tested).

Analysis of the Effect of Air Voids on APA Rut Depth at 8000 Cycles—The APA rut depth at 8000 cycles showed a significant sensitivity to changes in air void content (Table 10). According to the DMR groupings, only one of the projects exhibited no statistical changes in APA rut depth due to changes in air void content. The HMA mixture that showed no sensitivity to changes in air voids was a mixture that performed well for all but one asphalt content/air void combination (Monroe, US-24). The other nine projects that did demonstrate sensitivity to changes air voids showed the following:

- In three of the projects, the APA rut depths from specimens with 8 and 12 % air voids were statistically different than the 4 % specimens.
- In three of the projects, the APA rut depth from 12 % air void specimens were statistically different than specimens prepared to 4 and 8 % air voids.
- In three of the projects, the APA rut depth from specimens at all three air void levels was statistically different.

Research conducted by Linden and Van der Heide [27] stressed the importance of proper compaction and concluded that degree of compaction is one of the main quality parameters of placed mixtures. Proper compaction reduces the amount of rutting due to consolidation and also provides increased aggregate interlock. Normally, an HMA pavement is compacted to approximately 7–8 % air voids during construction. Table 10 illustrates that the 12 % air void mixtures performed statistically poorer than the 4 % and/or 8 % mixtures. This is in line with Linden and Van der Heide's findings.

Based on these findings it can be concluded that the APA rut depth is, in general, sensitive to air voids and, in particular, shows decreased performance with poorly compacted mixtures (air voids greater than 8 %). This lends credibility to the practice of taking field cores or beams from newly constructed pavements. If a pavement has been poorly compacted, the resulting decrease in pavement performance would be shown by decreased APA performance.

Statistical Analysis of the APA Cycles to Failure Results

Presently, most if not all state highway agencies that use the APA in HMA specifications use a pass/fail rut criterion to differentiate between rut resistant and rut prone HMA mixtures. The empirical model developed previously converts the amount of APA cycles needed to reach a failure APA rut depth to the ESALs needed to cause a pavement rutting failure. A 7 mm rut was shown to correlate with pavement failure, and thus the APA cycles needed to cause a 7 mm rut corresponds to ESALs to failure. Consequently, in order to validate the model, it is useful to know whether the amount of APA cycles needed to induce failure is sensitive to changes in air voids and asphalt content. It has been shown in the literature that high asphalt contents decrease HMA pavement stability, and high air voids increase consolidation rutting and decrease aggregate interlock. Both of these factors would decrease a pavement's life. Based on this it is thought that if a performance model is to be based upon APA data, the APA cycles to failure property should be sensitive to air voids and asphalt content.

The Effect that Changing Asphalt Content has on the Number of APA Cycles to Failure—The effect of changing asphalt content on the number of APA cycles to failure is summarized in Table 11. Only one HMA mixture out of ten is shown to be sensitive to a change in asphalt content. Consequently, it can be concluded based on this data that the amount of APA cycles to cause a 7 mm rut depth is insensitive to asphalt content. It is important to report that Hill's work [23] demonstrated that the APA results follow the correct trends, e.g., most of the results show decreasing APA cycles to failure with increasing asphalt content. This is what would be expected. The problem is the variability about the means. The standard deviations are consistently large throughout most of the APA results. Duncan's multiple range method of comparing means is sensitive to these large standard deviations, and thus it is difficult to statistically demonstrate that the means are different. One way to decrease the variability is to increase the sample size by creating and testing more APA specimens. However, this may not be economical since procuring and testing APA specimens is both timely and costly. It is thought that the sample size used in this study, three specimens, is a good sample size to use in APA testing. In conclusion, it appears that since statistical differences in the APA cycles to failure between mixture variations do not exist, the APA is unable to statistically discriminate changes in HMA pavement performance due to changes in asphalt content. Also, since there is a great amount of variability in the number of APA cycles to failure criterion, a PBS based upon APA data may be unrealistic.

TABLE 11—*Analysis of the effect of asphalt content on APA cycles until failure (α = 0.05).*

Superpave HMA Mixture Design Level	Project Location	Asphalt Content (% by Mass)	Tukey 95 % Grouping	Duncan 95 %Grouping
E1	Brimley, M-28	Low	A	A
		Optimum	A	A
		High	A	A
E3	Elk Rapids, US-31	Low	A	A
		Optimum	A	A
		High	A	A
	Monroe, US-24	Low	A	A
		Optimum	A	A
		High	A	A
	Brooklyn, M-50	Low	A	A
		Optimum	A	A
		High	A	A
E10	Lansing, M-43	Low	A	A
		Optimum	A	A
		High	A	A
	Indian River, I-75	Low	A	A
		Optimum	A	A
		High	B	B
	Grayling, US-27	Low	A	A
		Optimum	A	A
		High	A	A
E30	Auburn Hills, I-75	Low	A	A
		Optimum	A	A
		High	A	A
	Clarkston, I-75	Low	A	A
		Optimum	A	A
		High	A	A
	Saginaw, I-75	Low	A	A
		Optimum	A	A
		High	A	A

The Effect that Changing Air Voids has on the Number of APA Cycles to Failure—The sensitivity of the APA cycles to failure criterion to changes in air void content is summarized in Table 12. The statistical differences in the number of APA cycles to failure in Table 12 are similar to the differences in APA rut depth at 8000 cycles shown in Table 10. The statistical differences are summarized as follows:

- In five of the projects, the number of APA cycles to failure from 8 and 12 % specimens were statistically different then the 4 % specimens.
- In three of the projects, the APA cycles to failure for 12 % specimens were statistically different than specimens prepared to 4 and 8 % air voids.
- For one project, the APA cycles to failure for specimens prepared to all three air void levels were statistically different.

In most cases when an HMA mixture shows statistical differences in APA rut depths at 8000 cycles due to changes in air voids, it also shows the same or approximately the same statistical differences in the number of APA cycles to failure. This suggests a relationship between APA cycles to failure and the APA rut depth at 8000 cycles. This relationship is plotted in Fig. 7. It can be seen that the APA cycles to failure is related to APA rut depth at 8000 cycles. A decreased APA rut depth corresponds to increased APA cycles to failure.

TABLE 12—*Analysis of the effect of air void content on APA cycles until failure (α = 0.05).*

Superpave HMA Mixture Design Level	Project Location	Air Voids (percent)	Tukey 95 % Grouping	Duncan 95 % Grouping
E1	Brimley, M-28	4	A	A
		8	A B	A B
		12	B	B
E3	Elk Rapids, US-31	4	A	A
		8	A	A
		12	B	B
	Monroe, US-24	4	A	A
		8	A	A
		12	A	A
	Brooklyn, M-50	4	A	A
		8	B	B
		12	A B	B
E10	Lansing, M-43	4	A	A
		8	A	A
		12	B	B
	Indian River, I-75	4	A	A
		8	A	A B
		12	A	B
	Grayling, US-27	4	A	A
		8	A B	A B
		12	B	B
E30	Auburn Hills, I-75	4	A	A
		8	A	A
		12	A	A
	Clarkston, I-75	4	A	A
		8	A B	A B
		12	B	B
	Saginaw, I-75	4	A	A
		8	B	B
		12	B	C

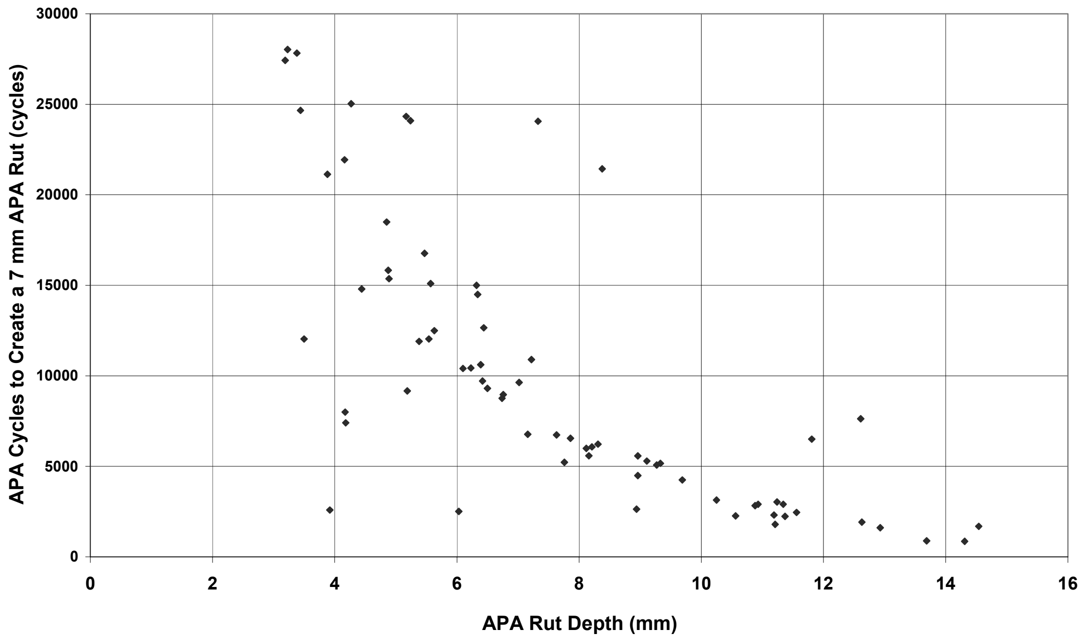

FIG. 7—*APA cycles to failure and APA rut depth at 8000 cycles.*

Conclusions

This paper presents the development of an empirical relationship between APA test results and field performance and the results of APA testing of ten different HMA mix designs. The following conclusions can be made:

- Neither the APA rut depth at 8000 cycles, the number of APA cycles to achieve a 7 mm rut depth, nor the APA cycles to failure are statistically affected by changes in asphalt content within ±0.5 % of the Superpave optimum design contents.
- The APA rut depth at 8000 cycles is sensitive to changes in air void content.
- The APA cycles needed to achieve a 7 mm rut (or APA cycles to failure) appear to be sensitive to changes in air void content. In eight of ten mix designs, the APA cycles to failure are statistically different at different levels of air voids.

Since the APA cycles to failure, and consequently the amount of ESALs to rutting failure predicted by the empirical rut prediction model, show a great deal of variability, it may not be feasible to base a rut prediction model based upon APA data. However, Fig. 7 lends credibility to the pass/fail criterion currently used by state highway agencies. In Fig. 7 it can be seen that low APA rut depths correspond to increased APA cycles to failure and increased pavement life.

References

[1] Witczak, M. W., Van Quintus, H. L., and Scwartz, C. W., "Superpave Support and Performance Models Management: Evaluation of the SHRP Performance Model Systems," *Eighth International Conference on Asphalt Pavements*, Vol. III, Seattle WA, 1997, pp. 175–195.

[2] Harvey, J. T. and Tsai, B., "Effects of Asphalt Content and Air Void Content on Mix

Fatigue and Stiffness," *Transportation Research Record 1543*, Transportation Research Board, National Research Council, 1997.

[3] Monismith, C. L., Epps, J. A., and Finn, F. N., "Improved Asphalt Mix Design," *Proceedings, The Association of Asphalt Paving Technologists*, Vol. 54, 1985, pp. 347–406.

[4] Eisenmann, J. and Hilmer, A., "Influence of Wheel Load and Inflation Pressure on the Rutting Effect at Asphalt Pavements – Experiments and Theoretical Investigations," *Proceedings, Sixth International Conference on the Structural Design of Asphalt Pavements*, Vol. 1, Ann Arbor, MI, 1987, pp. 392–403.

[5] Asphalt Institute, "Superpave Mix Design," Superpave Series No. 2, 1996.

[6] Mahboub, K. and Little, D. N., "Improved Asphalt Concrete Design Procedure," Research Report 474-1F, Texas Transportation Institute, 1988.

[7] Monismith, C. L., Epps, J. A., and Finn, F. N., "Improved Asphalt Mix Design," *Proceedings, The Association of Asphalt Paving Technologists*, Vol. 54, 1985, pp. 347–406.

[8] Haddock, J., Pan, C., Feng, A., Galal, K., and White, T. D., "Validation of SHRP Asphalt Mixture Specifications Using Accelerated Testing," Draft Interim Report, National Pooled Fund Study No. 176, December 1998.

[9] "Shell Pavement Design Manual – Asphalt Pavements and Overlays for Road Traffic," Shell International Petroleum Company Limited, London, 1978.

[10] Lai, J. S., "Development of a Laboratory Rutting Resistance Testing Method for Asphalt Mixes," Project No. 8717, Georgia Department of Transportation, August 1989.

[11] "Asphalt Pavement Analyzer User Manuel," Pavement Technology, Inc., Covington, GA, 2000.

[12] West, R. C., Page, G. C., and Murphy, K. H., "Evaluation of the Loaded Wheel Tester," Research Report FL/DOT/SMO/91-391, Florida Department of Transportation, December 1991.

[13] Williams, R. C. and Prowell, B. D., "Comparison of Laboratory Wheel-Tracking Test Results with WesTrack Performance," *Transportation Research Record 1681*, Transportation Research Board, National Research Council, November 1999, pp. 121–128.

[14] Lai, J. S., "Evaluation of Rutting Characteristics of Asphalt Mixes Using the Loaded Wheel Tester," Project No. 8609, Georgia Department of Transportation, December 1986.

[15] Choubane, B., Page, G. C., and Musselman, J. A., "Suitability of Asphalt Pavement Analyzer for Predicting Pavement Rutting," *Transportation Research Record 1723*, Transportation Research Board, National Research Council, 2000, pp. 107–115.

[16] Miller, T., Ksaibati, K., and Farrar, M., "Utilizing the Georgia Loaded Wheel Tester to Predict Rutting," Presented at the 74th Annual Meeting of the Transportation Research Board, Washington, D.C., January 22–28, 1995.

[17] Lai, J. S. and Lee, T., "Use of a Loaded-Wheel Testing Machine To Evaluate Rutting of Asphalt Mixes," *Transportation Research Record 1269*, Transportation Research Board, National Research Council, 1990, pp. 116–124.

[18] Kandhal, P. S. and Mallick, R. B., "Evaluation of the Asphalt Pavement Analyzer for HMA Mix Design," NCAT Report No. 99-4, National Center of Asphalt Technology, Auburn University, June 1999.

[19] Stuart, K. D., Izzo, R. P., and McRae, J. L., "Correlation of Superpave G*/sin □ with Rutting Susceptibility from Laboratory Mix Design Tests," *Transportation Research Record 1492*, Transportation Research Board, National Research Council, 1995.

[20] Barksdale, R. D., "Laboratory Evaluation of Rutting in Base Course Materials,"

Proceedings, Third International Conference on the Structural Design of Asphalt Pavements, Vol. 1, London, 1972, pp. 161–174.

[21] "Performance of Coarse-Graded Mixes at WesTrack-Premature Rutting," Federal Highway Administration, Report FHWA-RD-99-134, June 1998.

[22] Lee, C. E., Shankar, P. R., and Izadmehr, B., "Lateral Placements of Trucks in Highway Lanes," Report FHWA/TX-84/33+310-1F, Center for Transportation Research, The University of Texas at Austin, Austin, Texas, 1983.

[23] Hill, D. W., "The Development of an Empirical Rut Depth Prediction Model for HMA Pavements," Master of Science In Civil Engineering, Michigan Technological University, 2002.

[24] Mendenhall, W. and Sincich, T., "A Second Course in Business Statistics: Regression Analysis," Dellen Publishing Company, San Francisco, 1989.

[25] Carmer, S. G. and Swanson, M. R., "Evaluation of Ten Pairwise Multiple Comparison Procedures by Monte Carlo Methods," *Journal of the American Statistical Association*, Vol. 68, No. 314.

[26] Montgomery, D. C., "Design and Analysis of Experiments," John Wiley & Sons, New York, 2001.

[27] Linden, F. and Van der Heide, J. "Some Aspects of the Compaction of Asphalt Mixes and Its Influence on Mix Properties," *Proceedings, The Association of Asphalt Paving Technologies*, Vol. 56, pp. 408–426.

[28] "Standard Test Method for Determining Rutting Susceptibility Using the Asphalt Pavement Analyzer (ASTM Format)," Asphalt Pavement Analyzer User's Group Meeting Minutes, Jackson, MS, September 26–27, 2000.

Journal of ASTM International, Vol. 3, No. 5
Paper ID JAI12255
Available online at www.astm.org

Prithvi S. Kandhal[1] *and L. Allen Cooley, Jr.*[2]

Simulative Performance Test for Hot Mix Asphalt Using Asphalt Pavement Analyzer

ABSTRACT: Permanent deformation, or rutting, has been and continues to be a problem in the performance of hot mix asphalt (HMA) pavements. This paper presents a summary of work conducted under National Cooperative Highway Research Program (NCHRP) Project 9-17. This research project was undertaken to evaluate the Asphalt Pavement Analyzer (APA) to determine its suitability as a general method of predicting rut potential. There was a need to identify test conditions within the APA that produced results most related to field rutting performance. Ten HMA mixes of known field rutting performance were tested within a full factorial experiment designed to determine the combination of testing conditions for the APA that best predicts field rutting. The experimental plan consisted of different specimen types (beam and cylinder), air void contents in compacted test specimen (4 and 7 %), hose diameters (25 and 38 mm), and test temperatures (high temperature of standard PG grade based upon climate and 6°C higher temperature). Based upon the test results and analysis, a tentative standard method of test was developed and recommended. A standard practice for establishing maximum specified rut depth for APA by highway agencies has also been recommended.

KEYWORDS: Asphalt Pavement Analyzer (APA), loaded wheel tester, performance test, rutting, permanent deformation, hot mix asphalt, asphalt concrete, asphalt mixture, asphalt

Introduction

Permanent deformation, or rutting, has been and continues to be a problem in the performance of hot mix asphalt (HMA) pavements. Rutting is defined as the accumulation of small amounts of unrecoverable strain resulting from applied loads to the pavement. This deformation is caused by the consolidation and/or lateral movement of the HMA under traffic.

Some highway agencies have had success in identifying rut-prone mixes using the Asphalt Pavement Analyzer (APA), which is a simulative loaded wheel tester. The APA loosely simulates the effect of traffic on a pavement sample by tracking a wheel load onto a pressurized linear hose. This research project was undertaken to evaluate the APA to determine its suitability as a general method of predicting rut potential of HMA mixtures. Highway agencies use different test conditions for conducting the APA test. There was a need to identify a combination of test conditions within the APA that produced results most related to field rutting performance.

A standard practice for establishing maximum specified rut depth for APA by highway agencies has also been developed.

Development of Asphalt Pavement Analyzer

The Georgia loaded wheel tester (GLWT) was developed during the mid-1980s through a cooperative research study between the Georgia Department of Transportation and the Georgia Institute of Technology [1]. Development of the GLWT consisted of modifying a wheel tracking device originally designed by C. R. Benedict of Benedict Slurry Seals, Inc., to test slurry seals [2]. The primary purpose for developing the GLWT was to perform efficient, effective, and routine laboratory rut proof testing and field production quality control of asphalt mixtures [3].

Manuscript received December 1, 2003; accepted for publication December 1, 2005; published online February 2006. Presented at ASTM Symposium on Performance of Hot Mix Asphalt (HMA) including Fundamental and Empirical Procedures on 9 December 2003 in Tampa, FL; L. Mohammad, Guest Editor.
[1] Associate Director Emeritus, National Center for Asphalt Technology, 277 Technology Parkway, Auburn, AL 36830.
[2] Senior Pavements/Materials Engineer, Burns, Cooley, Dennis, Inc., 278 Commerce Dr., Ridgeland, MS 39157.

FIG. 1—*Asphalt Pavement Analyzer (APA).*

The GLWT is capable of testing asphalt beam or cylindrical specimens. Beam dimensions are generally 125-mm wide, 300-mm long, and 75-mm high (5 in. × 12 in. × 3 in.). Laboratory prepared cylindrical specimens are generally 150 mm in diameter and 75-mm high. Compaction methods for cylindrical specimens tested in the GLWT have included the "loaded foot" kneading compactor [1] and a Superpave gyratory compactor [4]. Both specimen types are most commonly compacted to either 4 or 7 % air void content.

Testing of samples within the GLWT has generally consisted of applying a 445 N (100 lb) load onto a pneumatic linear hose pressurized to 690 kPa (100 psi). The load is applied through an aluminum wheel onto the linear hose, which resides on the sample. Test specimens are tracked back and forth under the applied stationary loading. Testing is typically accomplished for a total of 8000 loading cycles (one cycle is defined as the backward and forward movement over samples by the wheel).

Test temperatures for the GLWT have ranged from 35 to 60°C (95 to 140°F). Initial work by Lai [1] was conducted at 35°C (95°F). This temperature was selected because it was representative of Georgia's mean summer air temperature [2]. Test temperatures within the literature subsequently tended to increase to 40.6°C (105°F) [2,5–7], 46.1°C (115°F) [7], 50°C (122°F) [2,8], and 60°C (140°F) [8].

At the conclusion of the 8000 cycle loadings, permanent deformation (rutting) is measured. Rut depths are obtained by determining the average difference in specimen surface profile before and after testing.

The Asphalt Pavement Analyzer (APA), shown in Fig. 1, is a commercial version of a modified version of the GLWT and was first manufactured in 1996 by Pavement Technology, Inc. Since the APA is the second generation of the GLWT, it follows the same general rut testing procedure. A wheel is loaded onto a pressurized linear hose and tracked back and forth over a testing sample to induce rutting. Similar to the GLWT, most testing is carried out to 8000 cycles. Unlike the GLWT, samples can also be tested while submerged in water.

Testing specimens for the APA can be either beam or cylindrical (Fig. 2). Currently, the most common method of compacting beam specimens is by the Asphalt Vibratory Compactor [9]. However, some have used a linear kneading compactor for beams [10]. The most common compactor for cylindrical specimens is the Superpave gyratory compactor [11]. Both specimen types are most commonly compacted to 4 or 7 % air voids [10]. Tests can also be performed on cores or slabs taken from an actual pavement.

Test temperatures for the APA have ranged from 40.6 to 64°C (105 to147°F). The most recent work with the APA has been conducted at or slightly above expected high pavement temperatures [11,12].

Wheel load and hose pressure have basically stayed the same as for the GLWT, 445 N and 690 kPa (100 lb and 100 psi), respectively. However, two recent research studies [12,13] did use a wheel load of 533 N (120 lb) and hose pressure of 830 kPa (120 psi) with good success.

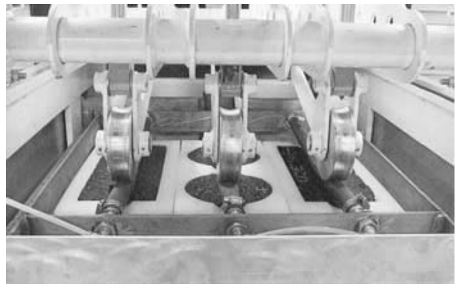

FIG. 2—*Close-up of beam and cylindrical specimens being tested in APA.*

Several states, including Georgia, Florida, and Virginia, have used the APA successfully in ranking a limited number of different asphalt mixtures for their potential for rutting. However, the correlation between APA rut depths and field rut depths of ten WesTrack test pavements subjected to the same traffic was attempted for the first time by Williams and Prowell [12]. The coefficient of determination (R^2) value of 82.3 % obtained in this correlation was encouraging (Fig. 3).

As mentioned earlier, researchers have used different test protocols in the past for the GLWT and APA in terms of specimen type (beam or cylinder), specimen dimensions, compaction method, air voids content in specimens, test temperature, hose pressure, and load. There was a need to optimize the test protocol for the APA which led to the undertaking of this project, NCHRP 9-17, "Accelerated Laboratory Rutting Tests: Asphalt Pavement Analyzer."

Refinement of Asphalt Pavement Analyzer

The primary objective of NCHRP Project 9-17 was to fine tune the APA by attempting different testing variables and correlating the laboratory APA rut depth data to actual field rut depth data obtained from controlled test sections in the field.

Based upon the review of literature, a controlled laboratory experimental plan was developed. The experimental plan was formulated with the primary objective of evaluating variables that could potentially influence the ability of the APA to predict the rutting potential of asphalt mixtures in the field and to select the combination of variables that best predict the rutting potential.

The overall research approach is shown in Fig. 4. After completion of the main experiment, the data were analyzed and conclusions drawn about the ability of the APA to predict rut depths.

Four factors (test variables) were included within the experimental plan. These factors along with their levels are as follows:

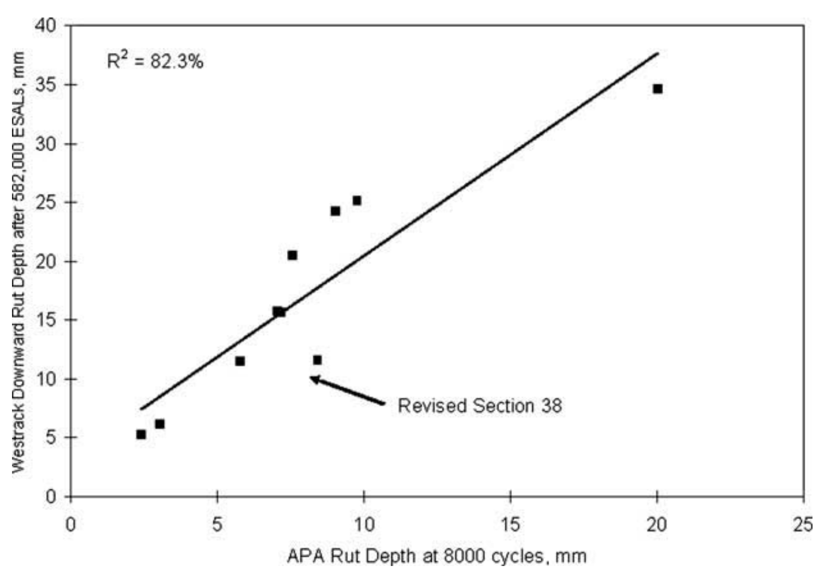

FIG. 3—*Evaluation of WesTrack pavement samples by Williams and Prowell [12].*

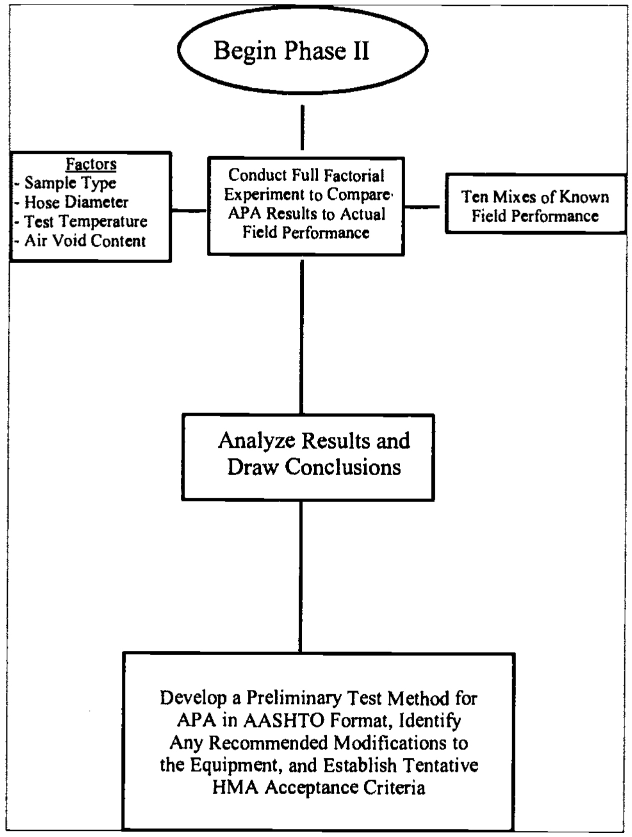

FIG. 4—*Overall research approach.*

- Specimen Type: (1) Beams compacted with an Asphalt Vibratory Compactor.
  (2) Cylinders compacted with a Superpave Gyratory Compactor.
- Hose Diameter: (1) The standard hose diameter of 25 mm (outside diameter).
  (2) Hose with a diameter of 38 mm (outside diameter).
- Test Temperature: (1) High temperature of standard PG grade based upon climate.
  (2) 6°C higher than high temperature of standard PG grade.
- Air Void Content: (1) 4.0±0.5 % (5.0±0.5 % for beams)
  (2) 7.0±0.5 %

A wheel load and hose pressure of 534 N (120 lb) and 827 kPa (120 psi), respectively, was used during the entire study because these values had been used successfully by Williams and Prowell [12] in evaluating WesTrack test pavements, as mentioned earlier.

Ten asphalt mixtures of known rutting performance in the field were included within a full factorial experiment designed to determine the combination of the aforementioned testing conditions for the APA that best predicts field rutting. These ten mixtures were selected from three full-scale pavement research projects and encompass climatic regions, project characteristics, and materials from throughout the United States. The three full-scale research projects include WesTrack (Nevada), MnRoad (Minnesota), and the FHWA Accelerated Loading Facility (ALF) at Turner-Fairbank Highway Research Center (Virginia).

Three test sections (15, 19, and 24) selected from WesTrack represent different gradations. Three test sections (cells 16, 20, and 21) selected from MnRoad represent different asphalt binders and optimum asphalt contents. Four test sections (Lane 5, 7, 10, and 12) from the FHWA ALF represent different asphalt binders and nominal maximum aggregate sizes.

Therefore, this experiment involved 160 factor-level combinations (2 sample types * 2 hose diameters * 2 test temperatures * 2 air void contents * 10 mixes). Three replicates of each factor-level combination were tested. Testing was conducted on mixes fabricated from original materials and subjected to short-term aging per AASHTO TP 2-96.

The detailed discussion of the experimental plan is given elsewhere [14].

The primary analysis tool selected for comparing laboratory and field rut depths was a simple

TABLE 1—*Six highest R^2 values for WesTrack.*

Air Voids	Test Temp	Hose Diameter	Specimen Type	R^2
5 %	PG	Large	Beam	1.000[a]
5 %	PG+6	Standard	Beam	0.982[a]
4 %	PG	Standard	Cylinder	0.856[a]
4 %	PG+6	Standard	Cylinder	0.855
5 %	PG	Standard	Beam	0.835[b]
4 %	PG	Large	Cylinder	0.386

[a]Laboratory results show the same trend as field rutting.
[b]Laboratory results ranked statistically similar to field rutting.

correlation/regression analysis. For each factor-level combination investigated in the APA, a scatter plot was developed that has the results of laboratory and field rut depths. Each plot reflected actual field rutting versus laboratory rut depth for a given factor-level combination, for a given full-scale research project. A correlation/regression analysis was then conducted on the data in order to determine the best fit line and the coefficient of determination (R^2).

Selection of the optimum factor-level combination for testing conditions in the APA was based upon the highest R^2 value obtained from the regression analyses. If one combination showed a significantly higher R^2 value than all other combinations, it would be selected and included in the tentative standard procedure.

Tables 1–3 show the six highest R^2 values, which were obtained with combinations of testing conditions for WesTrack, MnRoad, and ALF test sections.

Two typical plots with the four highest R^2 values for ALF and MnRoad mixtures are shown in Figs. 5 and 6, respectively. The legends for the combination of test variables in the figures has the following order. First, the air void content (4, 5, or 7 %); second, test temperature (PG or PG+6 C); third, large (L) or small (S) hose; and fourth, specimen type: cylinder (C) and beam (B).

Based on the detailed statistical analyses [14] of the field and APA rut depth data obtained from the three field projects, the following APA testing protocol was recommended:

- Both gyratory (cylinder) and beam specimens are acceptable.
- Four percent air voids in cylinders and 5 % in beams gave better results, compared to 7 % in both.
- 25 mm standard, small hose provided more repeatable results.
- PG high temperature gave better results compared to PG+6 C.

TABLE 2—*Six highest R^2 values for MnRoad.*

Air Voids	Test Temp	Hose Diameter	Specimen Type	R^2
5 %	PG	Large	Beam	0.997[b]
4 %	PG	Large	Cylinder	0.992[a]
7 %	PG	Large	Cylinder	0.876[a]
7 %	PG	Large	Beam	0.863[a]
4 %	PG	Standard	Cylinder	0.852[a]
5 %	PG+6	Large	Beam	0.848[a]

[a]Laboratory results show similar trend as field rutting.
[b]Laboratory rankings similar to field rankings.

TABLE 3—*Six highest R^2 values for ALF*

Air Voids	Test Temp	Hose Diameter	Specimen Type	R^2
7 %	PG	Large	Cylinder	0.999[a]
5 %	PG	Large	Beam	0.917[a]
4 %	PG	Large	Cylinder	0.910[a]
7 %	PG+6	Standard	Beam	0.889[a]
7 %	PG	Large	Beam	0.831
7 %	PG	Large	Cylinder	0.830

[a]Laboratory results show similar trend as field rutting.

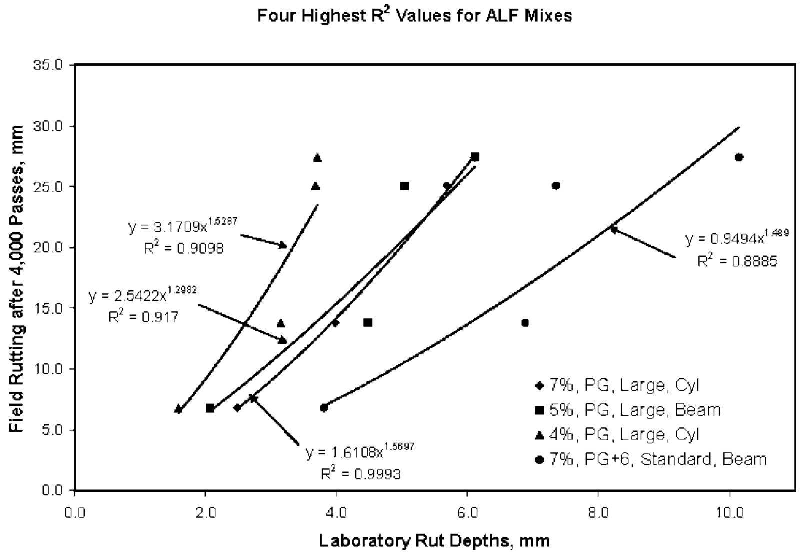

FIG. 5—*Typical plots for laboratory rut depth versus field rut depth (ALF mixes).*

Recommended Practice for Establishing Maximum Specified Rut Depth for Asphalt Pavement Analyzer

The objective of this recommended practice is to give highway agencies a method of calibrating APA rut depth criteria for local climate, traffic levels, and materials. There are two prevailing methods of calibrating laboratory permanent deformation tests to field rutting. The first entails testing mixes during production and then following the performance of these mixes over time. This method is the more time consuming, but provides a more accurate field calibration. The second method entails identifying existing pavements with a wide range of rutting performance. Samples of the pavement are cut from the roadway and the aggregates extracted. An asphalt binder similar to the original binder is then combined with the extracted aggregate and performance testing conducted. Results of the testing are then compared to performance in the field. The following sections describe these two calibration procedures.

Testing of Plant-Produced Mix

Identify HMA projects to be constructed that fall within the four primary traffic categories shown in Table 4. At each of the projects, compact samples of plant-produced mix were used to meet the sample requirements of the APA draft standard procedure. Depending upon the agency, cylinders, beams, or both can be

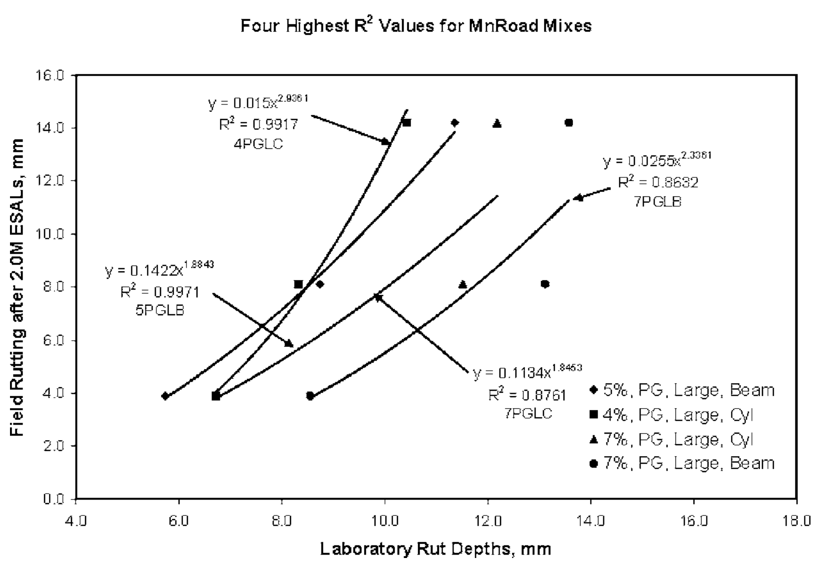

FIG. 6—*Typical plots for laboratory rut depth versus field rut depth (MnRoad mixes).*

TABLE 4—*Traffic categories to be evaluated.*

Traffic Category	20-year Design ESALs	N_{design} Gyrations
Very high	>30 million	125
High	3–30 million	100
Medium	0.3–3 million	75
Low	<0.3 million	50

investigated. At least four pavements should be tested for each traffic category, but preferably more. In order to evaluate repeatability, enough samples of the same mix should be compacted to conduct replicate tests (one replicate equals six cylindrical samples or three beams).

Evaluation of Test Data and Development of Critical Rut Depths—For all traffic categories of asphalt pavements sampled, prepare a table of data similar to the form shown in Table 5. Use engineering judgment in reviewing all the data in the table and establish a minimum APA rut depth specification requirement for each traffic category to ensure good rutting performance. The specification must take into account the repeatability and reproducibility of the APA test, if available.

Testing of Existing Asphalt Pavements

Identify at least three asphalt pavements (or overlays), which have been in service from three to five years, in the four 20-years design traffic categories given in Table 4.

The pavements in each traffic category should be selected to provide the following rutting performance in the field after three to five years in service: good (less than 5 mm rut depth), fair (5–10 mm rut depth), and poor (over 10 mm rut depth). Therefore, a minimum of 12 asphalt pavements should be sampled. The number in some or all traffic categories can be increased to improve confidence in specified acceptable rut depth criteria for APA.

Obtain hot mix asphalt (HMA) mix from each pavement by coring or sawing, which should be done within 600 mm (2 ft) of the pavement edge (outside wheel path) to represent as-placed HMA as much as possible. Sampling from wheel tracks is not desirable because of potential degradation of the HMA under traffic. If cores are obtained, the cores should be at least 150 mm in diameter to minimize inclusion of aggregate particles cut by the coring operation. Sampling should be done on a level stretch of the highway and within the region where the field rut depth was recorded. Enough cores or sawed samples should be obtained to make the following specimens or test samples:

- Six SGC specimens 150-mm diameter × 75-mm height *or*
- Three beam specimens 300 mm × 125 mm × 75 mm
- Three loose mixture samples (1500 g each) to determine the theoretical maximum density (TMD)
- Three loose mixture samples (2500 g each) for asphalt content

Obtain 40 % more material than needed above to account for wastage and/or retests.

TABLE 5—*Example table for field and APA rut depth data.*

Traffic Category[a]	Rutting Performance	Average Field Rut Depth (mm)	Average APA Rut Depth (mm)
Very high	good		
	fair		
	poor		
High	good		
	fair		
	poor		
Medium	good		
	fair		
	poor		
Low	good		
	fair		
	poor		

[a]Categories should recognize traffic speed, climatic conditions, and structural influences.

Analysis of In-Place Mix—Conduct three ignition or extraction tests on the HMA sample obtained from each asphalt pavement to obtain the average asphalt content and average gradation of the in-place mix.

If desired (optional), bulk specific gravity of the core or sawed samples and TMD of the in-place mix can be measured to determine the in-place air voids for information only.

Preparation of Test Samples—Conduct solvent extraction on the sampled, in-place mixture to extract aggregate for preparing fresh mixture using virgin asphalt binder. Obtain a virgin asphalt binder with the same PG grade as used on the project sampled. If a modified binder was used on the project, obtain a similarly modified binder of the same PG grade.

Mix the extracted aggregate and the virgin PG binder to obtain the average in-place asphalt content in the mix. Subject the prepared mix to short-term aging at the desired compaction temperature suited for the PG grade being used. Conduct three replicate tests to determine the average TMD of the aged mix, which will be used to control the air void content in the compacted specimens.

Compact six SGC samples to obtain 4 ± 0.5 % air void content in the samples. (Agencies that prefer beams should compact three beams at 5 ± 0.5 % air void content.) Where possible, replicate tests should be conducted.

Testing by APA—The six SGC specimens or three beam specimens should be tested to determine the average rut depth after 8000 loading cycles. Testing should be done at the high temperature of the PG grade recommended for the project location regardless of bumping. For example, a polymer modified PG 76-22 or PG 70-22 may have been used on a project which required a PG 64-22 corresponding to local climatic conditions. In that case, APA testing should still be conducted at 64?C.

Evaluation of Test Data and Development of Specifications—For all traffic categories of asphalt pavements sampled, tabulate the data as shown in Table 5. Use engineering judgment in reviewing all the data in the table and establish a minimum APA rut depth specification requirement for each traffic category to ensure good rutting performance. The specification must take into account the repeatability and reproducibility of the APA test, if available.

Conclusions

Based on the work on NCHRP Project 9-17, the following conclusions were obtained from this project. Not all data supporting these conclusions are included in this paper due to lack of space. The detailed supporting data are available in Ref. [14].

- Cylindrical samples compacted to 4 % air voids and beam samples compacted to 5 % air voids resulted in APA laboratory test results that were more closely related to field rutting performance than cylindrical and beam samples compacted to 7 % air voids.
- Samples tested in the APA at a test temperature corresponding to the high temperature of the standard PG grade for a project location better predicted field rutting performance than samples tested at 6EC higher than the high temperature of the standard PG grade.
- Samples tested with both the standard and large diameter hoses predicted field rutting performance about equally. However, samples tested with the standard hose produced less variability.
- Beam and cylindrical samples predicted field rutting performance about equally.
- Test temperature significantly affects measured rut depths in the APA. As test temperature increases, APA rut depths increase.
- APA-measured rut depths were collectively higher with the standard diameter hose than with the larger diameter hose.
- APA-measured rut depths were collectively higher with beam samples than with cylindrical samples.
- Based on the preceding conclusions, an improved test protocol was developed for the APA in this study in order to better identify rut prone HMA mixtures (included in Ref. [14]).
- Laboratory rut depths measured by the APA had good correlations on each individual project basis with the field rut depths in case of FHWA, ALF, WesTrack, and MnRoad.
- It is generally not possible to predict field rut depths from APA rut depths on a specific project using

relationships developed on other projects with different geographical locations and traffic.

A recommended standard practice for establishing maximum specified rut depth for APA by highway agencies has been presented.

References

[1] Lai, J. S., "Evaluation of Rutting Characteristics of Asphalt Mixes Using Loaded Wheel Tester," Georgia Department of Transportation Project No. 8609, December 1986.

[2] Collins, R., Watson, D., and Campbell, B., "Development of the Georgia Loaded Wheel Tester," *Transportation Research Record No. 1492*, Transportation Research Board, National Research Council, 1995.

[3] Lai, J. S., "Development of a Laboratory Rutting Resistance Testing Method for Asphalt Mixes," Georgia Department of Transportation Project No. 8717, August 1989.

[4] Hanson, D. I. and Cooley, L. A., Jr., "Study to Improve Asphalt Mixes in South Carolina, Volume III—Modified Mixes," Report No. FHWA-SC-98–02, January 1999.

[5] Lai, J. S., "Evaluation of the Effect of Gradation of Aggregate on Rutting Characteristics of Asphalt Mixes," Georgia Department of Transportation Project No. 8706, August 1988.

[6] Lai, J. S., "Results of Round-Robin Test Program to Evaluate Rutting of Asphalt Mixes Using Loaded Wheel Tester," *Transportation Research Record No. 1417*, Transportation Research Board, National Research Council, 1993.

[7] Miller, T., Ksaibati, K., and Farrar, M., "Utilizing the Georgia Loaded-Wheel Tester to Predict Rutting," *Presented at the 74th Annual Meeting of the Transportation Research Board*, Washington, DC, January 22–28, 1995.

[8] Collins, R., Shami, H., and Lai, J. S., "Use of Georgia Loaded Wheel Tester to Evaluate Rutting of Asphalt Samples Prepared By Superpave Gyratory Compactor," *Transportation Research Record No. 1545*, Transportation Research Board, National Research Council, 1996.

[9] Kandhal, P. S. and Cooley, L. A., Jr., "Accelerated Laboratory Rutting: Asphalt Pavement Analyzer," Phase 1—Interim Report, National Cooperative Highway Research Program Project 9–17, Transportation Research Board, August 1999.

[10] Neiderhauser, S., *Presentation at the Asphalt Pavement Analyzer User Group Meeting*, Auburn, AL, September 28–29, 1999.

[11] Kandhal, P. S. and Mallick, R. B., "Evaluation of Asphalt Pavement Analyzer for HMA Mix Design," NCAT Report No. 99–4, National Center for Asphalt Technology, June 1999.

[12] Williams, C. R. and Prowell, B. D., "Comparison of Laboratory Wheel-Tracking Test Results to WesTrack Performance," *Transportation Research Record No. 1681*, Transportation Research Board, National Research Council, 1999.

[13] Kandhal, P. S. and Cooley, L. A., Jr., "Accelerated Laboratory Tests: Asphalt Pavement Analyzer," Phase II—Interim Report, National Cooperative Highway Research Program Project 9–17, Transportation Research Board, December 2002.

[14] Kandhal, P. S. and Cooley, L. A., Jr., "Accelerated Laboratory Rutting Tests: Evaluation of the Asphalt Pavement Analyzer," National Cooperative Highway Research Program Report 508, Transportation Research Board, 2003.

Journal of ASTM International, November/December 2005, Vol. 2, No. 10
Paper ID JAI12259
Available online at www.astm.org

Gerald Reinke,[1] *Stacy Glidden,*[2] *Doug Herlitzka,*[3] *and John Jorgenson*[4]

Laboratory Investigation of HMA Performance Using Hamburg Wheel Tracking and DSR Torsional Creep Tests

ABSTRACT: Lack of existing fundamental mechanistic tests to evaluate performance potential of HMA mixtures has given rise to a number of empirical and mechanical-empirical test procedures. In an effort to understand how one of these tests, the Hamburg rutting test, was impacted by differences in HMA mixture variables, the following experimental work was conducted. Three aggregate types consisting of a crushed granite, a crushed siliceous gravel, and a crushed limestone were evaluated at four design ESAL levels. These four ESAL levels were 300 000, 1 million, 3 million, and 10 million. For each of these aggregate types and ESAL levels, 5 PG graded binders were investigated. The binders were PG 58-28, PG 64-28C (chemically modified), PG 64-28P, PG 64-34, and PG 70-28; the latter 3 binders were polymer modified. For all mixtures, Hamburg Wheel Tracking tests were performed under water at 50°C. In addition, a DSR Creep Test developed at MTE was performed on each mixture at 58°C and 34 kPa stress to determine the dry strength characteristics. The Hamburg test showed consistently better results as the ESAL level of the mix increased and as the high temperature PG grade of the binder increased for a given base asphalt. In the Hamburg test, mixes produced with PG 64-34 did not perform as well as PG 70-28 or PG 64-28P, while in the DSR Creep Test, mixes produced with PG 64-34 performed significantly better than PG 64-28P. This leads to speculation that the modulus of the base asphalt plays a more significant role in stress applied moisture resistance tests and that dry high temperature permanent deformation tests are influenced by the modified binder properties.

KEYWORDS: Hamburg Rut Tester, DSR Creep Test, ESAL, Polymer Modified Binders, VMA, VFA, ANOVA, p-value, multiple linear regression, cumulative strain test, zero shear viscosity

Introduction

The work presented in this paper is a laboratory investigation into the impact of aggregate types, binder grades, and mix design levels on the moisture sensitivity of mixtures and their resistance to high temperature deformation. Mixture moisture sensitivity was determined using the Hamburg Wheel Tracking (HWT) tester, and resistance to high temperature deformation was determined using the DSR Creep Test.

The Hamburg Wheel Tracking test (HWT) was originally developed in the 1970s by Esso in Germany and used by the city of Hamburg to develop specifications for their pavements. Several summaries and comparisons of various wheel tracking testers, including the HWT, have been published [1–3], and several papers have been published which show the development and utilization by agencies of the HWT in the US [4–6]. Interested readers are urged to examine these resources.

The DSR (dynamic shear rheometer) Creep Test was developed by MTE (Mathy Technology

---

Manuscript received 3 December 2003; accepted for publication 22 April 2005; published November 2005.
Presented at ASTM Symposium on Performance of Hot Mix Asphalt (HMA), including Fundamental and Empirical Procedures on 9 December 2003 in Tampa, FL.
[1] President, MTE Services, Inc, 915 Commercial Ct., Onalaska, WI 54650.
[2] Research Chemist, MTE Services, Inc., 915 Commercial Ct., Onalaska, WI 54650.
[3] Senior Asphalt Technician, MTE Services, Inc., 915 Commercial Ct., Onalaska, WI 54650.
[4] Senior HMA Mix Design Manger, Mathy Construction Co., 915 Commercial Ct., Onalaska, WI 54650.

and Engineering) in 2000. Description of the test procedure and results have been published elsewhere [7]. The test procedure detailing correlation to accelerated load testing results was presented at a session on Simple Performance Tests at TRB (Transportation Research Board) in 2002 [8].

Design of the Experiment

The goal of this investigation was to look at different types of aggregate, mix performance levels, and PG binders in an effort to understand how these factors combined to affect mixture performance as measured in the laboratory utilizing the Hamburg Wheel Tracker and the DSR Creep Test.

Materials Used

Three different aggregate types were employed: crushed granite, limestone, and siliceous gravel. Four different mix design levels that are utilized in Wisconsin were investigated. These are designated as E-0.3 (300 000 design ESALs), E-1 (1 million design ESALs), E-3 (3 million design ESALs) and E-10 (10 million design ESALs). The aggregate gradations, binder content, and other characteristics of each mix are summarized in Table 1. Five different binders were employed in the study: PG 58-28 (unmodified), PG 64-28C (acid modified), as well as PG 64-28P, PG 64-34, and PG 70-28, all three of which were polymer modified. All of the polymer-modified binders used DuPont Elvaloy®[5] as the modifier. With the exception of the PG 64-34, which utilized a PG 52-34 base, all of the modified binders used the PG 58-28 as the base asphalt. No anti-stripping additives were employed in any of the mixes. The high temperature DSR properties of the binders used in this study are summarized in Table 2.

Low shear rate viscosity as an approximation to zero shear viscosity (η_0) was determined at 0.01 radians per second, and a cumulative strain test was also performed on the RTFO residues of the binders using a procedure developed by Bahia at the University of Wisconsin [9]. Based on the cumulative strain test, a percent strain was obtained for each binder after 100 cycles at a stress level of 300 Pascals (Pa) at 50°C and at 58°C. Work published by Bahia et al. [9] and results presented by Reinke et al. [8] indicate that the cumulative percent strain of a binder is correlated to deformation resistance of mixes produced from those binders. Work published by Phillips and Robertus [14] and Sybiliski [15] suggest that zero shear viscosity is related to mixture deformation resistance.

An experimental design program, ECHIP®[6], was used to create the design and to analyze the results of the study. Since all variables were categorical, 60 trials were required to evaluate all possible interactions of terms. Although it seemed unlikely that three-way interactions between aggregate type, mix level, and binder type would exist, the necessary combinations were chosen to make that determination. In addition to the 60 trials, the ECHIP® program added replicate trials, which it used to determine how well the model being evaluated fit the data. In total, 74 trials were performed.

---

[5] E.I. DuPont de Neumors and Company, Wilmington, DE.
[6] ECHIP Inc, 724 Yorklyn Rd, Hockessin, DE.

TABLE 1—*Gradation and mixture data.*

	GRANITE AGGREGATE				GRAVEL AGGREGATE				LIMESTONE AGGREGATE			
% PASSING	E-0.3	E-1	E-3	E-10	E-0.3	E-1	E-3	E-10	E-0.3	E-1	E-3	E-10
25 mm	100	100	100	100	100	100	100	100	100	100	100	100
19 mm	100	100	100	100	100	100	100	100	100	100	100	100
12.5 mm	94.3	94.3	93.1	93.2	94.6	94.6	97	97.5	91.6	91.6	92.7	94.8
9.5 mm	84.2	84.2	80.7	80.8	86.5	86.5	87.4	89.6	82.9	82.9	85.1	89.4
4.75 mm	71.1	71.1	66.5	68.9	66.2	66.2	65.6	71.7	60.4	60.4	64.5	69
2.36 mm	53.1	53.1	46.3	47.4	51.1	51.1	46.8	51.7	46.2	46.2	47.3	46.3
1.18 mm	42	42	33.2	32.6	36.8	36.8	31.1	33.3	39.2	39.2	40.5	38.9
0.6 mm	31.3	31.3	24	22.9	24.4	24.4	20.6	22.1	26.8	26.8	27.7	29.5
0.3 mm	12.8	12.8	12.9	12.9	13.1	13.1	12.3	13.1	12.9	12.9	14.1	17.6
0.15 mm	6.1	6.1	7.4	7.2	5.3	5.3	7.6	7.5	6.8	6.8	7.1	8.8
0.075 mm	4.3	4.3	5.2	5.1	4	4	4.5	4.2	4.2	4.2	4.2	4.9
N design	40	60	75	100	40	60	75	100	40	60	75	100
N max	60	75	115	160	60	75	115	160	60	75	115	160
Optimum AC content, %	6.1	6.0	5.9	6.1	6.0	5.9	5.5	5.5	6.0	5.9	5.8	5.8
Effective AC content,%	5.67	5.57	5.52	5.52	5.52	5.42	5.03	5.26	5.14	5.04	4.80	4.62
VFA, %	76.3	76.0	75.9	75.9	76.0	75.8	74.7	75.3	74.7	74.4	73.7	73.2
VMA, %	16.90	16.7	16.6	16.6	16.7	16.5	15.8	16.2	15.8	15.6	15.2	14.9
Crush count 2 face, %	95.1	95.1	98.2	98.5	83.6	83.6	83	84.4	98.6	98.6	98.7	99.4
Flat & Elongated, %	1.9	1.9	1.9	1.8	1.6	1.6	1	1	0.4	0.4	0.4	0.4
FAA	42.6	42.6	45.3	45.1	45.1	45.1	45.1	45.1	40.4	40.4	45.7	45.7

TABLE 2—*High temperature DSR, cumulative strain, and zero shear viscosity results.*

BINDER, UNAGED	G*/SIN(δ) @ 58°C, kPa	PHASE ANGLE @ 58°C	G*/SIN(δ) @ Grade Temp, kPa	PHASE ANGLE @ Grade Temp
PG 58-28	1.265	87.09	1.265	87.09
PG 64-28P	3.090	68.90	1.731	70.44
PG 64-28C	2.544	80.75	1.259	82.47
PG 64-34	2.380	59.60	1.503	60.40
PG 70-28	4.186	60.10	1.526	63.00
BINDER, RTFO RESIDUE	Average % strain @ 50° C	Average η_0, Pa.sec, @ 50° C	Average % Strain @ 58° C	Average η_0, Pa.sec, @ 58° C
PG 58-28	1 886	1 606	9 140	356
PG 64-28P	279	5 640	969	1 821
PG 64-28C	609	3 751	2 026	1 811
PG 64-34	115	4 948	305	3 413
PG 70-28	82	7 272	262	4 067

Description of Specimen Preparation

Agencies that use the Hamburg Wheel Tracking Test typically require air voids of 7 % ± 1 % for specimens. The greater the air void range, the more variability we have observed in test results for a given mixture. Therefore, for each trial, four gyratory specimens 61 mm in height and 150 mm in diameter were compacted to a target void level of 6.5–7 %, and these were used to perform the Hamburg Wheel Tracking test. In addition, for each trial, a single specimen 95 mm in height and 150 mm in diameter was compacted to a target void level of 6.5–7 %. Test specimens were cut from the 95 mm high gyratory specimens to be used in the DSR Creep Test. All mixes were short-term oven aged (STOA) in the loose condition for 2 h prior to compaction. Statistics for the air voids of the 296 Hamburg Wheel Tracking specimens (Table 3) show that a range of 6.5–7.1 % voids was achieved with nearly equal numbers of specimens falling outside that range. Although we did not hit our target air voids range for all specimens, 86 % of all specimens were compacted to an air void range of 0.6 %. The air void range for all of our specimens was 1.4 % compared to a typically accepted value of 2 %.

TABLE 3—*Summary statistics of air voids data for Hamburg Wheel Tracking test specimens.*

Arithmetic Mean air voids	6.79
Maximum air voids	7.6
Minimum air voids	6.2
Median air voids	6.8
Range of air voids	1.4
Coefficient of Variation, %	3.52 %
Standard Deviation	0.239
Number of specimens < 6.5 % air voids	20 (6.5 % of total)
Number of specimens > 7.0 % air voids	39 (12.7 % of total)
Number of specimens > 7.1 % air voids	23 (7.1 % of total)

Hamburg Wheel Tracking Test

The Hamburg Wheel Tracking test was developed and is often performed using rectangular slabs of mix in the test machine. Testing utilized a machine manufactured by Precision Machine and Welding[7] to apply the requisite test load of 702 N (158 lb) at 52 wheel passes per minute [4] in water at 50°C. The advent of gyratory compaction and the ready availability of 150 mm diameter specimens resulted in development of specimen holders that would allow direct testing of gyratory specimens. To accomplish this, a slice was cut from the specimen producing a flat face (Fig. 1) approximately 90 mm wide.

The trimmed specimen was then placed in a polyethylene holder, and two such specimens were butted against each other to create a single specimen for wheel tracking. For this study, four gyratory specimens arranged into two-wheel tracking specimens were tested (Fig. 2). This yielded two test results for each trial that could be averaged. Because of the ability to average the results of two specimens per wheel and then further average the results from both pairs of specimens into a single data point for each trial, the range of average air voids for the trials conducted was 6.4–7.1 %.

FIG. 1—*One specimen cut for HWT testing.*

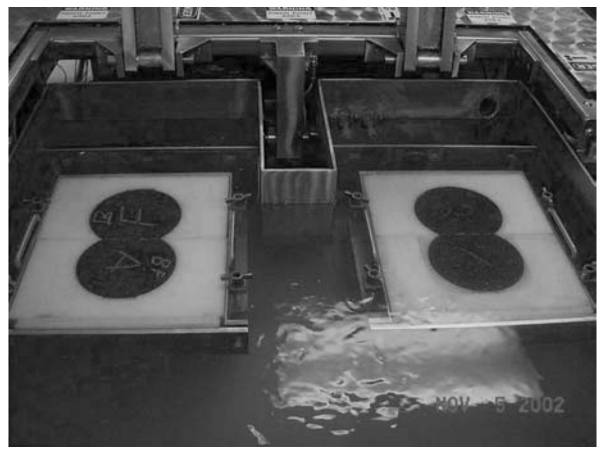

FIG. 2—*HWT specimens in test machine.*

DSR Creep Test

The DSR Creep Test was performed on a stress-controlled rheometer capable of applying up to 200 milli-Nm of torque. Two AR2000 rheometers manufactured by TA Instruments[8] were used for this testing. For the DSR Creep Test, specimens were prepared from a 95 mm high by 150 mm diameter gyratory specimen. Approximately 12–25 mm were sawed from one end of the specimen and discarded in an effort to obtain a mix representative of the entire specimen. A nominal 12 mm thick slice was cut from the trimmed gyratory specimen. This "wheel" of mix was then sawed into a rectangular slice approximately 150 mm long, 50 mm wide, and 12 mm thick. Finally, this rectangular piece was cut into test articles nominally 50 mm long, 12 mm thick, and 10 mm wide (Figs. 3 and 4).

Description of Test Procedures Performed

Hamburg Wheel Tracking Test

The specimens to be tested were placed into the holders and secured in the bath as described above. The bath was filled with water and brought to the test temperature (50°C in this study).

[7] Precision Machine and Welding, Salina, KS.
[8] TA Instruments, New Castle, DE.

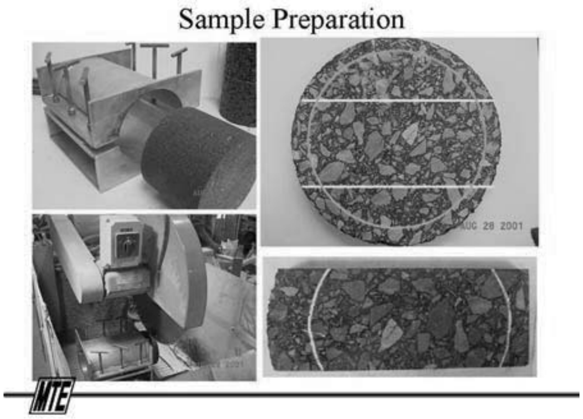

FIG. 3—*Cutting of gyratory specimen.*

FIG. 4—*Cutting of DSR creep specimen.*

The specimens are equilibrated for 30 min prior to applying the loaded wheels to the specimens and starting the test. The load applied by the steel wheels is 702 N (158 lb), and the wheel face is 47 mm wide. The wheels move reciprocally across the top of the specimens at 52 passes per minute. During this tracking procedure, the depth to which each wheel "cuts" into the specimens is tracked digitally via a LVDT, which is monitored by the computer software running the test. The HWT test is set up to run for a total of 20 000 cycles or end when one of the eleven monitoring points across the surface of the test specimen reaches a depth of 22 mm. Two pairs of specimens were tested for each trial in this study, and the data from both wheels were averaged to provide the final value used in the analysis.

DSR Creep Test

Test specimens (Fig. 6) are mounted vertically in the torsional fixture of the dynamic shear rheometer (Fig 5). A heated air system is used to bring the specimen to the test temperature of 58°C used in this study. This temperature was chosen because it is the high PG binder grade climatic temperature for most of Wisconsin. The test consists of applying repeated cycles of a torsional stress for 1 s and then zero stress for 9 s, during which time the strain induced into the specimen during the stress application is able to recover partially. The complete test consists of 2000 cycles or will terminate automatically when the sample ruptures or a permanent strain of 18 % is reached. For this study, a torsional stress of 34 kPa was used. This allowed measurable results to be obtained for the less stiff specimens, although it resulted in several of the better quality specimens not failing. In the analysis of the data, an attempt was made to adjust for this lack of failure in some of the specimens.

Data Collection and Data Analysis Methodologies

Hamburg Wheel Tracking Test

Three data measurements were obtained from the Hamburg Wheel Tracking test. Each test yielded two results, which were then averaged to produce the final value analyzed for each trial in the experimental design. The data values analyzed were: (1) the number of cycles to the onset of stripping, (2) the number of cycles to 12.5 mm of rutting, and (3) the number of cycles at sample failure or test completion. To reduce the data from each Hamburg Wheel Tracking test, the following procedure was employed. Examination of what is referred to internally as the Rut Profile (Fig. 7) shows that rutting at the ends of the specimen does not readily occur, nor should one expect that it would, given the confinement of the plastic holder. However, depending on the individual specimen, substantial rutting can occur anywhere between measurement points 3 and 9. Some agencies base their failure result for a Hamburg Wheel Tracking Test on the first measurement point to reach some target rut depth, such as 12.5 mm. This is an extremely conservative approach for a test, which is quite extreme in the stresses that it places upon test specimens, which are subject to typical production variability. Such an approach also assumes that the weakest location across the two gyratory specimens being tested is representative of the overall mix.

FIG. 5—*DSR creep specimen in rheometer.*

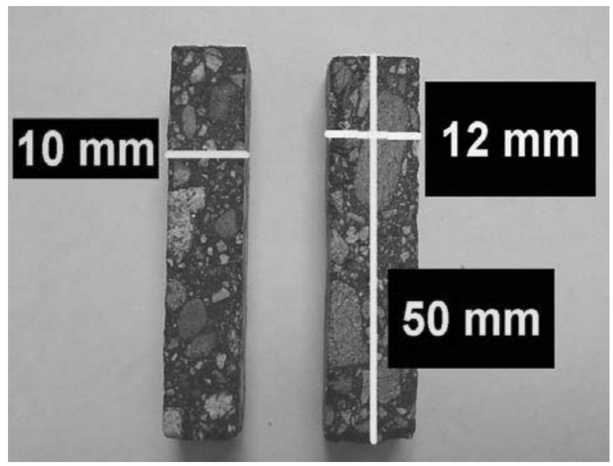

FIG. 6—*DSR creep specimen size.*

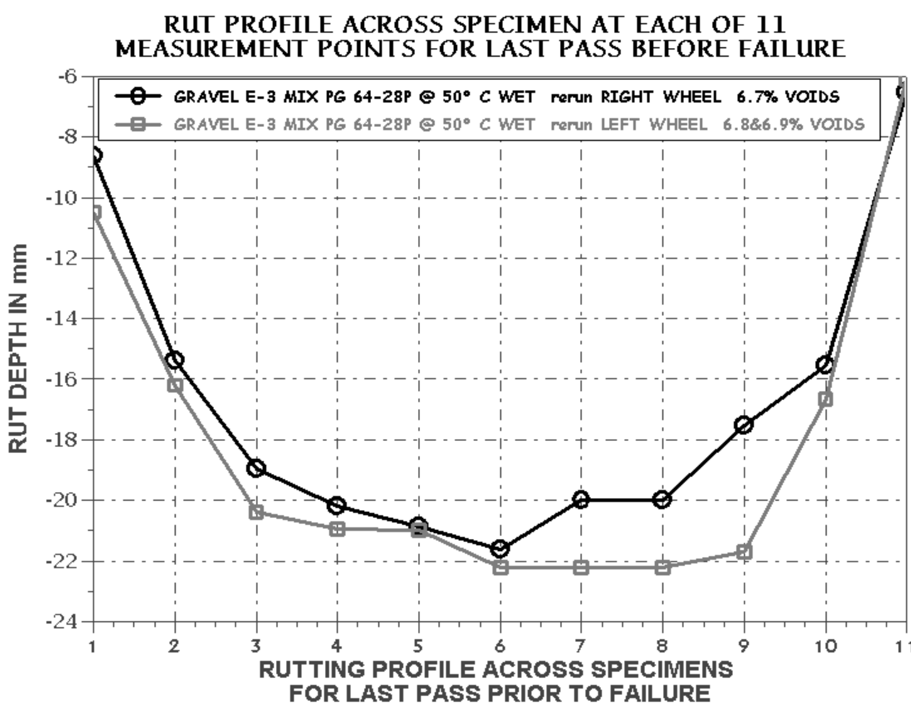

FIG. 7—*Rut profile plot.*

The approach was used to average the rut depths for measurement points 3–9 (Fig. 7) for each wheel at every cycle for which data are collected. Typically the software is set to collect a data value every 20 cycles. Regardless of the care taken in the preparation of lab specimens, density and aggregate distribution are not uniform in gyratory samples. By employing the data reduction procedures that are outlined some of those, inconsistencies in specimens were averaged out. All of the data values from the Hamburg Wheel Tracking Test used in this study were taken from rutting curves based on this data reduction procedure.

Figure 8 shows a typical data plot for one wheel of a test. The determination of cycles to onset of stripping is most easily seen by examination of the data trace. As the specimen tracking precedes, the mix deformation increases. For most mix specimens, a point will be reached where the wheel load, the heat, and the effect of the water will cause a rapid increase in the rate of rutting in the specimen. This point has been designated as the onset of stripping by various authors [4,5] and can be interpolated by determining the intersection point of tangent lines drawn on the data trace before and after the increase in the rate of rutting has occurred. These two regions of the data trace have been referred to as the “creep slope” and the “stripping slope,” respectively, by Ashenbrener [4], and other researchers have adopted this nomenclature [5,6]. The two other data values evaluated in this study, cycles to 12.5 mm and cycles at test termination, are apparent from the data trace.

The use of cycles at 12.5 mm was chosen because at least one agency [13] uses this rut depth in its mix design criteria.

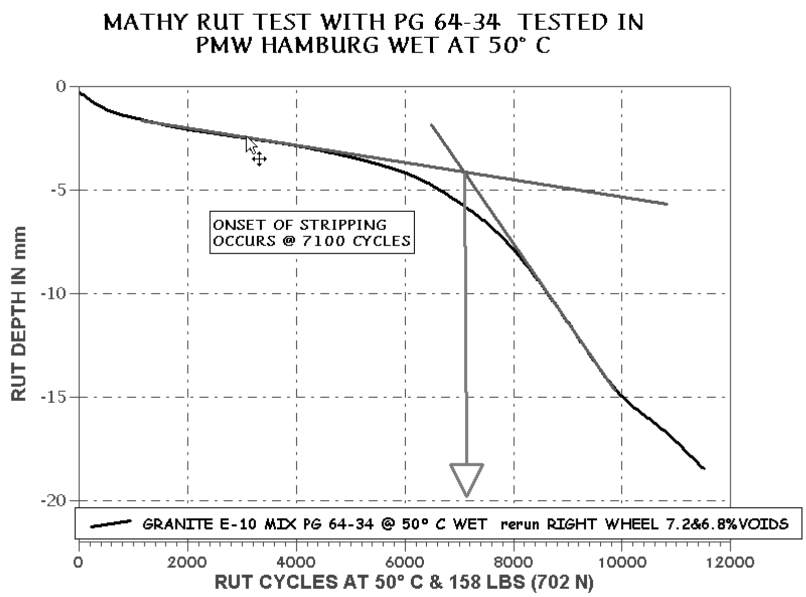

FIG. 8—*Rutting data showing onset of stripping.*

DSR Creep Test

The DSR Creep Test is not as well known as the Hamburg Wheel Tracking Test, and therefore the nature of the data collected and the manner in which they are evaluated requires some discussion. A typical data trace is shown in Fig. 9. Those familiar with the test results of the Repeated Shear at Constant Height test (AASHTO TP7) performed on the SST or Witczak’s work on the Simple Performance Test [10] will recognize the shape of the data output from the

DSR Creep Test. Examination of several creep and recovery test cycles (Fig. 10) gives some insight into how permanent deformation develops in the test specimens. During each 1 s of applied stress there is a resultant strain, and during the 9-s period of zero applied stress there is a relatively substantial amount of strain recovery. However, as Fig. 10 shows, the mixture specimen never completely recovers the total amount of strain; there is always a net amount of permanent strain accumulated. With repeated test cycles the specimen gradually goes through rapid strain development (primary flow), followed by a period when there is a linear rate of plastic deformation (secondary flow), and finally the point of failure when strain accumulates very rapidly (tertiary flow) (Fig. 11).

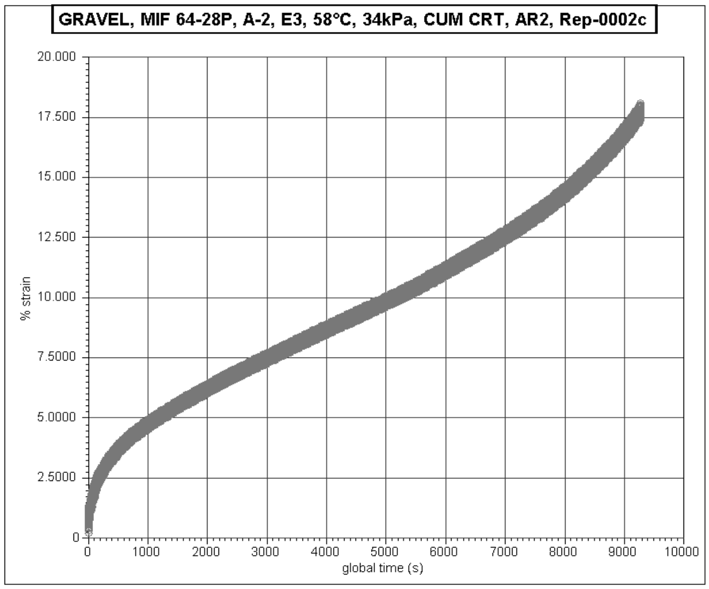

FIG. 9—*Typical DSR creep test result.*

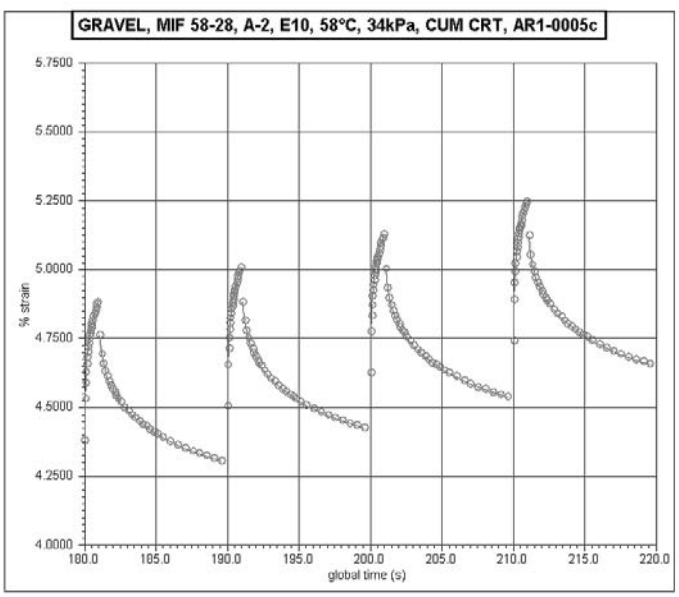

FIG. 10—*Creep and recovery test cycles.*

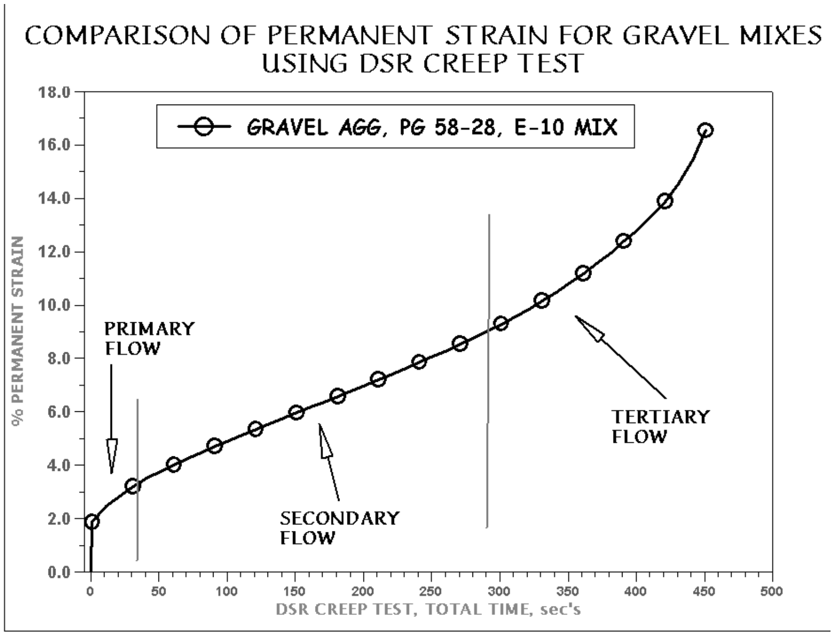

FIG. 11—*DSR creep showing primary, secondary, and tertiary flow.*

For the DSR Creep Test, three data values were collected for each specimen tested: the time to 5 % strain, the inverse of the slope in the region of secondary flow, and the time at which the specimen entered tertiary flow, which has been defined by Witczak as the Flowtime value [10]. Five specimens of each mix were tested, and the trimmed mean approach advocated by Romero and Anderson [11] was used to obtain three results, which were then averaged. Several of the mixture specimens failed to reach the point of tertiary flow during the 20 000 s of the DSR Creep Test. These were some of the E-3 and E-10 mixtures produced with PG 64-28P, PG 64-34, and PG 70-28. In an effort to obtain a reasonable value to enter as a response variable in the experimental design, curve-fitting software was employed to fit a mathematical model to the actual data, and then the model was extrapolated to a point where the fitted curve predicted failure. Several tests were evaluated using Tablecurve 2D[9] to determine whether this model could predict a tertiary flow type failure using data that had only entered the secondary flow region. The model that consistently provided a reasonable value for tertiary flow is shown as Eq 1, which is Eq 55 in the Tablecurve equations list.

$$Y^{-1} = a + b*\ln(X) \tag{1}$$

This mathematical model was used to predict Flowtime values and time to 5 % strain where necessary. After analysis, it appears as though the extrapolated results would under predict the Flowtime values, and therefore these values are conservative.

Experimental Design Input Variables and Responses

The experimental design that was employed in the investigation and the results of each experimental trial are summarized in Table 4. The Average Gyrations column of data is not part of the design, but it shows data that were collected for each trial and will be discussed later in the paper.

[9] Tablecurve 2D ver 5.01, Systat Software, Inc.

TABLE 4—*Experimental design trials and test results for each trial.*

TRIAL	AGGREGATE	BINDER	MIX	AVE GYRATIONS	Average stripping cycles	Average cycles to 12.5 mm	Average cycles to failure	1/SLOPE	TIME_5% STRAIN	FLOWTIME
1	GRANITE	PG58-28	E03	20.8	4 089	5 351	6 908	6.3	14.4	44.4
1	GRANITE	PG58-28	E03	27.0	4 769	5 419	6 710	17.1	44.4	114.4
4	GRANITE	PG58-28	E-1	25.5	3 968	4 958	6 218	7.0	11.1	54.4
8	GRANITE	PG58-28	E-10	56.8	4 194	6 211	7 921	44.5	87.7	141.1
6	GRANITE	PG58-28	E-3	58.8	4 152	5 441	6 991	20.1	51.1	291.1
62	GRANITE	PG64-28C	E03	22.3	3 518	4 465	5 514	23.3	58.1	174.8
36	GRANITE	PG64-28C	E-1	26.8	3 530	4 898	6 288	35.1	107.8	207.8
39	GRANITE	PG64-28C	E-10	61.5	5 216	7 511	9 171	72.1	121.1	517.8
19	GRANITE	PG64-28C	E-3	50.5	5 245	8 121	10 031	87.6	224.4	511.1
5	GRANITE	PG64-28P	E03	26.5	5 351	7 433	9 804	57.1	141.1	371.1
15	GRANITE	PG64-28P	E-1	22.8	6 765	10 184	13 324	44.6	101.1	351.1
33	GRANITE	PG64-28P	E-10	44.5	13 714	17 021	20 000	158.3	301.1	1 041.1
42	GRANITE	PG64-28P	E-3	43.8	13 490	17 100	20 000	144.7	264.4	971.1
11	GRANITE	PG64-34	E03	36.3	2 731	4 591	6 241	60.4	131.1	431.1
41	GRANITE	PG64-34	E-1	15.8	9 391	12 180	15 379	91.1	197.8	624.4
41	GRANITE	PG64-34	E-1	66.8	4 392	6 641	9 160	91.1	197.8	624.4
20	GRANITE	PG64-34	E-10	59.0	6 598	8 381	10 601	115.5	157.8	551.1
20	GRANITE	PG64-34	E-10	95.3	5 143	8 110	11 011	302.8	447.8	2 354.3
31	GRANITE	PG64-34	E-3	38.8	4 247	5 911	7 451	67.1	97.8	771.1
31	GRANITE	PG64-34	E-3	47.3	6 363	13 370	16 930	302.4	327.8	2 387.7
13	GRANITE	PG70-28	E03	25.5	10 910	17 147	20 000	231.8	388.1	1 828.0
23	GRANITE	PG70-28	E-1	21.0	14 530	20 000	20 000	393.0	554.4	3 214.3
43	GRANITE	PG70-28	E-10	55.0	16 247	20 000	20 000	926.4	1 114.4	2 797.7
37	GRANITE	PG70-28	E-3	57.5	15 735	20 000	20 000	390.4	484.4	6 671.0
3	GRAVEL	PG58-28	E03	28.3	3 725	4 755	5 716	16.7	37.7	104.4
16	GRAVEL	PG58-28	E-1	24.3	3 684	4 501	5 376	25.1	67.7	151.8
22	GRAVEL	PG58-28	E-10	42.0	4 239	5 301	6 561	49.0	147.8	294.4
9	GRAVEL	PG58-28	E-3	46.8	3 071	4 571	6 001	45.9	141.1	337.8
12	GRAVEL	PG64-28C	E03	27.3	4 115	6 126	7 526	85.9	211.1	554.4
53	GRAVEL	PG64-28C	E-1	27.5	4 115	6 326	8 176	61.8	141.1	407.8
46	GRAVEL	PG64-28C	E-10	45.3	5 726	8 021	10 151	151.5	341.1	1 164.3
27	GRAVEL	PG64-28C	E-3	58.8	5 581	8 451	10 691	88.3	214.4	661.1
24	GRAVEL	PG64-28P	E03	21.5	11 198	13 370	16 930	188.3	411.1	1214.3
48	GRAVEL	PG64-28P	E-1	25.3	6 375	9 300	10 901	108.6	301.1	574.4
48	GRAVEL	PG64-28P	E-1	32.3	8 689	12 951	16 611	186.1	337.8	1 437.7
35	GRAVEL	PG64-28P	E-10	47.8	5 741	9 451	13 201	256.6	527.8	1 771.0
55	GRAVEL	PG64-28P	E-3	51.8	9 116	12 071	15 080	362.2	621.1	3 191.0
55	GRAVEL	PG64-28P	E-3	33.5	7 889	11 080	15 251	706.9	1 397.7	5 807.7
28	GRAVEL	PG64-34	E03	31.3	3 705	5 526	8 625	308.3	517.8	2 481.0
28	GRAVEL	PG64-34	E03	21.3	3 087	5 640	9 260	734.6	1 134.4	4 737.7
45	GRAVEL	PG64-34	E-1	40.0	3 985	6 451	9 326	737.6	537.8	4 967.7
45	GRAVEL	PG64-34	E-1	23.8	3 822	6 251	9 371	846.4	877.7	5 884.0
57	GRAVEL	PG64-34	E-10	49.0	6 105	10 391	14 971	5 262.4	5 317.7	20 000.0
38	GRAVEL	PG64-34	E-3	47.8	6 559	10 781	15 441	10 861.6	10 960.3	20 000.0
18	GRAVEL	PG70-28	E03	25.0	14 021	20 000	20 000	2 687.2	2 987.7	18 573.3

TRIAL	AGGREGATE	BINDER	MIX	AVE GYRATIONS	Average stripping cycles	Average cycles to 12.5 mm	Average cycles to failure	1/SLOPE	TIME_5% STRAIN	FLOWTIME
18	GRAVEL	PG70-28	E03	31.3	11 775	18 901	20 000	13 975.9	20 304.0	131 728.0
32	GRAVEL	PG70-28	E-1	31.0	7 902	13 151	18 201	3 300.0	3 337.7	18 366.7
63	GRAVEL	PG70-28	E-10	41.5	20 000	20 000	20 000	3 722.1	4 881.0	26 287.3
52	GRAVEL	PG70-28	E-3	58.8	15 935	20 000	20 000	13 694.0	19 590.0	20 000.0
2	LIMESTONE	PG58-28	E03	16.5	1 965	2 781	3 681	49.2	147.8	297.8
7	LIMESTONE	PG58-28	E-1	19.3	1 668	2 921	3 951	19.2	54.4	121.1
14	LIMESTONE	PG58-28	E-10	62.3	3 517	5 991	7 571	487.3	1 464.3	2 264.3
21	LIMESTONE	PG58-28	E-3	41.0	2 263	3 611	4 700	44.9	154.4	227.8
25	LIMESTONE	PG64-28C	E03	18.3	2 567	3 671	4 921	15.4	44.4	84.4
40	LIMESTONE	PG64-28C	E-1	23.0	3 254	5 021	6 211	47.1	137.8	281.1
49	LIMESTONE	PG64-28C	E-10	56.3	3 170	5 611	7 601	356.6	1 107.7	1 707.7
56	LIMESTONE	PG64-28C	E-3	41.5	4 038	6 281	8 111	178.0	427.8	1 004.4
10	LIMESTONE	PG64-28P	E03	18.5	4 930	7 961	10 291	518.7	1491.0	2 984.3
26	LIMESTONE	PG64-28P	E-1	23.8	3 004	6 131	9 451	168.6	534.4	1 037.7
54	LIMESTONE	PG64-28P	E-10	55.0	6 104	10 771	14 811	9 694.9	17 360.0	19 600.0
47	LIMESTONE	PG64-28P	E-3	45.3	6 940	12 341	16 491	564.2	1 327.7	2 824.3
17	LIMESTONE	PG64-34	E03	20.8	2 621	5 050	8 161	1339.4	3 001.0	8 620.7
51	LIMESTONE	PG64-34	E-1	20.0	2 243	4 151	6 720	97.1	221.1	601.1
51	LIMESTONE	PG64-34	E-1	17.5	2 990	4 540	6 180	2 579.7	4 881.0	14 343.3
30	LIMESTONE	PG64-34	E-10	79.3	3 432	7 001	10 451	33 306.2	20 000.0	20 000.0
50	LIMESTONE	PG64-34	E-3	51.5	3 266	6 101	9 081	8 592.0	16 893.3	19 123.3
29	LIMESTONE	PG70-28	E03	19.0	6 070	12 031	16 291	171.9	471.1	937.7
64	LIMESTONE	PG70-28	E-1	46.0	6 119	12 311	16 820	3 367.0	6 231.0	18 258.7
64	LIMESTONE	PG70-28	E-1	46.3	9 210	17 760	20 000	3 367.0	6 231.0	18 258.7
44	LIMESTONE	PG70-28	E-10	105.5	6 915	13 591	17 581	67 522.2	20 000.0	20 000.0
44	LIMESTONE	PG70-28	E-10	59.3	8 326	17 050	18 630	44 550.5	179 300.0	561 252.0
34	LIMESTONE	PG70-28	E-3	43.8	12 508	18 781	20 000	10 914.1	15 766.7	20 000.0

Discussion of Data and Results

Table 5 shows the model terms used to analyze the data, and Table 6 is the ANOVA table for that model. No three-way interaction terms were found to be significant, and therefore initial analysis of all two-way interactions of variables was considered. This included all combinations of aggregate type and AC grade, aggregate type and mix level, and AC grade and mix level. This approach resulted in a 36-term model with all the AC grade and mix level interaction terms being non-significant. The 12 non-significant terms were removed from the model, and the data were re-analyzed. For the resulting 24-term model, none of the aggregate type/AC grade interaction terms were significant for the three response variables related to the Hamburg Wheel Tracking Test results. Some of the aggregate type/AC grade interaction terms were significant for the response variables of the DSR Creep Test, and some of the AC grade/mix level terms were significant for the response variables of both the Hamburg Wheel Tracking Test and the DSR Creep Test. Finally, the terms that were insignificant for all response variables were removed from the model, and a final analysis of the data was performed. The model shown in Table 5 contains those terms for which at least one of the response terms was significant. For this final model, the response variables for DSR Creep 1/Slope, DSR Creep Time to 5 % Strain, and DSR

Creep Flowtime were Log10 transformed. This was necessary to avoid Lack of Fit in the model. Considering the range of data for these response variables shown in Table 4, the need to log transform the data was not surprising.

TABLE 5—*Model terms used in the analysis.*

TERM	VARIABLE IN THE MODEL	TERM	VARIABLE IN THE MODEL
0	CONSTANT		
1	GRANITE	17	LIMESTONE*PG64-28C
2	LIMESTONE	18	LIMESTONE*PG64-34
3	GRAVEL	19	GRAVEL*PG58-28
4	PG58-28	20	GRAVEL*PG70-28
5	PG64-28P	21	GRANITE*E-03
6	PG64-28C	22	GRANITE*E-1
7	PG64-34	23	GRANITE*E-10
8	PG70-28	24	LIMESTONE*E-03
9	E-03	25	LIMESTONE*E-1
10	E-1	26	LIMESTONE*E-10
11	E-3	27	GRAVEL*E-03
12	E-10	28	GRAVEL*E-10
13	GRANITE*PG58-28		
14	GRANITE*PG64-28C		
15	GRANITE*PG64-34		
16	Granite*70-28		

TABLE 6—*ANOVA table for analysis model (p-values are shown for each response variable).*

Experimental Design Element	HWT Onset of Stripping	HWT Cycles to 12.5 mm Rut	HWT Cycles to Failure	DSR Creep 1/Slope	DSR Creep Time to 5 % Strain	DSR Creep Flowtime
Agg-Type	0.0000	0.0002	0.0024	0.0000	0.0000	0.0000
AC-Grade	0.0000	0.0000	0.0000	0.0000	0.0000	0.0000
Mix Level	0.0043	0.0004	0.0004	0.0000	0.0000	0.0000
Agg-Type*AC-Grade	0.1049	0.7378	0.8114	0.0017	0.0036	0.0015
Agg-Type*Mix Level	0.5877	0.5914	0.8002	0.0005	0.0001	0.0002

Note 1: p-Values in the Analysis of Variance Table describe levels of statistical significance of the design variable in predicting a given test result. A p-Value of less than 0.001 for a given response means that the particular design variable is a statistically significant cause at the 99.9 % confidence level, a p-Value of greater than 0.001 and less than 0.01 means that the design variable is statistically significant at the 99 % confidence level, and a p-Value of greater than 0.01 to 0.05 means that the design variable is statistically significant at the 95 % confidence level. P-Values greater than 0.05 mean the design variable is not a statistically significant factor in determining the test response. The proper way to read the ANOVA table, for example, is to say that the design variable Agg-Type is a statistically significant predictor of HWT Onset of Stripping at the 99.9 % confidence level.

Examination of the ANOVA table shows that neither the interaction term for Aggregate Type*AC Grade nor Aggregate Type*Mix Level was significant for the Hamburg Wheel Tracking results. Although intuitively one would think that the interaction of aggregate type and AC grade should be important for a test related to mixture moisture sensitivity, it may well be that the first order effects of the aggregate, binder, and mix level are so overwhelming that the interaction terms do not show up as important. Alternatively, these interaction terms show up as being significant for most of the response variables in the DSR Creep Test. The more in depth analysis of the model term coefficients shown in Tables 7 and 12 show the sign of the term coefficients and the statistical significance of the first order and the interaction terms. In Tables 7 and 12 the p-values are color coded to make it easier to discern statistical significance. There is a key at the bottom of each table, and any term for which the p-Value has a white background is not statistically significant for the particular response variable.

Evaluation of Results from Hamburg Wheel Tracking Test

Figures 12–14 are bar graphs for some of the moisture sensitivity responses of Hamburg test. Not all possible plots have been presented, in part because the information derived for each of the three response variables is very similar. Table 7 makes this point in a non-graphical form. For response variables “Onset of Stripping,” “Cycles to 12.5 mm,” and “Cycles to Failure,” the limestone aggregate is highly significant with a negative coefficient. For a given response variable, the ECHIP program evaluates all levels of a categorical input variable relative to the average value of all responses of that variable. Therefore, in the case of the limestone aggregate input variable the negative coefficient for “Onset of Stripping” means that relative to the average of the responses for all three aggregates (at all mix levels and using all binders), the limestone mixes reach the stripping slope faster. The p-value of 0.0000 coupled with the negative coefficient means that the limestone mixes reach the stripping slope faster than the average of all the mixes with statistical significance at the 99.9 % confidence level. Conversely, the coefficient for Onset of Stripping for the granite mixes is positive, which means that relative to the average for all three mixes, the granite mixes reach the stripping onset point in a longer number of cycles, and the significance level is 99 %. Table 7 also shows for the three response variables of the Hamburg Wheel Tracking Test that all binders (except PG 64-28P) and all mix levels are statistically significant at the 99 % or higher level. Based on the analysis of the model, the PG 64-28P and PG 70-28 mixes perform better than the average responses for all binders using all aggregates and all mix levels. Alternatively, the PG 58-28, PG 64-28C and the PG 64-34 mixes do not perform as well as the average.

ECHIP enables performance comparison of one input variable versus another. The results summarized in Table 8 show that for these three aggregate types both the granite and gravel outperform the limestone at a statistically significant level. Other groups have reported similar results when comparing Hamburg Wheel Tracking performance between diabase or igneous aggregates and limestone aggregates [12,13]. In one study [12] at least part of the reason for the more rapid failure of the limestone mixes was attributed to the Hamburg Wheel Tracker crushing the limestone aggregate and not crushing the diabase. In another report [13] no specific reasons were cited other than a comparison between hard (igneous) and soft (limestone) aggregates with the limestone aggregate failing more quickly. In the current study the gravel mixes have positive coefficients for HWT test responses, which means that the gravel mixes perform better than the average of all the aggregate mixtures. Based based on the p-value evaluation between granite and gravel for Cycles to Onset of Stripping (Table 8), Cycles to 12.5 mm Rut Depth, and Cycles to Failure, however, there is no statistically significant difference between the gravel and the granite for those responses. These conclusions may not be obvious through examination of the bar graphs, but one must bear in mind that the statistical conclusions are derived from evaluation of each aggregate relative to the aggregate average across all mix types with all binders. The bar graphs are, in essence, a one-dimensional picture of a multi-dimensional evaluation. Therefore, it is important to keep in mind that these results for the binders are averaged across all aggregate types and all mix levels.

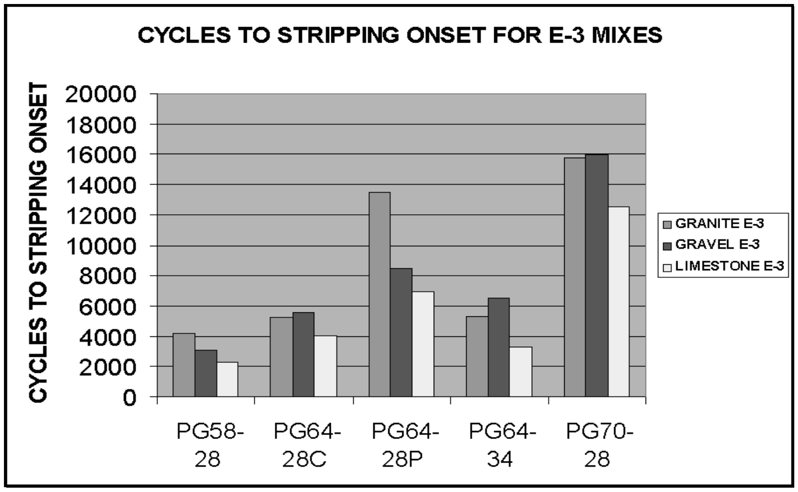

FIG. 12—*Cycles to stripping onset for granite, gravel, and limestone E-3 mixes.*

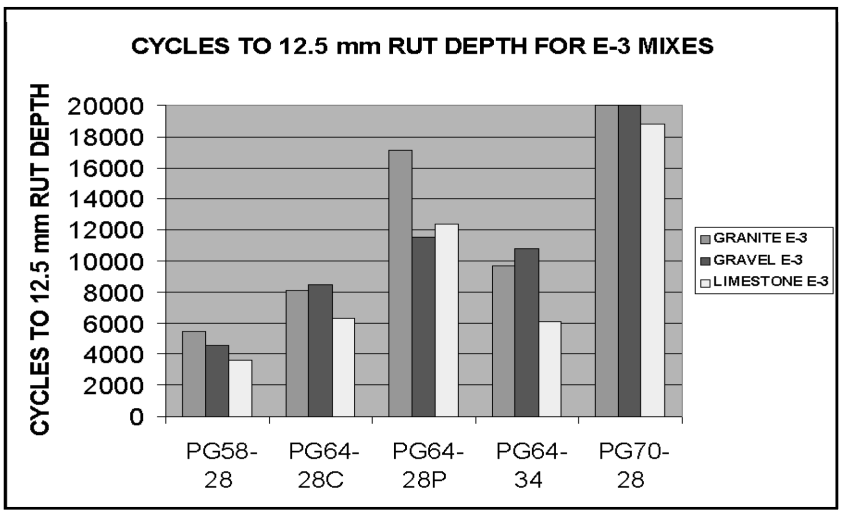

FIG. 13—*Cycles to 12.5 mm rut depth for granite, gravel, and limestone E-3 mixes.*

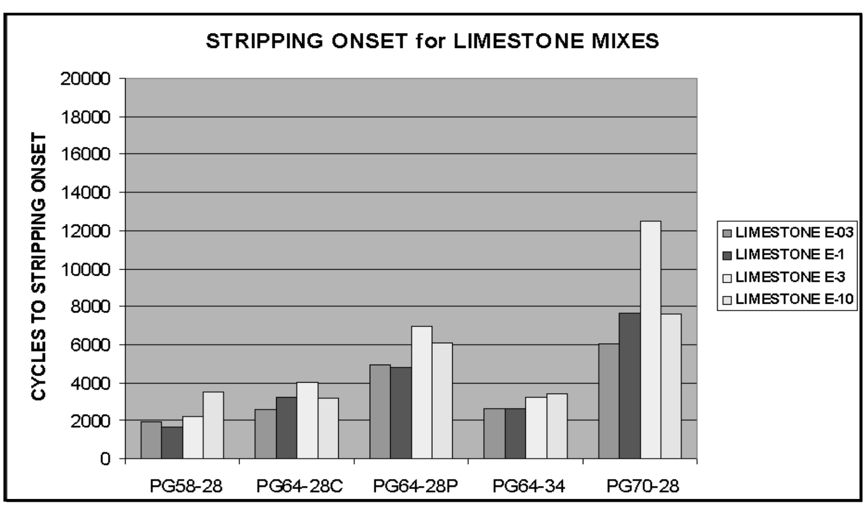

FIG. 14—*Cycles to stripping onset for limestone E-0.3, E-1, E-3, and E-10 mixes.*

TABLE 7—*Coefficients and p-values for HWT response variables.*

		Response	Onset of stripping	Response	Cycles to 12.5 mm	Response	Cycles to Failure
TERM		Coefficients	p-Value	Coefficients	p-Value	Coefficients	p-Value
0	CONSTANT	4346.27	NA	7894.48	NA	10541.2	NA
1	GRANITE	1045.42	0.0074	1024.49	0.0045	697.59	0.0602
2	LIMESTONE	-1721.27	0.0000	-1559.97	0.0000	-1355.37	0.0006
3	GRAVEL	723.2	0.0325	535.48	0.1262	657.77	0.0759
4	PG58-28	-2875.54	0.0000	-4558.14	0.0000	-5444.22	0.0000
5	PG64-28P	1496.24	0.0021	1866.68	0.0003	2836.36	0.0000
6	PG64-28C	-2369.61	0.0000	-3324.62	0.0000	-3804.4	0.0000
7	PG64-34	-2037.1	0.0000	-2247.13	0.0000	-1373.69	0.0058
8	PG70-28	5785.92	0.0000	8263.21	0.0000	7785.99	0.0000
9	E-03	-1063.69	0.0119	-1351.96	0.0026	-1448.3	0.0022
10	E-1	-715.7	0.0682	-872.87	0.0347	-929.05	0.0331
11	E-3	986.41	0.0199	1385.83	0.0022	1406.05	0.0031
12	E-10	793	0.0557	839	0.0533	971.3	0.0331
13	GRANITE*PG58-28	535.73	0.3631	337.74	0.5748	580.94	0.3724
14	GRANITE*PG64-28C	-206.98	0.685	-360.68	0.4908	-423.63	0.4536
15	GRANITE*PG64-34	-212.21	0.6592	60.98	0.9014	53.17	0.9203
16	GRANITE*PG70-28	-116.53	0.802	-38.04	0.9363	-210.48	0.6821
17	LIMESTONE*PG64-28C	206.983	0.6850	360.677	0.4908	423.628	0.4536
18	LIMESTONE*PG64-34	212.215	0.6592	-60.9838	0.9014	-53.1716	0.9203
19	GRAVEL*PG58-28	-116.53	0.802	-38.04	0.9363	-210.48	0.6821
20	GRAVEL*PG70-28	116.529	0.8020	38.0424	0.9363	210.48	0.6821
21	GRANITE*E-03	-423.36	0.357	-490.42	0.3385	-431.31	0.4349
22	GRANITE*E-1	201.86	0.6327	398.62	0.3582	533.09	0.2559
23	GRANITE*E-10	221.5	0.6456	91.8	0.8523	-101.79	0.8483
24	LIMESTONE*E-03	-592.91	0.3063	-808.33	0.175	-542.89	0.3963
25	LIMESTONE*E-1	-201.862	0.6327	-398.625	0.3582	-533.095	0.2559
26	LIMESTONE*E-10	794.774	0.1635	1206.86	0.0408	1075.98	0.0893
27	GRAVEL*E-03	1016.27	0.0424	-1298.65	0.0122	974.2	0.0772
28	GRAVEL*E-10	-1016.27	0.0424	-1298.65	0.0122	-974.195	0.0772
				Significant @ 95 %			
				Significant @ 99 %			
				Significant @ 99.9 %			
			NA	Not Applicable			

TABLE 8—*Evaluation of comparative aggregate performance for cycles to onset of stripping.*

Aggregate A	Aggregate B	Coefficient of A relative to B[NOTE 1]	p-value of A relative to B[NOTE 2]	COMMENT
Granite	Limestone	+2 115.89	0.0000	Granite performs better than Limestone at a statistically significant level
Gravel	Limestone	+ 2 642.74	0.0000	Gravel performs better than Limestone at a statistically significant level
Granite	Gravel	+ 473.15	0.4040	Granite performs better than Gravel but not at a statistically significant level

NOTE 1–Aggregate A column is compared to Aggregate B column; a positive coefficient means result for Aggregate A is greater than result for Aggregate B

NOTE 2–p-value determines whether performance of Aggregate A relative to Aggregate B is statistically significant. Lack of statistical significance implies no discernable difference in performance regardless of whether or not the result for Aggregate A is greater than the result for Aggregate B.

The ECHIP program's capability of evaluating the relative response of one binder versus another for all aggregates and all mix levels was used to calculate the relative binder performance results for Cycles to Onset of Stripping (Table 8) and for Cycles to 12.5 mm Rut Depth (Table 9).

TABLE 9—*Evaluation of comparative binder performance for cycles to onset of stripping.*

Binder A	Binder B	Coefficient of A relative to B[NOTE 1]	p-value of A relative to B[NOTE 2]	COMMENT
PG 64-28C	PG 58-28	+ 505.92	0.5144	PG 64-28C performs better than PG 58-28 but not at a statistically significant level
PG 64-34	PG 58-28	+ 838.52	0.2474	PG 64-34 performs better than PG 58-28 but not at a statistically significant level
PG 64-34	PG 64-28C	+ 332.6	0.6450	PG 64-34 performs better than PG 64-28C but not at a statistically significant level
PG 64-28P	PG 64-34	+ 3 533.25	0.0000	PG 64-28P performs better than PG 64-34 at a statistically significant level
PG 64-28P	PG 64-28C	+ 3 865.45	0.0000	PG 64-28P performs better than PG 64-28C at a statistically significant level
PG 70-28	PG 64-28P	+ 4 289.68	0.0000	PG 70-28 performs better than PG 64-28P at a statistically significant level

NOTE 1–Binder A column is compared to Binder B column, a positive coefficient means result for Binder A is greater than the result for Binder B

NOTE 2–p-value determines whether performance of Binder A relative to Binder B is statistically significant. Lack of statistical significance implies no discernable difference in performance, regardless of whether or not the result for Binder A is greater than the result for Binder B.

Examination of Table 9 shows that there is no statistical difference between PG 58-28, PG 64-28C and PG 64-34 with respect to the Cycles to Onset of Stripping. PG 64-28P performs significantly better than either PG 64-28C or PG 64-34 but is out performed by PG 70-28 at a significant level. The results are very similar for the binders' impact on Cycles to 12.5 mm Rut Depth (Table 10). PG 64-34 does outperform PG 58-28 at a significant level, and the p-value relationship between PG 64-28C and PG 58-28 and the relationship between PG 64-34 and PG 64-28C are reduced, but still not to a significant level. These results detailed in Tables 9 and 10 reflect the similarity in stripping potential (Table 9) for PG 58-28, PG 64-28C and PG 64-34, but they also reflect the greater resistance to rut development of the PG 64 grades compared to the PG 58 grade (Table 10).

Table 11 shows that mix levels E-0.3 and E-1 perform statistically significantly worse than the average of all four mix levels across all aggregate types and all binder grades. As might be expected, mix levels E-3 and E-10 perform better than the average of all four mixes for all aggregate types and binder grades. E-3 mixes are statistically significantly better than the average of all mixes, while E-10 mixes are nearly significant at the 95 % confidence level. Evaluation of Cycles to Onset of Stripping for mix levels relative to each other is shown in Table 11. This comparative evaluation shows that for the average of all three aggregate types, E-1 and E-0.3 mixes performed at the same level, and E-10 and E-3 mixes performed at the same statistical level. Furthermore, an analysis of these four mix levels for each specific aggregate type yielded the same results as the evaluation based on the average aggregate response.

TABLE 10—*Evaluation of comparative binder performance for cycles to 12.5 mm rut depth.*

Binder A	Binder B	Coefficient of A relative to B NOTE 1	p-value of A relative to B NOTE 2	COMMENT
PG 64-28C	PG 58-28	+ 1 233.51	0.1290	PG 64-28C performs better than PG 58-28 but not at a statistically significant level
PG 64-34	PG 58-28	+ 2 311.01	0.0023	PG 64-34 performs better than PG 58-28 at a statistically significant level (however not for granite aggregate)
PG 64-34	PG 64-28C	+ 1 077.5	0.1542	PG 64-34 performs better than PG 64-28C but not at a statistically significant level
PG 64-28P	PG 64-34	+ 4 113.81	0.0000	PG 64-28P performs better than PG 64-34 at a statistically significant level
PG 64-28P	PG 64-28C	+ 5 191.31	0.0000	PG 64-28P performs better than PG 64-28C at a statistically significant level
PG 70-28	PG 64-28P	+ 6 396.52	0.0000	PG 70-28 performs better than PG 64-28P at a statistically significant level

NOTE 1–Binder A column is compared to Binder B column, a positive coefficient means result for Binder A is greater than result for Binder B

NOTE 2–p-value determines whether performance of Binder A relative to Binder B is statistically significant. Lack of statistical significance implies no discernable difference in performance, regardless of whether or not the result for Binder A is greater than the result for Binder B.

TABLE 11—*Evaluation of comparative mix level performance for cycles to onset of stripping.*

Mix Level A	Mix Level B	Coefficient of A relative to B NOTE 1	p-value of A relative to B NOTE 2	COMMENT
E-1	E-0.3	+347	0.5876	E-1 mixes perform better than E-0.3 mixes but not at a statistically significant level
E-3	E-03	2 050.1	0.0354	E-3 mixes perform better than E-03 mixes at a statistically significant level
E-3	E-1	+ 1 702	0.0083	E-3 mixes perform better than E-1 mixes at a statistically significant level
E-10	E-3	-193.39	0.7730	E-10 mixes perform worse than E-3 mixes but not at a statistically significant level
E-10	E-1	+ 1 508.77	0.0482	E-10 mixes perform better than E-1 mixes at a statistically significant level

NOTE 1–Mix Level A column is compared to Mix Level B column, a positive coefficient means result for Mix Level A is greater than result for Mix Level B

NOTE 2–p-value determines whether performance of Mix Level A relative to Mix Level B is statistically significant. Lack of statistical significance implies no discernable difference in performance, regardless of whether or not the result for Mix Level A is greater than the result for Mix Level B.

Summary of Hamburg Wheel Tracking Results

Granite and gravel both performed better than limestone aggregate, but there was no statistical difference between the granite and the gravel. This may be due to the softer limestone aggregate and its tendency to disintegrate under the Hamburg wheel. PG 64-28P and PG 70-28 outperformed the other binders on the HWT. The performance of PG 64-34 was statistically comparable to the PG 58-28 and PG 64-28C when the data for all aggregates and mix types were considered. This is unexpected, considering that PG 64-34 and PG 70-28 have comparable levels of polymer. E-03 and E-1 mixes performed similarly, and E-3 and E-10 performed statistically similarly.

Evaluation of Results from the DSR Creep Test

Figures 15–17 are bar graphs for the DSR Creep Test Flowtime results. Once again, not all of the possible DSR Creep Test responses have been plotted, because the information shown by the "1/Slope" and "Time to 5 % Strain" plots provide information similar to those of the Flowtime response plots. Statistical analysis by ECHIP of the results is summarized in Table 14. The Granite, Limestone, and Gravel results are evaluated relative to the average for all three aggregates for all binders and all mix levels.

TABLE 12—*Coefficients and p-values for DSR creep test response variables.*

		Response	1/Slope	Response	Time to 5% Strain	Response	Flowtime
TERM		Coefficients	p-Value	Coefficients	p-Value	Coefficients	p-Value
0	CONSTANT	12146.7	NA	2.86851	NA	3.39624	NA
1	GRANITE	-0.52	0.0000	-0.55	0.0000	-0.5	0.0000
2	LIMESTONE	0.37	0.0000	0.451017	0.0000	0.308613	0.0000
3	GRAVEL	0.16	0.0054	0.0978053	0.0622	0.191361	0.0022
4	PG58-28	-0.9	0.0000	-0.78	0.0000	-0.92	0.0000
5	PG64-28P	0.1	0.9315	0.0634749	0.3949	0.0194795	0.8117
6	PG64-28C	-0.58	0.0000	-0.482166	0.0000	-0.593653	0.0000
7	PG64-34	0.51	0.0000	0.389879	0.0000	0.532378	0.0000
8	PG70-28	0.97	0.0000	0.809108	0.0000	0.965515	0.0000
9	E-03	-0.35	0.0000	-0.18	0.0726	-0.23	0.0348
10	E-1	-0.3	0.0000	-0.201814	0.0000	-0.32	0.0000
11	E-3	0.2	0.0052	0.0961893	0.0125	0.21	0.0049
12	E-10	0.44	0.0000	0.282372	0.0000	0.47	0.0000
13	GRANITE*PG58-28	0.22	0.0444	0.17	0.1341	0.26	0.0299
14	GRANITE*PG64-28C	0.32	0.0045	0.33	0.0022	0.33	0.0050
15	GRANITE*PG64-34	-0.35	0.0004	0.3	0.0024	-0.37	0.0009
16	GRANITE*PG70-28	-23	0.0354	-0.26	0.0192	-0.26	0.0338
17	LIMESTONE*PG64-28C	-0.28	0.0141	-0.33	0.0036	-0.31	0.0118
18	LIMESTONE*PG64-34	0.21	0.0497	0.25	0.0164	0.22	0.0490
19	GRAVEL*PG58-28	-0.18	0.1322	-0.1	0.4026	-0.2	0.0092
20	GRAVEL*PG70-28	0.26	0.0175	0.27	0.0429	0.027	0.0183
21	GRANITE*E-03	0.12	0.2219	0.14	0.1372	0.13	0.191
22	GRANITE*E-1	0.14	0.1437	0.18	0.0478	0.17	0.0892
23	GRANITE*E-10	-0.19	0.0407	-0.24	0.0073	-0.22	0.0248
24	LIMESTONE*E-03	-0.24	0.0135	-0.26	0.0019	-0.26	0.0144
25	LIMESTONE*E-1	-0.19	0.0356	-0.21	0.0189	-0.2	0.0312
26	LIMESTONE*E-10	0.49	0.0000	0.54	0.0000	0.55	0.0000
27	GRAVEL*E-03	0.13	0.1871	0.12	0.1997	0.12	0.216
28	GRAVEL*E-10	-0.3	0.0024	-0.29	0.0026	-0.33	0.0015
				Significant @ 95 %			
				Significant @ 99 %			
				Significant @ 99.9 %			
			NA	Not Applicable			

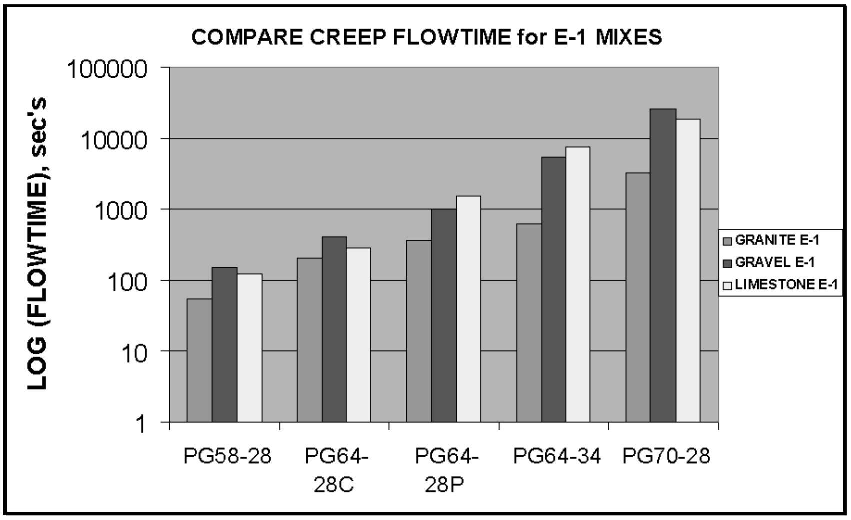

FIG. 15—*Compare DSR creep Flowtime for granite, gravel, and limestone E-1 mixes.*

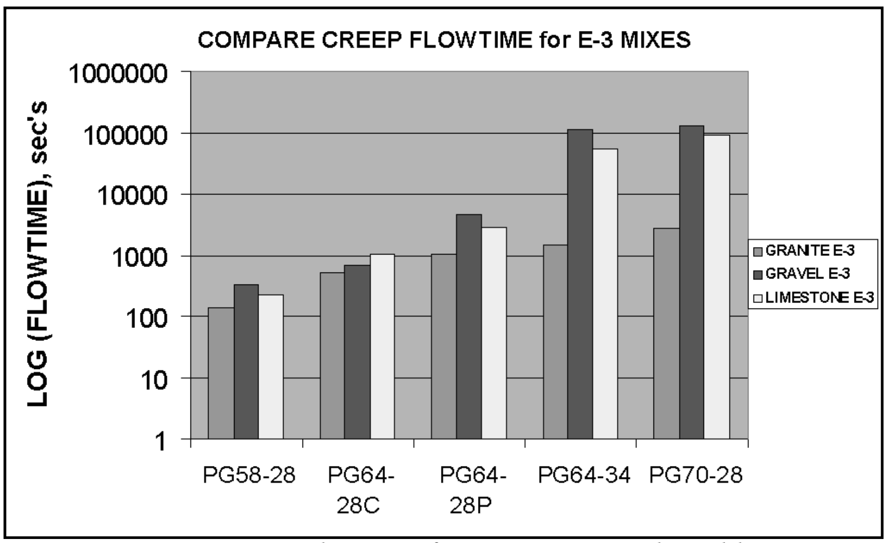

FIG. 16—*Compare DSR creep Flowtime for granite, gravel, and limestone E-3 mixes.*

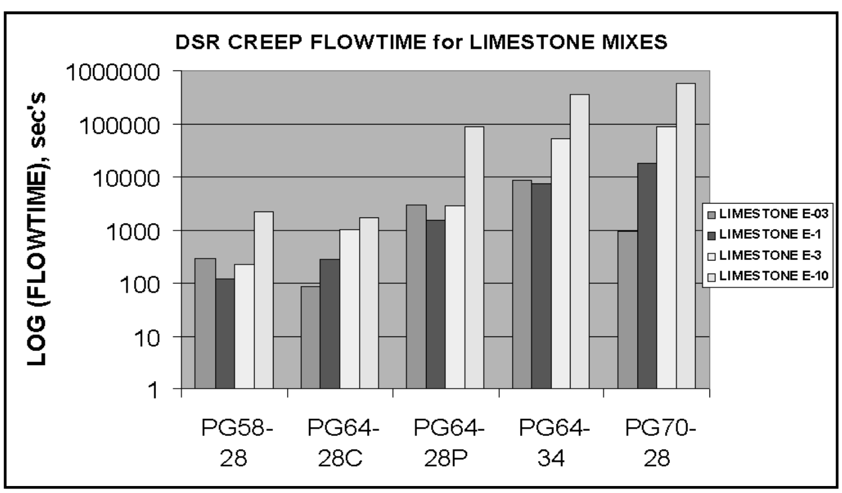

FIG. 17—*Compare DSR creep Flowtime for limestone E-0.3, E-1, E-3, and E-10 mixes.*

The Flowtime results for the limestone and gravel aggregates are statistically significantly better (positive coefficients) than the average Flowtime results for all three aggregates (Table 12). The granite aggregate has statistically significant lower (negative coefficient) Flowtime results than the average for all three aggregates.

DSR Creep Test Aggregate Evaluation

A comparison of the Flowtime results for the individual aggregates is shown in Table 13. The limestone aggregate performs significantly better than granite aggregate, while the gravel aggregate performs significantly better than the granite aggregate as well. However, the limestone aggregate does not have statistically significantly better Flowtime performance than the gravel aggregate.

Comparative aggregate evaluation of the Time to 5% Strain shows that limestone performs statistically significantly better than both granite and gravel and that gravel continues to perform better than granite (Table 14). Thus one could conclude that the ultimate failure strength of both the limestone and gravel mixes is similar but that the initial deformation rates of the gravel mixes are higher than those of the limestone mixes.

TABLE 13—*Evaluation of comparative aggregate performance for DSR creep test Flowtime to failure results. (Flowtime results are Log transformed; coefficient values reflect transformation.)*

Aggregate A	Aggregate B	Coefficient of A relative to B$^{\text{NOTE 1}}$	p-value of A relative to B$^{\text{NOTE 2}}$	COMMENT
Limestone	Granite	+ 0.81	0.0000	Limestone performs better than Granite at a statistically significant level
Limestone	Gravel	+ 0.12	0.1968	Limestone performs better than Gravel, but not at a statistically significant level
Gravel	Granite	+ 0.69	0.0000	Gravel performs better than Granite at a statistically significant level

NOTE 1–Aggregate A column is compared to Aggregate B column, a positive coefficient means result for Aggregate A is greater than result for Aggregate B.

NOTE 2–p-value determines whether performance of Aggregate A relative to Aggregate B is statistically significant. Lack of statistical significance implies no discernable difference in performance, regardless of whether or not the result for Aggregate A is greater than the result for Aggregate B.

TABLE 14—*Evaluation of comparative aggregate performance for DSR creep test time to 5 % strain results. (Time to 5 % strain results are log transformed; coefficient values reflect transformation.)*

Aggregate A	Aggregate B	Coefficient of A relative to B$^{\text{NOTE 1}}$	p-value of A relative to B$^{\text{NOTE 2}}$	COMMENT
Limestone	Granite	+ 1.02	0.0000	Limestone performs better than Granite at a statistically significant level
Limestone	Gravel	+ 0.356	0.0001	Limestone performs better than Gravel at a statistically significant level
Gravel	Granite	+ 0.65	0.0000	Gravel performs better than Granite at a statistically significant level

NOTE 1–Aggregate A column is compared to Aggregate B column; a positive coefficient means result for Aggregate A is greater than result for Aggregate B.

NOTE 2–p-value determines whether performance of Aggregate A relative to Aggregate B is statistically significant. Lack of statistical significance implies no discernable difference in performance, regardless of whether or not the result for Aggregate A is greater than the result for Aggregate B.

DSR Creep Test Binder Evaluation and Comparison to Hamburg Test Results

The binders have a different impact on the DSR Creep Test results than they do for the Hamburg Wheel Tracking results. The Flowtime result for PG 64-28P does not show up as statistically significantly different than the average Flowtime result for all binders across all aggregates and mix levels. PG 58-28 and PG 64-28C are significantly worse (negative coefficient), while the PG 64-34 and PG 70-28 are significantly better (positive coefficient) than the average Flowtime result for all binders. The comparative performance of individual binders on the Flowtime test shown in Table 15 ranks the binders from worst to best as PG 58-28, PG 64-28C, PG 64-28P, PG 64-34, and PG 70-28.

This is in contrast to the impact of the different binders on the Hamburg results. The ranking of binders for Cycles to Onset of Stripping from worst to best is PG 58-28, PG 64-28C, PG 64-34, PG 64-28P, PG 70-28, but there was no significant difference between PG 58-28, PG 64-28C, or PG 64-34.

TABLE 15—*Evaluation of comparative binder performance for DSR creep test Flowtime to failure results. (Flowtime results are log transformed; coefficient values reflect transformation.)*

Binder A	Binder B	Coefficient of A relative to B[NOTE 1]	p-value of A relative to B[NOTE 2]	COMMENT
PG 64-28C	PG 58-28	+ 0.33	0.0152	PG 64-28C performs better than PG 58-28 at a statistically significant level
PG 64-34	PG 58-28	+ 1.46	0.0000	PG 64-34 performs better than PG 58-28 at a statistically significant level
PG 64-34	PG 64-28C	+ 1.13	0.0000	PG 64-34 performs better than PG 64-28C at a statistically significant level
PG 64-28P	PG 64-34	- 0.54	0.0000	PG 64-28P performs worse than PG 64-34 at a statistically significant level
PG 64-28P	PG 64-28C	+ 0.61	0.0000	PG 64-28P performs better than PG 64-28C at a statistically significant level
PG 70-28	PG 64-28P	+ 1.02	0.0000	PG 70-28 performs better than PG 64-28P at a statistically significant level
PG 70-28	PG 64-34	+ 0.48	0.0001	PG 70-28 performs better than PG 64-34 at a statistically significant level

NOTE 1–Binder A column is compared to Binder B column, a positive coefficient means result for Binder A is greater than result for Binder B.

NOTE 2–p-value determines whether performance of Binder A relative to Binder B is statistically significant. Lack of statistical significance implies no discernable difference in performance, regardless of whether or not the result for Binder A is greater than the result for Binder B.

DSR Creep Test Mix Level Evaluation and Comparison to Hamburg Results

Evaluation of mix levels exhibits similar statistical significance on the DSR Creep Test Flowtime result (Table 16), as the impact of mix levels on the Hamburg Wheel Tracking Test results for Cycles to Stripping Onset (Table 11). The ranking of mix levels from worst to best is E-0.3, E-1, E-3, and E-10. However, E-0.3, compared to E-1 mix levels, and E-3 compared to E-10 mix levels, are not statistically different. The only difference between the mix level impact on the Hamburg and the DSR Creep results is that mix level, when significant, occurs (predominantly) at the 95 % confidence level for the Hamburg test and at the 99.9 % confidence level for the DSR Creep test.

TABLE 16—*Evaluation of comparative mix level performance for DSR creep test Flowtime to failure.*

Mix Level A	Mix Level B	Coefficient of A relative to B[NOTE 1]	p-value of A relative to B[NOTE 2]	COMMENT
E-1	E-0.3	+0.04	0.7385	E-1 mixes perform better than E-0.3 mixes, but not at a statistically significant level
E-3	E-0.3	+ 0.58	0.0000	E-3 mixes perform better than E-0.3 mixes at a statistically significant level
E-10	E-0.3	+0.83	0.0000	E-10 mixes perform better than E-0.3 mixes at a statistically significant level
E-3	E-1	+ 0.54	0.0000	E-3 mixes perform better than E-1 mixes at a statistically significant level (for all except granite)
E-10	E-1	+ 0.79	0.0000	E-10 mixes perform better than E-1 mixes at a statistically significant level
E-10	E-3	+ 0.26	0..0321	E-10 mixes perform better than E-3 mixes at a statistically significant level (for limestone mixes only)

NOTE 1–Mix Level A column is compared to Mix Level B column, a positive coefficient means result for Mix Level A is greater than result for Mix Level B.

NOTE 2–p-value determines whether performance of Mix Level A relative to Mix Level B is statistically significant. Lack of statistical significance implies no discernable difference in performance, regardless of whether or not the result for Mix Level A is greater than the result for Mix Level B.

Impact of Interaction Effects

The DSR Creep Test results are influenced to a greater extent by the interaction between input variables than were the Hamburg Wheel Tracking test results. Only two interaction terms (Gravel*E-0.3 and Gravel*E-10) had any level of impact on the HWT results. Most of the interaction terms listed in Table 5 are statistically significant at some level for the 1/Slope, Time to 5 % Strain, and Flowtime results. For the aggregate and binder interaction terms (terms 13–20 shown in Table 5), the result for any specific term is based on a comparison of the actual data, the specific combination of variables versus the value predicted by just adding together the first order effect values for each variable. As an example, the Flowtime result for the interaction term of Granite * PG 58-28 has a positive coefficient of 0.26 and a p-value of 0.0362. This means that the interaction of granite aggregate and PG 58-28 binder has an average Flowtime value that is greater than and statistically significant compared to the result that would be predicted by adding the average Flowtime result for granite to the average Flowtime result for PG 58-28. In other words, the interaction term predicts a synergistic result for this interaction. If the interaction had been antagonistic, the sign on the coefficient would have been negative, and if the interaction of the two variables was merely additive, the coefficient would have been zero, but it also would not be listed in Table 12 because it would not have been statistically significant. An example of a negative Flowtime coefficient is term 16, the interaction term of granite*PG 70-28. This interaction is statistically significant ($p = 0.0361$), but the coefficient is –0.26. Physically, this result means that there is an antagonistic interaction between the two variables compared to the result predicted from adding the average result for granite and the average result for PG 70-28. This is most likely due to the very good Flowtime results for most of the samples using PG 70-28 compared to the not very good Flowtime results for granite mixes. Based on these examples, it should be possible to understand where there are synergistic and antagonistic effects in Table 12.

For the aggregate binder interactions, there are 15 combinations that can be evaluated relative to each other. For example, this means that for just the Granite*PG 58-28 interaction term there are 14 possible combinations to evaluate. In total, there are 105 combinations to evaluate. All of those possible combinations are not shown in this paper. Concentrating just on the terms in Table 12, which are significant for Flowtime, there are 15 possible combinations to evaluate. Some comparisons, such as those involving Granite*PG58-28 are not very interesting because that combination is obviously a poor performer in the Flowtime test relative to other combinations. When comparing interaction terms, it is perhaps more interesting to examine those comparisons that are not statistically significant or those that might not be thought to be significant but are. Table 17 is a sampling of terms that are of interest. The data in Table 17 show that granite mix using polymer modified PG 64-28 performs at the same strength level as limestone mix using PG 64-28 acid modified. The same can be said of granite mix using polymer modified PG 64-28 and gravel mix using acid modified PG 64-28. Also note that gravel mix using PG 64-34 performs at a statistically superior level to granite mix using PG 70-28.

TABLE 17—*Evaluation of comparative aggregate*binder interaction performance for DSR creep test Flowtime to failure results. (Flowtime results were evaluated in non transformed format for the evaluation in the table.)*

Aggregate Binder A	Aggregate Binder B	Coefficient of A relative to B NOTE 1	p-value of A relative to B NOTE 2	COMMENT
Granite*58-28	Limestone*58-28	-255.2	0.00296	Granite*58-28 mix performs worse than Limestone*58-28 at a statistically significant level
Granite*64-34	Granite*64-28P	+212	0.5498	Granite*PG 64-34 mix performs better than Granite*PG 64-28P, but not at a statistically significant level
Granite*64-28P	Limestone*64-28C	+ 153	0.6061	Granite*64-28P mix performs better than Limestone*64-28C, but not at a statistically significant level
Gravel*64-28C	Granite*64-28P	+ 43.43	0.9026	Gravel*64-28C mix performs better than Granite*64-28P, but not at a statistically significant level
Gravel*70-28	Limestone*70-28	+ 16 772	0.4566	Gravel*70-28 mix performs better than Limestone*70-28, but not at a statistically significant level
Limestone*70-28	Limestone*64-34	+ 16 335	0.2487	Limestone*70-28 mix performs better than Limestone*64-34, but not at a statistically significant level
Gravel*70-28	Granite*70-28	51 477	0.0000	Gravel*70-28 mix performs better than Granite*70-28 at a statistically significant level.
Gravel*70-28	Gravel*64-34	+ 41 070	0.0044	Gravel*70-28 mix performs better than Gravel*64-34 at a statistically significant level.
Gravel*64-34	Granite*70-28	+ 10 406	0.0057	Gravel*64-34 mix performs better than Granite*70-28 at a statistically significant level

NOTE 1–Column A interaction is compared to Column B interaction, a positive coefficient means result for Column A is greater than result for Column B.

NOTE 2–p-value determines whether performance of Column A interaction relative to Column B interaction is statistically significant. Lack of statistical significance implies no discernable difference in performance, regardless of whether or not the result for Column A is greater than the result for Column B.

For the aggregate mix level interactions, there are 66 possible comparisons to be made between the 3 aggregates and 4 mix levels. Once again, the significant combinations are identified in Table 12. Comparisons of some combinations are shown in Table 18. Comparisons that might not be obvious have been selected. For example, the Gravel*E-3 combination shows up as statistically significant compared to Granite*E-10, even though the Gravel*E-3 interaction term did not show up as significant in comparison to overall average Flowtime response, and hence is not shown in Table 12. The same is true for Limestone*E-3 compared to Granite*E-3. The Limestone*E-10 combinations perform at the same statistical level as do Gravel and E-3; Limestone*E-3 mixes perform at the same statistical level as do the Gravel*E-10 mixes; and Limestone*E-1 mixes perform equivalently to Granite*E-10 mixes. It is possible that the overwhelming performance of the Limestone aggregate on the Flowtime test at all mix levels with all binder grades is responsible for many of the interaction results (both statistically significant and non-significant) shown in Table 18.

TABLE 18—*Evaluation of comparative aggregate*mix level interaction performance for DSR creep test Flowtime to failure results. (Flowtime results were evaluated in non transformed format for the evaluation in the table.)*

Aggregate Mix Level A	Aggregate Mix Level B	Coefficient of A relative to B[NOTE 1]	p-value of A relative to B[NOTE 2]	COMMENT
Gravel*E-3	Granite*E-10	+ 5 784	0.0000	Gravel*E-3 mix performs better than Granite*E-10 at a statistically significant level
Limestone*E-3	Granite*E-10	+ 4 000	0.0006	Limestone*E-3 mix performs better than Granite*E-10 at a statistically significant level
Limestone*E-10	Gravel*E-3	+ 33 066	0.0002	Limestone*E-10 mix performs better than Gravel*E-3, but not at a statistically significant level
Limestone*E-3	Gravel*E-10	+ 1 169	0.5979	Limestone*E-3 mix performs better than Gravel*E-10, but not at a statistically significant level
Limestone*E-1	Granite*E-10	+ 132	0.7646	Limestone*E-1 mix performs better than Granite*E-10, but not at a statistically significant level
Gravel*E-1	Granite*E-10	+ 454	0.3833	Gravel*E-1 mix performs better than Granite*E-10 at a statistically significant level
Gravel*E-1	Granite*E-3	+ 678	0.1576	Gravel*E-1 mix performs better than Granite*E-3, but not at a statistically significant level

NOTE 1–Column A interaction is compared to Column B interaction, a positive coefficient means result for Column A is greater than result for Column B.

NOTE 2–p-value determines whether performance of Column A interaction relative to Column B interaction is statistically significant. Lack of statistical significance implies no discernable difference in performance, regardless of whether or not the result for Column A is greater than the result for Column B.

Comparison of Rutting and Deformation Behavior from the Hamburg and DSR Creep

Although both the Hamburg Wheel Tracking Test and the DSR Creep Test are measures of mixture strength and resistance to deformation, they measure different aspects of the mix. When performed under water, the Hamburg Wheel Tracking Test indicates the response of a given mix to moisture and the mix's tendency to lose cohesive strength due to moisture damage. The DSR Creep Test, because it is performed dry, is a measure of mix strength due to aggregate structure and binder stiffness and elasticity. Figure 18 shows the difference between the same mix tested wet and dry in the Hamburg Wheel Tracker. The wet test, performed at 50°C compared to the dry test performed at 58°C, fails much more rapidly and displays the typical stripping and rutting slopes. The dry test displays a single, smooth line indicative of only rutting behavior. Allowing for these differences, it might be anticipated that results from the Hamburg Wheel Tracking Test and the DSR Creep Test should correlate to some extent. Linear regressions of non-transformed data between Cycles to 12.5 mm of Rutting and Time to 5 % Strain for several of the mix types for all the binders were examined. (R^2 data are shown in Table 19).

TABLE 19—*R^2 values for time to 5 % strain vs. cycles to 12.5 mm rut.*

Aggregate Type and Mix Level (all AC Grades were considered)	R^2 for the regression of DSR Creep Time to 5 % Strain as a function of HWT Cycles to 12.5 mm rut depth
Granite E-0.3	0.91
Granite E-1	0.90
Granite E-3	0.80
Gravel E-1	0.57
Gravel E-3	0.78
Gravel E-10	0.52
Limestone E-0.3	0.002
Limestone E-3	0.017
Limestone E-10	0.67

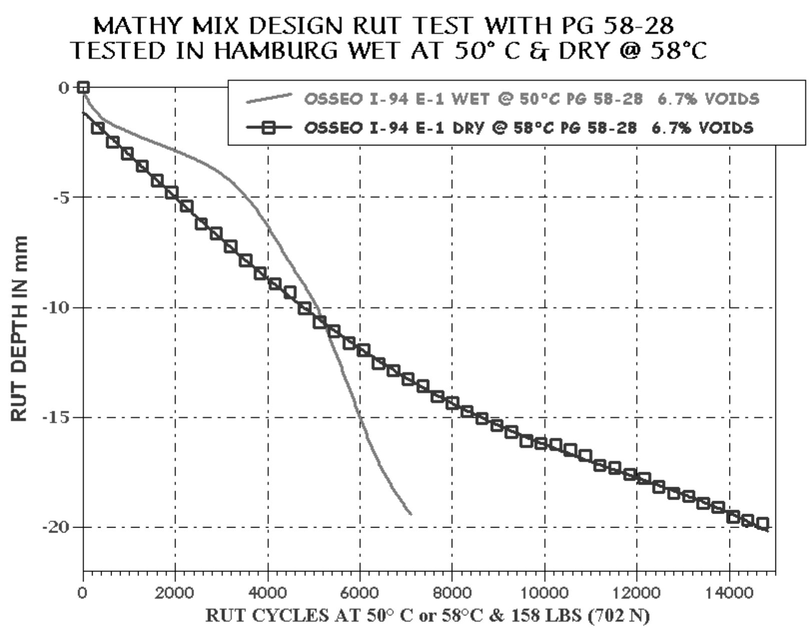

FIG. 18—*Plot comparing HWT results for wet and dry tests.*

It does appear for mixes that are more resistant to stripping (the granite mixtures) that the Hamburg Wheel Tracking test is a fairly good indicator of mixture strength as measured on dry sample using DSR Creep. However, as the mix becomes more susceptible to moisture attack, as shown in the gravel and the limestone mixtures, the resistance to permanent deformation as measured dry is less well predicted by the behavior in the rutting portion of the Hamburg Wheel Tracking Test. A plot comparing Hamburg Cycles to 12.5 mm and DSR Creep Test Time to 5 % Strain resulted in a very weak correlation of $R^2 = 0.27$ with a positive slope indicating that better Hamburg results were directionally matched to better DSR creep results. However, the lack of a strong correlation further demonstrates that the wet and dry tests are measuring different mixture properties.

Multiple Linear Regression of Aggregate, Binder, and Mix Properties

Analysis of the experimental design has shown the impact of different aggregate types, PG binder grades, and mix levels on moisture sensitivity as determined by the Hamburg Wheel Tracking test and resistance to permanent deformation as determined by the DSR Creep Test. These results are in some cases expected—the relative impact of PG binder grades, for example. In some cases the results are unexpected—the relatively poorer HWT performance of limestone mixes compared to granite and gravel mixes and yet the much better performance of limestone and gravel mixes compared to the granite mixes in the DSR Creep Test. The results in yet other cases are puzzling—the lack of significant difference between E-3 and E-10 mixes and between E-0.3 and E-1 mixes. The binders and mixtures have physical properties which should help to elucidate the impact of the design variables on the experimental outcomes and explain the unexpected results noted above. Early in the HWT testing it was noticed that differences in the number of gyrations required to produce the 61 mm specimens seemed to coincide with differences in performance during the test. Therefore, the gyration data for each specimen was recorded, and ultimately the average number of gyrations for the 4 specimens that were used for each trial was determined. In addition to the gyration data for the Hamburg test specimens, the high temperature binder properties at 50°C and 58°C (Table 2) and mixture properties of VMA, VFA, and Effective Asphalt Content (Table 1) were measured or calculated. Number of mix gyrations, VMA, and Effective Asphalt Content can also be viewed as indirect indicators of aggregate structure and absorption. This set of binder and mixture characteristics was used in a series of multiple linear regression analyses of the response outcomes of this study. This effort is somewhat compromised because, for example, all limestone E-0.3 mixes have the same Effective AC content and the same VMA, regardless of binder. All mixes produced with a given binder grade will use the same cumulative strain; phase angle and zero shear viscosity data. Nevertheless, the analysis has provided insight into binder and mixture physical properties influence on the outcomes of these tests.

An evaluation of log Flowtime for several of the mixtures as a function of log percent cumulative strain of binders at both 50°C and 58°C resulted in R^2 values greater than 0.8 and in many cases greater than 0.9. The slopes of the relationships were negative, showing that as binder cumulative strain decreased, the Flowtime to failure value increased. This is strong evidence that a substantial amount of the variation in the Flowtime results of the mixtures is due to the binders' elastomeric properties. Alternatively, looking at log Cycles to Onset of Stripping as a function of log percent binder cumulative strain at 50°C resulted in R^2 values that ranged from 0.114–0.726, with most being the in 0.3–0.5 range. Again, the slopes of these relationships were negative. Clearly, decreasing the binder cumulative strain (indicating greater elastomeric character) has some impact on the speed with which stripping begins in the Hamburg Wheel Tracking test, but there must be other factors that are equally or more important. To further pursue the materials' properties that influence the experimental design outcomes, several stepwise multiple linear regression analyses were performed using single term deletions and allowing for inclusion or removal of independent variables to improve the fit of the model.

Four response variables were investigated: Log of Cycles to Onset of Stripping, Log of Cycles to 12.5 mm Rut Depth, Log of Time to 5 % Strain, and Log of Flowtime. All possible input variables related to physical properties of the mixes or binders were available to the multiple linear regression software to enter into the model. These variables were Effective Asphalt Content, VMA, VFA, Gyrations, binder cumulative strain at 50°C, (binder cumulative strain at 50°C)^2, binder cumulative strain at 58°C, Phase Angle at 58°C, Eta Zero, η_0, at 50°C (Low Shear Viscosity at 0.01 radians/s), Eta Zero, η_0, (Low Shear Viscosity at 0.01 radians/s) at 58°C, and the SHRP DSR test value (G*/sin(δ)) at 58°C. The models chosen and the multiple R^2 results are shown in Table 20. Also included with the information for each term in Table 20 is an indication of whether the mathematical sign of the term is positive (POS) or negative (NEG) and the p-value significance of the term to the overall regression.

TABLE 20—*Results of multiple linear regression analysis.*

Response Variable	Multiple R^2	Term 1	Term 2	Term 3	Term 4	Term 5	Term 6	Term 7	Term 8
Log Cycles Onset to Stripping	0.827	Effective AC NEG p= 0.135	VMA POS p= 0.032	Gyrations POS p= 0.0000	% Strain @ 50°C NEG p= 0.0000	(% Strain @ 50°C)^2 POS p= 0.0000	% Strain @ 58° C POS p= 0.0698	Phase Angle at 58°C POS p= 0.0000	No term 8 in this model
Log Cycles to 12.5 mm Rut Depth	0.88	Effective AC NEG p= 0.1081	VMA POS p= 0.0394	Gyrations POS p= 0.0000	% Strain @ 50°C NEG p= 0.0000	(% Strain @ 50°C)^2 POS p= 0.0000	% Strain @ 58° C POS p= 0.0005	Phase Angle at 58°C POS p=0.1617	No term 8 in this model
Log Time to 5% Strain	0.869	Effective AC NEG p= 0.0000	VMA POS p= 0.0008	VFA NEG p= 0.0046	% Strain @ 50°C NEG p= 0.0684	(% Strain @ 50°C)^2 POS p= 0.0000	% Strain @ 58° C NEG p= 0.1368	Phase Angle at 58°C POS p= 0.0858	Eta zero @ 58° C NEG p= 0.0174
Log Flowtime	0.86	Effective AC NEG p= 0.0000	VMA POS p= 0.009	VFA NEG p= 0.0008	% Strain @ 50°C NEG p= 0.136	(% Strain @ 50°C)^2 POS p= 0.0159	% Strain @ 58° C NEG p= 0.0766	Phase Angle at 58°C POS p= 0.1265	Eta zero @ 58° C NEG p= 0.0105

For some of the terms, the mathematical sign is opposite that obtained by just calculating the impact of the data on the response. For example, Effective AC has a negative coefficient for Log of Cycles to Onset of Stripping, while the plot of Effective AC versus Log of Cycles to Onset has a positive slope. However, the R^2 for that plot is poor (0.047), and as the p-value for the multiple regression analysis shows, Effective AC is not a significant influence on the outcome.

When examining the data in Table 20, it is best to bear in mind that the multiple regression analysis is attempting to arrive at the best fit to the results data. The analysis program has no insight into the physical meaning of the inputs. Gyrations were not allowed as a potential variable for the Time to 5 % Strain or Flowtime responses because the gyration data collected applied only to the Hamburg test specimens. It is also worth pointing out that, although available to the model building process, the DSR G*/sin(δ) result at 58°C was never chosen for inclusion. Binder characteristics, which are capable of indicating the presence of elastomeric properties (% cumulative strain, phase angle) or resistance to flow (Eta zero), were the ones consistently included in the model. Also, Effective AC and VMA were consistently chosen for inclusion into all of the models.

In a separate investigation, multiple linear regression analysis was performed for the four responses shown in Table 20 using only binder properties as possible terms to include in the model. In all cases the multiple R^2 for only the binder related variables was 0.71 or greater. Alternatively when the multiple regression analysis was performed using only aggregate or mix related properties, the R^2 results were between 0.13 and 0.34. It would appear from these analyses that binder characteristics have a highly significant impact on mixture performance for both moisture sensitivity and permanent deformation.

The results discussed above lead to conclusions about the unexpected and puzzling results of the study. Traditionally, limestone aggregates have better moisture sensitivity resistance than granites and siliceous gravels. In this study the limestone performed worse than the gravel and granite on the Hamburg Wheel Tracking test. The relative softness of the limestone has already been discussed as a factor, but the low effective asphalt content of the limestone mixtures (Table 1) must also be considered as a factor explaining both the poorer moisture resistance values as well as the better performance of the limestone mixes on the dry DSR Creep Test compared to the other two aggregates. An examination of Table 4 shows that as a general trend for all aggregate types, the E-0.3 and E-1 mix levels had very similar (and relatively low) gyrations to achieve the target air voids level. Alternatively, the E-3 and E-10 mix levels had similar (and approximately double) gyrations to achieve the target air voids level. Voids filled and effective AC content (Table 1) also tended to be similar for E-03 and E-1 mix levels and for E-3 and E-10 mix levels. Given all of these factors, the similarity in performance between these two groupings of mix levels becomes less surprising.

Findings and Conclusions

A laboratory investigation using two mixture tests, the Hamburg Wheel Tracking Test and the DSR Creep Test, was conducted to evaluate the relative impact of aggregate type, PG binder grade, and mix level on mixture performance as determined by an empirical moisture sensitivity test and a mechanical-empirical permanent deformation test. Comparative results of the different mixture combinations were obtained. Although not part of the original experimental design, an effort was made to relate binder and mixture physical properties to the performance outcomes of the two tests. Based on data for the aggregates, binders, and mix levels, the following information can be summarized.

1. The granite and gravel aggregates performed comparably, and both performed better on the Hamburg Wheel Tracking Test than the limestone aggregate at mix levels above E-0.3 and for all polymer modified binders. There was little to distinguish performance of

E-0.3 level mixes produced using non-polymer modified binders for any of the aggregates.

2. Mixes produced using the two non polymer modified binders and polymer modified PG 64-34 did not perform as well on the Hamburg Wheel Tracking Test compared to mixes produced from the same aggregates and mix levels but using PG 64-28P or PG 70-28. Since the PG 64-34 contained polymer levels similar to the PG 70-28 and also exhibited cumulative strain, phase angle, and zero shear viscosity values comparable to the PG 70-28, it would appear that physical properties of the PG 64-34 and PG 70-28 binders related to their elastomeric character are not the most important factors when evaluating the performance of these binders on a test such as the Hamburg.
3. Limestone mixtures outperformed gravel mixtures, which outperformed granite mixtures on the DSR Creep Test for all binders and all mix levels. This is in contrast to the results for these aggregates on the Hamburg Wheel Tracking Test where the limestone mixtures had the poorest performance for a given aggregate and mix level.
4. The ranking of binder performance for the DSR Creep Test from worst to best was PG 58-28, PG 64-28C, PG 64-28P, PG 64-34, and PG 70-28. For the granite aggregate, PG 58-28, PG 64-28C, PG 64-28P, and PG 64-34 performed comparably with E-0.3, E-1, and E-3 mix levels. PG 70-28 mixtures performed statistically significantly better than other binders with E-3 and E-10 mix levels.
5. Neither the Hamburg Wheel Tracking Test nor the DSR Creep Test exhibited significantly different results for E-0.3 mix compared to E-1 mix or for E-3 mix compared to E-10 mix regardless of PG binder grade or aggregate type. If there are four mix levels that behave as two, then the need for this number of mix levels should be re-examined. Either the number of mix levels should be reduced or the performance requirements of the mix levels should be such that they do provide differentiated performance characteristics.

Evaluation of the information summarized above, combined with the mixture and binder data and the multiple linear regression analysis, lead to the following general conclusions.

1. Mix level appears to be equally as important for resistance to stripping onset and failure in the Hamburg test and the mix deformation failure in the DSR Creep Test. E-3 and E-10 mixtures, which performed better than E-0.3 and E-1 mixtures, generally required a higher number of gyrations to produce the 61 mm Hamburg specimens, implying a mix with greater internal angularity.
2. The harder aggregates, granite and gravel, performed better than the softer limestone in the Hamburg test, but the hardest aggregate (granite) performed worse than the limestone and gravel in the DSR Creep test. This may be due in part to the effective asphalt content of the mixtures. The limestone mixes had 5 % or less effective asphalt, the gravel mixes had 5–5.26 % effective asphalt, and the granite mixes generally had 5.5 % effective asphalt.
3. The Hamburg Wheel Tracking Test and the DSR Creep Test do not provide the same information about bituminous mixtures. The R^2 for a log-log regression between DSR Creep Test Flowtime and Hamburg Wheel Tracking Test Cycles to Failure was 0.42 with a positive slope implying, at best, a directional trend between outcomes from the two tests. This is not surprising, considering the differences in relative performance of the

aggregates and binders on the two tests. These differences in performance, however, reinforce the fundamental mechanistic differences between the two tests and possibly between permanent deformation tests performed on dry specimens versus loaded wheel tests performed on submerged specimens.

4. For both the HWT and the DSR Creep Test, binder properties play a significant role. Binder related variables explained approximately 70 % of variation for both HWT results and DSR Creep Test results. Furthermore, binder properties such as cumulative percent strain, zero (low shear) shear viscosity, and phase angle were important in predicting performance as opposed to G*/sin(δ) at the 58°C.
5. For both the HWT and DSR Creep Test mix and aggregate, related properties predicted about 20 % of the variation in HWT and DSR Creep Test results. Gyrations to compact Hamburg specimens and VMA, which reflect internal structure, were the most important mix related factors in predicting HWT results. Effective asphalt content, VMA, and VFA were the mix related factors that were important in predicting DSR Creep Test results. There appears to be no performance trend for either test directly related to crushed faces of larger particles. The gravel aggregate had the lowest percent (83–85 %) of crushed faces and performed better than limestone with 99 % two crushed faces on the Hamburg Wheel Tracking Test and better than the granite (95–98 % two crushed faces) mixes on the DSR Creep Test.

References

[1] Cooley, L. A. Jr., Kandhal, P., Buchanan, Shane, M., Fee, F., and Epps, A., "Loaded Wheel Testers in the United States: State of the Practice," *Transportation Research E-Circular,* Number E-C016, July 2000, 21 pp.

[2] Aschenbrener, T., McGennis, R. B., and Terrel, R. L., "Comparison of Several Moisture Susceptibility Tests to Pavements of Known Field Performance," *Proceedings of the Association of Asphalt Paving Technologists*, Vol. 64, 1995, pp. 163–208.

[3] Romero, P. and Stuart, K., "Evaluating Accelerated Rut Testers," Turner Fairbanks Website, at http://www.tfhrc.gov/pubrds/julaug98/evaluating.htm, viewed on 24 May 2003.

[4] Aschenbrener, T., "Evaluation of Hamburg Wheel-Tracking Device to Predict Moisture Damage in Hot-Mix Asphalt," *Transportation Research Record 1492-Hot-Mix Asphalt Design, Testing, Evaluation and Performance*, 1995, pp. 193–201.

[5] Izzo, R., and Tahmoressi, M., "Testing Repeatability of the Hamburg Wheel-Tracking Device and Replicating Wheel-Tracking Devices Among Different Laboratories," *Proceedings of the Association of Asphalt Paving Technologists*, Vol. 68, 1999, pp. 589–612.

[6] Mohammad, L., Zhang, X., Huang, B., and Tan, Z., "Laboratory Performance Evaluation SMA, CMHB, and Dense Graded Asphalt Mixtures," *Proceedings of the Association of Asphalt Paving Technologists*, Vol. 68, 1999, pp. 252–283.

[7] Reinke, G., and Dai, S., "Performance Properties of Three Mixes Constructed at the MNROAD Test Site," *Canadian Technical Asphalt Association Proceedings*, Vol. XLVI, 2001, pp. 213–248

[8] Reinke, G. and Glidden, S., "Development of Mixture Creep Performance Tests Using a Dynamic Shear Rheometer," An invited presentation for Session 300 at the 2002 Transportation Research Board meeting, *TRB E-Circular E-C068 New Simple Performance Tests for Asphalt Mixes*, September 2004, Transportation Research Board.

[9] Bahia, H. U., Hanson, D. I., Zeng, M., Zhai, H., Khatri, M. A., and Anderson, R. M., "NCHRP Report 459: Charcterization of Modified Asphalt Binders in Superpave Mix Design," *National Cooperative Highway Research Program* 2001, pp. 49–59.

[10] Witczak, M. W., Kaloush, K., Pellinen, T., El-Basyouny, M., and Von Quintus, H., "NCHRP Report 465: Simple Performance Test for Superpave Mix Design," *National Cooperative Highway Research Program*, 2002, p. 10.

[11] Romero, P. and Anderson, R. M., "Variablility of Asphalt Mixture Tests Using Superpave Shear Tester Repeated Shear at Constant Height Test," *Transportation Research Record 1767—Asphalt Mixtures*, 2001, pp. 95–101.

[12] Stuart, K. D., Youtcheff, J. S., and Mogawer, W. S., "Understanding the Performance of Modified Asphalt Binders in Mixtures: Evaluation of Moisture Sensitvity," *National Cooperative Highway Research Program Project 90-07, FHWA-RD-02-029*, December 11, 2001.

[13] Rand, D. A., "HMA Moisture Sensitivity: Past, Present, and Future TxDOT Experiences," *Moisture Damage Symposium*, Western Research Institute, July 17–19, 2002, Laramie, WY. Available at: http://www.westernresearch.org/content/technology_areas/asphalt_materials/MDSymp.shtml.

[14] Phillips, M. C. and Robertus, C., "Binder Rheology and Asphaltic Pavement Permanent Deformation: The Zero Shear Viscosity," First Eurasphalt and Eurobitume Congress, Strasbourg, 1996, Paper No. 5.134.

[15] Sybiliski, D., "Zero Shear Viscosity of Bituminous Binder and Its Relation to Bituminous Mixtures Rutting Resistance," Transportation Research Record 1535, TRB, 1996.

Journal of ASTM International, April 2005, Vol. 2, No. 4
Paper ID JAI12261
Available online at www.astm.org

Rebecca S. McDaniel,[1] *Victor L. Gallivan,*[2] *Gerald A. Huber,*[3] *David H. Andrewski,*[4] *and Mark Miller*[4]

Use of HMA Stiffness Results as a Referee Test in Indiana

ABSTRACT: The Indiana Department of Transportation (INDOT) began implementing volumetric acceptance of hot mix asphalt (HMA) mixtures in 2001. In some cases the air void contents of the plant-produced mixtures have been less than 2.0 %. Rather than require removal and replacement of low air void mixes in all cases, INDOT implemented an optional referee testing procedure. This procedure allows contractors to leave low air void material in place, at reduced pay, if the stiffness of the placed material is equal to or greater than a specified minimum. If the stiffness is less, that sublot must be removed and replaced. The rationale is that if the stiffness is high enough, even if the air voids are low, the material would be expected to perform adequately. If the low air voids are accompanied by low stiffness, rutting performance would likely be compromised. This paper describes the rationale, development, and implementation of this program.

KEYWORDS: hot mix asphalt, air voids, stiffness, volumetric acceptance, referee testing, frequency sweep

Introduction

The Indiana Department of Transportation (INDOT) began implementing volumetric acceptance of hot mix asphalt (HMA) mixtures in 2001. The program was fully implemented on all INDOT HMA projects in 2003. Under this program, Voids in the Mineral Aggregate (VMA), air voids, binder content, and roadway density (from cores) are considered in determining payment. The values needed to calculate the volumetric properties are based on roadway (plate) samples from behind the paver. Binder content and maximum specific gravity are determined from the plate samples. Other plate samples are compacted in the Superpave Gyratory Compactor to N_{design} for determination of the bulk specific gravity of the mix, VMA, and air voids. Indiana uses N_{design} values as specified in AASHTO PP28, "Standard Practice for Superpave Volumetric Design for Hot Mix Asphalt (HMA)."

The plate samples are located at randomly selected locations within each sublot. Two plate samples are collected. The first is located at the random location, and the second is 0.6 m (2 ft) from the first plate toward the center of the mat. A third plate sample is collected for surface mixtures at a location 0.6 m (2 ft) back from the first. Minimum sample sizes and plate sizes are specified in Indiana Test Method 580, "Sampling HMA" [1].

Lots are 4000 Mg (4000 t) for base or intermediate mixtures and 2400 Mg (2400 t) for

---

Manuscript received 1 December 2003; accepted for publication 23 September 2004; published April 2005.
Presented at ASTM Symposium on Performance of Hot Mix Asphalt (HMA), including Fundamental and Empirical Procedures on 9 December 2003 in Tampa, FL.
[1]Technical Director, North Central Superpave Center, P.O. Box 2382, West Lafayette, IN 47906.
[2] Pavement and Materials Engineer, Federal Highway Administration, Indiana Division, 575 N. Pennsylvania Street, Room 254, Indianapolis, IN 46204.
[3]Associate Director of Research, Heritage Research Group, 7901 West Morris Street, Indianapolis, IN 46231.
[4]Materials Engineer and Chief, respectively, Division of Materials and Tests, Indiana Department of Transportation, 120 South Shortridge Road, Indianapolis, IN 46219.

surface mixtures. Each lot is sub-divided into sublots of 1000 Mg (1000 t) or less for base or intermediate mixtures or 600 Mg (600 t) for surface mixtures.

Initial experience with the volumetric acceptance program revealed some cases where the air void contents of the gyratory compacted plant-produced mixtures were low (less than 2.0 %). According to standard INDOT procedures, after one failing test result, retained samples were also tested. If these samples also exhibited low air void contents, the program called for that sublot to be treated as failed material and to be referred to the Failed Materials Committee for adjudication. Removal and replacement of the suspect sublots at the contractor's expense was the obvious solution, though the Failed Materials Committee does have the latitude to consider extenuating circumstances.

Rather than require removal and replacement of low air void mixes in all cases, INDOT implemented an optional referee testing procedure that could be used for sublots with low air voids. This procedure allows contractors to leave low air void material in place, at reduced pay, if the stiffness of the placed material is adequate. If the results of frequency sweep testing in the Superpave Shear Tester (SST) show that the material has a modulus (G*) equal to or greater than a minimum specified value, the material may be left in place. If the stiffness is less, that sublot must be removed and replaced. The rationale is that if the stiffness is high enough, even if the air voids are low, the material would be expected to perform adequately. If the low air voids are accompanied by low stiffness, performance would likely be compromised.

The remainder of this paper describes the procedures, rationale, development, and implementation of this referee testing program in Indiana. A summary of experiences to date is also provided.

Referee Testing Procedures

In those cases where initial acceptance testing of the retained samples reveals mixtures with air void contents at N_{design} of less than 2.0 %, the contractor may elect to submit pavement samples for stiffness testing before the sublot is considered by the Failed Materials Committee. Pavement cores are taken at locations within the sublot specified by the INDOT Engineer; these locations approximate the location of the acceptance sample. INDOT witnesses the coring and takes immediate possession of the cores for transport to the testing laboratory. Three cores are required for base and intermediate course mixtures, and six cores are required for surface courses. The contractor is responsible for coring, traffic control and SST testing costs.

Cores are then submitted to a laboratory for SST frequency sweep testing. Four laboratories are cited in the testing procedure, including the North Central Superpave Center, Heritage Research Group, the Asphalt Institute, and the National Center for Asphalt Technology.

The cores are sawn to isolate the suspect layer and are prepared for testing. The SST testing requires a specimen 150 mm in diameter and 50 mm thick. Since surface courses in Indiana are generally thinner than 50 mm, the protocol allows for gluing two cores together, as described later.

Each of the three final specimens is then tested in the frequency sweep test at 40°C in accordance with AASHTO TP7, Standard Test Method for Determining the Permanent Shear Strain and Stiffness of Asphalt Mixtures Using the Superpave Shear Tester (SST). The frequency sweep test applies a repeated shear load in a horizontal direction at a wide range of frequencies from 0.01 Hz to 10 Hz, producing a controlled peak strain of 0.005 %. During the test, an axial load is applied as required to keep the specimen height constant. The frequency sweep test allows determination of the complex shear modulus (G*) and phase angle (δ) of a mixture. This referee testing is conducted at 40°C (AASHTO TP7-94, Procedure E). The stiffness at 10 Hz is used to determine the shear stiffness of the material for referee testing purposes.

If the average shear modulus of three tests is greater than or equal to 250 MPa (36 200 psi), at 10 Hz and 40°C, the suspect material can be left in place, at reduced pay. If the stiffness is less than 250 MPa (36 200 psi), the material must be removed and replaced at contractor's expense.

Rationale for the Referee Testing

This referee testing program is based on the results of several research projects coupled with experience in the state. It is important to understand that INDOT adopted and implemented Superpave technology at a more aggressive pace than many other states. The first Superpave project was placed in Indiana in 1993, and implementation of the binder and mixture specifications proceeded rapidly. INDOT was one of the AASHTO Lead States for Superpave based on their early experiences with the system. For one of Indiana's first HMA warranty projects in 1995, the contractor elected to use a Superpave mix design instead of a more familiar Marshall mix design to get some indication of the performance of the mix over the life of the warranty (five years). In short, INDOT and industry were generally receptive to Superpave technology.

Marshall designed mixtures were accepted based on asphalt content and gradation. Volumetric properties, air voids, and VMA were quality control properties monitored by the contractor. When Superpave was implemented, the same acceptance and quality control procedures were initially used. Once Superpave mix design was fully implemented, however, it was a logical extension to move from acceptance by asphalt content and gradation to acceptance by volumetric properties. Implementation of volumetric acceptance began in 2001, and the program was fully implemented in 2003.

When some low air void material was observed on a few projects in 2001, concerns about possible pavement rutting arose. Industry conducted additional testing in the SST to evaluate the expected rutting performance of these low air void mixes. Results showed, in some cases, that pavement cores had adequate stiffness despite the low air voids measured on gyratory compacted, plant-produced mixture samples. Due to questions about possible test variability in determining the bulk and maximum specific gravities and in internal angles in the Superpave gyratory compactor, the Department was willing to consider other mixture properties when determining whether material had to be removed and replaced.

Shear stiffness of a given HMA is influenced by the temperature and time of loading. At high temperatures, it is well known that HMA becomes softer and more susceptible to rutting. At longer loading times (low frequency) the mix also acts softer. At shorter loading times (high frequency) the mix seems stiffer. This is analogous to dipping a toe in a swimming pool (low frequency) as opposed to diving off the high dive (high frequency). The water feels much stiffer when you hit it at high speed.

An HMA will remain rut resistant as long as the mixture stiffness remains above a minimum. In other words, if the mix is stiff, it will not rut. If the mix becomes too soft, it will rut. The question is, how stiff is stiff enough?

The Asphalt Institute determined a minimum stiffness guideline of 250 MPa (36 200 psi) for high traffic (greater than 10 million ESALs) at free flowing traffic speeds [2]. The validity of this value was confirmed by an evaluation of the performance of the first four pilot Superpave projects conducted by the Heritage Research Group and the Asphalt Institute, when the four pilot sections were six years old [3]. The pilot projects, located in Wisconsin, Indiana, and Maryland, were all performing well. This study revealed that the pilot projects exhibited rutting of six millimeters or less after 3.5–16.5 million ESALs. Mechanical property testing in the SST showed that the frequency sweep test correctly ranked the pavements in terms of rutting. That is, as the shear stiffness decreased, the observed permanent deformation increased. All of these intermediate and surface course mixtures had a stiffness at 10 Hz and 40°C greater than 250 MPa (36 200 psi).

On the strength of this research, INDOT adopted 250 MPa (36 200 psi) as the minimum acceptable stiffness for a low air void mixture to remain in place. INDOT applied this value to base, intermediate, and surface mixtures regardless of traffic, application, or binder grade. It could be argued that base mixtures are subjected to lower stress or that mixes for lower traffic volumes could perform acceptably with a lower stiffness than, say, a surface mix for high traffic. However, the research has been done only for the high traffic condition, and, as a result, INDOT uses a single criterion. In most cases, all mixtures are subjected to traffic during construction, when they are at their most vulnerable. Also, mixtures that are tested under this procedure have already failed two quality tests on the acceptance and retained samples. Lastly, INDOT can consider mitigating factors such as depth in pavement, traffic level, or location (mainline versus shoulder), etc., when determining the appropriate reduced pay factor. That is, a mix used in a less critical application may be subject to a smaller pay reduction than a mix used in a critical application (high stresses, high traffic). Pay reductions are applied because the mixture did not meet specifications.

The temperature of 40°C was selected as the standard test temperature because it is the approximate effective temperature for rutting in Indiana as defined in the Strategic Highway Research Program.

Gluing Specimens for Thin Lifts

To estimate the effect of gluing cores together, Heritage Research Group experimented in the laboratory using road cores [4]. Cores were obtained from lifts that were sufficiently thick to provide a 50 mm test specimen. The mixtures were tested. Then the specimens were sawn in two while still glued to the testing platens. The two halves were glued together using the same epoxy glue used to attach the cores to the platens. The resulting specimen was then approximately 45 mm thick.

Gage points for the shear deformation gages were repositioned on the specimen to provide the required 38 mm gage length, and the specimens were re-tested. Stiffness measurements of the cut and glued specimens were compared to uncut specimens.

Table 1 contains data used for the comparison. For this study, done before the referee testing protocol was established, specimens were tested at 30°C and 50°C. Since the referee protocol for Indiana calls for a test temperature of 40°C, the data were interpolated.

The data in Table 1 are for single test specimens. The comparison shows that there is some variability in the effect. The difference is always negative; that is, the cut and glued specimens are always less stiff than the uncut specimens. The range of difference is 5–35 %. The average difference is 17 %, and the standard deviation is 13 %.

Based on the data in Table 1, if the stiffness of glued specimens is measured in triplicate, there is a 95 % probability that the measured stiffness will be 3–31 % lower than the stiffness of uncut specimens. There is a 67 % probability that the stiffness of the cut specimens would be 10–24 % lower than the uncut specimens.

TABLE 1—*Shear stiffness of cut and uncut specimens.*

Measured Stiffness (10 Hz), psi				Interpolated Stiffness, psi		Change in Stiffness
50°C		30°C		40°C		
Uncut	Cut	Uncut	Cut	Uncut	Cut	Delta
27 605	26 000	132 652	127 662	80 129	76 831	–4 %
34 564	29 681	159 749	136 163	97 157	82 922	–15 %
27 643	25 949	151 293	128 500	89 468	77 225	–14 %
27 049	22 555	149 021	91 735	88 035	57 145	–35 %
					Average	–17 %
					Std Dev	13 %

Note: Percent delta is percent difference of uncut stiffness to cut specimens.

If duplicate specimens are used, there is a 95 % probability that the measured stiffness will be between 5 % higher to 41 % lower than the stiffness of uncut specimens. There is a 67 % probability that the stiffness of the cut specimens would be 5–29 % lower than the uncut specimens.

Based on this analysis, it was recommended that the stiffness of glued specimens be measured in duplicate, and the measured stiffness be divided by 0.85 to estimate the stiffness of an uncut sample. This was later changed to require triplicate specimens be tested and averaged in all cases.

In many cases, it has proven possible to get thick enough surface course specimens without gluing, which allows application of the minimum stiffness requirement without adjusting. From the six field cores submitted for testing, three with thicknesses of at least 38 mm can usually be found. For example, the NCSC lab has never had to glue specimens for testing.

Implementation of the Referee Testing Program

INDOT began implementation of this program in 2002 and continued it through the 2003 construction season. Contractors have elected to use referee testing on many occasions. Records of the number of suspect and acceptable sublots are not maintained, but the percentage of suspect sublots is estimated by INDOT as very low.

In those cases where the contractor has elected to use referee testing, the results have gone both ways. There have been cases where the stiffness was indeed low, and the mixture had to be removed and replaced at the contractor's expense. There have also been cases where the stiffness was high, despite the low air voids, and the mixture was allowed to remain in place. Of the 30 sublots tested to date in 2003, 15 have passed the stiffness limit, and 15 have not. Pay reductions in the cases with acceptable stiffness have ranged from approximately 15–50 %.

Future Application of Referee Testing for Low Air Void Mixtures

The Department intends to monitor the performance of some of these questionable mixtures to determine whether they do in fact perform acceptably. After two years, none of the mixtures that were allowed to remain in place have exhibited premature rutting. These observations may help to refine the criteria for acceptable stiffness in the future. In addition, another research project [5] is looking at HMA stiffness and performance in Indiana using dynamic modulus.

This may also lead to further refinements in the referee testing protocol, although that is not the objective of the project.

Although there are relatively few sublots that exhibit low air voids compared to the vast majority of sublots that meet the desired 3–5 % air void level, INDOT recognizes that the economic impact on the contractor can be significant. A sublot left in place for little or no pay, or one where the contractor has to pay to remove and replace material, can have a major effect on the contractor's profitability on the project. The Department and industry continue to work together to reduce failed materials.

INDOT is sponsoring research aimed at assessing the variability in common testing protocols in Indiana [6]. The Department is also considering basing the pay adjustments for the failed sublot on the overall quality of production. For example, they may look at the mean and/or standard deviation of five sublots (two before and two after) instead of basing decisions on each sublot in isolation. The initial decision to look at individual sublots was made in order to get acceptance testing results back to the contractor as quickly as possible. The result, however, is that there is a great deal riding on the results of one or two test results. The five sublot average could help to reduce the effects of sampling and testing variability and could reduce the number of cases where referee testing is applicable.

Conclusion

Mixture stiffness as measured by the Superpave Shear Tester is being used in Indiana to judge the expected performance of mixtures that fail a minimum air void criterion of 2.0 %.

INDOT will continue allowing referee testing using the SST for the foreseeable future. The SST has been, and will continue to be, a useful tool in this application. The Department will also continue working with industry to reduce the number of times referee testing is applied by improving the quality of the mixtures produced and by understanding and controlling sampling and testing variability where possible.

References

[1] Indiana Department of Transportation, "Indiana Test Method 580, Sampling HMA," August 2003, http://www.in.gov/dot/pubs/itm/index.html.

[2] Heritage Research Group, "Superpave Shear Tester Performance Testing on RS-25519, US 50," October 2001.

[3] Anderson, R. M., Huber, G. A., Walker, D., and Zhang, X., "Mixture Testing, Analysis and Field Performance of the Pilot Superpave Projects: The 1992 SPS-9 Mixtures," *Asphalt Paving Technology 2000*, Association of Asphalt Paving Technologists, Vol. 69, 2000, pp. 177–211.

[4] Heritage Research Group, "Estimation of Effect of Gluing Specimens on Measured Shear Stiffness," June 2002.

[5] Pellinen, T., "Stiffness of Hot Mix Asphalt," Joint Transportation Research Project, SPR 2644, Purdue University, http://rebar.ecn.purdue.edu/JTRP/.

[6] Pellinen, T. and Weiss, J., "Comparison of Various INDOT Testing Methods and Procedures to Quantify Variability in Measured Bituminous and Concrete Properties," Joint Transportation Research Project, SPR 2645, Purdue University, http://rebar.ecn.purdue.edu/JTRP/.

Journal of ASTM International, October 2005, Vol. 2, No. 9
Paper ID JAI12256
Available online at www.astm.org

Soheil Nazarian,[1] *Vivek Tandon,*[2] *and Deren Yuan*[3]

Mechanistic Quality Management of Hot Mix Asphalt Layers with Seismic Methods

ABSTRACT: Realistic field-test protocols and equipment, which in a rational manner, combine the results from laboratory and field tests with those used for quality control during construction, have been developed. Seismic nondestructive testing technology has been used for this purpose. Simple laboratory tests that are compatible with the field tests have been recommended. All these tests have several features in common. They can be performed rapidly (less than 3 min.), and their data reduction processes are simple and almost instantaneous.

KEYWORDS: quality control, seismic methods, mechanistic pavement design, modulus

Introduction

Aside from traffic and environmental loading, the primary parameters considered for structural design of a flexible pavement section are the modulus, thickness, and Poisson's ratio of each layer. A number of procedures for structural design of flexible pavements consider these parameters. Although, the state-of-the-art test procedures have been developed to obtain laboratory modulus of hot-mix asphalt (HMA), the acceptance criteria are typically based on either adequate density of the placed and compacted materials or laboratory modulus tests on materials that are retrieved from the site but compacted in the laboratory. To successfully implement any mechanistic pavement design procedure and to move toward performance-based specifications, it is essential to develop tools that can measure the modulus of each layer in the field.

Under concentrated efforts primarily funded by TxDOT, realistic field-test protocols and equipment, which in a rational manner, combine the results from laboratory and field tests with those used for quality control during construction, have been developed. Seismic nondestructive testing technology has been used for this purpose. Simple laboratory tests that are compatible with the field tests have been recommended.

The significance of this project is evident. These types of tests are one of the major components needed to develop a mechanistic pavement design and performance-based construction specifications. A gradual transition from the existing specifications to performance-based specifications may be necessary. Performing the simplified laboratory and field tests on pavement materials will allow us to develop a database that can be used to smoothly unify the design procedures and construction quality control.

Manuscript received 5 January 2004; accepted for publication 24 January 2005; published October 2005. Presented at ASTM Symposium on Performance of Hot Mix Asphalt (HMA), including Fundamental and Empirical Procedures on 9 December 2003 in Tampa, FL.
[1] Director, Center for Transportation Infrastructure Systems, The University of Texas, El Paso, TX 79968.
[2] Assistant Professor, Center for Transportation Infrastructure Systems, The University of Texas, El Paso, TX 79968.
[3] Research Engineer, Center for Transportation Infrastructure Systems, The University of Texas, El Paso, TX 79968.

The main objective of this paper is to present the implementation issues. The test protocols and devices are first briefly described. A methodology developed for combining laboratory complex modulus tests and seismic tests to estimate design modulus is also introduced. This methodology provides the moduli that can be readily used in many mechanistic design procedures including the newly developed design guide for the Federal Highway Administration (FHWA). In addition, several case studies are included to demonstrate the new quality management concepts discussed.

Test Equipment

The focus of the study is on measuring moduli with two devices. An ultrasonic device is used for testing HMA field cores and lab compacted specimens (briquettes). The other device is the Portable Seismic Pavement Analyzer (PSPA) for testing HMA layers nondestructively in the field. Each device is described below.

Laboratory Testing

The laboratory setup used in this study is shown in Fig. 1. The elastic modulus of a specimen, being a field core or a briquette, is measured using an ultrasonic device containing a pulse generator and a timing circuit, coupled with piezoelectric transmitting and receiving transducers. The dominant frequency of the energy imparted to the specimen is 54 kHz. The timing circuit digitally displays the time needed for a wave to travel through a specimen. To ensure full contact between the transducers and a specimen, special removable epoxy couplant caps are used on both transducers. To secure the specimen between the transducers, a loading plate is placed on top of it, and a spring-supporting system is placed underneath the transmitting transducer. The receiving transducer, which senses the propagating waves, is connected to an internal clock of the device. The clock automatically displays the travel time, t_ν, of compression waves The Young's modulus, E_ν, is then calculated using

$$E_\nu = \rho(\frac{L}{t_\nu})^2 \frac{(1+\nu)(1-2\nu)}{(1-\nu)} \tag{1}$$

where L, ρ and ν are the length, bulk density and Poisson's ratio of the specimen, respectively.

The Poisson's ratio can be either estimated or can be calculated from laboratory tests as discussed in Nazarian et al. [1].

Portable Seismic Pavement Analyzer

The Portable Seismic Pavement Analyzer (PSPA), as shown in Fig. 2, is a device designed to determine the average modulus of a concrete or HMA layer. The operating principle of the PSPA is based on generating and detecting stress waves in a medium. The Ultrasonic Surface Wave (USW) method, which is an offshoot of the Spectral-Analysis-of Surface-Waves (SASW) method [2], can be used to determine the modulus of the material. The major distinction between these two methods is that in the USW method the modulus of the top pavement layer can be directly determined without an inversion algorithm. The theoretical and experimental background behind this method can be found in Baker et al. [2]. Typically, a seismic source and at least two receivers are needed. The source impacts the surface of the medium to be tested and the transmitted waves are monitored with the receivers. By conducting a spectral analysis, a so-called dispersion curve (a plot of velocity of propagation of surface waves with wavelength) is obtained. The average modulus of the top layer, E_{USW}, can be simply obtained from the average phase velocity, V_{ph}:

$$E_{USW} = 2\rho(1+\nu)[(1.13-0.16\nu)V_{ph}]^2 \tag{2}$$

FIG. 1—*Ultrasonic test device for HMA specimens.*

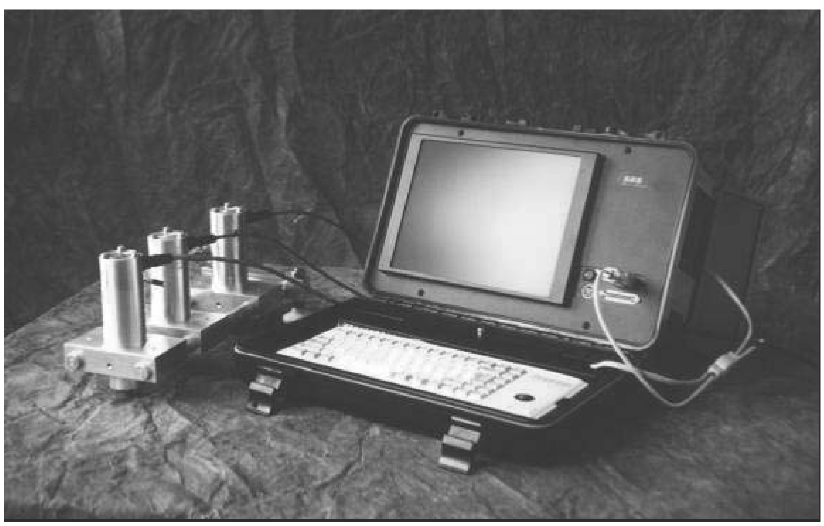

FIG. 2—*Portable seismic pavement analyzer.*

Design Modulus from Seismic Modulus

Moduli obtained with seismic measurements are low-strain high–strain-rate values. Vehicular traffic causes high strain deformation at low strain rates. One of the main concerns of the pavement community throughout the years has been how seismic moduli can be used in the design. It is of utmost importance to address this question before further discussion in the methodology is performed.

The most desirable way of calculating the design modulus is to develop the master curve based on the recommendations of Witczak et al. [3]. The response of a viscoelastic material, such as asphaltic cement or binder, is dependent on the loading frequency and temperature. The general practice has been that the testing is performed at various temperatures at similar loading frequencies and a master curve is generated at a reference temperature by using time-temperature shift factors. The following sigmoid function proposed by Ferry (1970) [4] can be used to generate a master curve

$$\log(E^*) = \delta + \frac{\alpha}{1 + e^{\beta + \gamma \times \log t_r}} \tag{3}$$

where E* = dynamic modulus, t_r = loading period, δ = minimum value of dynamic modulus, δ + α = maximum value of dynamic modulus, and β and γ = sigmoidal function shape parameter. Once the master curve is established, the design modulus can be readily determined from the design vehicular speed and the design temperature as recommended in the new FHWA mechanistic design guide.

Tandon et al. [5], based on tests on two dozen mixtures, have shown that the seismic modulus and the master curve from complex modulus correlate well. Typical results from one material when the seismic and dynamic moduli are combined are shown in Fig. 3. The process of defining the design modulus is marked on the figure as well. First, a reference temperature is defined for the region. A design frequency is then determined based on the vehicular speed. The desired design modulus based on these two input parameters can be readily defined.

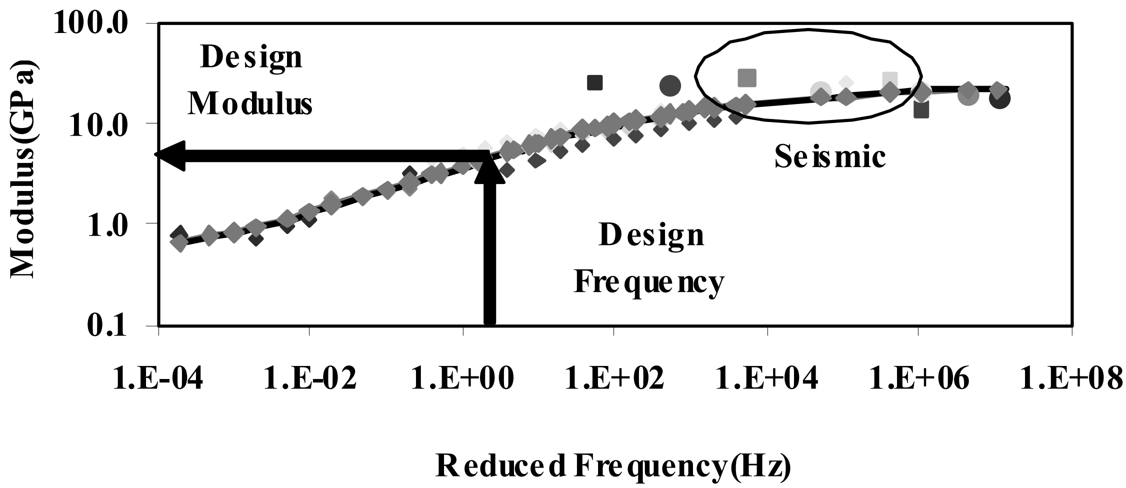

FIG. 3—*Master curve concept for defining seismic modulus.*

Proposed Protocol

The proposed quality management procedure consists of five steps. The first step consists of selecting the most suitable material or mix for a given project. In the second step, a suitable modulus value is determined based on variation in modulus with the primary parameter of interest. For a particular hot mix asphalt (HMA) mixture, this step may consist of developing air voids-modulus curve. In the third step, the variation in modulus with environmental factors is considered. In the case of a HMA layer, the variation in modulus with temperature is important. The fourth step consists of determining the design modulus for the material. The fifth and final step is to compare the field modulus with the acceptable laboratory modulus. All steps are described.

Step 1: Selecting the Most Suitable Material (Development of Job Mix Formula)

For the last century, the focus of the highway agencies has been towards placing the most durable pavement layers. For the most part, the characteristics of a durable material for a given layer depend on the collective experience of a large and diverse group of scientists and practitioners. Each highway agency's specifications clearly define how to obtain a durable HMA material. Parameters, such as angularity of the aggregates, the hardness of aggregates, percent allowable fines, degree and method of compaction, all impact the modulus and strength of an HMA layer. However, the selection of acceptable levels for these parameters is for the most part experienced based. Very little effort has been focused to routinely define the impact of these parameters on the modulus of the layer.

Even though the durability of a material cannot be directly included in the structural design of a pavement, the durability definitely do impact the performance of that pavement. The process of volumetric design, from the simplest, Marshall Method, to the most sophisticated, Strategic Highway Research Program (SHRP) Method, is meant to ensure a constructible and durable material. As such, we cannot over-emphasize that the material selection and mix design should be based on the existing collective experience acquired by the highway community. The following steps, even though more quantitative, do not replace this knowledge.

Step 2: Selecting the Most Suitable Moduli

After the job mix formula (JMF) and the binder grade are ascertained in Step 1, its most suitable modulus is determined. The modulus can be related to one of the primary construction parameters such as the compaction effort (i.e., air voids) similar to Fig. 4. Two moduli should be selected from the seismic modulus-air voids curves: the modulus corresponding to the air voids at placement (typically 7–8 %), and the modulus at design air voids from the JMF (typically 4 %). The modulus at the design air voids is used by the pavement engineer to determine the modulus that should be used in structural design as discussed in Step 4. The modulus at placement is used by the construction engineer for field quality control as described in Step 5.

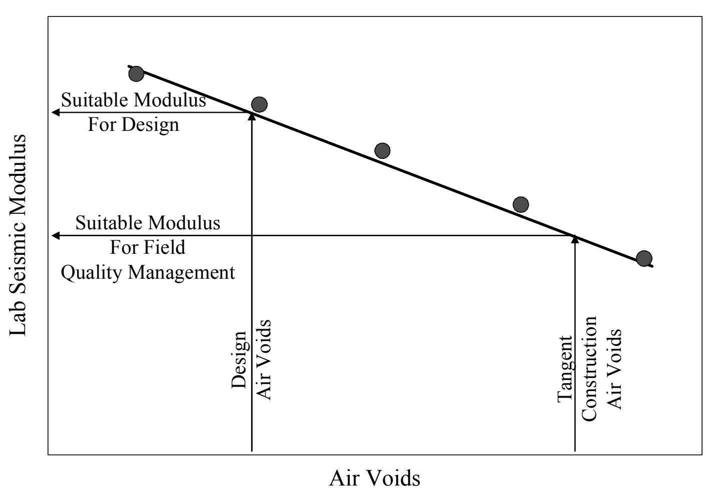

FIG. 4—*Process of determining most suitable moduli.*

Step 3: Characterizing the Variation in Modulus with Temperature

After the compaction of a layer is completed, it may be exposed to different temperatures. The simplest way of relating modulus to temperature consists of preparing two specimens: one at the JMF air voids and another at the target placement air voids. These specimens are subjected to a sequence of temperatures. The suitable temperature range for the region being considered can be determined based on the guidelines set forward by SHRP for selecting the regional air temperature extremes. It should be emphasized the binder grade is obtained in Step 1 as part of the mix design. At the end of each temperature sequence, the specimens are tested as described in the next sections. An example for the variations in modulus with temperature for one mixture is shown in Fig. 5.

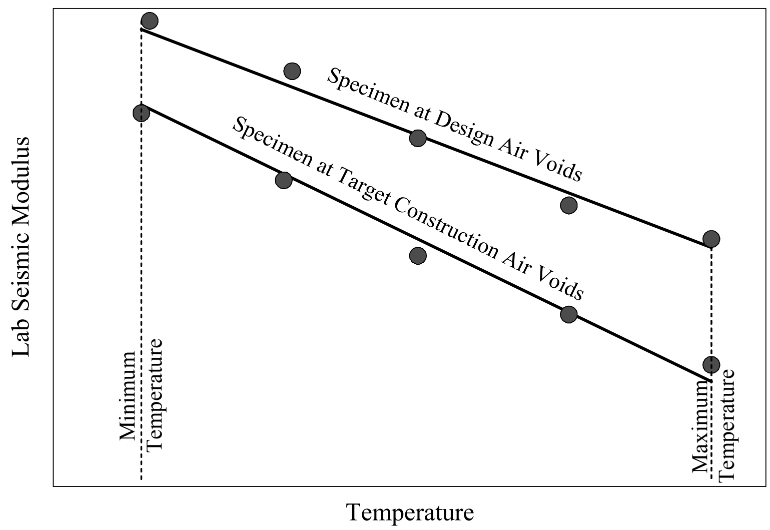

FIG. 5—*Process of characterizing variation in modulus with temperature*.

Step 4: Determining Design Modulus of Material

The most suitable seismic modulus at JMF air voids, determined in Step 2, should be translated to a design modulus as discussed in the previous section. As schematically shown in Fig. 6, the most rigorous way of calculating the design modulus is to develop a master curve. Based on a reference temperature and a design frequency, the desired design modulus can be readily defined from the master curve. The new FHWA design guide contains comprehensive guidelines for selecting the design temperature (primarily based on geographical location), and design frequency (primarily based on the vehicular speed).

If the modulus assumed by the designer and the one obtained from this analysis are significantly different, either an alternative material should be used, or the layer thickness should be adjusted. In that manner, the design and material selection can be harmonized.

Step 5: Field Quality Control

Tests are performed at regular intervals or at any point that the construction inspector suspects segregation, lack of compaction, or any other construction related anomalies. The field moduli should be greater than the most suitable laboratory seismic modulus determined at the placement air voids in Step 2. An example is shown in Fig. 7.

As emphasized in Step 2, it is important to make a distinction between the most suitable modulus for design reported to the pavement engineer and the most suitable modulus used as a guideline for quality management.

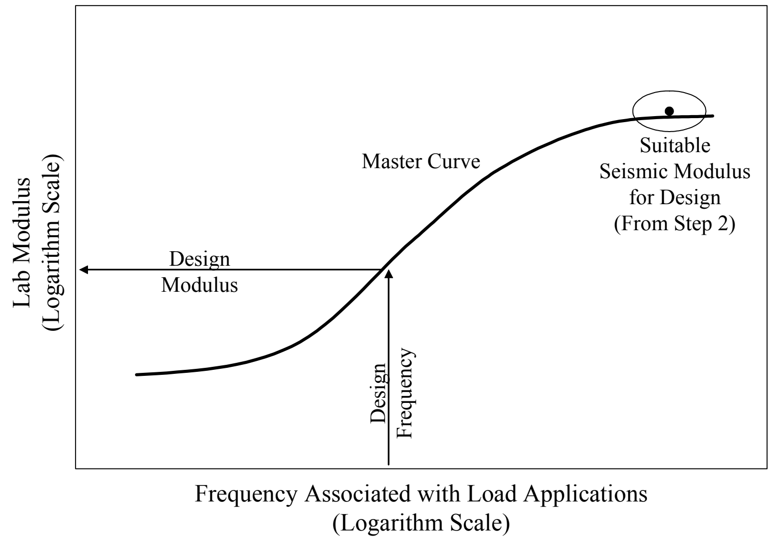

FIG. 6—*Process of estimating design modulus*.

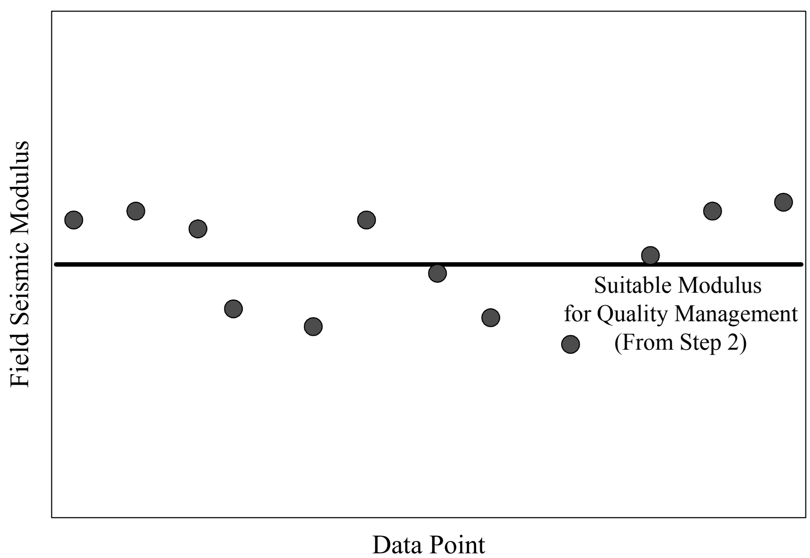

FIG. 7—*Process of field testing for HMA materials.*

Case Study

Our focus of the HMA layer testing has been an experimental test section in east Texas. The site is located near Marshall on IH-20 consisting of a 100 mm overlay placed on top of a Portland cement concrete pavement (PCCP). The overlay was placed in two lifts. The bottom 50 mm was a typical TxDOT type mixture, the top layer was a combination of nine different mixtures. In summary, the nine mixtures consisted of a combination of three aggregates using traditional TxDOT and SuperPave gyratory compactors to obtain the job mix formula. The gradations of the mixtures are summarized in Table 1. All mixes met the SuperPave gradation requirements. All mixes except for Section 5 pass below the restricted zone. The other relevant information is included in Table 2. The design voids in total mix (VTM) are 4 % for all mixtures. The binder contents varied between 4.5 % and 5 %. For all nine mixtures the same PG 76-22 asphalt binder was used.

TABLE 1—*Gradations of mixtures used in I-20 site.*

Sieve Size (mm)	Cumulative Percent Passing								
	Siliceous Gravel			Sandstone			Quartzite		
	Section 1 SuperPave	Section 4 CMHB	Section 7 Type C	Section 2 Super Pave	Section 5 CMHB	Section 8 Type C	Section 3 Super Pave	Section 6 CMHB	Section 9 Type C
22.2		100.0	100.0		100.0	100.0		100.0	100.0
19.0	100.0	…	…	100.0	…	…	100.0	…	…
15.8		99.7	100.0		…	99.8		99.6	99.8
12.5	92.0	…	…	92.1	--	…	93.7	…	…
9.5	84.8	64.5	75.8	79.4	65.4	80.7	81.7	65.6	79.1
4.75	52.4	34.3	49.2	49.0	38.0	46.2	45.5	34.2	51.4
2.36	30.9	…	…	29.2	…	…	31.4	…	…
2.00	…	21.8	31.5		24.0	30.9		24.0	34.0
1.18	20.4	…	…	22.4	…	…	21.0	…	…
0.6	13.9	…	…	18.9	…	…	17.7	…	…
0.425	…	16.2	18.2		16.4	15.6		14.5	17.9
0.3	8.8	…	…	14.9	…	--	11.8	…	…
0.15	4.5	9.8	11.7	10.2	10.9	9.6	8.2	9.1	10.0
0.075	3.2	6.4	5.8	6.5	6.4	5.8	5.6	5.9	5.3
Pan	0.0	0.0	0.0	0.0	0.0	0.0	0.0	0.0	0.0

TABLE 2—*Volumetric information for mixture used in I-20 site.*

Section No.	Mix Method	Major Aggregate	Properties from Job Mix Formula			
			G_{mb}[1]	G_{mm}[2]	VTM[3], %	BC[4], %
1		Siliceous	2.328	2.425	4.0	5.0
2	SuperPave	Sandstone	…	…	…	…
3		Quartz	3.352	2.456	4.0	5.1
4		Siliceous	2.280	2.381	4.0	4.7
5	CMHB-C	Sandstone	2.245	2.339	4.0	4.7
6		Quartz	2.315	2.412	4.0	4.8
7		Siliceous	2.315	2.411	4.0	4.4
8	Type C	Sandstone	2.275	2.370	4.0	4.5
9		Quartz	2.342	2.440	4.0	4.6

[1]G_{mb} = Bulk Specific Gravity [2]G_{mm} = Maximum Specific Gravity, [3]VTM = Voids in Total Mix, [4]BC = Binder Content.

TABLE 3—*Moduli measured with PSPA and volumetric information from I-20 sites.*

Section No.	Mix Method	Major Aggregate	Field Modulus			Field Volumetric Information	
			No. of Samples	Average, GPa	COV, %	VTM, %	Binder Content, %
1		Siliceous	27	3.98	10.8	8.8	4.4
2	SuperPave	Sandstone	42	3.86	5.9	10.4	4.5
3		Quartz	51	4.28	7.7	7.0	4.5
4		Siliceous	35	4.71	12.0	5.7	4.6
5	CMHB-C	Sandstone	44	3.55	8.6	10.1	3.9
6		Quartz	50	4.20	13.4	8.9	4.8
7		Siliceous	40	3.95	11.5	8.2	4.0
8	Type C	Sandstone	42	3.66	8.0	9.3	4.6
9		Quartz	29	3.90	7.2	8.9	4.7

Tests were performed in three phases: 1) field control using the PSPA shortly after the completion of the project; 2) testing cores extracted from field with the ultrasonic device; and 3) conducting the ultrasonic and complex modulus tests on lab prepared specimens.

The modulus values obtained from measurements made in the field using the PSPA for the nine sites are shown in Table 3 after adjusting to a frequency of 15 Hz and a temperature of 25°C. The moduli vary from a minimum of 3.5 GPa for the CHMB mixture with sandstone aggregate to 4.7 GPa for the CMHB mixture with the siliceous gravel. The number of samples and the coefficient of variation for each section are also included in Table 3. Typically 30 points were tested per section. The coefficient of variation in the measurements for each section is about 10 %.

Table 3 also contains the average VTM and binder content for each section. It would have been desirable to report results from individual test points where the coring and PSPA were performed concurrently. However, due to time constraint, the in situ volumetric information has to be determined from cores obtain from other locations than PSPA tests. A comparison of Tables 2 and 3 indicates that the field binder contents were within 0.6 % of the design binder contents for all sections except for Section 5 where the difference was about 0.8 %. The field VTM is between a low of 5.7 % at Section 4 and a high of 10.4 % at Section 2. For most sections the VTM is about 8–9 %.

The variation in modulus with VTM is presented in Fig. 8. The mixtures follow more or less the same trend. As the VTM increases, the modulus decreases. The best fit line through the data provides an R^2 of about 0.78. When the variation in the binder content (BC) was considered, the best fit line provided the following relationship

$$E = 4299 + 318\ BC - 198\ VTM \quad (R^2 = 0.85) \tag{4}$$

This relationship can be improved by considering one mixture at a time. This study clearly shows a trend between the modulus and VTM. As such, with proper calibration for a given mixture, the VTM may be potentially estimated from the modulus.

From each section, the cores used for verifying the thickness were shipped to UTEP for laboratory ultrasonic testing. The statistical information from this activity is included in Table 4. From Eq 2, the Poisson's ratio of the material is needed to obtain the seismic modulus from ultrasonic tests. To do so the results from one core is used to calibrate the results.

The average moduli from the cores and the PSPA are compared in Fig. 9. For the most part, the two moduli are quite close. In oneoCcasion, Section 6, the results differ by about 20%. The reason for such a difference is unknown at this time.

Several 150-mm high, 100-mm diameter briquettes were prepared from AC mixtures collected during construction by the staff of the Texas Transportation Institute and shipped to UTEP. The dynamic modulus and seismic measurements were performed on the specimens. The seismic moduli are summarized in Table 5. The results from Section 2 are not included because sufficient material was not available to prepare specimens. In general, the moduli from the specimens prepared in the lab (pills) were higher than those obtained from the cores or the PSPA (see Fig. 9). The AC contents of the specimens were typically slightly greater than the job mix formula reported in Table 2. The VTM values, on the other hand, were generally lower than those obtained from the cores. In some instances, the VTM values were even lower than the design value of about 4 %. This study shows that the laboratory prepared specimens may not be representative of the field condition. Any quality control based on lab prepared specimens should be done with caution. Part of the explanation for higher moduli observed in the lab can be attributed to the differences in the method of compaction and the thickness of the layers.

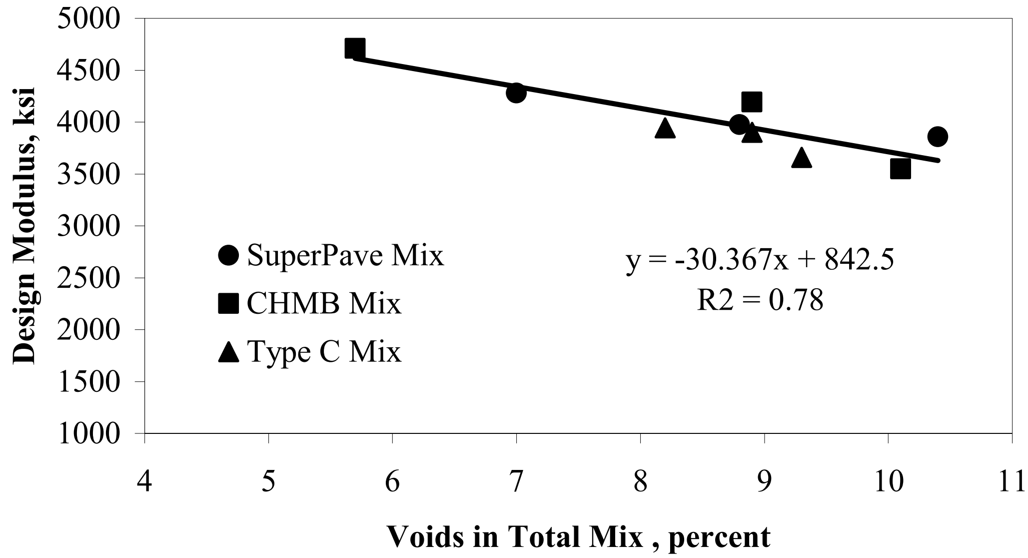

FIG. 8—*Variation in Modulus Measured with PSPA with Air Voids from I-20 Sites.*

TABLE 4—*Comparison of moduli measured with PSPA and ultrasonic device on cores.*

Section No.	Mix Method	Major Aggregate	Average Field Modulus, GPa	No. of Samples	Core Modulus Average, GPa	Core Modulus COV, %
1		Siliceous	3.98	4	3.96	9.2
2	Super Pave	Sandstone	3.86	4	4.09	5.2
3		Quartz	4.28	4	4.32	10.7
4		Siliceous	4.71	4	4.57	4.8
5	CMHB-C	Sandstone	3.55	4	3.54	3.2
6		Quartz	4.20	4	3.50	11.2
7		Siliceous	3.95	4	4.39	0.9
8	Type C	Sandstone	3.66	4	3.74	4.8
9		Quartz	3.90	4	4.07	2.7

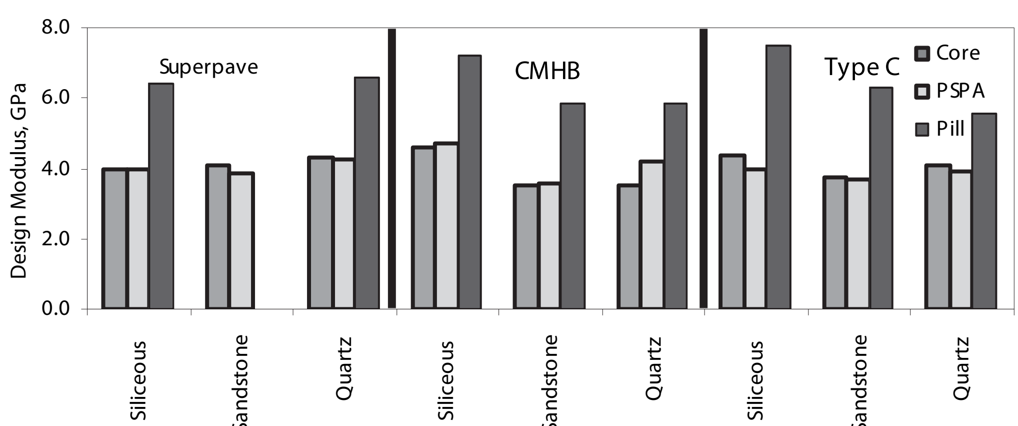

FIG. 9—*Comparison of Moduli Measured in Situ, on cores retrieved from field and from specimens prepared from loose material retrieved during paving.*

TABLE 5—*Moduli measured with ultrasonic device and volumetric information from briquettes.*

Section No.	Mix Method	Major Aggregate	No. of Samples	Seismic Modulus		Volumetric Information	
				Average, GPa	COV, %	AC Content, %	VTM, %
1	Super Pave	Siliceous	4	6.39	7.9	4.6	4.9
2		Sandstone	…	…	…	…	…
3		Quartz	4	6.60	3.2	6.4	2.7
4	CMHB-C	Siliceous	4	7.19	1.9	5.1	2.5
5		Sandstone	4	5.84	2.3	5.2	2.4
6		Quartz	4	5.87	2.0	5.6	3.1
7	Type C	Siliceous	4	7.50	3.7	5.0	1.3
8		Sandstone	4	6.30	9.4	5.3	4.2
9		Quartz	4	5.56	6.4	5.3	1.9

The type and gradation of aggregates, the viscosity of the binder and to a lesser extent the asphalt content typically impact the seismic moduli. The complex modulus is also impacted by these parameters but the impact of the binder content is more prominent. In this case study, the moduli of the nine mixes both from the field and lab tests are fairly similar. The binder used for all nine mixes was similar. Even though it is not shown here, the master curves from all mixes were similar down to a frequency of about 5 Hz (see Tandon et al. [5] for more details).

This case study demonstrates that the quality control of the HMA layer can be performed with the seismic data. The moduli measured in situ with PSPA and on cores are reasonably close. The seismic and dynamic moduli of a given material can be readily related through a master curve. The use of lab-prepared specimens to characterize the field performance of a given material should be performed with caution.

Conclusions

Procedures have been developed to measure the moduli of each pavement layer shortly after placement and after the completion of the project. These procedures allow rapid data collection and interpretation. Thus, any problem during construction process can be identified and adjusted. The outcomes from this study exhibit that the proposed equipment and methodologies may strike a balance between the existing level of sophistication in the design methodology, laboratory testing and field testing. Performing the simplified laboratory and field tests along with more traditional tests may result in a database that can be used to smoothly unify the design procedures and construction quality control.

The major advantage of seismic methods is that similar results are anticipated from the field and laboratory tests as long as the material is tested under comparable conditions. This unique feature of seismic methods in material characterization is of particular significance, if one is interested in implementing performance-based specifications.

The methodology proposed can be used to determine the quality of the completed layer. Through the complex modulus tests, the measured modulus can be readily related to the design modulus. The methods have also shown some potential in terms of estimating the degree of compaction for a given mixture. The primary construction parameter that impacts the seismic modulus seems to be the voids in total mix.

References

[1] Nazarian S., Yuan D., Tandon V. and Arellano M., "Quality Management of Flexible Pavement Layers with Seismic Methods," Research Report 1735-3, The Center for Transportation Infrastructure, The University of Texas, El Paso, TX, 2003, 120 p.

[2] Nazarian, S., Baker, M. and Crain, K., "Assessing Quality of Concrete with Wave Propagation Techniques," *Materials Journal, American Concrete Institute,* Vol. 94, No. 4, 1997, pp. 296–306.

[3] Witczak, M. W., Bonaquist, R., Von Quintus, H. and Kaloush, K., "Specimen Geometry and Aggregate Size Effects in Uniaxial Compression and Constant Height Shear Tests," *Journal of Association of Asphalt Paving Technologist,* Vol. 69, 1999, pp. 733–793.

[4] Ferry, J.D, *Viscoelastic Properties of Polymers,* 2nd ed., John Willy, New York, 1970.

[5] Tandon, T., Nazarian, S. and Bai X., "Assessment of Relationship between Seismic and Dynamic Modulus of Hot Mix Asphalt Concrete," *International Journal of Road Materials and Pavement Design,* 2004 (submitted for publication).

Journal of ASTM International, March 2005, Vol. 2, No. 3
Paper ID JAI12281
Available online at www.astm.org

Jingna Zhang,[1] *Hongbin Xie,*[2] *Prithvi S. Kandhal,*[3] *and R. D. Powell*[4]

Field Validation of Superpave Shear Test on NCAT Test Track

ABSTRACT: When the National Center for Asphalt Technology Test Track was built in 2000, one of the primary objectives was to determine the ability of a number of laboratory tests to predict the permanent deformation of various mixtures. Repeated Shear at Constant Height (RSCH) was included as one of the tests in the laboratory study. The subject of this paper is field validation of the Superpave Shear Tester (SST) based on the field rutting data from the Test Track. Permanent shear strain, slope of the deformation rate, repetitions to a certain strain level, and shear modulus were the parameters evaluated for RSCH. The sensitivity of SST test to asphalt binder type in the various test track sections was analyzed. The relationship between RSCH test results and field rut depth was poor. This was partly due to the good quality of the track construction, thick pavement structure, and mild summers during the loading of the 2000 track, which did not cause any significant rutting. The sensitivity study indicated that PG 76-22 binder performed better than the PG 67-22 binder in the RSCH test. The criteria developed by the Asphalt Institute seem to be in a reasonable range.

KEYWORDS: Superpave Shear Test, Repeated Shear at Constant Height, NCAT Test Track, HMA, Rutting, permanent deformation, SST, asphalt concrete

Introduction

The Superpave Shear Tester (SST) was developed as a means to characterize asphalt mixture properties during the Strategic Highway Research Program (SHRP), a five-year $150 million dollar United States research effort established and funded in 1987. The SST is a servo-hydraulic machine that can apply both axial and shear loads at constant temperatures using closed-loop control. The SST consists of four major components: a testing apparatus, a test control unit, an environmental control chamber, and a hydraulic system. The SST simulates, among other things, the comparatively high shear stresses that exist near the pavement surface at the edge of vehicles tires – stresses that lead to the lateral and vertical deformations associated with permanent deformation in surface layers.

The current SST protocols consist of three different modes of operation: 1) simple shear at constant height (SSCH), 2) frequency sweep at constant height (FSCH), and 3) repeated shear at constant height (RSCH). In each mode, different types of information are available. Of these three modes, RSCH (AASHTO TP7, Procedure F) is most commonly selected to assess the permanent deformation response characteristics of the asphalt mixtures. This test operates by applying repeated shear load pulses to an asphalt mixture specimen. As the specimen is being sheared, the constant height prevents specimen dilation, thereby promoting the accumulation of permanent shear strain. The test can be used for comparatively analyzing shear response characteristics of mixtures subjected to similar loading and temperature conditions.

Manuscript received 1 December 2003; accepted for publication 19 November 2004; published March 2005.
[1] Research Engineer, National Center for Asphalt Technology, 277 Technology Parkway, Auburn, AL 36832.
[2] Ph.D. Candidate, Auburn University, 277 Technology Parkway, Auburn, AL 36832.
[3] Associate Director, National Center for Asphalt Technology, 277 Technology Parkway, Auburn, AL 36832.
[4] Test Track Manager, National Center for Asphalt Technology, 277 Technology Parkway, Auburn, AL 36832.

Background

Since the SST was first introduced in 1993, researchers have used it to evaluate mixture properties such as permanent deformation and fatigue. The information obtained from the SST is utilized conventionally by researchers to compare generated data for any proposed mixture of unknown performance with another mixture with known performance under the same conditions at identical temperatures. This practice is certainly useful, but it is limited to those specific sets where there is available information on mixtures with known performance for comparison. Several parameters were developed and employed to evaluate the results of the RSCH test. Permanent shear strain is most commonly used to interpret this test, while some other parameters, such as slope of the deformation rate, repetitions to a certain strain level, and shear modulus, have been also found in the literature. However, only a limited field validation of the SST has been conducted. Hence, there is no universally accepted parameter that can be used to evaluate the RSCH test results and to predict the rutting potential.

Recent studies [1–5] have indicated that the RSCH test can be used successfully to evaluate the relative rutting potential of HMA mixtures. Unfortunately, even under the most controlled circumstances and operated by experienced technicians, the data from the RSCH test have been shown to have high variability [1–5]. To remedy the high variations, Romero and Anderson [6] recommended that five specimens be tested and the two extremes discarded from further analysis. The remaining three should be averaged to provide an effective way to reduce the coefficient of variation. As a result, this will significantly increase the time and effort needed.

When the National Center for Asphalt Technology (NCAT) test track was built, one of the primary objectives was to determine the capability of a number of laboratory tests to predict the permanent deformation of various mixtures. The SST was included as one of the laboratory tests; therefore it provided an opportunity to determine the practicality of the test procedure and to evaluate the SST parameter as a predictor of performance at the NCAT test track.

Objective

The primary objective of this study was to perform a validation of the SST test based on the field rutting data from the NCAT Test Track. If possible, best parameters from these tests will be identified as specification parameter(s). The secondary objective was to evaluate the sensitivity of the SST test to the mixture components in the various test track sections.

NCAT Test Track Experimental Design

An oversight committee was formed at the beginning of the construction of the NCAT test track, in which sponsors were encouraged to work together as much as they could so that an overall test plan for the facility could be developed. Most sponsors chose to ship in their own local aggregates while using common asphalt binders for most of the test sections. Table 1 is included herein to provide an overall summary of the various test sections [7].

Since each sponsor could use any mix they desired, as shown in Table 1, a wide range of mixture types and properties was provided. Several aggregates were used on the track, including limestone, granite, marine limestone, gravel, and slag. Reclaimed asphalt pavement (RAP) was also used in a few sections. These test sections provided some opportunity to evaluate the effect of aggregate type on performance.

TABLE 1—*Overview of mix types evaluated [7].*

Track Quad	Section Num	Aggregate Blend Type	Mix Type	Design NMA	Grad Type	Binder Grade	Binder Modifier	Lift Type	Design Thick
E	2	Granite	Super	12.5	BRZ	67-22	N/A	Dual	4.0
E	3	Granite	Super	12.5	BRZ	76-22	SBR	Dual	4.0
E	4	Granite	Super	12.5	BRZ	76-22	SBS	Dual	4.0
E	5	Granite	Super	12.5	TRZ	76-22	SBS	Dual	4.0
E	6	Granite	Super	12.5	TRZ	67-22	N/A	Dual	4.0
E	7	Granite	Super	12.5	TRZ	76-22	SBR	Dual	4.0
E	8	Granite	Super	12.5	ARZ	67-22	N/A	Dual	4.0
E	9	Granite	Super	12.5	ARZ	76-22	SBS	Dual	4.0
E	10	Granite	Super	12.5	ARZ	76-22	SBR	Dual	4.0
N	1	Slag/Lms	Super	12.5	ARZ	76-22	SBS	Dual	4.0
N	2	Slag/Lms	Super	12.5	ARZ	76-22+	SBS	Dual	4.0
N	3	Slag/Lms	Super	12.5	ARZ	67-22+	N/A	Dual	4.0
N	4	Slag/Lms	Super	12.5	ARZ	67-22	N/A	Dual	4.0
N	5	Slag/Lms	Super	12.5	BRZ	67-22+	N/A	Dual	4.0
N	6	Slag/Lms	Super	12.5	BRZ	67-22	N/A	Dual	4.0
N	7	Slag/Lms	Super	12.5	BRZ	76-22+	SBR	Dual	4.0
N	8	Slag/Lms	Super	12.5	BRZ	76-22	SBR	Dual	4.0
N	9	Slag/Lms	Super	12.5	BRZ	76-22	SBS	Dual	4.0
N	10	Slag/Lms	Super	12.5	BRZ	76-22+	SBS	Dual	4.0
N	11	Granite	Super	19.0	BRZ	67-22	N/A	Lower	2.5
		Granite	Super	12.5	TRZ	76-22	SBS	Upper	1.5
N	12	Granite	Super	19.0	BRZ	67-22	N/A	Lower	2.5
		Granite	SMA	12.5	SMA	76-22	SBS	Upper	1.5
N	13	Gravel	Super	19.0	BRZ	76-22	SBS	Lower	2.5
		Gravel	SMA	12.5	SMA	76-22	SBS	Upper	1.5
W	1	Granite	SMA	12.5	SMA	76-22	SBR	Dual	4.0
W	2	Slag/Lms	SMA	12.5	SMA	76-22	SBR	Dual	4.0
W	3	Granite	Super	12.5	BRZ	76-22	SBR	Lower	3.3
		Slag/Lms	OGFC	12.5	OGFC	76-22	SBR	Upper	0.7
W	4	Limestone	SMA	12.5	SMA	76-22	SBR	Lower	3.3
		Granite	OGFC	12.5	OGFC	76-22	SBR	Upper	0.7
W	5	Limestone	SMA	12.5	SMA	76-22	SBS	Lower	3.3
		Granite	OGFC	12.5	OGFC	76-22	SBS	Upper	0.7
W	6	Slag/Lms	Super	12.5	TRZ	67-22	N/A	Dual	4.0
W	7	Limestone	SMA	12.5	SMA	76-22	SBR	Dual	4.0
W	8	Sandstn/Slg/Lms	SMA	12.5	SMA	76-22	SBR	Dual	4.0
W	9	Gravel	Super	12.5	BRZ	67-22	N/A	Dual	4.0
W	10	Gravel	Super	12.5	BRZ	76-22	SBR	Dual	4.0
S	1	Granite	Super	19.0	BRZ	76-22	SBS	Lower	2.5
		Granite	Super	12.5	BRZ	76-22	SBS	Upper	1.5
S	2	Gravel	Super	19.0	BRZ	76-22	SBS	Lower	2.5
		Gravel	Super	9.5	BRZ	76-22	SBS	Upper	1.5
S	3	Limestone	Super	19.0	BRZ	76-22	SBS	Lower	2.5
		Lms/Gravel	Super	9.5	BRZ	76-22	SBS	Upper	1.5
S	4	Lms/RAP	Super	19.0	ARZ	76-22	SBS	Lower	2.5
		Limestone	Super	12.5	ARZ	76-22	SBS	Upper	1.5
S	5	Lms/Grv/RAP	Super	19.0	BRZ	76-22	SBS	Lower	2.5
		Gravel	Super	12.5	TRZ	76-22	SBS	Upper	1.5
S	6	Lms/RAP	Super	12.5	ARZ	67-22	N/A	Dual	4.0

S	7	Lms/RAP	Super	12.5	BRZ	67-22	N/A	Dual	4.0
S	8	Marble-Schist	Super	19.0	BRZ	67-22	N/A	Lower	2.1
		Marble-Schist	Super	12.5	BRZ	76-22	SBS	Upper	1.5
S	9	Granite	Super	12.5	BRZ	67-22	N/A	Dual	4.0
S	10	Granite	Super	12.5	ARZ	67-22	N/A	Dual	4.0
S	11	Marble-Schist	Super	19.0	BRZ	67-22	N/A	Lower	2.1
		Marble-Schist	Super	9.5	BRZ	76-22	SBS	Upper	1.5
S	12	Limestone	Hveem	12.5	TRZ	70-28	SB	Dual	4.0
S	13	Granite	Super	12.5	ARZ	70-28	SB	Dual	4.0
E	1	Gravel	Super	12.5	ARZ	67-22	N/A	Dual	4.0

Notes:

- Mixes are listed chronologically in order of completion dates.
- "Dual" lift type indicates that the upper and lower lifts were constructed with the same mix.
- ARZ, TRZ, and BRZ refer to gradations intended to pass above, through, and below the restricted zone
- SMA and OGFC refer to stone matrix asphalt and open-graded friction course mixes, respectively.
- Shaded sections/layers were not conducted for SST tests.

There were five gradation types used at the test track: below the restricted zone (BRZ), above the restricted zone (ARZ), through the restricted zone (TRZ), stone matrix asphalt (SMA), and open-graded friction course (OGFC).

PG 76-22, PG 70-28, and PG 67-22 were the three PG binder grades used throughout the track. There were several direct comparisons of mixtures containing PG 76-22 and PG 67-22, while all other mix properties were held constant. This allowed a direct comparison of the performance of mixes containing the two grades of asphalt binders. Modifier types for PG 76-22 were mainly styrene butyl rubber (SBR) and styrene butadiene styrene (SBS).

An additional 0.5 % asphalt cement was added to five mixtures to determine the effect of the extra binder. This was done for both the modified and unmodified binders.

After the 200-ft long test sections were constructed, 10 million total ESALs were applied over a 2-year period. Before construction of experimental sections had been completed, random numbers were used to identify longitudinal positions at which transverse profiles could be measured over time [8]. Allowing 25 ft for transition into and out of each section, the middle 150 ft of each experimental mat were divided into three 50-ft statistical observations. A random location was selected within each observation area where transverse profiles were measured for the duration of the research. Transverse profiles were measured weekly to evaluate the change in permanent deformation over time. Three different methods of measuring the transverse profile were utilized: precision differential level, inertial laser profiler, and wireline. For the purpose of this paper, the final wireline measurements after 10 million ESALs were utilized.

Unfortunately, due to the good quality of the track construction, thick pavement structure, and generally mild summers during the loading of the 2000 Track, significant rutting did not occur. Therefore the range of rutting data is smaller than what might be desired to evaluate tests for permanent deformation. Since the performance samples were produced at the density of the quality control samples compacted to N_{design}, this eliminates the majority of the densification, and, therefore, only shear flow would be expected in the laboratory test samples [8].

In total, RSCH tests for 51 different mixes from the NCAT test track were conducted in this project. All RSCH test data will be presented and analyzed along with the NCAT test track rut depth data in this paper.

SST Test Procedure and Data Analysis

Test samples for SST RSCH testing were prepared at the time of construction using fresh mix without reheating. The original goal of the performance testing for the test track mixes was to identify methods that could be used in quality control and quality assurance. Therefore, samples were prepared using the SGC to match the density of samples compacted to N_{design} with a reference SGC used to prepare all of the tracks' quality control samples. Two test samples were sawed from each gyratory sample.

Tests were conducted following the procedure outlined in the AASHTO TP7-01, test procedure C. The RSCH test consists of applying a repeated haversine shear stress of 68 kPa (0.1-s load and 0.6-s rest) to a compacted HMA (150 mm diameter × 50 mm height) specimen while supplying necessary axial stress to maintain a constant height. The RSCH test is performed at 64°C to 5000 load cycles. Permanent strain is measured as the primary response variable at certain interval load cycles throughout the test and recorded using LVDTs and a computerized data acquisition system. Permanent shear strain, slope of the deformation rate, repetitions to a certain strain level, and shear modulus at certain cycles were the parameters to interpret the RSCH test results. Each of these parameters will be discussed later in this paper.

Figure 1 shows a typical RSCH test deformation curve for the mixes evaluated in this study.

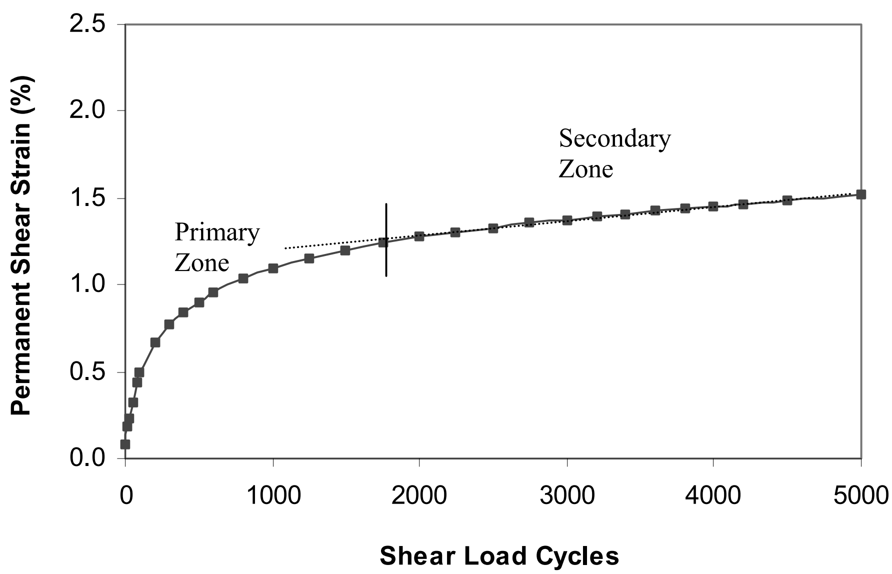

FIG. 1—*Typical repeated shear at constant height test for test track mixes.*

It indicates how the amount of permanent shear deformation accumulates with increasing load repetitions in a test. The specimen deforms quite rapidly during the first several hundred loading cycles. The rate of unrecoverable deformation per cycle decreases and becomes quite steady for many cycles in the secondary region. For some mixes, at some number of loading cycles, the deformation begins to accelerate, leading to failure in the tertiary portion of the curve. Due to the good performance of the mixes studied in this project, none of them yielded the tertiary zone. Therefore, at 5000 load cycles, the mixes were still in the secondary zone. Linear model regression, $y = kx + b$, was used to simulate the shear strain versus loading cycles at the secondary zone. In this study, the linear portion was identified from 2500–5000 cycles.

The development of the permanent shear strain as a function of loading also can be represented by the power law regression [9], yielding an equation of the form:

$$\gamma_p = ax^m \quad (1)$$

where, γ_p = permanent shear strain; x = loading cycles; and a, m = regression coefficients.

Thus, the plastic strain versus the number of loading repetitions plotted on a log-log scale is nearly a straight line.

Repetition to a certain shear strain is also a factor used by some researchers to differentiate between mixes. In this study, repetitions to 3 % shear strain were calculated from the data obtained. For the mixes which had less than 3 % shear strain when the tests stopped, data were extrapolated to the repetitions corresponding to 3 % shear strain using the linear model developed previously.

Shear modulus is a variable that has been used by Tayebali et al. [10] in their study on Westrack fine mixes. It was typically calculated either from 100 or 5000 cycles.

Test Results and Discussion

As discussed above, the RSCH tests provided permanent shear deformation γ, modulus, and some other parameters such as slopes and repetitions to 3 % shear strain. Table 2 summarizes these results for the 51 mixes from the NCAT test track. Each value in the table is the average of the corresponding parameters from the replicates. Rut depths from the test track are also presented in this table.

TABLE 2—*Repeated shear at constant height test results versus test track rut depth.*

Test Section		RSCH Test					NCAT Test Track
		$y = ax^m$, m	$y = kx+b$, k (10^{-5})	$\gamma_{5000}{}^{a}$, %	$G^*_{100}{}^{b}$, MPa	Reps to $\gamma = 3$ %	Rut Depth mm
E	1	0.290	7.333	2.422	37.7	12 966	6.37
E	2	0.350	5.667	1.548	103.3	32 875	5.11
E	3	0.234	1.100	*0.373*	137.7	365 675	4.03
E	4	0.340	4.000	0.587	104.6	68 414	2.50
E	5	0.355	6.000	1.402	53.0	41 280	3.06
E	6	0.292	3.333	0.850	129.2	81 258	3.79
E	7	0.327	2.667	0.347	223.3	108 568	2.84
E	8	0.341	3.000	1.735	64.3	79 587	3.48
E	9	0.328	6.333	0.939	131.0	39 418	2.02
E	10	0.226	1.400	1.119	61.4	438 619	1.80
N	1	0.192	7.500	1.628	51.8	22 717	2.07
N	2	0.225	4.333	0.945	70.2	53 077	2.00
N	3	0.225	10.000	2.788	29.4	2 191	7.27
N	4	0.283	9.000	2.379	90.8	11 909	5.29
N	5	0.223	5.000	1.428	106.1	38 796	7.06
N	6	0.240	10.000	3.624	78.4	1 379	3.80
N	7	0.408	8.333	1.417	65.6	24 298	1.58
N	8	0.354	7.333	1.465	93.9	26 420	0.89
N	9	0.334	7.667	1.837	38.4	20 868	0.51
N	10	0.309	8.000	2.319	21.2	13 493	0.93
N	11 Top	0.375	2.000	0.317	264.9	138 920	1.42
N	12 Top	0.322	1.500	0.302	191.7	210 870	2.10
N	13 Top	0.453	6.000	1.011	143.0	38 121	3.44
W	1	0.332	2.567	1.248	104.7	146 825	4.86

W	2	0.341	12.333	2.113	79.5	16 536	2.30
W	6	0.220	8.667	1.830	59.1	41 495	1.75
W	7	0.363	8.333	1.790	90.1	19 788	1.97
W	8	0.362	20.000	2.998	71.8	4 515	4.84
W	9	0.220	8.667	3.187	28.3	4 242	3.39
W	10	0.281	6.667	1.478	74.4	29 869	2.24
S	1 Top	0.305	2.367	0.538	163.2	913 106	1.83
S	2 Top	0.327	1.667	0.232	253.9	190 335	0.46
S	3 Top	0.319	1.000	0.195	265.4	285 540	0.52
S	4 Top	0.268	3.000	0.793	80.0	78 650	0.66
S	5 Top	0.258	6.000	1.999	38.2	21 609	0.68
S	6	0.340	6.667	1.859	94.5	24 643	2.06
S	7	0.273	8.667	2.789	48.6	9 011	3.30
S	8 Top	0.222	2.500	0.834	75.3	93 441	1.75
S	9	0.247	6.333	1.982	38.1	21 002	2.01
S	10	0.237	6.333	2.134	40.2	19 181	4.14
S	11 Top	0.247	3.000	0.735	60.4	79 800	1.60
S	12	0.286	6.667	1.238	119.7	37 515	2.52
S	13	0.412	5.000	0.750	117.3	71 651	1.58
N	11 Bottom	0.303	3.000	0.812	176.6	77 609	…
W	5 Bottom	0.273	8.500	1.992	103.5	14 926	…
S	1 Bottom	0.282	1.500	0.259	196.3	212 035	…
S	2 Bottom	0.303	3.000	0.683	96.9	80 591	…
S	3 Bottom	0.280	4.000	0.872	84.8	57 800	…
S	4 Bottom	0.284	4.667	1.259	60.6	43 202	…
S	5 Bottom	0.311	2.333	0.396	121.0	120 444	…
S	11 Bottom	0.285	7.000	1.890	69.3	21 410	…

[a] Permanent shear strain at 5000 load cycles.
[b] Modulus at 100 load cycles.

Comparison of Laboratory Permanent Deformation Tests to Field Performance

Figure 2 illustrates the shear permanent strain (γ_p) versus rut depth from the test track. The coefficient of correlation $R^2 = 0.17$ indicates a poor relationship.

As indicated earlier, due to the good quality of the track construction, thick pavement structure, and generally mild summers during the loading of the 2000 Track, the range of rutting data is smaller than what might be desired to evaluate tests for permanent deformation.

The Asphalt Institute (AI) had recommended criteria (shown in Table 3) for interpreting RSCH maximum permanent shear strain as related to rut resistance [11]. Numbers of mixes that have shear strain in each of the four categories are presented in Table 3. Based on the criteria recommended by AI, there are only two mixes that have poor rut resistance. Most of the track mixes have good and even excellent rut resistant property based on the RSCH shear strain criteria. These criteria seem reasonable considering the small rut depth in the field. It should be mentioned that the AI criteria were based on a lower test temperature than used in this study.

Using the poor relationship shown in Fig. 2, the field rut depth would be about 4.0 mm for the poor mixes in the track. Practically, sections with such a small rut depth cannot be considered to have poor rut resistance. This again resulted from the good quality mixes used on the test track.

Figures 3–6 illustrate the repetition to 3 % shear strain, shear modulus, linear slope "k," power slope "m" versus field rut depth from the test track. The low R^2 values indicate none of these variables has good relationship with field rut depths. The modulus and slope "m" did not follow the trend as expected.

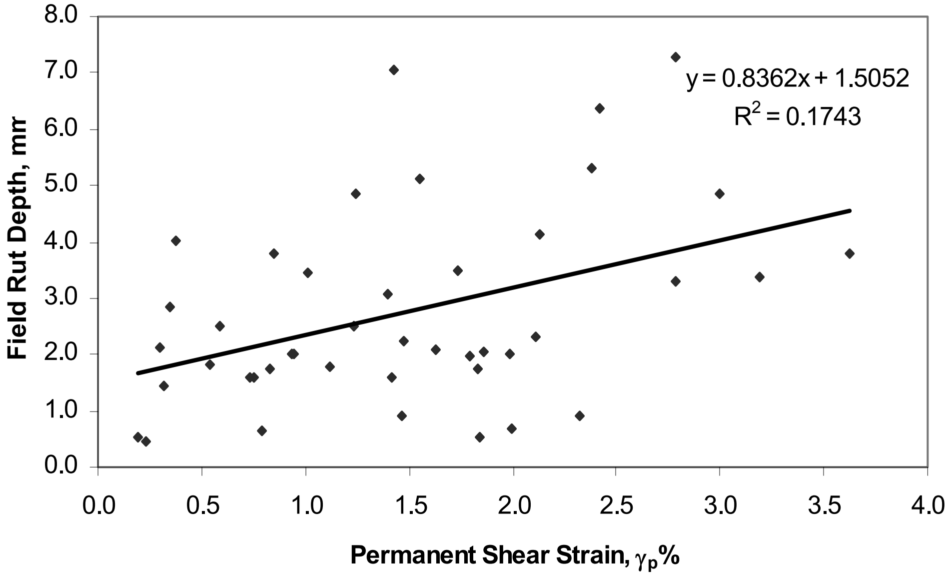

FIG. 2—*Permanent shear strain versus track rut depths after 10 million ESAL.*

TABLE 3—*Criteria for evaluating rut resistance using RSCH permanent shear strain.*

RSCH Shear Strain at 50°C (%)	Rut Resistance	Test Track Mixes RSCH		Rut Depth from Model y = 0.8362x + 1.5052
		Number	Percent	
< 1.0	Excellent	20	39 %	2.3
1.0 to < 2.0	Good	21	41 %	2.3–3.2
2.0 to < 3.0	Fair	8	16 %	3.2– 4.0
≥ 3.0	Poor	2	4 %	≥ 4.0

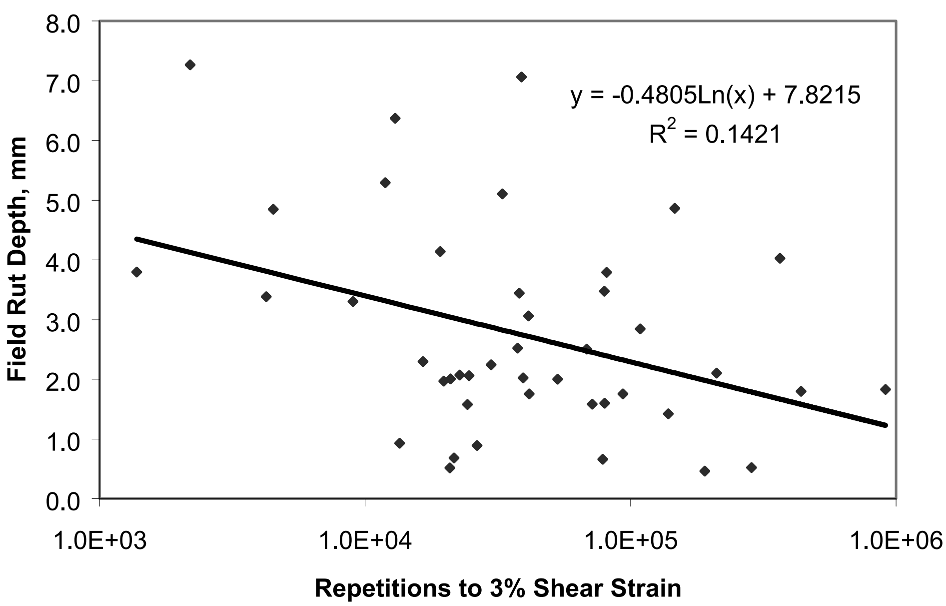

FIG. 3—*Repetitions to 3 % shear strain versus track rut depths.*

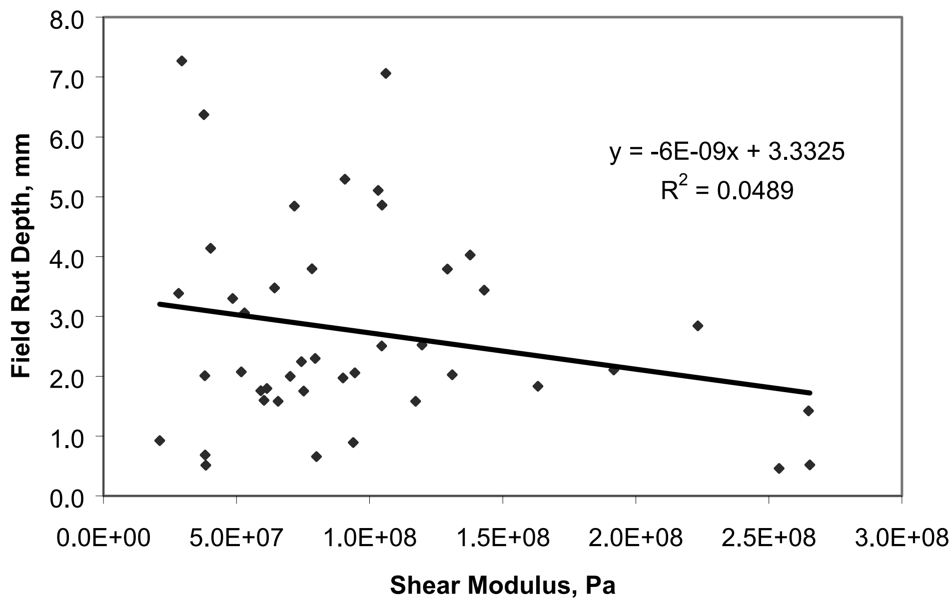

FIG. 4—*Shear modulus versus track rut depths.*

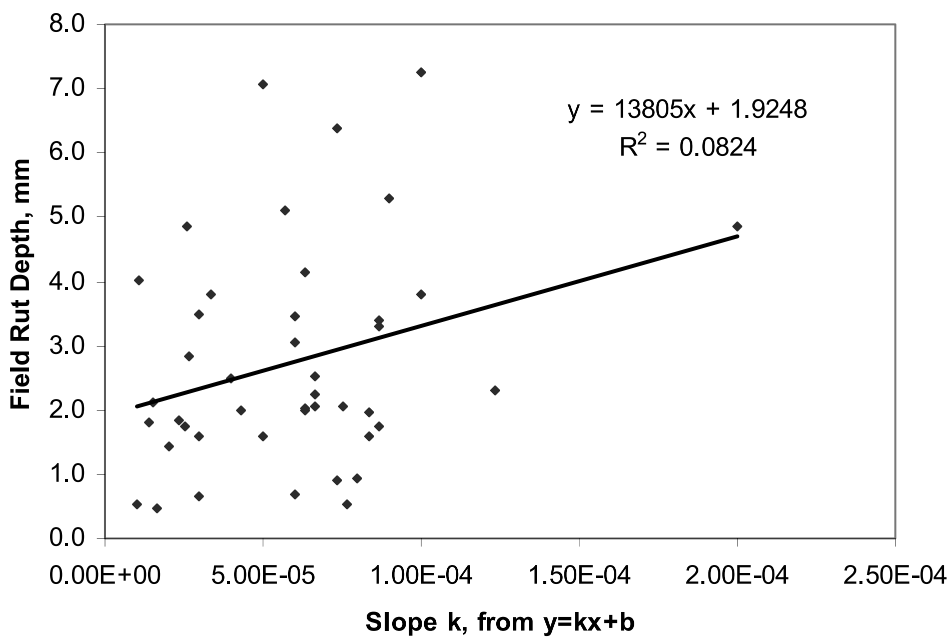

FIG. 5—*Linear slope "k" versus track rut depths.*

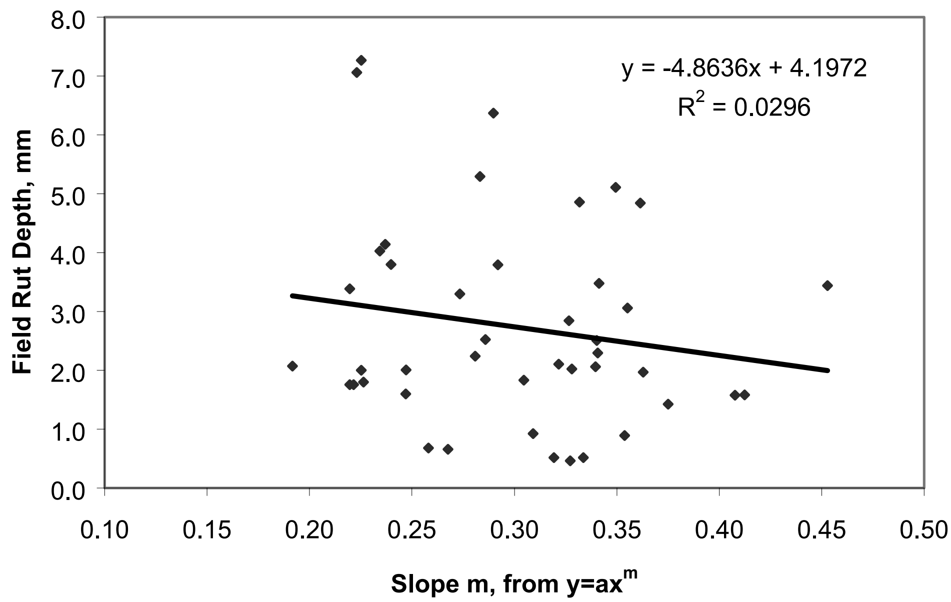

FIG. 6—*Power slope "m" versus track rut depths.*

Sensitivity of RSCH Test to the Test Track Mixes

The secondary objective of this paper was to evaluate the sensitivity of the RSCH test to the various mixture components in the test track sections. The experimental design allowed sensitivity analysis of the asphalt binder type on the RSCH test. Permanent shear strain at 5000 cycles was the factor most commonly used to interpret RSCH test, therefore, it was decided to conduct the sensitivity analysis with this parameter only.

Sections N1-N10—One mini experiment involving 10 sections was set up to look at the effect of PG grade, asphalt content, and fine grade versus coarse grade mixes. These sections were identified as N1 through N10. Analysis of the RSCH shear strain data consisted of conducting an analysis of variance (ANOVA) using general linear model (GLM). For this analysis, usually three replicate observations were included for each section. Because there were three replicate observations, a measure of experimental error was available for calculating the F-statistics. Table 4 indicates the analysis result. PG grade, asphalt content, gradation type, and the two-way and three- way interactions were included in this table.

TABLE 4—*Results of ANOVA on permanent shear strain.*

Source of Variation	Degree of Freedom	Seq SS	Adj SS	Adj MS	F	P-value
Gradation	1	0.0575	0.0021	0.0021	0.01	0.930
PG Grade	1	3.9642	5.6359	5.6359	21.47	0.000
OAC	1	0.8737	1.0714	1.0714	4.08	0.062
Gradation*PG Grade	1	0.8006	0.632	0.632	2.41	0.142
Gradation*OAC	1	0.0406	1.1317	1.1317	4.31	0.055
PG Grade*OAC	1	0.2041	0.0923	0.0923	0.35	0.562
Gradation*PG Grade*OAC	1	3.8891	3.8891	3.8891	14.81	0.002
Error	15	3.9377	3.9377	0.2625		
Total	22	13.7676				

It appears that the asphalt binder PG grade and the three-way interaction significantly affected the shear strain ($P<0.05$). As shown in Fig. 7, on average, mixes using PG 76-22 had lower permanent shear strain than mixes using PG 67-22 (1.5 % versus 2.7 %). This is as expected.

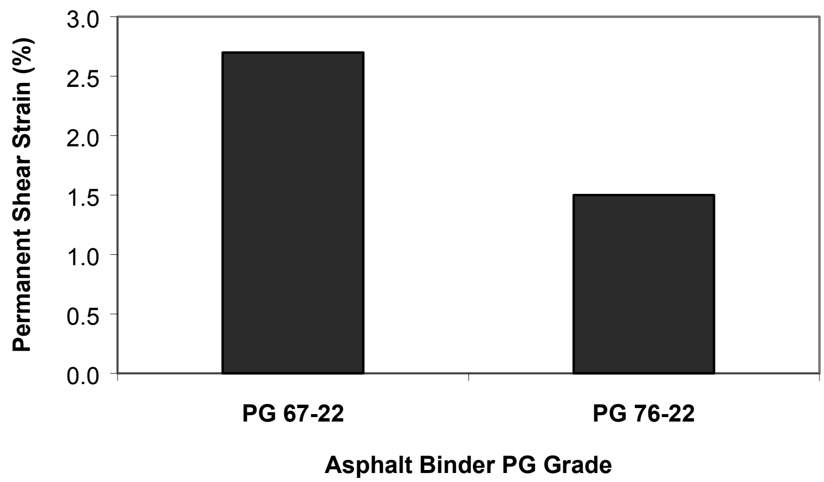

FIG. 7—*Effect of asphalt binder on RSCH permanent shear strain.*

This conclusion pertains to a specific aggregate and a nominal maximum aggregate size (NMAS). The effect of binder type was also evaluated by conducting t-Tests on mixes containing more aggregate types as follows.

Modifier (SBS, SBR) and PG 67-22—Mixtures with same components other than asphalt binder type are compared through t-Tests. There were seven paired experiments to look at the effect of modifier (SBS and SBR) on shear strain. The test section numbers were E9 versus E10, E4 versus E3, N12 versus W1, E5 versus E7, W5 versus W7, N9 versus N8, and N10 versus N7. Table 5 shows the t-Test results. P values indicated that there is no significant difference between these two modifiers at 95 % reliability. However, on average, mixes using SBR modified asphalt had approximately 0.3 lower shear strain than the SBS mixes.

The SBS modified and SBR modified PG 76-22 were compared separately with PG 67-22 binder. The first analysis compared PG 67-22 to PG 76-22 SBS. There were five paired experiments to evaluate the PG 67-22 and SBS based on shear strain. The mixture IDs were E8, S10 versus E9, E2, S9 versus E4, S1Top, E6 versus E5, N11Top, N6 versus N9, and N5 versus N10. In the cases where more than one mix was included, the average permanent shear strain was then used in the t-Test. The results are presented in Table 5. As shown in Table 5, p-value is 0.149 for PG 67-22 versus SBS. The t-Test did not show a significant difference between the mixes using PG 67-22 and SBS modified PG 76-22 binder. However, on average, PG 67-22 had higher shear strain than the SBS modified PG 76-22. The next analysis compared PG 67-22 to SBR modified PG 76-22. Six paired experiments, E8, S10 versus E10, E2, S10 versus E3, E6 versus E7, W9 versus W10, N6 versus N8, and N5 versus N7, were available to conduct t-tests. The results are also presented in Table 5. There is a significant difference between PG 67-22 and SBR modified PG 76-22 at $P = 0.010$.

TABLE 5—*T-test: paired two sample for means on shear strain.*

T-test: Paired Two Samples for Mean	SBS versus SBR		PG 67-22 versus SBS		PG 67-22 versus SBR	
	SBS	SBR	67-22	SBS	67-22	SBR
Mean	1.39331	1.087905	1.824833	1.303267	2.051917	1.025944
Variance	0.463191	0.288974	0.885732	0.548518	1.017987	0.293208
Observations	7	7	5	5	6	6
Pearson Correlation	0.59775	…	0.345245	…	0.682614	…
Hypothesized Mean Difference	0	…	0	…	0	…
Degree of Freedom	6	…	4	…	5	…
t Stat	1.440185	…	1.194694	…	3.342435	…
P(T<=t) one-tail	0.099942	…	0.149101	…	0.010249	…
t Critical one-tail	1.943181	…	2.131846	…	2.015049	…
P(T<=t) two-tail	0.199884	…	0.298202	…	0.020498	…
t Critical two-tail	2.446914	…	2.776451	…	2.570578	…

In summary, mixes using SBR modified PG 76-22 binder provided higher rut resistance (lower permanent shear strain) than PG 67-22. SBS modified PG 76-22 had slightly higher shear strain than the SBR modified PG 76-22 binder. As for SBS modified PG 76-22 and PG 67-22, although on average SBS did provide higher rut resistance (lower shear strain) than PG 67-22, there is no significant difference between these mixes using the two binders.

Summary

The relationship between RSCH test permanent shear strain and NCAT Test Track field rut depth was poor. This was partly due to the good quality of the track construction, thick pavement structure, and mild summers in 2001 and 2002, which did not produce any significant rutting. The other parameters of the RSCH test, such as repetitions to 3 % shear strain, modulus, linear portion slope, and power law slope did not show good relationship with field rut depth either.

Criteria for interpreting RSCH permanent shear strain recommended by the Asphalt Institute to differentiate good and poor mixes seem to be reasonable based on the laboratory tests and field rut depth data in this study.

Sensitivity analysis for RSCH shear strain conducted for asphalt binder indicated that mixes using PG 76-22 binder performed better than the mixes using PG 67-22 binder.

References

[1] Romero, P. and Mogawer, W., "Evaluating of Superpave Shear Tester Using 19-mm Mixtures from the Federal Highway Administration's Accelerated Loading Facility," *Proceeding of the Association of Asphalt Paving Technologists*, Vol. 67, 1998.

[2] Wiliams, R. C., Romero, P., and Stuart, K., "Comparison of Superpave Shear Test Results to Westrack Performance," *Symposium on Highway and Runway Technology*, The 1998 International Conference of Computational Science (ICES 98), 1998.

[3] Anderson, R. M., Huber, G. A., Walker, D. E., and Zhang, X., "Mixture Testing, Analysis and Field Performance of the Pilot Superpave Project – The 1992 SPS-9 Mixtures," *Proceeding of the Association of Asphalt Paving Technologists*, Vol. 69, 2000.

[4] Tayebali, A. A., Khosla, N., Malpass, G., and Waller, F., "Evaluation of Superapve Repeated Shear at Constant Height Test to Predict Rutting Potential of Mixtures – Performance of Three Pavement Sections in North Carolina," Transportation Research Board, Transportation Research Record 1681, 1999.

[5] Anerson, R. M., Bulowski, J. R., and Turner, P. A., "Using Superpave Performance Tests to Evaluate Asphalt Mixtures," Transportation Research Board, Transportation Research Record 1681, 1999.

[6] Romero, P. R. and Anderson, M., "Variability of Asphalt Mixtures Tests Using the Superpave Shear Tester Repeated Shear at Constant Height Test," *80th Annual Meeting of the Transportation Research Board*, Washington, D.C., January 2001.

[7] Brown, E. R., Cooley Jr., L. A., Hanson, D., Lynn, C., Powell, B., Prowell, B. D., et al., "NCAT Test Track Design, Construction, and Performance," NCAT Report No. 2002-12, November 2002.

[8] Brown, E. R., Prowell, B., Cooley, A., Zhang, J., and Powell, R. B., "Evaluation of Rutting Performance on the 2000 NCAT Test Track," *Association of Asphalt Paving Technologists Meeting*, April 2004.

[9] Anderson, R., Michael, R. B., McGennis, W., Kennedy, T. W., "Sensitivity of Mixture Performance Properties to Changes in the Laboratory Compaction Using the Superpave Gyratory Compactor," *Proceeding of the Association of Asphalt Paving Technologists*, Vol. 69, 2001.

[10] Tayebali, A., "Evaluation of the Sensitivity of RSCH Based on Laboratory Rutting Characteristics of Westrack Fine Mixes," ATM 1142.

[11] Bukowski, J. R. and Harman, T., "Minutes of the Superpave Mixture Report Task Group," Meeting, September 1997.

Journal of ASTM International, March 2005, Vol. 2, No. 3
Paper ID JAI12262
Available online at www.astm.org

T. F. Fwa[1] *and S. A. Tan*[1]

C-ϕ Characterization Model for Design of Asphalt Mixtures and Asphalt Pavements

ABSTRACT: This paper reports the results of a research effort initiated in the early 1990s to develop a C-ϕ (cohesion-angle of friction) characterization model for the design of asphalt mixtures and asphalt pavements. It is demonstrated that, since the model is based on the fundamental material properties represented by C and ϕ, it can derive analytically other asphalt mix design parameters such as Marshall stability and flow, and indirect tensile strength. The C-ϕ characterization model therefore offers a useful basis for the development of a comprehensive design framework that integrates asphalt mix design with asphalt pavement structural design. To demonstrate this capability, the research developed an empirical-mechanistic rutting prediction model of asphalt pavement layer using the C-ϕ characterization model. In addition, the model allows stresses and strains under design loading to be computed, which can be applied as input to structural analysis for asphalt material selection and pavement thickness design.

KEYWORDS: triaxial test, asphalt mixtures, mix design, cohesion, friction angle, elastic modulus, pavement design, rutting prediction

Introduction

The conventional methods of asphalt mix design, such as the Marshall test procedure [1] and the stabilometer test method [2], are not related directly to pavement thickness design and performance analysis. The Superpave mix design method based on volumetric properties of the asphalt mixture [3] developed in the early 1990s also is not derived directly from engineering properties that permit mechanistic analysis of pavement structures. It is of practical interest to have an integrated asphalt mix design and pavement structural design approach based on a common set of fundamental engineering properties of the asphalt mixture. That would enable pavement engineers to predict or study analytically the performance of a particular design mix during service and have a better understanding of the behavior of the design mix under service conditions.

Research has been conducted by the authors at the National University of Singapore since the early 1990s with the aim of developing an integrated framework of asphalt mix design and asphalt pavement structural design based on C–ϕ (cohesion and angle of friction) characterization of asphalt mixtures. This paper presents the findings of the research so far. It is demonstrated that with the fundamental material properties of C and ϕ, and by means of finite element analysis, one can analytically compute conventional mix design parameters such as the Marshall stability and flow and the indirect tensile strength. This means that one could replace empirical Marshall test by the triaxial test that provides the C–ϕ material properties and proceed to performing mix design based on the Marshall procedure. This concept of applying the C–ϕ model to asphalt mix design is further illustrated by an example of mix design based on the Smith's mix design criteria [4].

Manuscript received 28 November 2003; accepted for publication 23 November 2004; published March 2005.
[1] Professor and Associate Professor, respectively, Center for Transportation Research, Department of Civil Engineering, National University of Singapore, 10 Kent Ridge Crescent, Singapore 119260.

Given the mix design, structural design of the asphalt pavement can be performed with trial thickness of pavement layers since the C-ϕ characterization model allows stresses and strains under design loading to be computed. As an illustration, the research has developed a rutting prediction model of asphalt pavement layer using the C-ϕ characterization model. The empirical-mechanistic rutting prediction model was developed from laboratory rutting tests by relating measured rut depths to the applied stresses, loading characteristics, and bearing capacity of the asphalt layer computed using the C-ϕ model. Examples are also given to explain how the C-ϕ model could be employed to perform pavement thickness design and performance analysis based on other structural failure considerations, such as fatigue cracking or excessive deflection.

Asphalt Mix Design Using the C-ϕ Model

It is illustrated that in this section that by determining the C-ϕ properties of an asphalt mixture, one is able to compute its Marshall stability and flow of the mixture and conduct mix design based on the Marshall criteria. While it is not the intention to perform Marshall mix design by computing Marshall stability and flow from the C-ϕ model, one must be aware of the significant added value of a new mix design method that can link and evaluate the past 50 years of experience in asphalt mix design based on the Marshall method. The C-ϕ model can also be used to compute the indirect tensile strength of an asphalt mixture for any mix design procedure that requires this property. A third illustration of mix design using the C-ϕ model is an application of the design criteria proposed by Smith [4] for asphalt mix design.

The triaxial cell used in the present research was modified from a conventional triaxial cell for soil testing. It was designed for testing 102 mm diameter × 200 mm tall specimens. During testing, the entire cell is immersed in a perspex water bath maintained at the desired test temperature. The water reservoir that provides the required confining pressure for testing is also kept at the same test temperature. The main test variables involved include test temperature, speed of loading, and the magnitude of confining pressure.

The cohesion C and the angle of friction ϕ are determined by constructing Mohr circles, each representing the average of the peak stresses of three test specimens tested at a given confining pressure. A failure envelope is defined by a line tangent to the Mohr circles. The cohesion C is given by the intercept of the line with the vertical axis, and the angle of friction ϕ is equal to the angle of inclination of the line. For the triaxial test associated with each Mohr circle, an elastic modulus E_p corresponding to confining pressure p can be computed from the initial linear portion of the deviator stress versus strain curve of the test [5,6]. A more detailed description of the test procedure and determination of C, ϕ, and E_p is given by the authors elsewhere [7].

Deriving Marshall Mix Design Parameters from C-ϕ Model

With the triaxial test determined properties of C, ϕ, and E_p, the Marshall stability and flow can be derived without performing the Marshall stability test. This is achieved by means of finite element analysis based on the C-ϕ model. Figure 1 shows the finite element mesh used for modeling the Marshall stability test. The stress-strain behavior of the asphalt mixture is modeled by an elasto-plastic idealization with the Drucker-Prager failure criterion [8,9]. In accordance with the Drucker-Prager criterion, a yield function f can be defined as:

$$f = \sqrt{J_{2D}} - \alpha J_1 - k \tag{1}$$

where J_1 is the first invariant of the stress tensor, J_{2D} is the second invariant of the deviator stress tensor, and α and k are positive material parameters. The material parameters α and k can be expressed in terms of C and ϕ by matching with the Mohr-coulomb failure criterion. As has been shown by a number of researchers [10,11], α and k in Eq 1 can be computed as follows for compression tests:

$$\alpha = \frac{2\sin\phi}{\sqrt{3}\,(3 - \sin\phi)} \tag{2}$$

$$k = \frac{6C \cdot \cos\phi}{\sqrt{3}\,(3 - \sin\phi)} \tag{3}$$

The material properties required as input to the finite element analysis based on Drucker-Prager model are thus fully defined by C and ϕ through the use of Eqs 2 and 3.

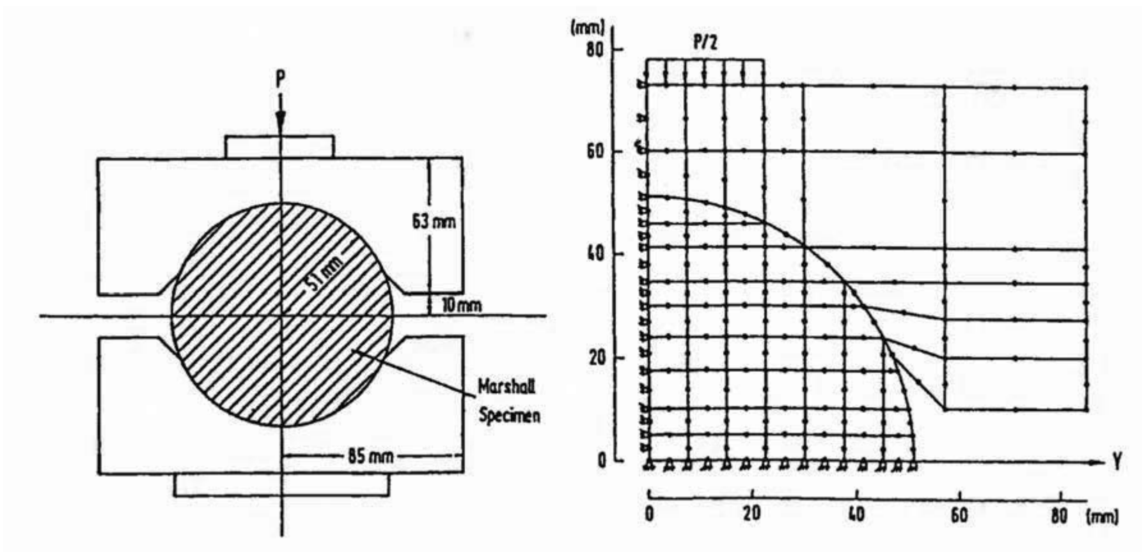

FIG. 1—*Finite element mesh for modeling Marshal test.*

Figures 2 and 3 show the results of a typical finite element analysis. The computed stress contours at failure are depicted in Fig. 2, while the load-deformation curves for different confining pressures p (hence different elastic moduli E_p) are given in Fig. 3. It is evident from Fig. 3 that the Marshall stability computed by the finite element analysis for a given pair of C and ϕ values is constant, regardless of the choice of elastic modulus E_p. However, the choice of E_p has a direct effect on the magnitude of the computed flow value. Based on the experimental evidence of Geotz [12] and the authors [13], the elastic modulus E_p at confining pressure of 70 kPa (10 psi) described the Marshall test condition best and provided a good estimate of the Marshall flow value.

The finite element mesh shown in Fig. 1 will provide asufficiently accurate estimation of Marshall stability and flow for common road paving mixtures. Therefore, the user of the computer software for computing Marshall stability and flow is only required to provide input values of C, ϕ, and E_p for p = 70 kPa. Alternatively, statistical predictive equations can be derived by regression techniques to relate C-ϕ properties to Marshall test parameters. For instance, based on the common dense-graded wearing surface asphalt mixes used in Singapore, the following regression equations have been established:

$$S = -14.0 + 0.0447C + 0.4960\phi \qquad (R^2 = 0.918, \text{standard error} = 1.913 \text{ kN}) \tag{4}$$

$$F = 15.1 + 0.00639C - 6.3444 \log E_0 \qquad (R^2 = 0.860, \text{standard error} = 0.871 \text{ mm}) \tag{5}$$

where S = Marshall stability in kN; F = Marshall flow in mm; and C and ϕ are in kPa and degree, respectively. E_0 in kPa is the elastic modulus determined by an unconfined triaxial test, i.e., with zero confining pressure. E_0 was chosen for the regression model because of the relative ease of performing triaxial tests at zero confining pressure.

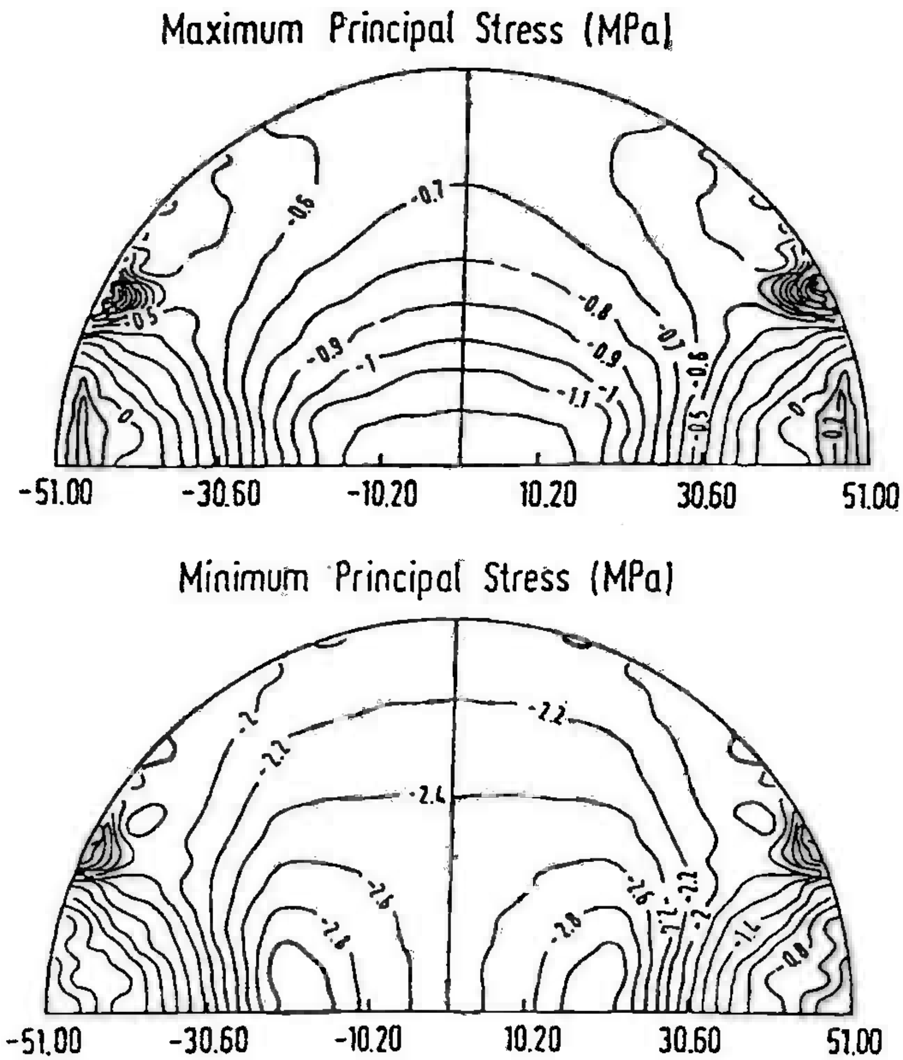

FIG. 2—*Finite element prediction of stress contours in Marshal test specimen at failure.*

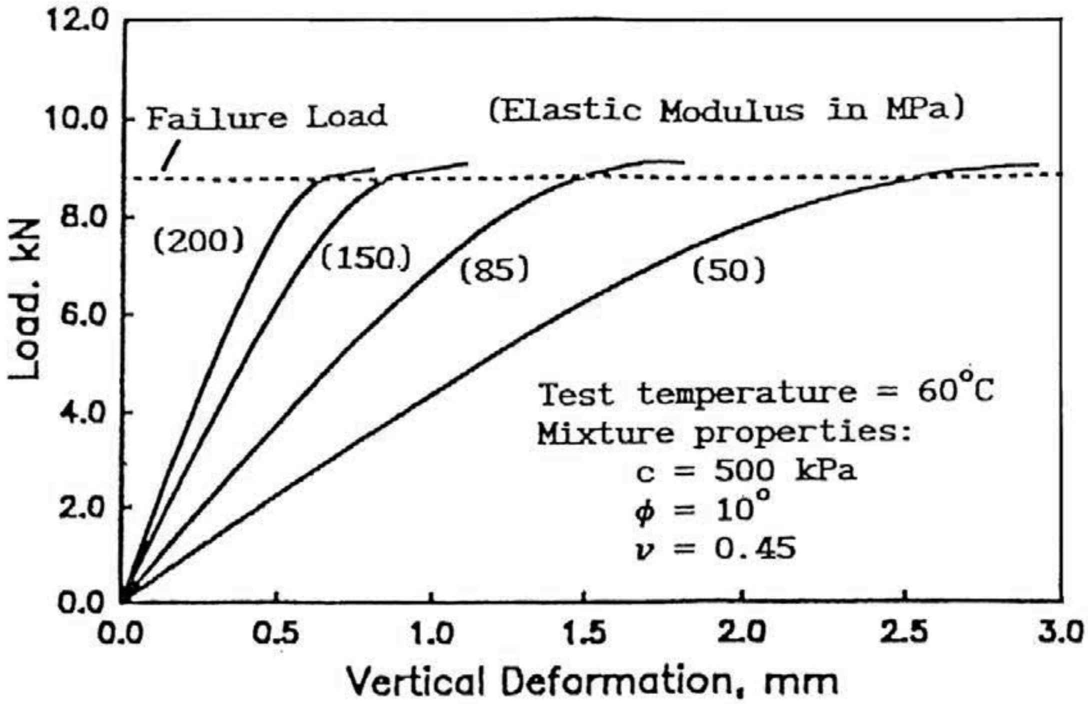

FIG. 3—*Finite element prediction of Marshal stability.*

Deriving Indirect Tensile Strength Using C-ϕ Model

A major benefit of using the C-ϕ model for mix design is the fact that other forms of test properties of the asphalt mixture could be derived analytically from the C-ϕ properties. This section illustrates that indirect tensile strength, which is an important property of asphalt mixture for pavement structural analysis, can be estimated with good accuracy from the C-ϕ model using finite element analysis. In the simulation of indirect tension tests, the elastic modulus obtained from unconfined triaxial tests (i.e., zero confining pressure) were applied. Figure 4 shows the finite element mesh adopted for the analysis. An example of the test results are plotted in Fig. 5. The finite element simulation of the indirect tensile test was able to provide a very good estimate of the measured indirect tensile strength. The overall correlation coefficient between the computed and measured indirect tensile strength was 0.930.

Similar to the case for Marshall test properties, statistical regression models can be developed to predict the indirect tensile strength of an asphalt mixture from its C-ϕ properties. Tests on the dense-graded asphalt mixtures commonly used in Singapore concluded that the indirect tensile strength was dependent only on the cohesion C of the mixtures, as given by the following predictive equation,

$$S_T = 36.74 + 0.6705\ C \qquad (R^2 = 0.834,\ \text{standard error} = 40.39\ \text{kPa}) \tag{6}$$

where S_T is the indirect tensile strength in kPa, and C is the cohesion in kPa.

Smith's Stability Concept for Asphalt Mix Design

In 1952, Smith [4] proposed a set of asphalt mix design criteria based on C and ϕ. The design criteria were established by examining the C and ϕ values of two classes of mix design according to their service performance under traffic loading. The two classes were satisfactory and unsatisfactory mixes. The criteria proposed by Smith are shown graphically in Fig. 6. Unsatisfactory mixes were those that exhibited excessive rutting and shoving, while satisfactory mixes were those with superior service performance.

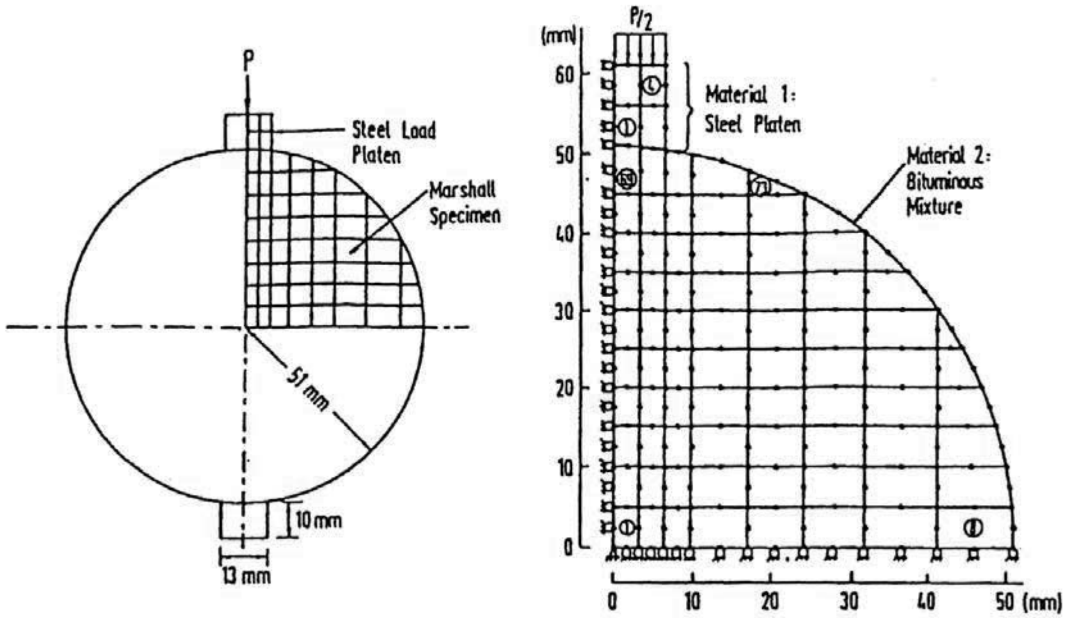

FIG. 4—*Finite element mesh for modeling indirect tension test.*

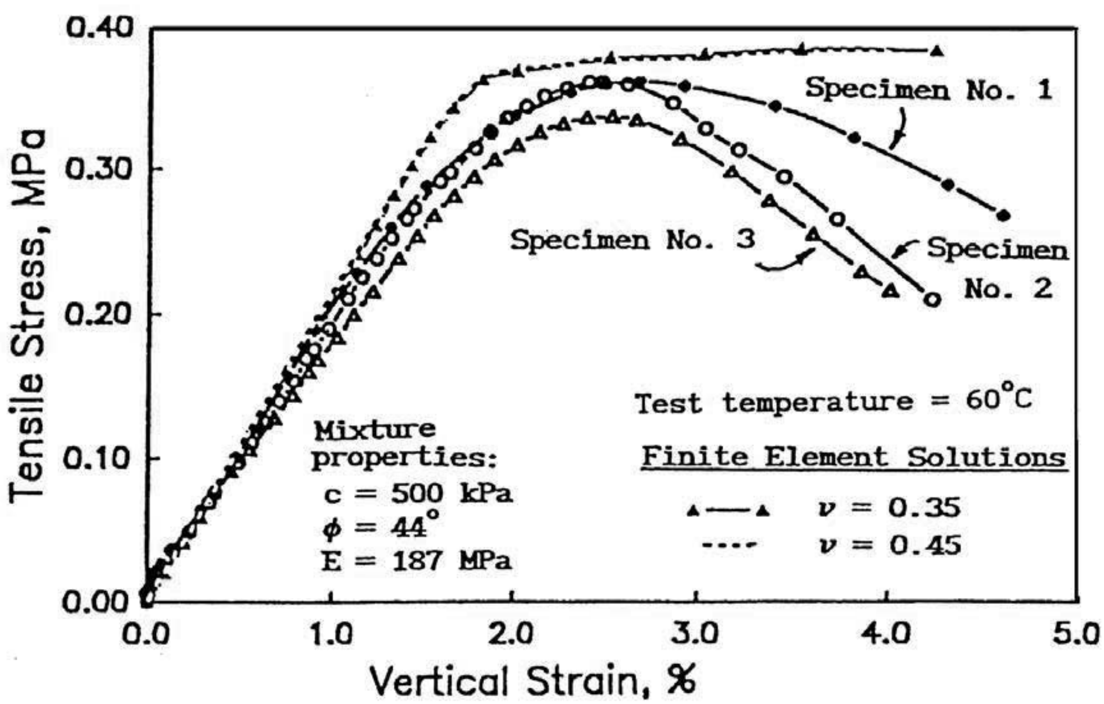

FIG. 5—*Predicted and measured stress-strain behavior of indirect tension test specimen.*

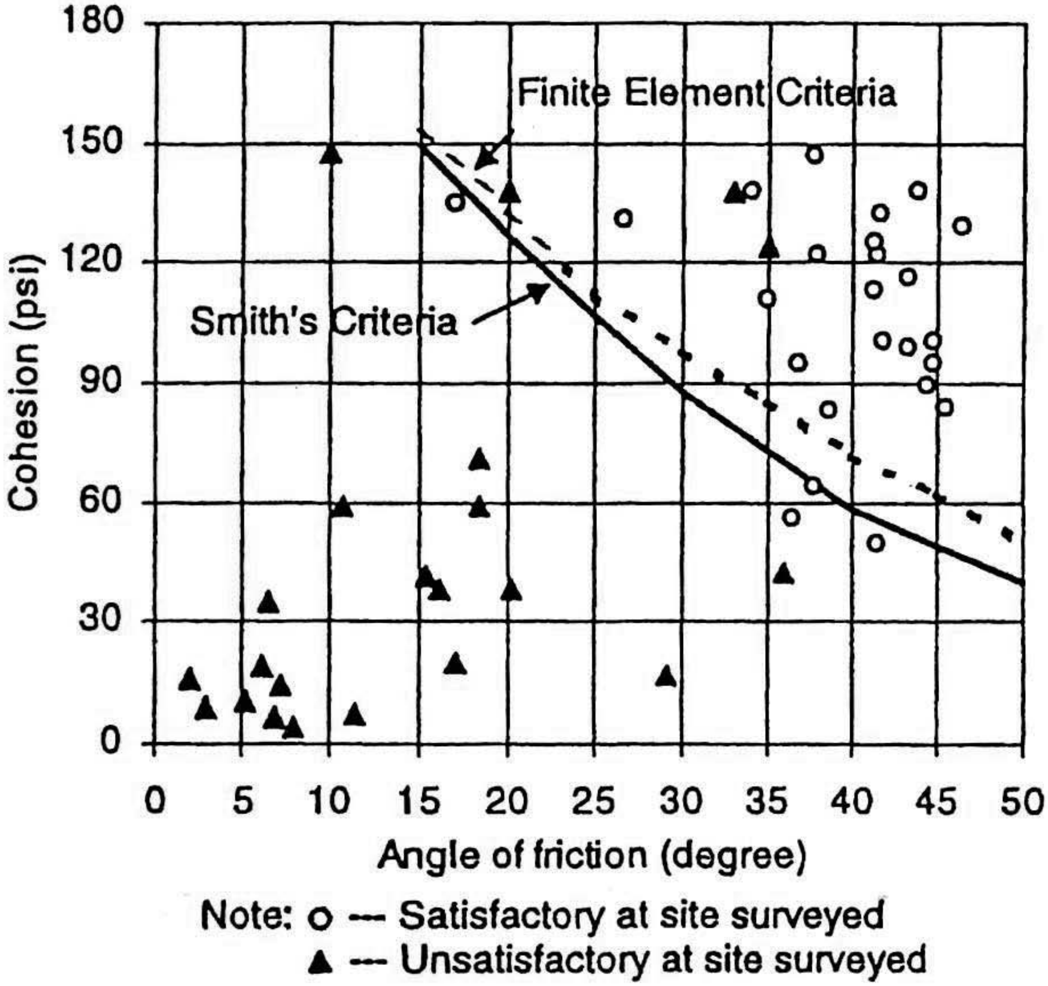

FIG. 6—*Mix design based on C-ϕ concept.*

Smith went on to derive the boundary that differentiated satisfactory and unsatisfactory mixes by means of the concept of Coulomb C-ϕ stability analysis. He considered the stresses within a semi-infinite layer of asphalt mixture below a uniformly loaded circular area and checked against the Coulomb shear strength of the mixture defined by the following equation:

$$S = C + q \tan\phi \tag{7}$$

where S is the shear strength of the mixture, and q is the applied normal pressure. Assuming that the most critical stresses occurred at the top surface, Smith found that the failure curve corresponding to an applied pressure q = 100 psi (690 kPa) provided a satisfactory divide between the satisfactory and unsatisfactory mixes. This failure curve is labeled as "Smith's criteria" in Fig. 6. Also shown in the same figure is a dashed-line curve labeled as "Finite element criteria," which is obtained by means of finite element analysis using the C-ϕ approach proposed in the present paper. The differences between the two criteria are relatively small and acceptable for practical applications.

Smith's mix design criteria suffer from the following obvious shortcomings: 1) Smith's criteria remain unchanged regardless of the thickness design of the actual pavement. This is inconsistent with experience of pavement design because pavement performance is known to be affected by the thickness of asphalt surface layer and the properties of underlying pavement layers. 2) The choice of q = 100 psi (690 kPa) as the mix selection criterion was made based on field experience, not derived analytically. It does not provide the flexibility of adjusting the mix design according to the design loading.

Both of the two shortcomings highlighted in the preceding paragraph can be overcome by the C-ϕ approach proposed in the present paper. Instead of considering an asphalt surface layer of infinite thickness as assumed by Smith, the multi-layer structure of the pavement and the true thickness of all layers can be analyzed to obtain the actual allowable applied load of the pavement. In this manner, the effects of layer thickness and magnitude of design load can be incorporated into the mix design process. An example is presented in Fig. 7, where it is shown that increasing the thickness of the asphaltic surface layer significantly raises the magnitude the failure load of a pavement. The same example also illustrates the beneficial effect of having a stronger base layer.

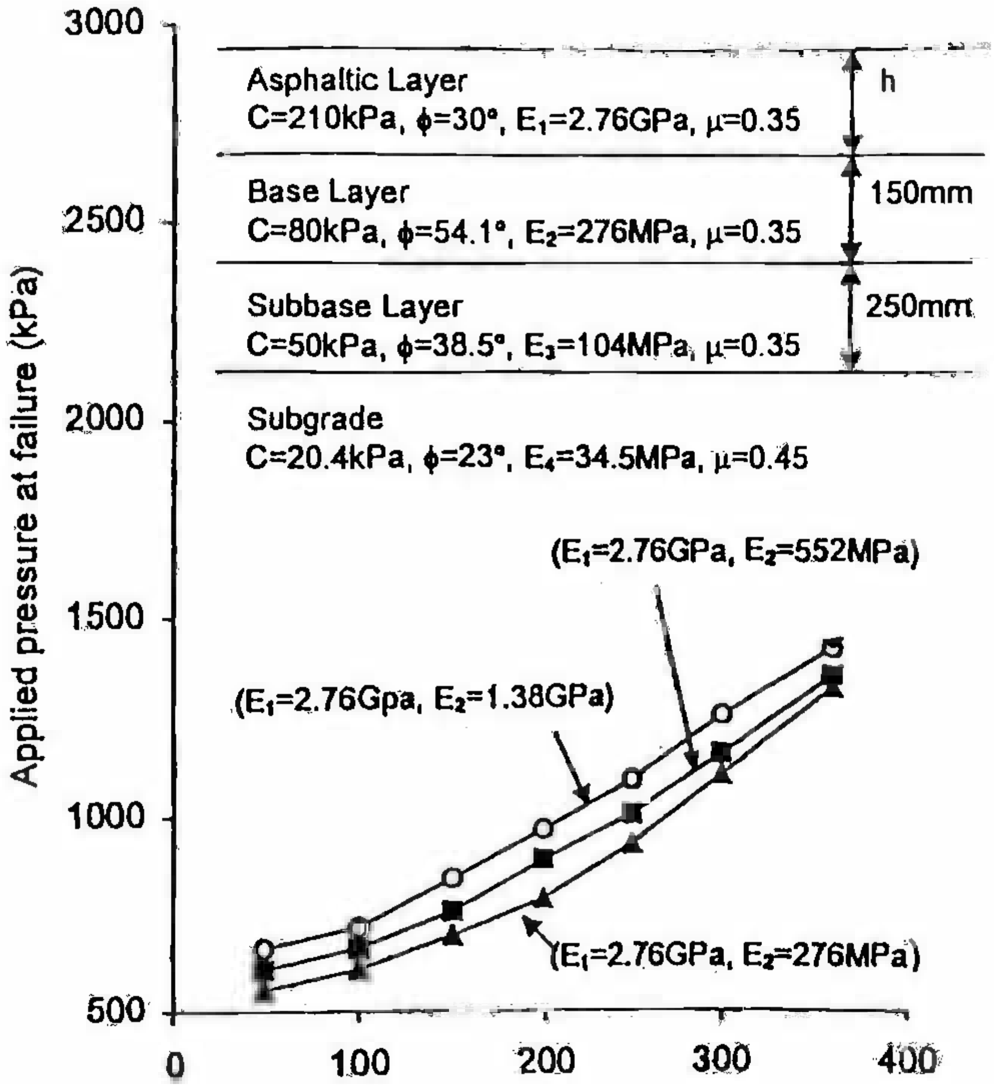

FIG. 7—*Computation of maximum applied load.*

Remarks on C-ϕ Model for Asphalt Mix Design

The preceding sections serve to illustrate the applicability of the proposed C-ϕ approach for asphalt mix design. While it is possible to establish mix design criteria based directly on the C-ϕ properties of the asphalt mixture, as with the case of Smith's design criteria, a highly significant benefit of the proposed approach is the possibility of linking up with other analytical or empirical mix design procedures. This has been demonstrated for the case of Marshall mix design method and the case of Smith's design procedure. Combining the C-ϕ approach with finite element analysis enables one to simulate other test methods and derive analytically the material parameters required for selected mix design methods. This is of great practical importance in switching from an empirical to an analytical mix design procedure, because the practical experience and knowledge accumulated through many years' of application of an empirical mix design can be passed on to achieve continuity in the process of migrating to a new mix design procedure.

The adoption of the C-ϕ approach should not present an implementation problem. Triaxial test is an established standard test procedure for determining the C-ϕ properties of soils. An advantage of using a triaxial test is that it is already a widely accepted test in civil engineering, and the triaxial test apparatus has been standard equipment available in all geotechnical engineering laboratories. With modern day test facilities and supporting systems, triaxial testing of asphalt paving mixtures is no longer prohibitive.

Structural Design Using C-ϕ Model

This section provides examples of possible applications by which the proposed C-ϕ model could be employed for structural design of asphalt pavements. By means of the C-ϕ model and finite element analysis, one could compute the stresses and strains of all pavement layers, including the asphaltic surface layer, under the design wheel loads. This offers the necessary information for mechanistic or semi-mechanistic analysis and design of various pavement layers against different modes of failure.

Structural Analysis of Pavement Using C-ϕ Model

In the finite element analysis of a pavement structure under the action of a wheel load, the problem can be considered as a half-space of layered structure acted upon by a circular uniform load. Figure 8 shows a typical axisymmetric finite element mesh used for the analysis. For highway pavement design, a depth of H = 1.5 m and width of W = 2.0 m would be adequate to produce sufficiently accurate stress and strain data for pavement design. The Drucker-Prager failure criterion as described by Eqs 1–3 is adopted. The following four material properties are required as input: cohesion C, angle of friction ϕ, elastic modulus E_p, and Poisson ratio ν. If one is interested in establishing the allowable load that a pavement structure can withstand, the finite element analysis will involve applying a series of sufficiently small load increments until the peak load is reached. The peak load may be defined as the load when the first element of the finite element mesh reached the yield state.

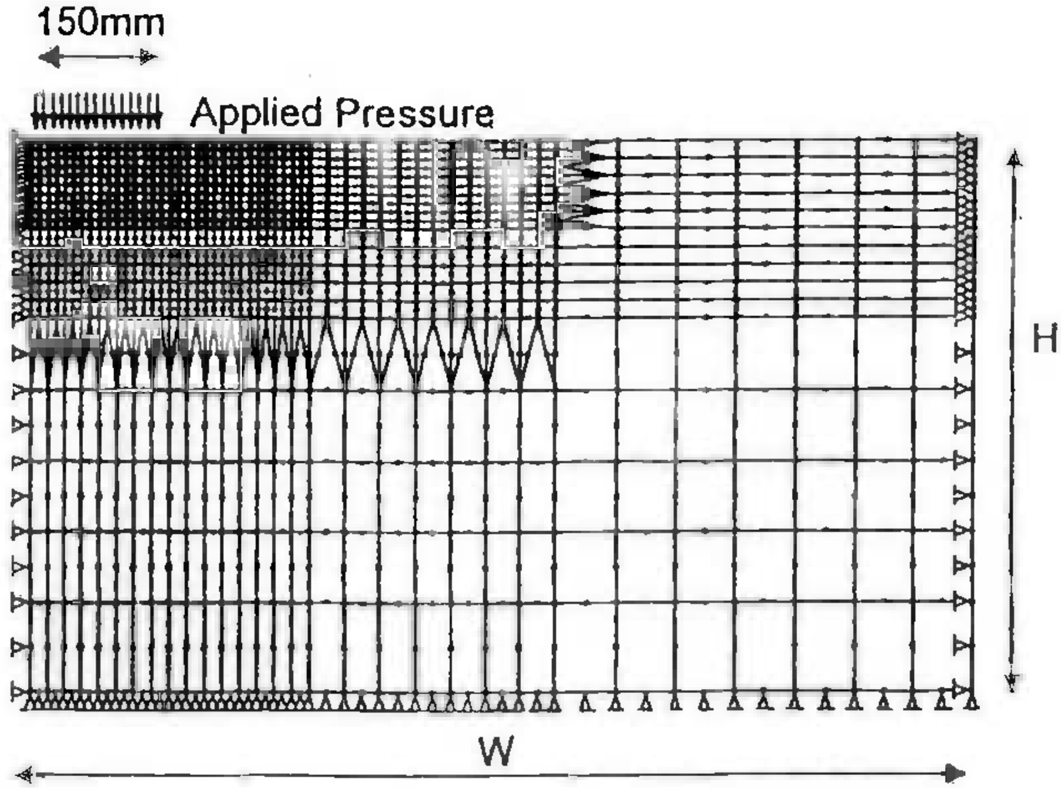

FIG. 8—*Axisymmetric finite-element mesh for pavement under circular load.*

Figure 9 gives a simple example as an illustration of pavement layer thickness design based on the maximum surface deflection. The maximum surface deflection has been used by some road agencies as an indicator of the structural capacity of the pavement in question and as a basis for computing the remaining service life of the pavement. In Fig. 9, the maximum surface deflections for different thickness of the asphaltic surface layer under different applied loads are presented. Depending on the maximum surface deformation and the design load specified, an appropriate thickness of the asphaltic surface layer can be determined. An elaborate trial-and-error process is involved if one decides to try out different materials and thicknesses for other pavement layers as well, although the basic nature of the analysis remains unchanged.

Rutting Prediction Model Based on C-ϕ Concept

Another example of application of the C-ϕ concept is recently illustrated by the authors in developing a rutting prediction model of an asphalt pavement layer using the C-ϕ properties of pavement materials [14]. The rut depth prediction model adopts the common power equation form to account for the cumulative development of rut depth with the number of load applications as follows:

$$R = k \cdot (N)^a \tag{8}$$

where R is the rut depth after N number of load repetitions, a is a model constant, and k is a model coefficient.

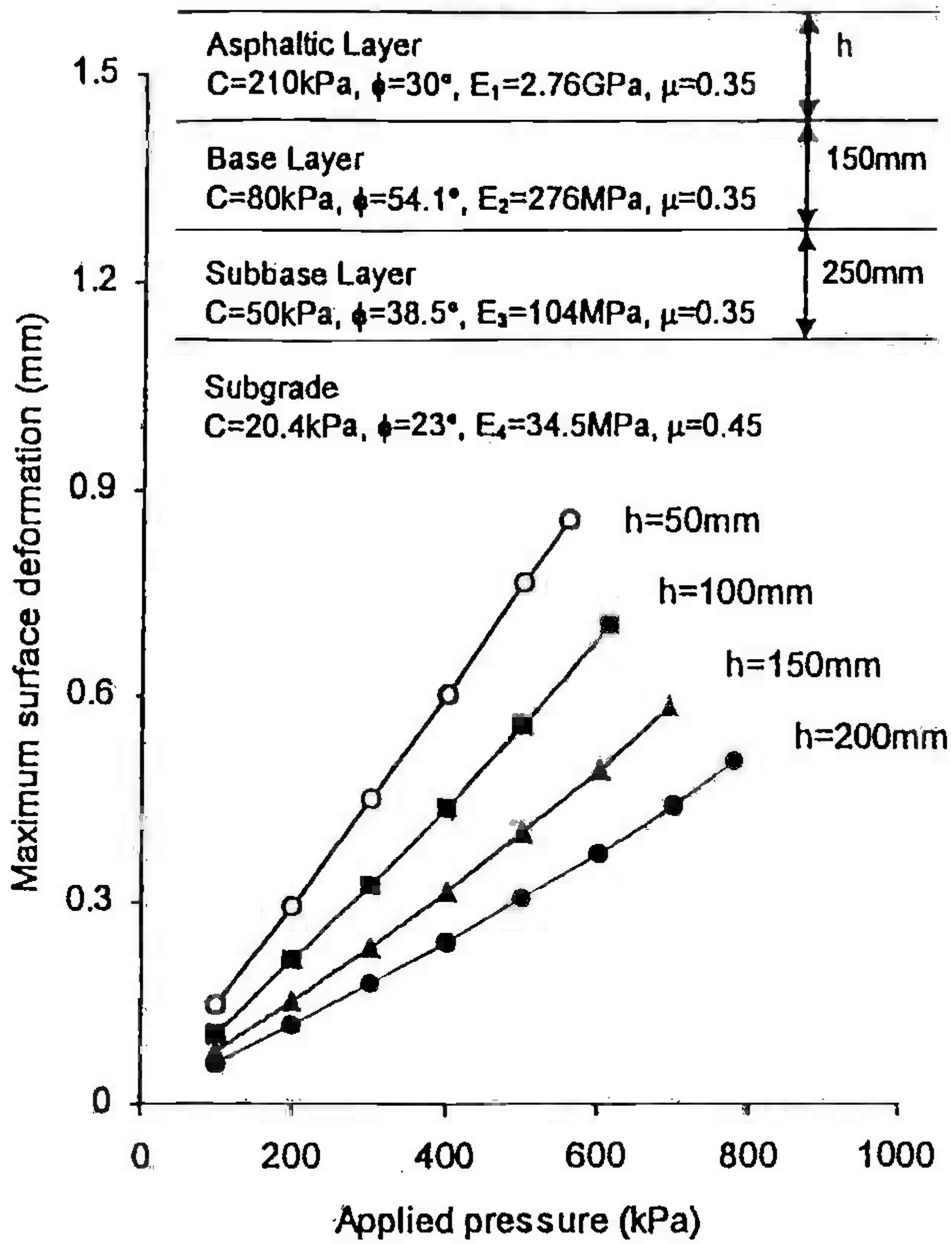

FIG. 9—*Computation of maximum surface deflection.*

To take the effects of pavement layer properties, magnitude of applied load, loading speed, and pavement temperature into consideration, the k function was defined as follows:

$$k = (L)^b \cdot (T)^c \cdot (t)^d \quad \text{with } L = P/B \tag{9}$$

where L is a load ratio of the magnitude of the repeated load P to the maximum allowable load B that defines the bearing capacity of the asphalt pavement layer; T is the pavement temperature, t is the loading duration of each load application; and b, c, and d are model constants.

It is noted that the load bearing capacity B of the asphalt layer of a pavement structure is the maximum applied load it can withstand before shear failure in the asphalt layer takes place. It is a function of the layer thickness and structure properties (i.e., C, ϕ, and E_p) of the asphalt layer as well as the underlying pavement layers. The finite element method of computing the peak load as explained in the preceding section was adopted in the computation of the load bearing capacity B.

The model constants a, b, c, and d are to be calibrated for an asphalt mix type. They characterize the rutting behavior of the asphalt mix considered. For instance, the following are rut depth prediction models for three different asphalt mix types used in Singapore:

$$\text{Mix type 1:} \quad R = (N)^{0.45} \cdot (L)^{2.02} \cdot (T)^{0.53} \cdot (t)^{0.40} \tag{10}$$

$$\text{Mix type 2:} \quad R = (N)^{0.50} \cdot (L)^{2.27} \cdot (T)^{0.51} \cdot (t)^{0.16} \tag{11}$$

$$\text{Mix type 3:} \quad R = (N)^{0.28} \cdot (L)^{1.22} \cdot (T)^{0.29} \cdot (t)^{0.28} \tag{12}$$

In the above equations, rut depth R is in mm, load ratio L in numerical value, temperature T in degree Celsius, and loading duration t in seconds. It should be mentioned that the load ratio L covers the effects of structural design and the bearing capacity of the asphalt surface layer computed based on the C-ϕ model.

To apply the proposed rut depth prediction model for actual traffic consideration, a procedure using the following rut depth estimation equation is proposed:

$$R = \sum_{i=1}^{n} \left[(N_i)^a \cdot (L_i)^b \cdot (T_i)^c \cdot (t_i)^d \right] \tag{13}$$

where the number of traffic loading is divided into n groups according to the magnitude of wheel load, travel speed, and pavement temperature. As indicated earlier, the values of coefficients a, b, c, and d vary with mix type and have to be determined experimentally.

Further Remarks on Pavement Design Using C-ϕ Model

Besides the deflection and rutting in the asphaltic surface layer, there are other possible failure modes which must be examined in a comprehensive asphalt mix and pavement design framework. For example, the possibility of tensile cracking and subgrade rutting potential are two other common considerations for pavement design. With the proposed C-ϕ model and finite element analysis, indirect tensile strength of the design mix can be determined, and tensile stresses in the asphaltic surface layer under different wheel loads can be computed for the trial design pavement structure. These computed data can be analyzed using an appropriate fatigue model to check against fatigue cracking. Similarly, compressive strains caused by repeated applications of different wheel loads can be computed and applied to derive the cumulative deformation by means of a suitable mechanistic or semi-empirical subgrade rutting model. The computed rutting deformation in the subgrade may then be added to the predicted rutting depth in the asphaltic surface layer and checked for excessive rutting.

It must be mentioned that there are aspects of mix and pavement performance that cannot be addressed by the proposed C-ϕ approach. These include durability of mix, resistance of mix against water damage, and its susceptibility to low temperature cracking. One must also take note that asphaltic mixtures may harden due to aging, and that their cohesion, angle of friction, and elastic modulus are likely to change during the service life of pavements.

Conclusion

The main aim of this paper is to present a framework for integrated asphalt mix and pavement design using C-ϕ model. The proposed integrated asphalt mixture and asphalt pavement design approach provides a logical link between the mix design phase and the pavement design phase, based on fundamental material properties that are determined experimentally. The cohesion, angle of friction, and elastic modulus are the basic engineering properties employed for the analysis. These properties are determined by the triaxial test, which is a widely accepted standard test in civil engineering.

It has been demonstrated in this paper that, with the help of finite element analysis, the C-ϕ model can be a powerful tool for the design of asphalt paving mixtures. It enables the pavement engineer to examine analytically the expected behavior of the asphalt mixture under different design loading conditions. It also allows the pavement engineer to determine, through finite-element simulated analysis, mix design parameters (such as Marshall stability and flow) used in other empirical or semi-empirical mix design methods.

Since the proposed C-ϕ model and the method of analysis compute pavement stresses and strains under wheel loads, mechanistic or semi-empirical models can be applied for pavement design against failures such as fatigue cracking and rutting. Examples are presented to demonstrate applications of the C-ϕ model in surface deflection computation and rut depth prediction. In summary, the proposed finite-element C-ϕ model has been demonstrated to be able to evaluate mix design and pavement structural design in an integrated manner using a consistent set of fundamental engineering properties. It appears to be a potentially useful design approach and analytical tool to address the main issues in mix design, pavement design, and pavement performance evaluation, although other tests to examine mix durability, water damage potential, and low temperature cracking are still necessary.

References

[1] Asphalt Institute, "Mix Design Methods for Asphalt Concrete and other Hot-Mix Types," Manual Series MS-1, 5th ed., 1983.

[2] Yoder, E. J. and Witczak, M. W., *Principles of Pavement Design*, John Wiley & Sons, Inc., New York, 1975.

[3] Kennedy, T. W., Moulthrop J. S., and Huber G. A., "Development of SHRP Mixture Specification and Design and Analysis Aystem," *J. of the Association of Asphalt Paving Technologists*, Vol. 62, 1993, pp. 508–528.

[4] Smith, V. R., "Application of the Triaxial Test to Bituminous Mixtures," *ASTM STP 106*, ASTM International, West Conshohocken, PA, 1951.

[5] Worley, H. E., "Triaxial Design Correlated with Flexible Pavement Performance in Kansas," *ASTM STP 106*, ASTM International, West Conshohocken, PA, 1951, pp. 112–137.

[6] Huang, Y. H., "Deformation and Volume Change Characteristics of a Sand-Asphalt under Constant Direct and Triaxial Compressive Stresses," Highway Research Record No. 178, Highway Research Board, 1967.

[7] Fwa, T. F., Tan, S. A., and Zhu L. Y., "Re-Examining C-ϕ Concept for Asphalt Paving Mix Design," *J. of Transportation Engineering*, American Society of Civil Engineers, Vol. 127, No. 1, 2001, pp. 67–73.

[8] Drucker, D. C. and Prager, W., "Soil Mechanics and Plasticity Analysis or Limit Design," *Quarterly of Applied Mathematics*, Vol. 10, 1952, pp. 157–165.

[9] Desai, C. S. and Siriwardane, H. J., *Constitutive Laws for Engineering Materials with Emphasis on Geologic Materials*, Prentice-Hall, Inc., Englewood Cliffs, New Jersey, 1984.

[10] Cumaraswamy, V., "Mechanical Behavior of Chemically Grouted Sand," *J. of Geotechnical Engineering*, Vol. 112, No. 9, 1986, pp. 869–887.

[11] Fourie, A. B. and Beer, B., "An Illustration of the Importance of Soil Nonlinearity in Soil Structure Interaction Problems," *Computer and Geotechnics*, Vol. 8, 1989, pp. 219–241.

[12] Geotz, W. H., "Comparison of Triaxial and Marshall Test Results," *Proc. Association of Asphalt Paving Technologists*, Vol. 20, 1951, pp. 200–245.

[13] Fwa, T. F., Low, B. H., and Tan, S. A., "Behavior Analysis of Asphaltic Mixtures Using Triaxial Test-Determined Properties," *STP 1265*, ASTM International, West Conshohocken, PA, 1995, pp. 97–111.

[14] Fwa, T. F., Tan, S. A., and Zhu, L. Y., "Rutting Prediction of Asphalt Pavement Layer Using C-ϕ Model," *J. of Transportation Engineering*, American Society of Civil Engineers, 2003.

Journal of ASTM International, March 2005, Vol. 2, No. 3
Paper ID JAI12264
Available online at www.astm.org

Zhong Wu,[1] Louay N. Mohammad,[1] L.B. Wang,[2] and Mary Ann Mull[3]

Fracture Resistance Characterization of Superpave Mixtures Using the Semi-Circular Bending Test

ABSTRACT: The fracture resistance of asphalt mixture is an important property directly related to pavement distresses, such as cracking. This paper reports the investigation of a newly-developed semi-circular bending (SCB) test as a candidate test for the fracture resistance characterization of asphalt mixtures. Thirteen Superpave mixtures, designed with four different binder types (AC-30, PAC-40, PG70-22M, and PG76-22M) and four different compaction levels (N_{design} = 75, 97, 109, and 125), were considered in this study. The SCB tests were conducted at 25°C using a three-point bending fixture in a MTS testing system. The fracture resistance was analyzed based on an elasto-plastic fracture mechanics concept of critical strain energy release rate, also called the critical value of J-integral (J_C). Preliminary results indicate that the J_C values were fairly sensitive to changes in binder type and nominal maximum aggregate size (NMAS) used in Superpave mixtures. This study suggests that the SCB test could be a valuable correlative tool in the evaluation of fracture resistance of asphalt mixtures.

KEYWORDS: Superpave mixture, fracture resistance, semi-circular bending, energy release rate

Introduction

An increasing number of researchers in recent years has expressed concern over the cracking resistance of asphalt pavements and has realized the limitations associated with predicting true fracture (cracking) properties of asphalt mixtures based on tests performed on un-notched samples, such as the indirect tensile (IT) and beam fatigue tests [1–3]. As a consequence, a number of studies has started to investigate the application of the more complex fracture mechanics concepts to the behavior of bituminous materials [4,5]. A recent research effort in the mechanistic testing of asphalt mixtures has resulted in the development of a Semi-Circular Bending (SCB) test as an alternative to the IT test to determine the fracture and fatigue behavior of asphalt concrete [6,7]. This method is based on the elasto-plastic fracture mechanics concept that leads to the laboratory determination of the critical strain energy release rate of mixtures using notched semi-circular samples. The major advantage of the SCB test is that different notch depths can be introduced easily on the semi-circular test specimen. Hence, the true fracture properties of asphalt mixtures with regard to the crack propagation can be evaluated directly. Other advantages of the SCB test include: (1) the test setup and procedure are fairly simple and rapid; (2) the SCB specimens can be prepared directly from cylindrical samples obtained from standard cores prepared in the Superpave gyratory compactor (SGC) or taken from the field; and (3) multiple specimens can be obtained from one core, reducing the error caused by

Manuscript received 6 January 2004; accepted for publication 29 July 2004; published March 2005. Presented at ASTM Symposium on Performance of Hot Mix Asphalt (HMA), including Fundamental and Empirical Procedures on 9 December 2003 in Tampa, FL.
[1] Ph.D., Louisiana Transportation Research Center and Louisiana State University, 4101 Gourrier Ave., Baton Rouge, LA 70808.
[2] Ph.D., Louisiana State University, Baton Rouge, LA 70803.
[3] Technology Resources, Inc., Auburn, AL 36832.

heterogeneities from one core to the next. While the semi-circular notched bending test offers a direct evaluation for cracking performance of asphalt mixtures, there has been very little experience with it.

Objective and Scope

The primary objective of this research was to evaluate the fracture resistance of Superpave mixtures using the proposed SCB test. The scope of this study included conducting a total of 117 SCB tests at 25°C, which were resulted from 13 mixtures × 3 notch depths (25.4-, 31.8-, and 38.0-mm) × 3 duplicates for each mixture.

Laboratory Mixture Characterization

Materials

Thirteen Superpave mixtures were evaluated in this paper. Table 1 provides the general project information for the mixtures considered. As shown in Table 1, four asphalt binder types: AC-30, PAC-30, PG70-22M, and PG76-22M were selected. According to the Louisiana Standard Specifications for Road and Bridges [8], binders AC-30 and PAC-40 grades as a PG 64-22 and a PG70-22, respectively. More details about these binders can be found elsewhere [8]. The Superpave mixture design was performed as per AASHTO TP4 specifications. Four SGC compaction levels – N_{design} = 75, 97, 109, and 125 – were included in the mixture design. All mixtures used crushed limestone aggregates except two mixtures – 361W and 191W – which contained the granite and rhyolite, respectively. In addition, these two mixtures (361W and 191W) were the only two fine-graded mixtures (gradation curve passes above the restricted zone) in this study; the remaining eleven mixtures were coarse-graded (gradation curve passes below the restricted zone). Finally, the thirteen mixtures considered included two nominal maximum aggregate sizes (NMAS): 19 mm and 25 mm. Only three mixtures (4B, 61B, and 90B) had a 25 mm NMAS, Table 1.

TABLE 1—*Project information and mixtures designation.*

Project Route	Mixture Type	Binder Type	Aggregate			N_{design}	Mix Designation
			NMAS (mm)	Type	Gradation		
LA 361	WC	PG70-22M*	19	Granite	Fine	75	361W
LA 191	WC	PG70-22M	19	Rhyolite	Fine	75	191W
LA 874	WC	PG70-22M	19	Limestone	Coarse	75	874W
LA 121	BC	AC-30	19	Limestone	Coarse	97	121B
LA 22	BC	AC-30	19	Limestone	Coarse	97	22B
LA 4	BC	AC-30	25	Limestone	Coarse	97	4B
US 61	WC	PAC-40	19	Limestone	Coarse	109	61W
US 61	BC	PAC-40	25	Limestone	Coarse	109	61B
US 90	BC	PAC-40	25	Limestone	Coarse	109	90B
Westbank Express	WC	PAC-40	19	Limestone	Coarse	125	WEW
I-10	WC	PG76-22M	19	Limestone	Coarse	125	10W
I-49	WC	PG76-22M	19	Limestone	Coarse	125	49W
I-12	WC	PG76-22M	19	Limestone	Coarse	125	12W

*M = polymer-modified binder; WC = wearing course; BC = binder course.

Specimen Preparation and Experimental Procedure

The SCB test specimens in this study were obtained by slicing the SGC compacted cylindrical cores along their central axes. Figure 1 provides the geometry of a SCB specimen used in this study. Each SGC cylindrical core was compacted at an air void content of 7.0 ±0.5 % with a dimension of 150 mm ($2r_d$) in diameter and 57 mm (b) in height. Two SCB test specimens were then cut from one SGC core. As shown in Fig. 1, a vertical notch (the symbol "a" in Fig. 1) was introduced along the symmetrical axis of each SCB specimen in order to study the true fracture properties of asphalt mixtures with regard to the crack propagation. The notches were cut using a special saw blade of 3.0 mm thickness. Three nominal notch depths: 25.4 mm, 31.8 mm, and 38 mm, were used. For each notch depth three duplicate SCB specimens were prepared.

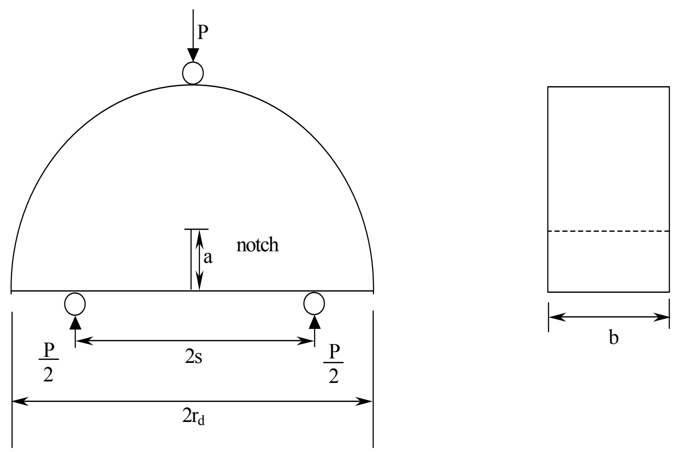

FIG. 1—*SCB test specimen configuration.*

An MTS model 810 closed-loop electro-hydraulic testing machine was used to perform the SCB tests. Figure 2 shows the three-point bend load SCB test configuration developed in this study together with the initial and final orientation of a SCB specimen. The distance between the support rollers of load application, 2s, was 125 mm. The SCB test procedure used in this study was first introduced by Mull et al. [6] to characterize the fracture resistance of crumb rubber modified asphalt mixtures. During an SCB test, the semi-circular specimen was loaded monotonically until fracture failure under a constant cross-head deformation rate of 0.5 mm/min at a test temperature of 25 ±1°C. The load and vertical deformation were continuously recorded, and a load-vertical displacement curve was plotted.

A preliminary finite element (FE) simulation was performed in this study to analyze the stress distribution in a SCB test. A commercial FE software, ABAQUS, was chosen for the simulation. For simplicity, only elasticity was considered. Because of double symmetry, only half of the SCB specimen was modeled. Figure 3 presents the stress distribution in two major directions (S11 and S22) of a semi-circular specimen. It shows, as expected, that the SCB specimen is primarily under tension around the notch tip and the bottom of specimen in the horizontal direction (S11 in Fig. 3). Meanwhile, a significant amount of compression is also found around the notch tip and the bottom of specimen in the vertical direction (S22 in Fig. 3).

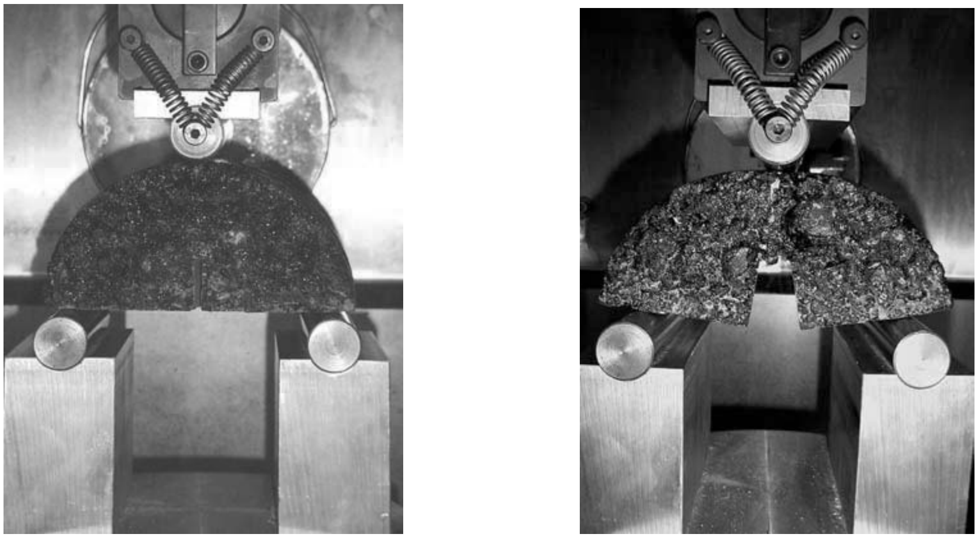

FIG. 2—*SCB bending test apparatus.*

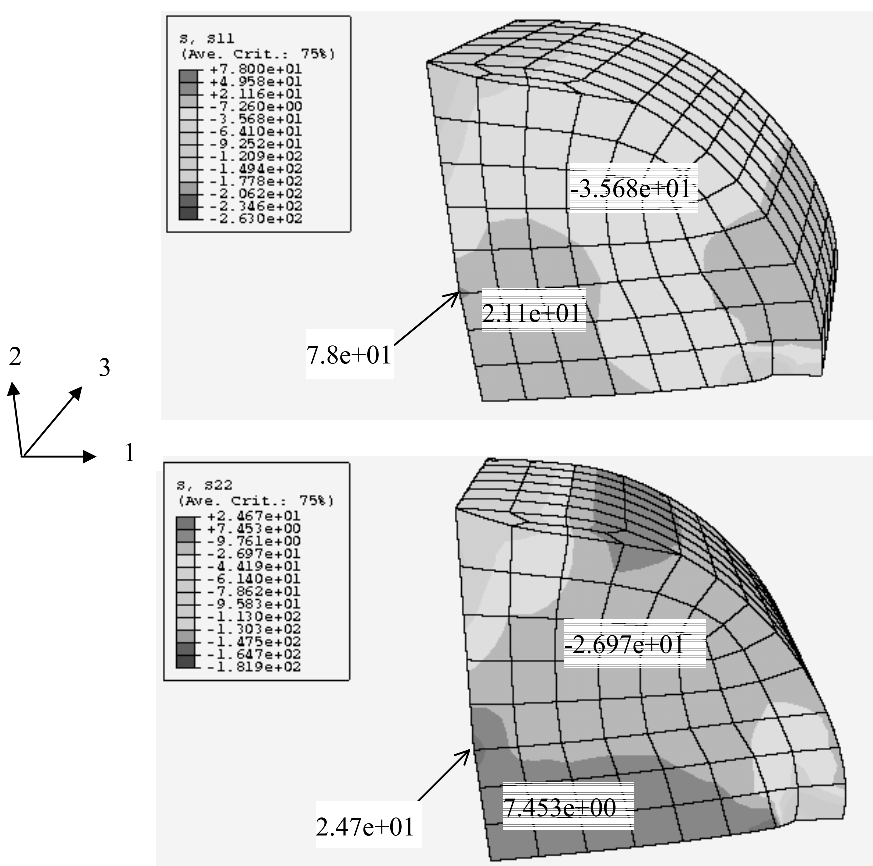

FIG. 3—*Finite element simulation of the SCB test.*

Determination of the Critical J-integral, J_C

As shown in Fig. 4, according to the linear-elastic fracture mechanics (LEFM), the strain energy release rate (G) of a cracked member under Mode I displacement mode (also called the opening mode) can be defined as follows:

$$\begin{aligned} G &= -\left(\frac{1}{b}\right)\frac{dU}{da} \\ &= K^2/E' \end{aligned} \tag{1}$$

where,

b = thickness of the specimen,
a = the notch depth,
U = the strain energy to failure,
K = stress intensity factor,
E' = Young's modulus, E (plane stress), and
E' = $E/(1-u^2)$ (plane strain) where u is the Poisson ratio.

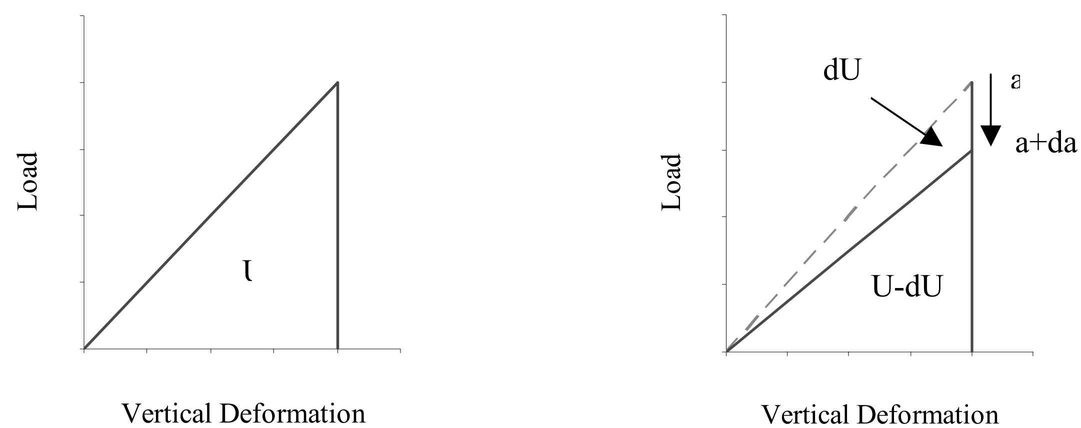

FIG. 4—*Potential energies for two neighboring crack lengths of a and a + da.*

According to Dowling [9], for a material whose stress-strain behavior is nonlinear due to elasto-plastic behavior, such as asphalt mixtures, the concept of J-integral can be thought of as the generalization of the strain energy release rate, G, as illustrated in Fig. 5.

Since the plasticity limitations of LEFM can now be exceeded according to the J-integral concept, according to Rice [10], the critical value of J-integral or the fracture resistance, J_C, can be determined with the following equation:

$$J_c = -\left(\frac{1}{b}\right)\frac{dU}{da} \tag{2}$$

Figure 6*a* shows typical load-vertical deflection curves obtained in the SCB test at three nominal notch depths of 25.4, 31.8, and 38.0 mm. In order to obtain the critical value of fracture resistance, J_C, the area under the loading portion of the load deflection curves, up to the maximum load, needs to be measured for each notch depth of each mixture. This area represents the strain energy to failure, U.

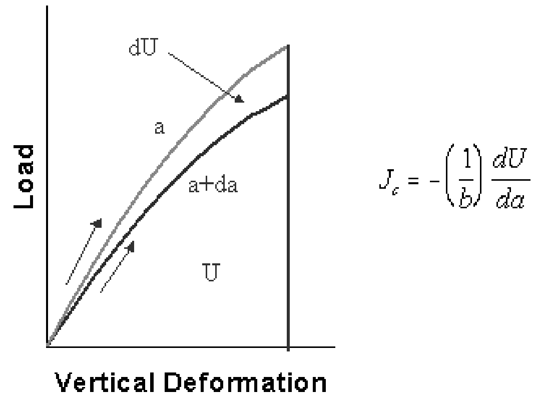

FIG. 5—*Definition of the J-integral in terms of the potential energy difference.*

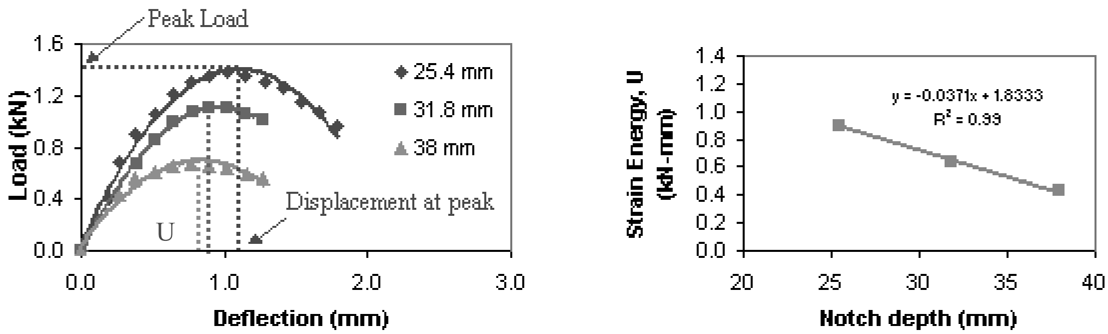

FIG. 6—*Typical load-deflection curves from semi-circular fracture test.*

The average values of U at each notch depth are then plotted versus notch depth to obtain a changing slope of U from a regression line, Fig. 6*b*. This slope is the value of (dU/da) in Eq 2. Finally, the J_C can be computed by dividing the dU/da value by the specimen width of b.

Discussion of Test Results

Notch Depth of 25.4 mm

Figure 7 presents the mean SCB test results at the notch depth of 25.4 mm for the thirteen Superpave mixtures considered, which including the peak load, vertical displacement at peak load and strain energy to failure (as defined in Fig. 6). The mean values showed in the figure were averaged from three duplicate test results of each mixture. Mixtures containing the same asphalt binder types were graphically grouped together, which resulted into four mixture groups as shown in Fig. 7: the PG70-22M, the AC-30, the PAC-40 and the PG76-22M. In addition, an overall average value per mixture group was also computed and presented together within each mixture group.

As for the peak load shown in Fig. 7*a*, the PAC-40 mixture group had the highest average load value (1.62 kN), followed by the mixture groups of PG76-22M (1.53 kN), AC-30 (1.47 kN), and PG70-22M (1.12 kN). Considering the fact that the same specimen geometry was used in all SCB tests and the tensile failure occurred at the bottom of a SCB sample, this largest peak load value implies that the PAC-40 mixture group possessed the highest tensile strengths. The PG70-

22M had the lowest strengths, among the four mixture groups considered at the notch depth of 25.4 mm.

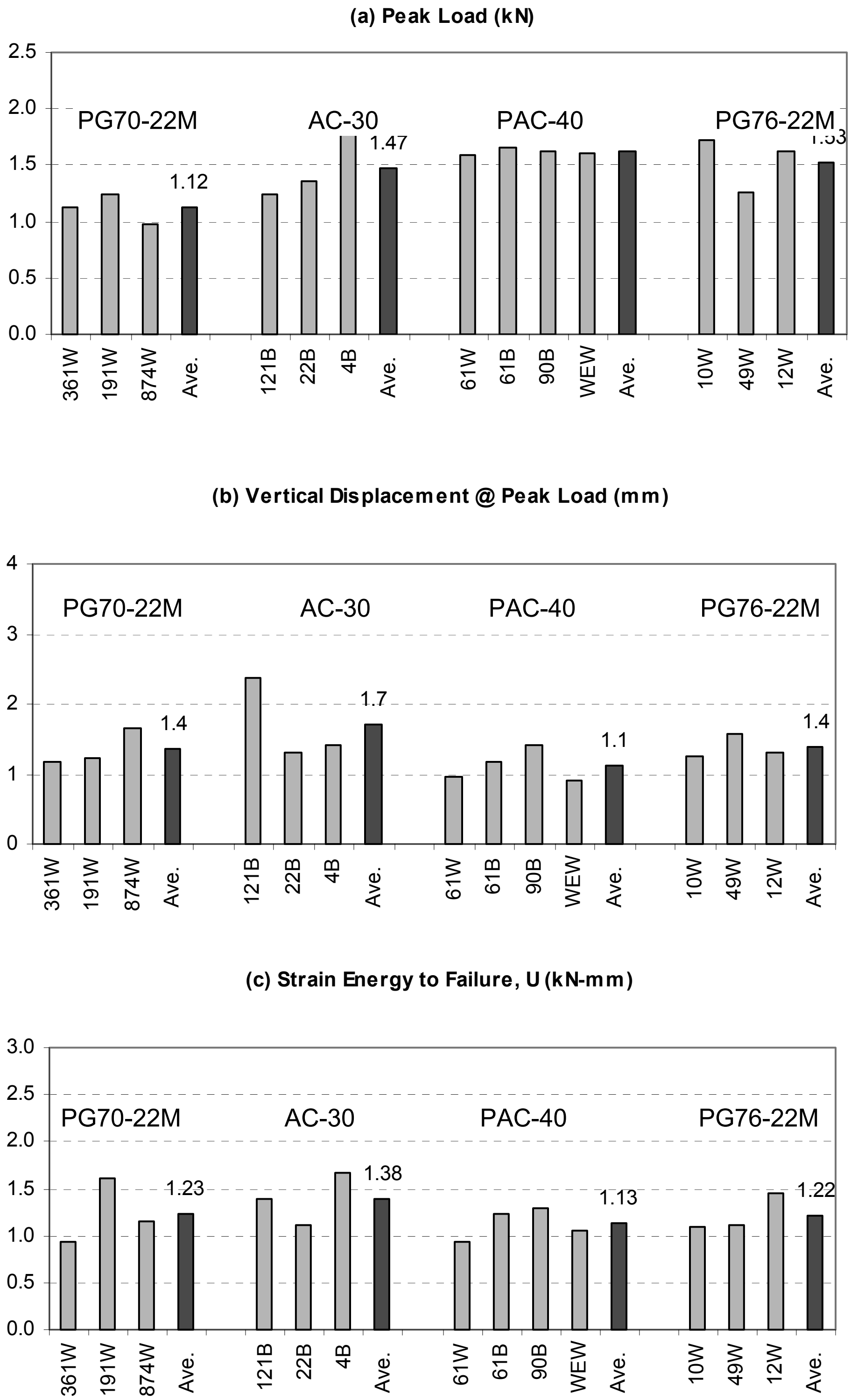

FIG. 7—*Average SCB test results for Superpave mixtures with 25.4 mm notch depth.*

However, the vertical displacement results plotted in Fig. 7*b* showed a completely different ranking order from the peak load results. The AC-30 mixture group had the highest average displacement value at the peak load, followed by either PG70-22M or PG76-22M mixture groups, and the lowest average displacement value was for the PAC-40 mixture group. The data in Figs. 7*a* and *b* indicate that, although the PAC-40 mixtures possessed the highest tensile strengths at the notch depth of 25.4 mm, they were actually very brittle and failed at the smallest vertical deformations among the four mixture groups studied. On the other hand, the AC-30 mixture group had an intermediate tensile strength but possessed the highest average displacement value or the most ductility (flexibility) at the peak load.

The strain energy results showed in Fig. 7*c* confirmed the observation obtained in Fig. 7*b*. Since the strain energy to failure reflects the nonlinear load-displacement behavior in a SCB test, a higher strain energy value will result in a more fracture resistant mixture. In summary, the overall result at the notch depth of 25.4 mm indicates that the AC-30 mixture group possesses the highest fracture resistance, followed by mixture groups PG70-22M, PG76-22M, and PAC-40.

Notch Depth of 31.8 mm

Figure 8 presents the mean SCB test results (the peak load, vertical displacement at peak load, and strain energy to failure) at the notch depth of 31.8 mm for the thirteen Superpave mixtures considered.

Similar to the average peak load results at the notch depth of 25.4 mm, the PAC-40 and the PG70-22M mixture groups displayed the highest and lowest load values, respectively, at the notch of 31.8 mm, Fig. 8*a*. However, the numerical order for the mixture groups AC-30 and PG76-22M at the notch of 31.8 mm was reverse from that at the notch of 25.4 mm (Figs. 7*a* and 8*a*, respectively). Further, except that the highest average displacement value of the AC-30 mixture group was observed in both the notch depths of 25.4 mm and 31.8 mm, the vertical displacement results were completely different at the two notch depths as shown in Figs. 7*b* and 8*b*. Unlike at the notch depth of 25.4 mm, the PAC-40 mixture group showed better flexibility or larger vertical deformation at the notch depth of 31.8 mm than the mixture groups PG76-22M and PG70-22M. This observation was further confirmed by the strain energy results shown Fig. 8*c*.

In summary, the overall result presented in Fig. 8 indicates that, at the notch depth of 31.8 mm, the AC-30 mixture group possesses the highest fracture resistance, followed by mixture groups PAC-40, PG76-22M, and PG70-22M. The inconsistent ranking between test results at the notch depths may be partially explained by the non-linear, elasto-plastic behavior of asphalt mixtures in a SCB test, and partially due to variations in sample fabrication/testing and the difference existed in individual mixture design variables, which will be further discussed below.

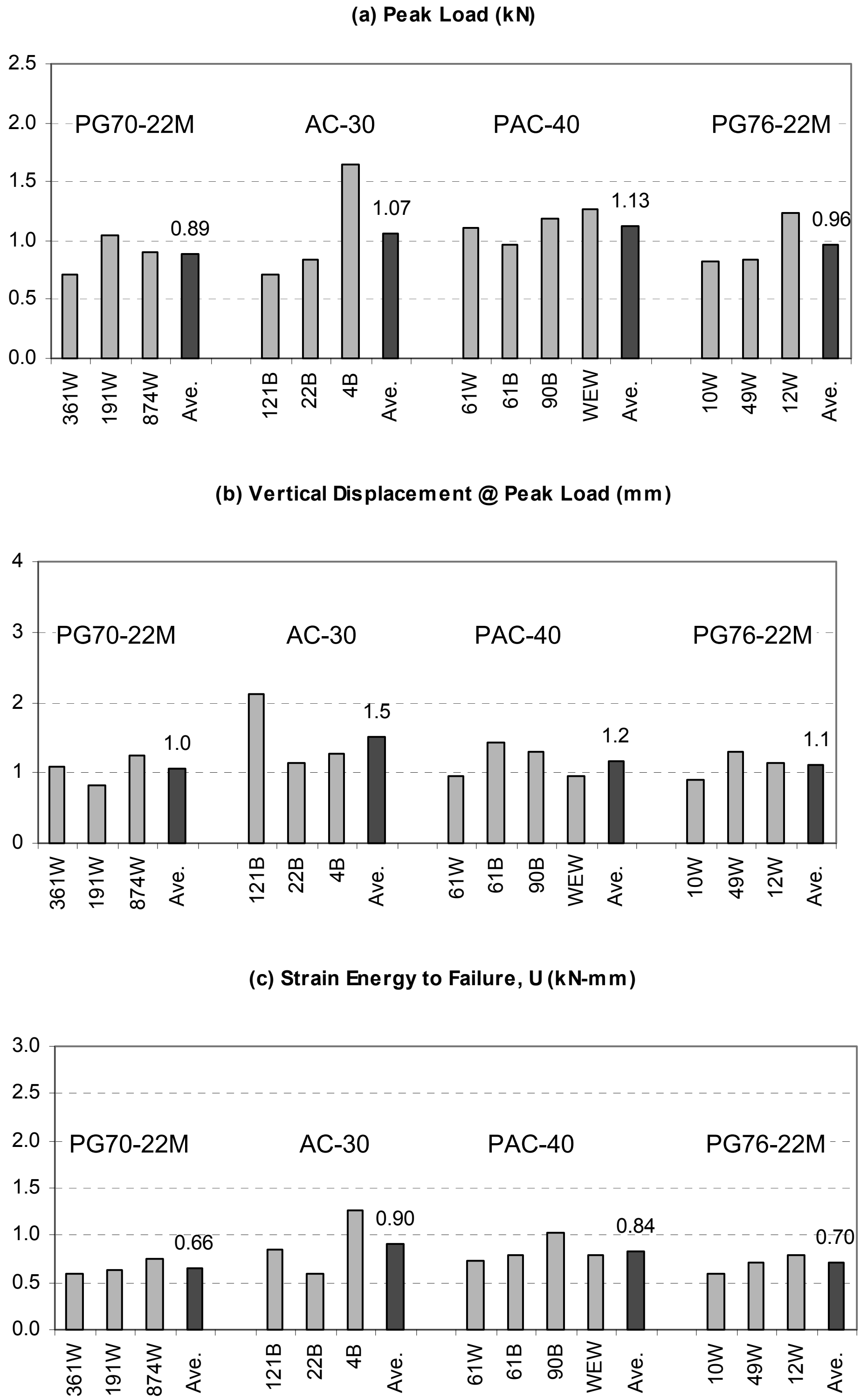

FIG. 8—*Average SCB test results for Superpave mixtures with 31.8 mm notch depth.*

Notch Depth of 38.0 mm

Figure 9 presents the mean SCB test results at the notch depth of 38.0 mm for the thirteen Superpave mixtures considered. As pointed earlier, due to possible variations that existed among each mixture group, a completely different set of numerical orders was observed for the test results at the notch depth of 38.0 mm. Based on the overall average results shown in Fig. 9, the following numerical orders can be observed for each test results:

- Peak load, Fig. 9*a*: PAC-40 > AC-30 > PG70-22M > PG76-22M
- Vertical displacement at peak load, Fig. 9*b*: AC-30 > PG76-22M > PG70-22M = PAC 40
- Strain energy to failure, Fig. 9*c*: PAC-40 > AC-30 > PG76-22M > PG70-22M

In summary, based on the ranking of the strain energy to failure, the overall result at the notch depth of 38.0 mm indicates that the PAC-40 mixture group possesses the highest fracture resistance, followed by mixture groups AC-30, PG76-22M, and PG76-22M.

Effects of Mixture Design Variables

A two-way analysis of variance (ANOVA) statistical test was performed to analyze the effects of mixture design variables on the SCB test results. Two sets of variable combinations – (1) binder type versus NMAS and (2) compaction effort (N_{design}) versus NMAS – were selected for the two-way ANAVA analysis. Tables 2–4 present the p-values obtained from the two-way ANOVA analysis on the test results at notch depths of 25.4 mm, 31.8 mm, and 38.0 mm, respectively. Statistically, a smaller p-value indicates the more significant effect of an independent variable on the dependent variable. Base on a significant level of 0.95, the following observations can be made from Tables 2–4:

- Table 2 indicates that, based on the p-value > 0.05, neither the binder type nor the NMAS had a significant effect on any of the SCB test results of the peak load, vertical displacement, and strain energy at the notch depth of 25.4 mm. The interaction between the two variables did not have a significant effect on any of the three SCB test results, either. The similar non-significant effects were found to be true for the variables of the compaction effort, the NMAS, and their interaction. However, at a degraded significant level of 0.90, both the binder type versus the NMAS and the compaction effort and the NMAS will have an effect on the peak load results from the SCB tests, which indicates that the peak load at the notch depth of 25.4 may be sensitive to the binder type, the NMAS, or the compaction effort at the 0.90 statistically significant level.
- Table 3 showed that, at the notch depth of 31.8 mm, both the NMAS and the binder-NMAS interaction would have a significant effect on the peak load results. Also, both the NMAS and the compaction-NMAS interaction would have a significant effect on the peak load results at this notch depth. The NMAS alone was also found to have an effect on the strain energy at the 0.95 significant level. Neither the binder type nor the compaction effort was observed to have any significant effects on any of the three SCB test results at the notch depth of 31.8 mm.
- All p-values shown in Table 4 were much greater than 0.05. This indicates that at the notch depth of 38.0 mm none of those independent variables have a significant effect on any of the SCB test results.

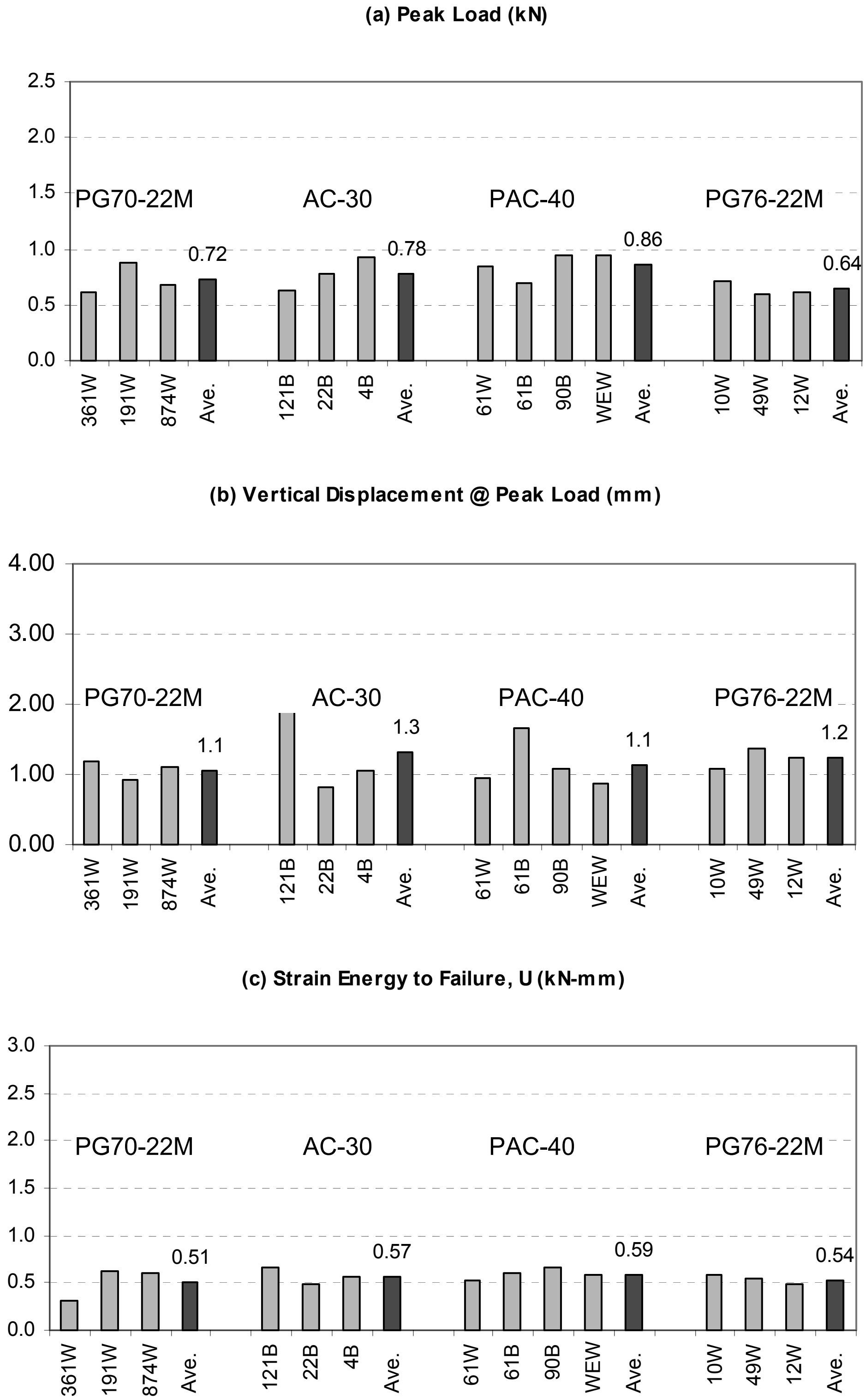

FIG. 9—*Average SCB test results for Superpave mixtures with 38.0-mm notch depth.*

TABLE 2—Two-way ANOVA analysis of 25.4-mm notch depth test results.

	p-value		
	Binder	NMAS	Binder*NMAS
Peak Load	0.051	0.055	0.098
Vertical Displacement	0.346	0.903	0.181
Strain Energy (U)	0.361	0.103	0.683
	Compaction	NMAS	Compaction*NMAS
Peak Load	0.042	0.074	0.134
Vertical Displacement	0.430	0.888	0.274
Strain Energy (U)	0.408	0.109	0.824

TABLE 3—Two-way ANOVA analysis of 31.8-mm notch depth test results.

	p-value		
	Binder	NMAS	Binder*NMAS
Peak Load	0.833	0.027	0.008
Vertical Displacement	0.484	0.943	0.148
Strain Energy (U)	0.328	0.007	0.063
	Compaction	NMAS	Compaction*NMAS
Peak Load	0.698	0.042	0.029
Vertical Displacement	0.463	0.947	0.186
Strain Energy (U)	0.334	0.010	0.107

TABLE 4—Two-way ANOVA analysis of 38.0-mm notch depth test results.

	p-value		
	Binder	NMAS	Binder*NMAS
Peak Load	0.374	0.441	0.132
Vertical Displacement	0.930	0.939	0.203
Strain Energy (U)	0.936	0.718	0.624
	Compaction	NMAS	Compaction*NMAS
Peak Load	0.960	0.478	0.349
Vertical Displacement	0.965	0.989	0.280
Strain Energy (U)	0.976	0.654	0.573

In summary, the two-way ANOVA analysis results illustrate that 1) the peak load might be sensitive to the binder type or the compaction level or the NMAS at the notch depth of 25.4 mm; but it was only sensitive to the NMAS at the notch depth of 31.8 mm and is not sensitive to any variables at the notch depth of 38.0 mm; 2) the strain energy was found to be sensitive only to the NMAS and only at the notch depth of 31.8 mm; and 3) the vertical displacement was found not to sensitive to any independent variables selected.

The Critical J-Integral (J_C)

The critical J-integral (J_C) values for the thirteen Superpave mixtures were calculated using the methods described, and the results are presented in Table 5. Also shown in Table 5 are p-values from the two-way ANOVA analysis on the J_C results with the two sets of variable combinations: 1) binder type and NMAS; 2) N_{design} and NMAS.

TABLE 5—*Critical J-integral of Superpave mixtures and the corresponding p-values.*

Mixture	J_C (kJ/m^2)	Binder Type	NMAS (mm)	p-value	Compaction (N_{design})	NMAS (mm)	p-value
361W	0.87	PG70-22M	19	$p_{binder} = 0.047$ $p_{NMAS} = 0.026$ $p_{binder*NMAS} = 0.301$	75	19	$p_{compaction} = 0.050$ $p_{NMAS} = 0.031$ $p_{compaction*NMAS} = 0.422$
191W	1.38						
874W	0.74						
121B	1.01	AC-30			97		
22B	0.88						
4B	1.53		25			25	
61W	0.57	PAC-40	19		109	19	
61B	0.86		25			25	
90B	0.89						
WEW	0.67		19		125	19	
10W	0.73	PG76-22M					
49W	0.81						
12W	0.83						

From Table 5, the following observations can be made:

- The value of J_C ranges from 0.57–1.53 for the thirteen Superpave mixtures in this study. This J_C data range for Superpave mixtures is on the same order of magnitude as those found for other asphalt mixtures [6].
- The values of J_C for the mixture groups of PG70-22M and AC-30 seem to be generally higher than those for mixture groups of PAC-40 and PG76-22M.
- Two-way ANOVA analysis indicates that J_C is fairly sensitive to all mixture variables of binder type, NMAS, and compaction effort (N_{design}).
- J_C is not sensitive to either interactions of binder-NMAS or compaction-NMAS.

Based on above statistical analysis results, Fig. 10 summarizes the J_C results with four binder types and two NMASs. The following conclusions an be made from Fig. 10:

- Superpave mixtures with larger NMAS tend to have better fracture resistance or larger values of J_C. This implies that Superpave mixtures with larger NMAS may have stronger aggregate structures than those with smaller NMAS primarily due to the stone-to-stone contact.
- Superpave mixtures with harder asphalt binders (e.g., PG 76-22M and PAC 40 in this study) appear to have less fracture resistance or smaller J_C values than those with softer binders (e.g., AC-30 and PG 70-22M).

The compaction efforts in this study were coincidently changed with the changes of binder type in the Superpave mix design; therefore, similar effects were observed for the compaction efforts on the results of J_C.

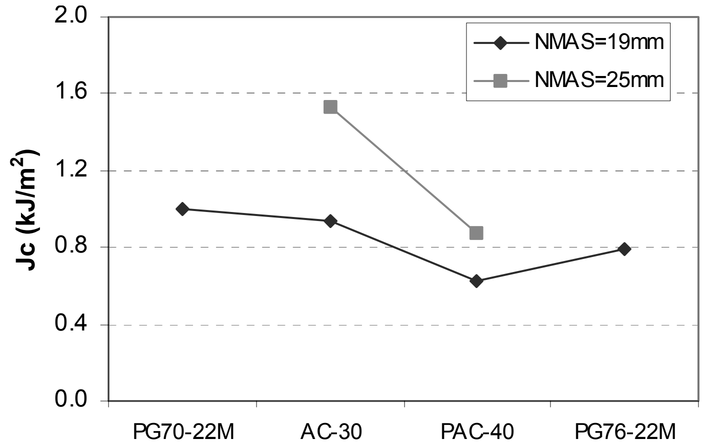

FIG. 10—*The critical J-integral at 25°C.*

Conclusions and Recommendations

The following conclusions can be made from this study:

- In an SCB test at a single notch depth, the order of fracture resistance based on the average strain energy (U) results for the four mixture groups in this study was found to be generally consistent with that from the average vertical displacement results, but completely different from that based on the peak load measurements.
- Superpave mixtures with higher tensile strengths could be more brittle and less fracture resistant than those with lower tensile strengths, and vice versa.
- None of individual test results (peak load, vertical displacement, or strain energy to failure) obtained from the SCB tests with a single notch depth were found to be able to correctly rank the fracture resistance of Superpave mixtures in a consistent order. The explanation for this may include: the non-linear, elasto-plastic behavior of asphalt mixtures in a SCB test, the possible variations in sample fabrication/testing, and the different individual mixture design variables in different mixture groups.
- Results of the two-way ANOVA analysis indicate that the individual SCB test results - peak load, vertical displacement, or strain energy (U) at different notch depths were not sensitive, or consistently sensitive, to mixture design variables. On the other hand, the critical J-integral, J_C, determined from the SCB tests was found fairly sensitive to all mixture variables selected, including binder type, NMAS, and compaction effort (N_{design}).
- Superpave mixtures with larger NMAS were found to have better fracture resistance or larger J_C values. This indicates that asphalt mixtures with larger NMAS tend to have stronger aggregate structures than those with smaller NMAS, probably due to the larger stone-to-stone contact.
- Superpave mixtures with harder asphalt binders appeared to have less fracture resistance or smaller J_C values than those with softer binders.
- The SCB test can be a valuable tool in the evaluation of fracture resistance of asphalt mixtures.

Acknowledgments

This study was supported by funds from the Louisiana Transportation Research Center (LTRC). The authors are grateful to Mr. Amar Raghavedra, Mr. Keith Beard, and Mr. C. G. Zhang for their experimental testing and data analysis.

References

[1] Little, D. and Mahmoub, K., "Engineering Properties of First Generation Plasticized Sulfur Binders and Low Temperature Fracture Evaluation of Plasticized Sulfur Paving Mixtures," Transportation Research Record, 1034, National Research Council, Washington, DC, 1985, pp. 103–111.

[2] Abdulshafi, A. A. and Majidzadeh, K., "J-Integral and Cyclic Plasticity Approach to Fatigue of Asphaltic Mixtures," Transportation Research Record, 1034, TRB, National Research Council, Washington, DC 1985, pp. 112–123.

[3] Dongre, R., Sharme, M. B., and Anderson, D. A., "Development of Fracture Criterion for Asphalt Mixes at Low Temperatures," Transportation Research Record 1228, TRB, National Research Council, Washington, DC 1989, pp. 94–105

[4] Molenaar, A. A. A., Scarpas, A., Liu, X., and Erkens, S., "Semi-Circular Bending Test: Simple but Useful?," *Journal of the Association of Asphalt Paving Technologists*, Vol. 71, 2002, pp.795–815.

[5] Roque, R. and Zhang, Z., "Determination of Crack Growth Rate Parameters of Asphalt Mixtures Using the Superpave IDT," *Journal of the Association of Asphalt Paving Technologists*, Vol. 68, 1999, pp. 404–433.

[6] Mull, M. A., Stuart, K., and Yehia, A.,"Fracture Resistance Characterization of Chemically Modified Crumb Rubber Asphalt Pavement," *Journal of Materials Science*, Vol. 37, 2002, pp. 557–566.

[7] Mohammad, N. L., Wu, Z., and Aglan, M., "Characterization of Fracture and Fatigue Resistance on Recycled Polymer-Modified Asphalt Pavements," The 5th RILEM Conference on Pavement Cracking, France, 2004 (in press).

[8] Louisiana Standard Specifications for Roads and Bridges, Louisiana Department of Transportation and Development, Baton Rouge, Louisiana, 2000.

[9] Dowling, N .E., Mechanical Behavior of Materials, Prentice Hall, Englewood Cliffs, NJ, 1993.

[10] Rice, J. R. "A Path Independent Integral and the Approximate Analysis of Strain Concentration by Notches and Crack," *Journal of Applied Mechanics*, Vol. 35, 1968, pp. 379–386.

Journal of ASTM International, April 2006, Vol. 3, No. 4
Paper ID JAI12258
Available online at www.astm.org

Terhi K. Pellinen, Ph.D.,[1] *Shangzhi Xiao, M.Sc.,*[2] *and Sunil Y. Raval, B.S.*[3]

Dynamic Modulus Testing of Thin Pavement Cores

ABSTRACT: A novel method of testing thin surface cores using the dynamic (complex) modulus test is proposed that utilizes composite mechanics theory. Rectangular specimens are sawed from the round surface layer cores, and the sawed blocks are simply stacked horizontally without bonding. Two hydrostone caps are made to provide flat and smooth loading ends, as well as to restrain the blocks from moving during loading. Two Linear Vertical Differential Transformers are attached 180° apart to the flat uniform side of the horizontally stacked cores to obtain the strain response without measuring over the joint of the cores. The advantage of this approach over the diametral loading mode, used for resilient modulus testing, is that it provides homogenous testing conditions, which gives direct access to stress and strain and, therefore, constitutive equations.

KEYWORDS: hot mix asphalt, dynamic complex modulus, thin pavement cores, pavement design, mix design, performance testing, capping, composite theory

Introduction

The recent development of the new national pavement design guide by the National Cooperative Highway Research Program (NCHRP) contract 1-37A for the American Association of State Highway and Transportation Officials (AASHTO) has prompted new interest in the dynamic (complex) modulus testing of asphalt concrete. The studies conducted in the 1970s [1–3] produced ASTM Test Method for Dynamic Modulus of Asphalt Concrete Mixtures (D 3497), which was published in 1977. A draft new protocol for conducting dynamic modulus testing has been developed by the design guide research team with detailed steps of sample preparation, specimen instrumentation, and testing [4]. The current resilient modulus test, AASHTO Standard Test Method of Determining the Resilient Modulus of Bituminous Mixtures by Indirect Tension for the 1993 AASHTO Pavement Design Guide will be replaced by the dynamic modulus test as a primary material characterization test for designing asphalt pavements in the new 2004 AASHTO pavement design guide. The dynamic modulus test is also a candidate Simple Performance Test for the Superpave volumetric mix design procedure enhancement [5].

The dynamic modulus testing is performed by applying a frequency sweep of uniaxial compressive sinusoidal loading to obtain dynamic modulus $|E^*|$ of the mix. Testing is performed at five different temperatures to construct a master curve of the mix to evaluate its viscoelastic behavior. The new dynamic modulus test protocol requires that test specimens have a height to diameter ratio (H/D) of 1.5, which means that a 100-mm diameter test specimen must have a height of 150 mm. During the new design guide development, a comprehensive study of specimen size and geometry effects on various material parameters were conducted, investigating mixtures with different nominal aggregate sizes and specimens with varying height to diameter ratios [6]. Research recommended using a minimum height to diameter ratio of 1.5 to obtain a true and accurate stiffness response of asphalt mixtures tested using uniaxial dynamic modulus testing. This recommendation was based on the concept of representative volume element (RVE) for studied materials; therefore, the recommended test specimen diameter was 100 mm, although for the dynamic modulus testing, 75 mm could be used also. Thus, only laboratory-fabricated or compacted specimens or both will yield to the acceptable height to diameter ratios, and testing of asphalt cores taken from a thin surface layer or a thin base layer cannot be tested according to the protocol. This unsatisfactory

Manuscript received December 1, 2003; accepted for publication November 2, 2005; published online January 2006. Presented at ASTM Symposium on Hot Mix Asphalt (HMA) including Fundamental and Empirical Procedures on 9 December 2003 in Tampa, FL; L. Mohammad, Guest Editor.
[1] Assistant Professor, Purdue University, School of Civil Engineering, West Lafayette, Indiana 47907.
[2] Graduate Research Assistant, Purdue University, School of Civil Engineering, West Lafayette, Indiana 47907.
[3] Undergraduate Assistant, Purdue University, School of Civil Engineering, West Lafayette, Indiana 47907.

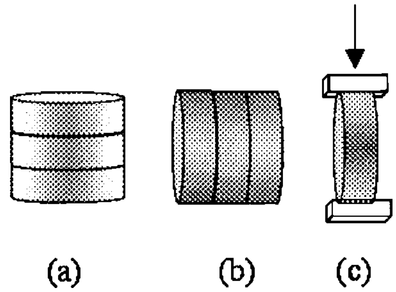

FIG. 1—*Different options of stacking and testing thin pavement cores.*

situation has been heavily criticized by industry. The need for testing actual pavement cores for quality control and forensic studies is essential; furthermore, testing of cores is the only way to correlate the laboratory and field performance of asphalt mixtures.

Therefore, the objective of the study was to develop an effective and practical test procedure for measuring the stiffness of thin pavement cores using dynamic modulus testing. The development work was done using gyratory-compacted specimens instead of using actual field cores to have better control over different variables, such as air void content, that can affect the mix stiffness. After the sample preparation procedure was established, actual field cores were tested for verification.

Hypothesis and Research Approach

The first thought that comes to mind is simply to stack thin cores vertically to obtain the desired height, as Fig. 1(*a*) shows. Another way, of course, would be to stack the cores horizontally, Fig. 1(*b*). But why stack cores if they can be measured using just indirect loading mode, Fig. 1(*c*), as the resilient modulus test of pavement cores has been conducted over the years?

The dynamic modulus $|E^*|$ is a measure of a viscoelastic property of an asphalt mixture and the linear viscoelastic theory is applied to obtain the modulus from the measured stress and strain response; the dynamic modulus $|E^*|$ is defined as the modulus of the complex number E^*, where σ_o is the stress amplitude and ε_o is the recoverable strain amplitude, Eq 1.

$$|E^*| = \frac{\sigma_o}{\varepsilon_o} \tag{1}$$

The phase angle φ between stress and strain signals can be obtained from Eq 2, where t is the time lag between the signals and ω is the angular velocity.

$$\varphi = t\omega \tag{2}$$

The test protocol for obtaining the dynamic modulus of asphalt concrete calls for applying a uniaxial compressive sinusoidal frequency sweep using a cylindrical specimen. This type of testing is a homogeneous test, which means that it gives direct access to the applied stress and strain and to the constitutive equation; thus, the dynamic modulus is easily obtained by dividing the applied force by the circular loading area and dividing the measured resilient deformation by the used gage length.

The indirect resilient modulus test is a nonhomogeneous test, which means that the solution for obtaining stresses and strains is specimen-shape-dependent and needs to be postulated first, assuming either elastic or viscoelastic material behavior before the modulus can be obtained. A linear elastic material behavior has been postulated for the resilient modulus testing while solving stresses and strains from the indirect loading configuration of a cylindrical specimen.

Because the behavior of an asphalt mixture is viscoelastic, the elastic solution for an indirect loading configuration gives an approximation of stresses and a true viscoelastic solution is needed to obtain stresses and strains correctly. Another issue is the high temperature testing of dynamic modulus; at high test temperatures the loading strip is penetrating to the thin specimen during loading, causing large stress concentrations, which in turn are causing erroneous stress/strain measurements regardless of what solution is used to obtain them. Therefore, due to the mathematical simplicity of solving the constitutive equation

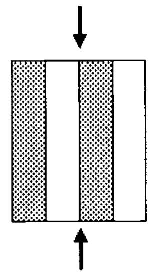

FIG. 2—*Parallel phases model.*

for the dynamic modulus for uniaxial loading mode, and the ability to avoid large stress concentrations during high temperature testing, the axial testing of cylindrical specimens is preferred over the indirect loading mode to obtain the dynamic modulus of asphalt mixtures.

A concept of stacking specimens vertically has been studied by the pavement design guide development team [7] in order to obtain higher height to diameter ratios for the gyratory-compacted, laboratory-fabricated specimens. Stacked specimens were glued or just pressed together to form tight joints across the specimens. Research indicated that there were no differences in the mixture stiffness $|E^*|$ values between the stacked and monolithic specimens. However, the specimen stacking and instrumentation were arranged in such a way that the strains were not measured across the joint of the stacked specimens.

A preliminary laboratory study tried to verify this finding, but the results indicated that stacking of thin cores vertically is not an option because it was not possible to stack cores in such a way that strain measurements over the specimen joints was not needed. The specimen joints were causing too much movement, which will cause erroneous strain measurements if the gage length expands over the joint. Therefore, the vertical stacking of thin cores is not an option to obtain the dynamic modulus of the mix.

If the thin cores are stacked horizontally side by side, Fig. 1(*b*), the combination of stacked cores is analogous to the springs in parallel. Figure 2 shows a simple parallel arrangement phase distribution model that can be applied to the horizontally stacked cores. The stiffness of the composite shown in Fig. 2 can be obtained from the mixture rule of composite materials [8]. The mixture rule uses weighting procedures that depend on the phase distribution geometry of the components used. Therefore, the stiffness of the composite is given by Eq 3:

$$k = \sum_{i=1}^{n} \nu_i k_i \tag{3}$$

where
ν_i = the volume fractions of the individual components
and
k_i = the stiffness of the individual components.

The application of the composite materials theory for testing thin horizontally stacked pavement cores can be accomplished by using the following specimen preparation arrangements, see Fig. 3. A rectangular slice is sawed from the surface layer of the pavement core and the sawed slices are stacked vertically

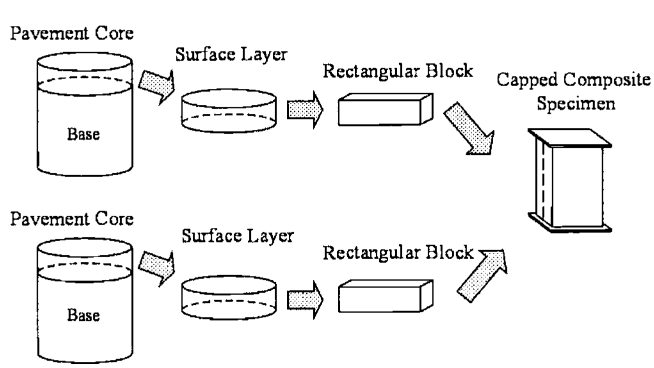

FIG. 3—*A schematic plan for testing of thin cores (not in scale).*

without bonding. Two caps will provide flat and smooth loading ends, as well as to restrain slices from moving during loading. Stiffness $|E^*|$ of composite specimen is the weighted average $|E^*|$ value of the stiffness of the individual slices. The slices are not glued in order to avoid any confinement that gluing may introduce. Also capping forces the slices to move as a monolithic specimen eliminating possible friction between the slices during loading. Depending on the thickness of the cores, two or three cores are needed to form a composite specimen with a height to diameter ratio of 1.5. A 150-mm diameter core would allow sawing of a 75- by 130-mm rectangular slice. If three 25-mm thick slices are combined, a total loading cross section of 75 by 75 mm can be obtained. This cross section is needed to obtain a large enough loading area for a load cell capacity of 25 kN, which is rather typical in asphalt laboratories.

The advantages of this method are that the loading does not span across the interfaces, strain measurements are not done over joints, and flat and parallel end conditions can be obtained. The disadvantages of the method are the possible specimen anisotropy effects due to a change in the specimen loading direction and possible confinement effects caused by specimen capping.

Apparently, a change in specimen loading direction is unavoidable in order to obtain a composite specimen from the gyratory-compacted pill or from the pavement core; therefore, it is important to consider the anisotropic effects on mixture stiffness obtained from the composite specimens. The stiffness variation due to the anisotropy effects may be separated into two causes, aggregate orientation and air void distribution; although in many cases the air voids distribution is caused by the aggregate orientation and shape.

A study by Witczak, Mamlouk, and Ho [9] found that for the fine mix with 12.5-mm nominal size aggregate, the anisotropy effects were not significant for the measured creep modulus in compression and tension. The study used gyratory compacted pills, from which all test specimens were sawed and cored. The sawed specimens had an air voids content of approximately 4 %; therefore, the gyratory pills were compacted to 6 % air void content.

Another study by Witczak, Pellinen, and Kaloush [10] quantified the air void distribution in a gyratory compacted specimen. Cores measuring 100 mm in diameter and 150 mm in height were taken from the gyratory-compacted pills and the air void distribution in the outer ring and the inner core were compared. The study found that the inner ring had as an average 1.8 % higher air void content than the core. Furthermore, the vertical air void distribution within the ring and core varied substantially (3 to 4 %), when the measured air voids of five 30-mm thick slices obtained from the core were compared.

The capping of specimens using sulfur compound, which has been used to ensure parallel specimen ends according to the old ASTM protocol, was studied by Witczak et al. [6]. They found that for the unaxial testing for permanent deformation of asphalt cores, the capping would restrain the lateral movement of the mix (dilatation), which affects the state of stresses along the height of the specimen. Therefore, the recommendation was not to cap specimens, even for small strain dynamic modulus testing. This was recommended despite the fact that the specimen is not expected to dilate when less than 100 microstrains response is measured and capping therefore should not have any effect on the measured modulus values.

The air void effects on the stiffness of asphalt mixtures have been studied extensively, and several stiffness-predictive models are available to estimate the air voids influence for the stiffness of the mix. These stiffness models include the Bonnaure et al. model [11], Witczak et al. model [12], and a newest Hirsch model from Christensen et al. [13], Eqs. 4 and 5. The Hirsch model was developed employing composite mechanics theory for a three-phase system of aggregate, binder, and air. The sensitivity of stiffness to variation in air voids content varies between these models.

$$|E^*| = Pc\left[4\,200\,000\left(1 - \frac{\text{VMA}}{100}\right) + 3|G^*|_{\text{binder}}\left(\frac{\text{VFA} \times \text{VMA}}{10\,000}\right)\right] + (1 - Pc)\left[\frac{1 - \text{VMA}/100}{4\,200\,000} + \frac{\text{VMA}}{3\text{VFA}|G^*|_{\text{binder}}}\right]^{-1} \tag{4}$$

where $|E^*|$ = dynamic (complex) modulus, psi, Pc = contact factor, given by Eq 5, VMA = voids in mineral aggregate (%), $|G^*|_{\text{binder}}$ = complex shear modulus of the binder (psi), and VFA = voids filled with asphalt (%).

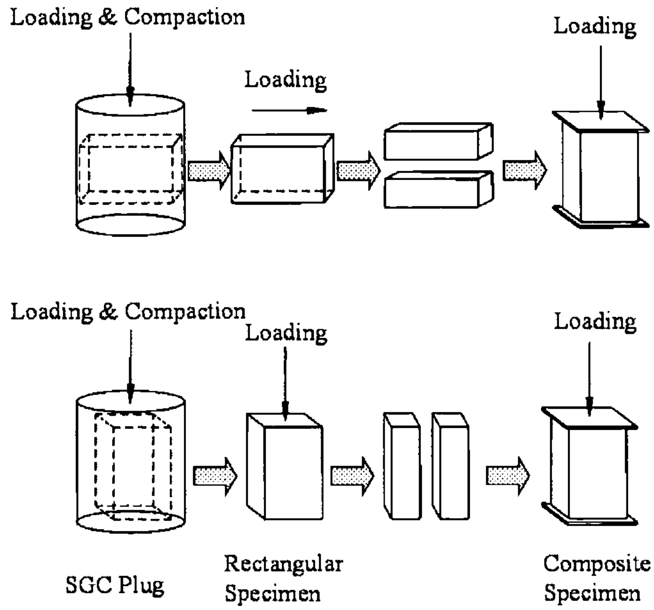

FIG. 4—*Sample preparation scheme.*

$$Pc = \frac{\left(20 + \frac{VFA \times 3|G^*|_{binder}}{VMA}\right)^{0.58}}{650 + \left(\frac{VFA \times 3|G^*|_{binder}}{VMA}\right)^{0.58}} \tag{5}$$

Experimental Plan

As discussed in the previous sections, the horizontal stacking of thin pavement cores is a viable solution for obtaining the stiffness of the asphalt mix. However, there are two questions that need to be answered by the research:

1. How should composite specimens be prepared to reliably measure $|E^*|$ of the mix?
2. Is the measured $|E^*|$ from composite specimens comparable to the $|E^*|$ obtained from axial testing of cylindrical specimens of equal height to diameter ratio of 1.5?

To answer these questions, it was important that all the variables that could affect the stiffness measurements were controlled. The development and verification work was done using gyratory-compacted specimens instead of using actual field cores in order to have better control over all variables, such as air void content, that can affect the mix stiffness. After the procedure was established, actual field cores were tested for verification.

The experimental testing plan was constructed based on the two issues that arose from the literature: (1) the loading direction effects caused by anisotropy of asphalt mixture and (2) the possible confinement effects caused by the specimen capping. To study these effects, the following specimen preparation, testing, and analysis scheme was selected, see Fig. 4.

1. Four cylindrical gyratory-compacted pills were prepared using the sample preparation of the proposed new test protocol [4]. The stiffness of the pills was measured according to the proposed test protocol.
2. A control sample comparable to the 100 mm in diameter and 150 mm in height cylindrical specimen requirement was obtained from gyratory pills. However, instead of coring a cylindrical specimen, a rectangular block was sawed with the same height-to-diameter ratio. Due to the homogeneity of the axial dynamic modulus testing, the specimen shape should not affect the measured modulus values. Two rectangular blocks were sawed in both the vertical and horizontal directions to study the anisotropy effects caused by the change in loading direction. The size of the blocks was dictated by the dimensions of the block sawed from the lateral direction because it was

TABLE 1—*Air void continent of prepared specimens.*

Cylindrical gyratory (SGC) specimens Size: 150×172 mm	V_a [%]	Sawed rectangular (-R) specimens Size: 80×75×130 mm	V_a [%] Overall	V_a [%] End-1	V_a [%] Middle	V_a [%] End-2
SGC01	9.3	SGC01-R-L	7.8	7.8	7.2	8.4
SGC03	9.2	SGC03-R-L	8.1	9.0	7.4	8.7
SGC02	9.3	SGC02-R-A	7.3	7.8	7.6	7.5
SGC04	9.4	SGC04-R-A	7.6	7.3	8.2	8.2
Average	9.3		7.7	8.0	7.6	8.2

desired to have the same dimensions for the blocks in both directions. The stiffness of the blocks was measured, again according the proposed new test protocol.

3. The measured blocks were sliced in half and composite specimens were constructed by joining the two pairs of blocks using capping. The stiffness of the composite specimens was measured. By comparing the capped and rectangular specimens, it should be possible to assess the confinement effects due to the capping.
4. To validate the sample preparation and testing protocol, actual road cores were prepared and tested using the developed sample preparation protocol.

Specimen Preparation and Instrumentation

An asphalt plant-fabricated dense-graded 9.5-mm nominal maximum size mix was used for preparing specimens for testing. The unmodified binder used in the mix was PG 64-22 and the binder content was 5.6 % by weight. The maximum theoretical specific gravity of the mix was 2.488, and the aggregate bulk specific gravity was 2.682. Specimens were compacted using the Superpave Gyratory compactor and were sawed using a one-blade masonry saw.

A hydrostone capping compound was used instead of the traditional sulfur compound in the capping of composite specimens. Compared with the sulfur compound, the hydrostone is not hazardous, it is easier to handle and it does not damage asphalt specimens because it is mixed with water instead of applying heat to obtain the suitable viscosity for capping.

Preparation of Gyratory Compacted Specimens

The 150-mm diameter and 172-mm high cylindrical specimens were gyratory compacted to the target air void content of 9 %, which was selected to obtain a 7 % air void content for the samples obtained from the pills. The 7 % air void content is considered to be the average in situ density. The specimen compaction was successful by producing almost the same air void content for all four specimens as shown in Table 1.

The specimen instrumentation followed the proposed new dynamic modulus test protocol, and spring-loaded Linear Vertical Differential Transformers (LVDT) were used for the strain measurements. Three sets of buttons were glued directly to the surface of the specimen to attach the three LVDTs on each specimen at mid-height at an angle of 120° apart. The gage length used in the testing was 100 mm. This gage length was selected to assure that the measured stiffness represents the same part of the specimen where the composite specimens were obtained, see Fig. 5.

After testing all four gyratory pills, the reference specimens were obtained by sawing two rectangular specimens in the axial and in the lateral direction. The sawed specimens were 80 by 75 by 130 mm. A thicker side would allow further cutting of a specimen by counting the mix loss during sawing. The measured overall air voids content of each rectangular block is shown in Table 1. The average air void content was 7.7 % for all four rectangular blocks. The gage length used in the dynamic modulus testing was 75 mm. There were two LVDTs attached on the long side of each specimen, see Fig. 5. The aim was to obtain approximately the same gage length-to-height ratio as for the gyratory pills.

Table 1 also shows the air void distribution in each rectangular block measured by slicing the specimen into three equal slices after all of the testing was completed and the capping removed from the specimen. The inner part of the gyratory specimen was the densest as was expected based on the literature.

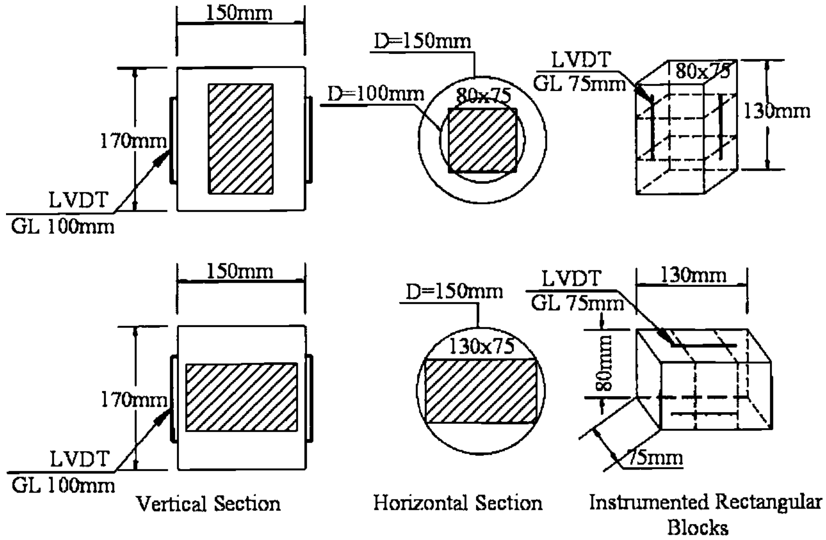

FIG. 5—*Specimen instrumentation plans.*

Preparation of Composite Specimens

The four rectangular specimens were sliced into two equal halves of 37.5 by 75 by 130 mm. Then, each pair of the sawed halves was combined together by capping both ends of the slices. A special jig was designed to keep the sliced specimens vertical and fixed while capping was in progress, Fig. 6(*a*). With an adjustable sliding block, the jig could accommodate a wide range of specimen/core thicknesses, Fig. 6(*b*). As an example, Fig. 7 shows two composite specimens prepared from road cores, instrumented and ready for testing. The specimen at the left side has two cores stacked together, and the specimen at the right side

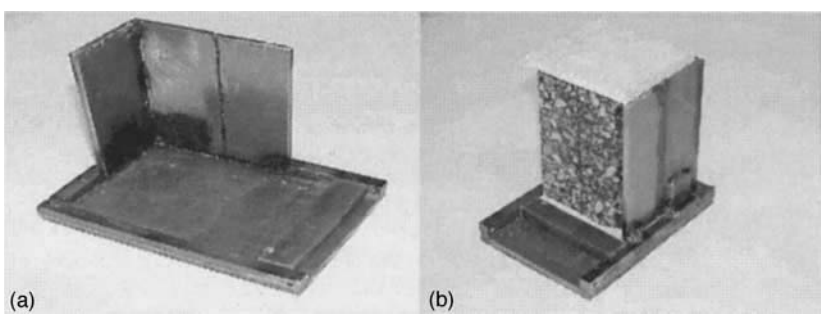

FIG. 6—*Developed capping jig a) and capping of specimen b).*

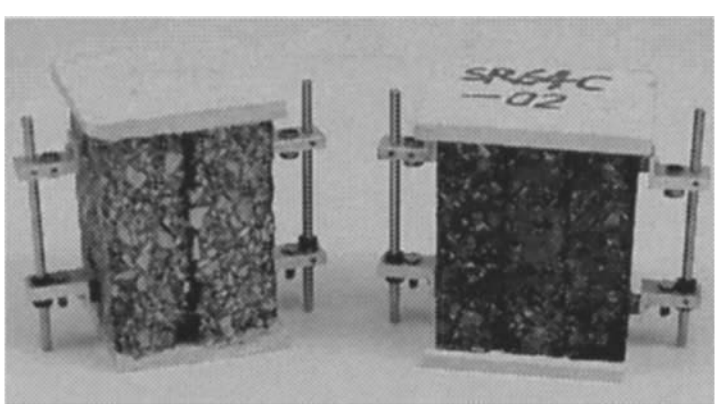

FIG. 7—*Composite specimens with instrumentation (actual road cores).*

TABLE 2—*Dynamic modulus test results.*

Frequency	25 Hz	10 Hz	5 Hz	1 Hz	0.5 Hz	0.1 Hz
Specimen ID	Original/Normalized, Dynamic Modulus $\|E^*\|$, (MPa)					
SGC01-S-A	1842/2063	1291/1447	987/1106	573/637	462/510	325/352
SGC03-S-A	1530/1715	1032/1149	776/862	440/482	357/387	245/257
SGC02-S-A	1833/2053	1278/1433	966/1082	552/613	452/499	312/337
SGC04-S-A	1562/1751	1113/1255	858/966	524/584	437/484	311/337
SGC01-R-L	2558/2509	1709/1676	1327/1301	836/820	713/700	559/549
SGC03-R-L	2194/2180	1678/1667	1326/1317	907/901	786/781	512/509
SGC02-R-A	2140/2154	1461/1471	1193/1201	781/786	688/692	541/544
SGC04-R-A	1599/1673	1114/1165	844/882	500/520	421/437	329/339
SGC01-C-L	2345/2300	1674/1641	1320/1294	878/861	812/797	699/686
SGC03-C-L	1983/1970	1473/1463	1186/1178	761/756	682/678	605/601
SGC02-C-A	2108/2122	1537/1547	1216/1224	774/779	667/671	536/539
SGC04-C-A	1735/1815	1292/1352	1051/1099	729/761	665/694	588/613
Specimen ID	Original/Normalized, Phase Angle φ, (Deg)					
SGC01-S-A	35.15/34.81	35.53/35.45	34.53/35.14	31.51/32.35	29.58/30.41	24.91/26.12
SGC03-S-A	34.88/34.43	35.43/35.49	34.83/35.13	30.72/31.56	27.98/29.22	22.66/23.40
SGC02-S-A	33.84/33.18	34.71/34.59	34.12/34.53	30.34/31.25	27.72/29.02	21.88/23.25
SGC04-S-A	35.25/35.28	35.33/35.36	34.21/34.60	29.91/31.07	27.36/29.05	23.08/24.12
SGC01-R-L	34.07/34.33	33.88/33.28	32.08/31.78	27.28/27.38	25.13/25.37	22.57/21.81
SGC03-R-L	34.16/34.15	33.29/33.26	31.92/31.87	28.52/28.46	26.87/26.79	20.66/20.57
SGC02-R-A	32.07/32.14	31.25/31.12	29.55/29.66	24.61/24.57	22.06/22.50	17.94/17.91
SGC04-R-A	35.99/35.72	35.83/35.94	33.99/34.77	29.22/29.38	26.33/26.68	20.98/21.97
SGC01-C-L	33.79/33.73	32.59/32.70	30.77/30.41	24.27/23.46	21.74/21.69	18.44/17.91
SGC03-C-L	32.32/31.98	31.72/32.25	30.45/30.73	24.13/23.07	20.89/20.25	16.03/16.73
SGC02-C-A	32.64/32.49	32.46/32.80	32.01/31.91	27.48/27.49	25.21/25.25	21.05/21.26
SGC04-C-A	31.04/30.57	30.30/30.91	28.49/29.26	21.82/22.49	19.24/20.01	14.17/16.20

has three thinner cores stacked together. Although the target loading area of 75×75 mm was aimed while sawing the road cores, there will be some variation in the size of the loading area due to the thickness variation of cores.

Laboratory Testing and Test Results

The dynamic modulus testing was conducted following the newest test protocol proposed by the pavement design guide development team [4]. All samples were measured at 40°C temperature, applying a frequency sweep of 25, 10, 5, 1, 0.5, and 0.1 Hz. A sinusoidal compressive loading was applied and the consequent resilient strain was measured. The loading magnitude was adjusted to keep the measured resilient strains below 100 microstrains. The two viscoelastic parameters, the dynamic modulus $|E^*|$ and the phase angle φ, were obtained from the measured stress and strain signals using Eqs 1 and 2.

Table 2 shows the dynamic modulus $|E^*|$ test results for all tested specimens. The test data is presented in two different ways in the table. The first number is the actual measured stiffness of the mix and the second number is the normalized stiffness. Normalization was done by adjusting the air void content of all specimens to 7.5 % for equal comparisons. The coefficient of variation between two replicate test results ranged from 11.2 to 13.5 %, which aggress well with the variation of 13 to 15 % reported by other researchers [4,5].

Normalization for the modulus values was done using the Hirsch model [13] to estimate the stiffness change due to the air void change, see Eqs 4 and 5. The phase angle values were normalized by fitting a second-order polynomial through the modulus and phase angle data in the black space and computing new phase angle values by using the normalized modulus values. For the rectangular and composite specimens, the air void content of the center specimen was used in the normalization process. The air void content was selected over the overall density of a rectangular specimen because it represents the part of the specimen where the strains were measured, as Fig. 5 shows. All consequent analysis of test data was done using normalized data.

The complex plane allows the investigation of a viscoelastic behavior and assessment of viscoelastic parameters, modulus, and phase angle simultaneously. In the complex plane the *x* axis is the real axis and

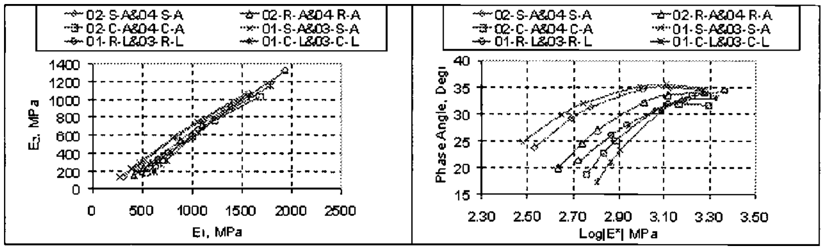

FIG. 8—*Summary of test data averaged over two replicate test results.*

the *y* axis is the imaginary axis. The elastic part of the dynamic modulus, storage modulus E_1 is computed using Eq 6a and 6b, and the viscous part, loss modulus E_2 by using Eq 6a and 6b.

$$E_1 = |E^*|\cos\varphi \quad \text{and } E_2 = |E^*|\sin\varphi \tag{6ab}$$

If a perfectly homogeneous asphalt mix sample is tested repeatedly at the same temperature and frequency, the test data should plot to a single point in a complex plane. If the temperature is kept constant and frequency is varied, the test data should form a single continuous curve. If temperature and frequency are varied, the test data should still plot to the same single curve, but now extending from both ends, depending on the temperatures and frequencies used. The test data can also be plotted to the black space to investigate the viscoelastic behavior of asphalt mixtures. Again, the test data should form a single curve if the only variables are the test temperature and loading frequency.

The test data is summarized in Fig. 8 by presenting the average of two replicate test results. Figure 8(*a*) shows the test data in the complex plane and Fig 8(*b*) in the black space. Both plots show that the test data does not form a single curve, indicating that the measured samples have some variation in their viscoelastic behavior. Both plots also show that the variation increases as a function of testing frequency. The rectangular and composite specimens seem to have more elastic behavior, i.e., higher stiffness than the gyratory pills because the pills have the lowest storage modulus E_1 values, Fig. 8(*a*), and the highest phase angle values, Fig 8. The laterally loaded rectangular and composite specimens seem to have very similar behavior while the axially loaded composite specimens seem to have slightly higher modulus than the rectangular specimens, Figs. 8(*a*) and 8(*b*).

Comparison of Rectangular and Composite Specimens

By comparing the axially loaded rectangular (control) and composite specimens, it is possible to assess the goodness of the proposed sample preparation protocol. The control specimens are comparable to the 100 mm in diameter and 150 mm in height cylindrical specimens required by the dynamic modulus test protocol [4], see Fig. 5.

The normalized test data was further processed by comparing the modulus ratios of the rectangular and composite specimens. The base modulus used was the control (average axially loaded rectangular) specimens to which all other values were compared. Figure 9 shows the modulus ratios for the storage modulus E_1 and the loss modulus E_2. The stiffness difference is increasing or decreasing as a function of frequency,

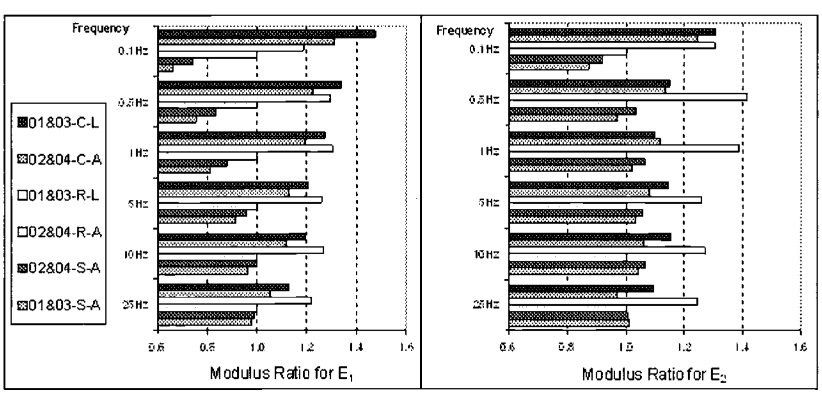

FIG. 9—*Modulus Ratio for E_1 and E_2.*

TABLE 3—*Summary of modulus ratios averaged over all frequencies.*

Specimen processing	Specimen ID	Loading direction	Modulus Ratio			Phase Ratio
			E_1	E_2	$\lvert E^*\rvert$	φ
Rectangular	02&04-R-A	Axial-Reference	1.00	1.00	1.00	1.00
	01&03-R-L	Lateral	1.25	1.31	1.26	1.02
Composite	02&04-C-A	Axial	1.17	1.10	1.16	0.94
	01&03-C-L	Lateral	1.27	1.16	1.25	0.91
Gyratory	02&04-S-A	Axial	0.90	1.02	0.92	1.11
	01&03-S-A	Axial	0.85	0.99	0.88	1.13

as discussed earlier. The computed modulus ratios are summarized in Table 3 by averaging E_1, E_2, and $|E^*|$ over all six frequencies. Table 3 also summarizes the respective phase angle ratios for the studied specimens.

The dynamic modulus $|E^*|$ of the laterally loaded rectangular specimens was approximately 26 % higher than that of the axially loaded specimens. The laterally loaded composite specimens were 25 % stiffer and the axially loaded 16 % stiffer than the reference specimens. The phase angle values of the composite specimens were 6 to 9 % lower than the reference specimens, while for the rectangular specimens they were about 2 % higher. Overall, the test results seemed to indicate that the loading direction was affecting the measured stiffness values but the capping did not have much influence.

Analysis of variance (ANOVA) was performed to statistically evaluate the measured stiffness differences due to the varying testing conditions. The significance of the statistical analysis for the overall research conclusions is however limited due to the small sample size. Because there were two factors that might influence the mix behavior, i.e., loading direction and specimen processing, a nested factorial ANOVA was performed at a significance level of $\alpha = 0.05$. The variables used in the ANOVA were the dynamic modulus $|E^*|$, phase angle φ, storage modulus E_1, and loss modulus E_2 over a frequency sweep of six frequencies. The ANOVA results, summarized in Table 4, suggest that the observed variation in the measured mix stiffness, shown in Figs. 8 and 9, was not statistically significant.

To investigate further why the observed stiffness variation was not statistically significant, the measured replicate test results were plotted to the complex plane. Figure 10(*a*) shows the replicate and the average results for the rectangular specimens, and Fig. 10(*b*) shows the same data for the composite specimens. The measured stiffness of the rectangular 02-R-A specimen was lower than the stiffness of the replicate specimen 04-R-A, see Fig. 10(*a*). For the composite specimens, the replicate measurements were very close, see Fig. 10(*b*). The large variation between the axially tested rectangular specimens was

TABLE 4—*Summary of ANOVA for comparing rectangular and composite specimens.*

Test parameter	Loading direction effect statistically significant $\alpha = 0.05$	Capping effect statistically significant $\alpha = 0.05$
$\lvert E^*\rvert$	No	No
φ	No	No
E_1	No	No
E_2	No	No

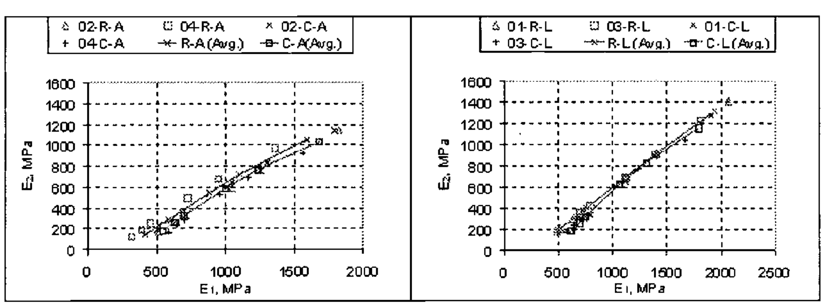

FIG. 10—*Loading direction effects.*

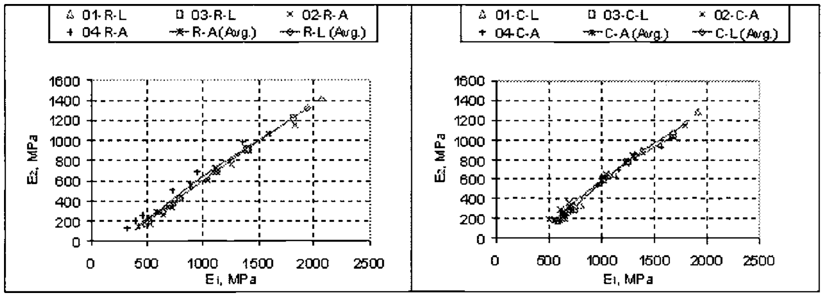

FIG. 11—*Capping Effects.*

causing the statistical analysis to conclude that the specimen processing and loading direction did not affect the measured stiffness values.

The capping effect was studied by comparing rectangular and capped specimens loaded in the axial and lateral direction. Figure 11 shows the replicate test results and the average stiffness of the rectangular and capped specimens. Figure 11(*a*) suggests that the capping does not affect the measured modulus values in the lateral direction because the stiffness difference was very small, which confirmed the ANOVA results. In the axial direction the capped specimens have slightly higher modulus values, but again the specimen 02-R-A may be distorting the results, Fig 11(*b*).

Comparison of Gyratory Pills and Sawed Specimens

Figures 8 and 9 suggest that the cylindrical gyratory-compacted pills have lower modulus values than the sawed specimens. Figure 12 compares the replicated measurements of the pills and the axially Fig. 12(*a*) and laterally Fig. 12(*b*) loaded rectangular specimens. Table 3 shows that the storage modulus E_1 of the cylindrical pills was 10 to 15 % softer than that of the rectangular specimens, while the loss modulus did not change much, see Fig. 9.

A nested factorial ANOVA was performed on the cylindrical pills, rectangular specimens, and composite specimens tested in both the axial and lateral direction. The analysis results are shown in Table 5. The storage modulus values were statistically significantly different at lower frequencies of 1, 0.5, and 0.1 Hz. The stiffness of loss modulus deviated significantly from the stiffness of the rectangular specimens only at the lowest frequency of 0.1 Hz. These results confirm the observations based on Figs. 8 and 9.

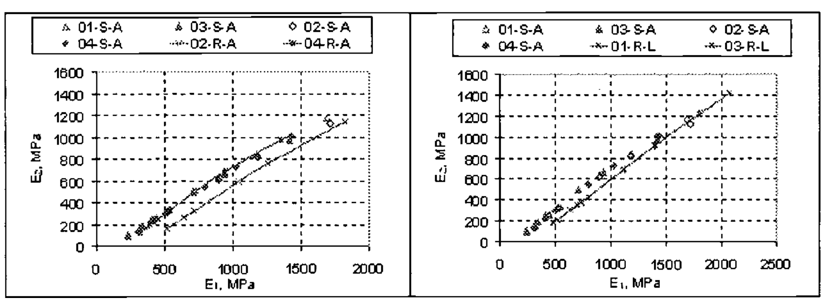

FIG. 12—*Gyratory pills versus axially loaded rectangular specimens.*

TABLE 5—*Summary of ANOVA results for the gyratory compacted specimens.*

Test Parameter	Specimen preparation effect statistically significant $\alpha=0.05$						Loading direction effect statistically significant $\alpha=0.05$
Frequency (Hz)	25	10	5	1	0.5	0.1	All frequencies
$\|E^*\|$	No	No	No	No	Yes	Yes	No
φ	No	No	No	Yes	Yes	Yes	No
E_1	No	No	No	Yes	Yes	Yes	No
E_2	No	No	No	No	No	Yes	No

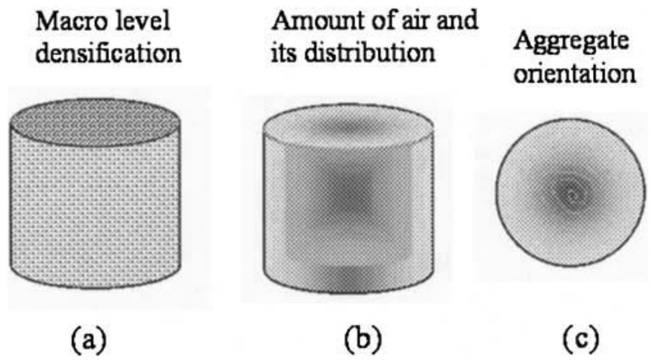

FIG. 13—*Variables affecting mechanical response of aggregate skeleton.*

Discussion

As the above analysis suggests, the sawed rectangular and composite specimens had a higher stiffness than the gyratory-compacted cylindrical pills. The stiffness measurements were obtained by essentially testing the fabricated gyratory pills three times because the rectangular specimens were obtained from the pills by sawing, and composite specimens were obtained by splitting the rectangular specimens. The difference in the air voids content of the prepared specimens explains only partially the increase in the measured stiffness values. It can be hypothesized that the observed modulus increase can be explained by the aggregate skeleton response for the applied mechanical loading, which is comprised of three different variables: mixture macrolevel densification, amount of air void and its distribution in the specimen, and anisotropy due to the aggregate orientation, see Fig. 13.

The unaixial compressive loading causes creep in the viscoelastic material. The accumulated creep strain measured during the dynamic modulus testing had fair to good correlation to the measured stiffness increase suggesting that some densification or aggregate orientation occurred during testing. This densification cannot be detected by the air void measurements because it happens in the microscopic level in the specimen, see Fig. 13(*a*).

The overall air void content of the tested specimens cannot explain the stiffness variation, because the normalization process was unable to correct the response caused by the air void distribution in the specimen. The gyratory compacted specimens have a denser inner core compared to the air void consent of the outer ring, see Fig. 13(*b*).

The shear action in the tilted gyratory mold arranges the aggregates to a spiral form which is expanding from the center of the specimen, as Fig. 13(*c*) shows. This aggregate orientation can cause a mechanical response of the specimen skeleton to deviate in the lateral and axial direction.

The changes in the specimen response can be attributed mainly to the specimen/aggregate skeleton effects because that testing was performed for the same specimen and viscous response of the mix and was not altered by changing the amount of binder and/or stiffness of the binder in the specimens. However, there might have been some minor binder stiffening due to aging of binder during testing. The gyratory pills had the low storage modulus values because the aggregate skeleton response manifests itself in the elastic, not in the viscous response of the mechanical loading. This behavior created a lateral shift in the complex plane, see Fig. 8(*a*).

The anisotropy caused by the aggregate orientation is manifesting itself in a slightly different way in the complex plane. The observed stiffness difference in the lateral and axial loading directions (Fig. 9 and Table 3) can be seen in a shift of the data points because both the storage and loss modulus are changing simultaneously, although they seem to be plotting to form a single curve. This suggests that the anisotropy due to the aggregate orientation is causing a shift in the mix behavior similar to the shift caused by the time temperature superposition.

A small separate laboratory experiment by the authors, not related to this research, was conducted earlier where three asphalt mix specimens were tested at 24°C temperature on subsequent dates. The measured dynamic modulus $|E^*|$ increased systematically from 5 to 14 %, apparently due to the specimen densification, although part of the variation can be contributed to the testing variation itself. Therefore, the modulus increase by repeated testing can be expected to be more than the 14 % at higher testing temperature, and perhaps only 10 % of the average modulus increase of 25 % (Table 3) can be attributed to the anisotropy effects caused by aggregate orientation. The 8 to 12 % lower stiffness in the gyratory pills (after air void normalization) can be explained by the specimen densification during testing and different air void distribution within the specimen. The air void normalization tries to address the amount of air in the test specimen but it cannot address the air void distribution which in most cases is unknown.

Statistical analysis indicated that the observed modulus increases in the lateral loading direction was not statistically significant, which can be attributed to the small sample size and quite large testing variation associated to the dynamic modulus testing. The combined specimen preparation and testing variation can be as high as 47 % expressed as the coefficient of variation [5]. Therefore, the 10 to 15 % modulus increase measured in the lateral direction can be considered acceptable and the presented sample preparation protocol can be used to test thin pavement cores. As the analysis suggests capping did not affect the measured modulus values.

A verification of specimen preparation protocol using actual road cores was conducted successfully and prepared specimens were tested at 40 and 54°C with no noticeable problems. An attempt was made to measure composite specimens at −10°C, but the hydrostone capping was cracking and chipping because the specimen ends were not parallel enough to apply uniform loading so the specimen could not be tested.

Concluding Remarks

The proposed composite specimen procedure provides a feasible approach to measure the axial stiffness of thin pavement cores at elevated temperatures and the laboratory performance thus can be tied to the field performance. Due to the preliminary nature of the research a verification study is needed to confirm the findings and further enhance the specimen preparation protocol. A key feature in the protocol development work is a sample preparation that is effective and least time consuming but that will still produce acceptable specimens for testing. The prepared test specimens must meet the requirements of parallel specimen ends so that the dynamic modulus of the mix can be measured at all test temperatures to produce the mix master curve. A modification of the capping jig is needed to produce better quality specimens and to allow more fast and effective methods of constructing composite specimens for testing.

Disclaimer

This work was supported by the Joint Transportation Research Program administered by the Indiana Department of Transportation and Purdue University. The contents of this paper reflect the views of the authors, who are responsible for the facts and the accuracy of the data presented herein and do not necessarily reflect the official views or policies of the Federal Highway Administration and the Indiana Department of Transportation, nor do the contents constitute a standard, specification, or regulation.

References

[1] Kallas, B., "Dynamic Modulus of Asphalt Concrete in Tension and Tension-Compression," *Proceedings of Association of Asphalt Paving Technologist*, Vol. 39, 1970, pp. 1–23.

[2] Khanal, P., and Mamlouk, M., "Tensile Versus Compressive Moduli of Asphalt Concrete," *Transportation Research Board, 74th Annual Meeting*, Transportation Research Board, Washington, D.C, January, 1995.

[3] Shook, J. F. and Kallas, B. F., "Factors Influencing Dynamic Modulus of Asphalt Concrete," *Proceedings of the Association of Asphalt Paving Technologist*, Vol. 38, 1969, pp. 140–178

[4] Witczak, M. W., "Draft Test Method DM-1 Standard Test method for Dynamic Modulus of Asphalt Concrete Mixtures," Superpave Support and Performance Models Management, NCHRP 9-19, Arizona State University, Tempe, AZ.

[5] Pellinen, T. K., "Investigation of the Use of Dynamic Modulus as an Indicator of Hot-Mix Asphalt Performance," Doctoral dissertation, Arizona State University, Tempe, AZ.

[6] Witczak, M. W., Bonaquist, R., Von Quintus, H., and Kaloush, K., "Specimen Geometry and Aggregate Size Effects in Uniaxial Compression and Constant Height Shear Test," *Journal of the Association of Asphalt Paving Technologists*, Vol. 68, 1999, pp. 1–54.

[7] Kaloush, K., "Simple Performance Test for Permanent Deformation of Asphalt Mixtures," Doctoral dissertation, Arizona State University, 2001, Tempe, AZ.

[8] Nicholls, R., *Composite Construction Materials Handbook*, Prentice-Hall, Inc., Englewood, NJ, 1976, pp. 296–297.

[9] Witczak, M. W., Mamlouk, M., Ho, and Yow-Shi, "Anisotropy Study," Superpave Support and Performance Models Management, NCHRP 9-19, Task F–Advanced Mixture Characterization. Arizona State University, 2001, Tempe, AZ.

[10] Witczak, M. W., Pellinen, T. Kaloush, K., "Air Void Distribution in Gyratory Compacted Specimens," Superpave Support and Performance Models Management, NCHRP 9-19, Arizona State University, 2000, Tempe, AZ

[11] Bonnaure, F., Guest, G., Gravois, A., and Uge, P., "A New Method of Predicting the Stiffness of Asphalt Paving Mixtures," *Journal of the Association of Asphalt Paving Technologist*, Vol. 46, 1977, pp. 64–104.

[12] Andrei, D., Witczak, M. W., and Mirza, M. W., "Development of Revised Predictive Model for the Dynamic (Complex) Modulus of Asphalt Mixtures," Development of the 2002 Guide for the Design of New and Rehabilitated Pavement Structures, NCHRP 1-37A. Interim Team Technical Report. Department of Civil Engineering, University of Maryland of College Park, MD, 1999.

[13] Christensen, D. W., Pellinen, T., and Bonaquist, R., "Hirsch Model for Estimating the Modulus of Asphalt Concrete," *Journal of the Association of the Asphalt Paving Technologists*, Vol. 72, 2003, pp. 97–121.

Journal of ASTM International, March 2005, Vol. 2, No. 3
Paper ID JAI12318
Available online at www.astm.org

Christos A Drakos,[1] *Reynaldo Roque,*[1] *Bjorn Birgisson,*[1] *and Marc Novak*[1]

Identification of a Physical Model to Evaluate Rutting Performance of Asphalt Mixtures

ABSTRACT: The objective of this study is to identify a physical model that can provide reliable predictions about a mixture's ability to resist permanent deformation under realistic stress states. Key differences were identified between stress states under the existing Asphalt Pavement Analyzer (APA) loading device (hose) and stress states under radial truck tires, which may indicate potentially different rutting mechanisms. It was shown that the APA hose was not capturing the critical lateral stresses found to be detrimental to rutting and cracking of HMA pavements. A new loading device (rib) was designed and constructed for use in the APA that more closely represents stress states found under radial tires.

Contact-stress measurements under the two loading devices – hose and rib – showed that the rib was able to reproduce the lateral stresses found under individual ribs on a radial-tire tread. Subsequent finite element modeling also showed that the rib appeared to generate similar shear stress patterns to those found under the modeled radial-tire load.

A new method was developed to measure deformations on the surface of APA specimens, where a contour gauge was used to record and store the entire surface profile of the sample throughout the progress of the test. An area-change parameter, which reflects volume change, was introduced to calculate the volumetric changes in the specimen. The area-change parameter can be used to determine whether specimen rutting is primarily due to shear instability or consolidation.

Two mixtures of known field performance – poor and good – were tested to evaluate the test's ability to predict performance with the new loading device and the new measurement and interpretation system. Results showed that the new system (loading strip and profile measurement method) appears to have greater potential of evaluating a mixture's potential for instability rutting than the original (hose and single rut-depth measurement) configuration.

KEYWORDS: rutting, instability, HMA, APA

Introduction

Background

A major distress mode of flexible pavements is permanent deformation, also known as rutting. Rutting is characterized by a depression that forms in the wheel paths and can be the result of permanent reduction in volume (consolidation/traffic densification), permanent movement of the material at constant volume (plastic deformation/shear), or a combination of the two. This mode of failure reduces serviceability and creates the hazard of hydroplaning because of accumulated water in the wheel-path ruts. Rehabilitation of rutted pavements usually involves asphalt concrete (AC) overlay, recycling, or replacement of all structural layers.

Manuscript received 10 December 2003; accepted for publication 29 July 2004; published March 2005. Presented at ASTM Symposium on Performance of Hot Mix Asphalt (HMA), including Fundamental and Empirical Procedures on 9 December 2003 in Tampa, FL.
[1] Assistant-In Engineering, Professor, Assistant Professor, and Doctoral Candidate, respectively, University of Florida, Gainesville, FL 32611.

The Superpave™ mix design and analysis method was developed more than a decade ago under the Strategic Highway Research Program (SHRP) [1]. Many agencies in North America – including the Florida Department of Transportation (FDOT) – have adopted the Superpave™ method of performance-grade (PG) binder specification and the volumetric mixture design method. Although the Superpave™ volumetric design procedure has resulted in some improvements over the Marshall method of mixture design, it is still devoid of a general strength test that would determine the mixture's suitability for resistance to rutting and cracking. The industry has expressed the need for a simple 'pass–fail' type of test to complement the Superpave™ volumetric mix design method, especially for use on design–build or warranty projects.

Numerous performance prediction models – numerical and physical – have been implemented to classify an asphalt mixture's ability to resist rutting. In an effort to control this type of distress, many institutions and agencies are searching for a simple performance test that would indicate the rutting potential of HMA. For this purpose the suitability of various loaded-wheel testers (LWT), as a physical model, is being examined throughout the country. The LWTs provide an accelerated performance evaluation by subjecting the designed mixture to repeated loading under various environmental conditions (moisture and temperature). Some of the most popular devices used are the Georgia Loaded Wheel Tester (GLWT), Asphalt Pavement Analyzer (APA), Hamburg Wheel Tracking Device (HWTD), and the French Pavement Rutting Tester (FPRT) [2,3].

Objectives

The main objective of this study was to identify the loading, environmental, and construction (density) factors that are critical to defining the mechanism of rutting. The identification of these conditions will lead to the development of a reliable physical model. The current version of the APA was selected for the experimental program; necessary modifications will be made to incorporate new testing procedures that more realistically simulate traffic and environmental conditions existing in pavements.

The primary objectives of this research study are listed below:

- Identify the characteristics of a loading device necessary to represent a tire load more realistically.
- Design and construct a new loading device to induce more realistic contact stresses.
- Verify the effects of loading characteristics on rutting performance.
- Evaluate the importance of density/loading history on rutting performance.
- Investigate the sensitivity of the physical model to mixtures with different densities as produced by compaction and/or aggregate gradation of the mixtures.
- Recommend test configuration and procedure for mixture evaluation. As envisioned, the procedure will define the magnitude and sequence of loading as well as test-temperature requirements.

Scope

The research focuses on identifying some of the most critical conditions that contribute to the mechanism(s) of rutting. Defining the conditions that might initiate and propagate rutting will lead to the development of better performance prediction models – physical and numerical. This research will focus on the effects of the following:

- A new loading device (loading strip) will be evaluated against the existing pressurized hose. The contact stresses will be measured for both devices and then used in finite element modeling (FEM) to calculate the induced stress states in the specimen.
- Two temperatures – 64 and 70ºC – have tentatively been selected for evaluation of mixture's sensitivity to temperature changes.
- Mixtures will be tested at two levels – 93–94, and 95–96 % – of maximum theoretical density (MTD).
- Two mixtures of known field performance – poor field performing mixture (I-10 Madison County), good field performing mixture (Turnpike Palm Beach) – will be used for the initial development and the evaluation/validation of the physical model.

The Pine gyratory compactor will be used to prepare 150-mm diameter by 75-mm thick mixture specimens. In this research, beams will not be considered because of compaction issues and the potential for variability that may influence the analysis.

Asphalt Pavement Analyzer

The APA is a further modification of the Georgia Loaded Wheel Tester, first manufactured in 1996 by Pavement Technology, Inc. Since it is a new generation of the GLWT, it follows the same testing philosophy. Load is applied to a pressurized linear hose by a pneumatically loaded wheel and tracked back and forth over a testing sample to induce rutting. The APA has the additional capability of testing for moisture susceptibility and fatigue cracking while the specimens are submerged in water.

Extensive studies have been conducted to evaluate the ability of the APA to distinguish the rutting susceptibility between mixtures of known performance. Most of these studies tried to establish a relation between rut depths obtained in the laboratory tests and the field performance of the mixture. A study by Epps et al. [4] compared test results from WesTrack to rutting predictions from three LWT devices. The APA ranked the mixtures according to their WesTrack performance with 89 % accuracy [5]. The National Center for Asphalt Technology indicated that the APA was sensitive to mixtures with different asphalt binder and varying gradation (ARZ, BRZ, and TRZ) [6]. The Federal Highway Administration also conducted a study at Turner-Fairbank Highway Center. Comparison of LWT test results to the Accelerated Loading Facility (ALF) showed that the LWTs were able to distinguish between good and poor performance mixtures that were prepared with the same aggregate gradation and different binder. However, when the aggregate gradations were varied, none of the LWTs were able to separate the mixtures, even though the ALF testing showed that there were significant differences in pavement performance [7].

Limitations of Wheel Testers

Loaded wheel testers operate on the same basic principle: a test specimen of mixture is subjected to repetitive loading by a traversing wheel, and the surface depression in the sample is then measured and reported as a function of load cycles. These types of torture tests are classified as empirical or performance-related tests because they do not measure a fundamental property that can be used to explain and identify the mechanisms resulting in surface distress.

The APA, like most LWTs, attempts to replicate field conditions in a controlled laboratory environment. In this sense, good correlation between results from the APA with field performance relies on how well (realistically) conditions have been simulated in the lab. The following issues raise some considerations on the ability of the APA to approximate field conditions:

- Loading scale effects. The loaded area under the pressurized hose is very small (narrow) in proportion to the nominal maximum aggregate size [3,8].
- Boundary conditions. Test specimens are resting on a metal plate that limits deflections and increases confinement.
- Load application. Earlier work [9,10] showed that radial truck tires induce high lateral stresses that can cause tension on the surface of the pavement [11]. It is believed that the pressurized hose of the APA does not simulate the effects of the stiff tread of the radial tire, thus not inducing any lateral stresses.

New Loading Mechanism

The concept for a new APA loading mechanism is based on the observations and conclusions from the tire-pavement interface stresses studies [10,11] that showed the importance of lateral stresses in the development of critical stress-states near the surface of the pavement. These studies have shown that radial tires induce stresses that are more detrimental to pavements than bias-ply tires and that the difference has been attributed mainly to tire structure. Analyses performed with the elastic layer analysis program BISAR and the finite element program ADINA provided information on the pavement's response under modeled tires from measured contact stresses. Researchers have identified the lateral stresses induced by radial tires as the fundamental cause of stress reversals (tension) and high magnitude shear stresses near the surface of the pavement [12]. These stress states cause a reduction in confinement near the pavement's surface near the edge of the loaded area, which reduces the resistance to shear stress within the mixture.

The hypothesis was that the stiff pressurized hose used by the APA to load the specimen does not reproduce the lateral stresses found under radial truck tires. The objective was to develop a new loading mechanism, modeled after a radial truck tire, to replicate these stress conditions in the APA specimen.

The initial task was to develop a reasonable finite element model that represents the structural behavior and response of a typical radial truck tire tread. Earlier work by Roque et al. [13] showed that the radial tire loading behavior can be simulated with a combination of steel and rubber. Results from this research were used to estimate the right amount of steel and rubber needed to build a device that captures the loading behavior of the radial tire. The idea for the APA loading mechanism was to substitute the pressurized hose with a steel-rubber configuration based on the tire finite element model. Figure 1 shows a schematic of the concept device, called the *loading strip*, where a thin rectangular steel plate (14 gauge) is attached on top of a medium-durometer (45–55) rubber. The solid steel wheel applies the load on the thin steel plate that distributes the stresses on the sample through the rubber part of the device.

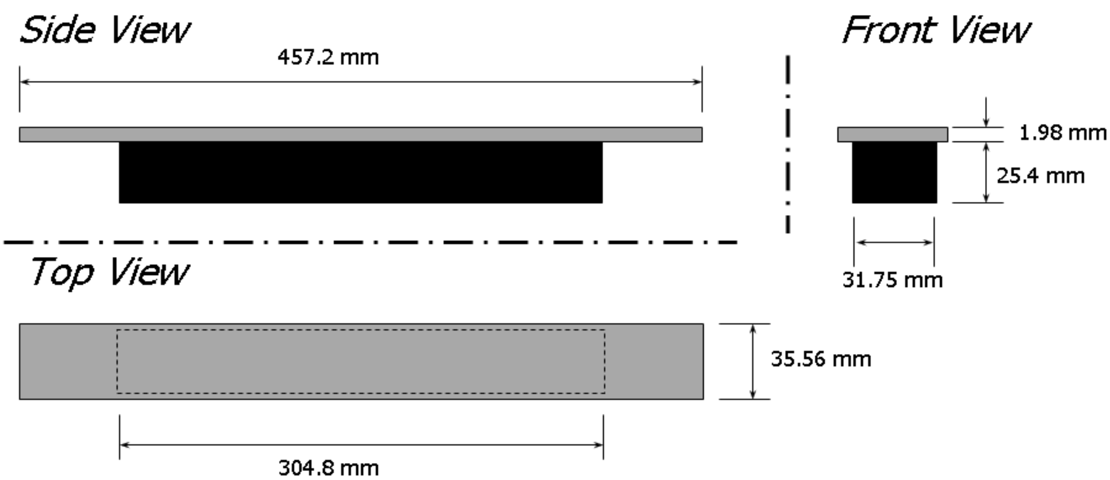

FIG. 1—*Schematic of the loading strip.*

Ideally, the loading strip stress-distribution behavior would represent that of a single rib from the radial tire tread. It was determined that the magnitude of the applied stresses would be lower because of limitations in the range of applied load in the APA; however, the stress-distribution pattern was expected to be similar. The steel plate would uniformly distribute the stresses to the rubber and also increase the stiffness of the device, whereas the rubber member would apply the vertical load and also create the Poisson's effect that induces lateral stresses as found under radial tires.

Measured Contact Stresses in the APA

Preliminary measurements of the APA hose contact patch (traced with carbon paper) revealed that the initial contact area is approximately 8 mm wide. The initial hypothesis was that the limited width of the pressurized hose contact patch cannot generate the essential lateral stresses found under radial tires. A new loading device (loading strip) was designed and tested with the help of numerical modeling that would simulate real tire stress distribution. In order to verify the above hypothesis, both loading devices – pressurized hose and the loading strip – were sent to Smithers Scientific Services, Inc. in Ravenna, Ohio, to measure the actual contact stresses at the loading device-specimen interface.

Smithers Scientific Services, Inc. developed the Flat Surface Tire Dynamics Machine (FSTDM) to measure contact stresses at the tire-pavement interface. The device measures vertical, transverse, and longitudinal forces and displacements under a moving tire by using a series of 16 transducers. Dr. Pottinger of Smithers Scientific Services, Inc. fabricated custom end-restraints and a loading foot that allowed load control to within ±1 lb (±0.45 kg), to accommodate the pressurized hose and the loading strip on the FSTDM.

The loading strip was tested at three load levels – 110-, 130-, and 150-lb – whereas the pressurized hose was tested at two load levels – 100-, and 120-lb. The loading foot with the steel wheel remained stationary, while the bed with the loading device (hose/loading strip) moved in the longitudinal direction. The movement of the bed forced the steel wheel over the loading device, and the transducers measured the displacements and stresses at the contact interface. Proprietary software developed by Smithers Scientific then compiled the data and created an array of the contact patch stresses.

APA Hose Interface Stresses

Results from the APA pressurized hose contact stresses verified the initial hypothesis that the contact area under the hose was too narrow to produce any significant lateral stresses. Figure 2 shows the pressurized hose, which is attached to the moving bed, and the concave steel wheel loading the hose directly above the transducers. In their report, Smithers Scientific showed that the narrow (8 mm) contact area was not wide enough to record any lateral stress on the transducers. Figure 3 illustrates the vertical stress distribution under the hose. The measured vertical stresses show two humps at each side of where the steel wheel loads the hose, caused by the semi-rigid structure of the hose.

Loading Strip Interface Stresses

Smithers Scientific Services measured the contact stresses under the loading strip for three load levels – 110-, 130-, and 150-lb. In the case of the loading strip, Dr. Pottinger used the solid wheel to load the loading strip, and he noted that the wheel had to be centered over the loading strip to avoid asymmetric stress distribution; the concave wheel acts as a ‘channel’ that continuously aligns the rubber hose with the traversing movement of the loading arm.

Figure 4 illustrates the vertical stress distribution under the loading strip for the three load levels. Unlike the pressurized hose results, the vertical stress distribution under the loading strip resembles that of an elastic material with the stress peaking in the middle of the normal distribution. As expected, the magnitude of the vertical stresses is much lower under the loading strip due to the increase of the contact area. The highest measured vertical stress under the loading strip for the 150-lb (68 kg) load was 241 kPa, whereas the pressurized hose recorded 896-kPa vertical stress for the 100-lb (45 kg) load.

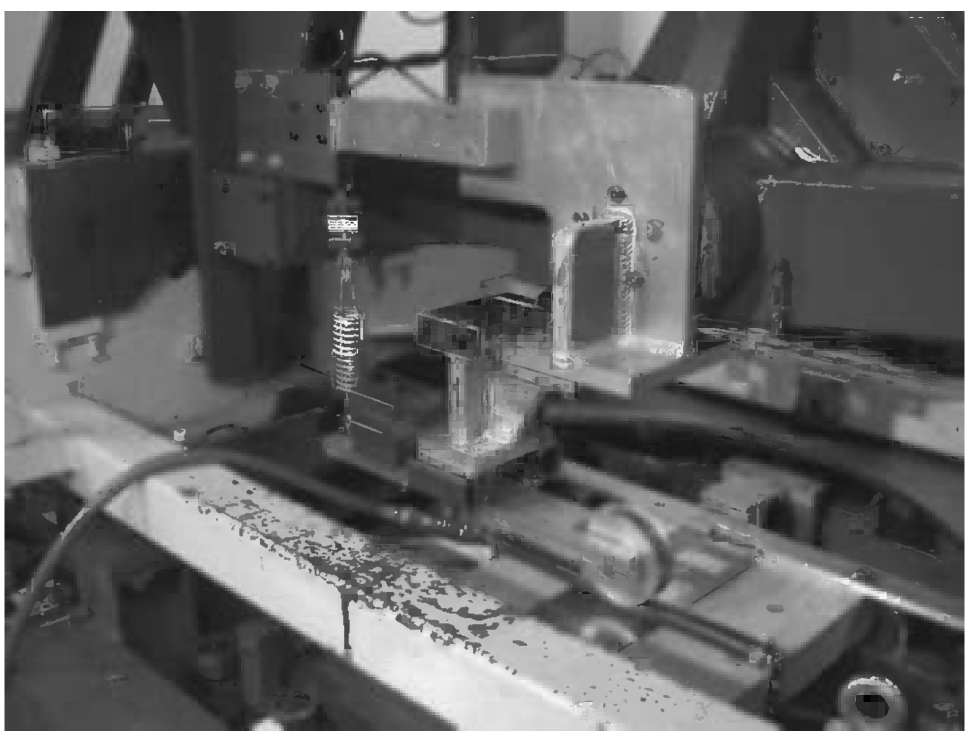

FIG. 2—*Picture of the APA pressurized hose test.*

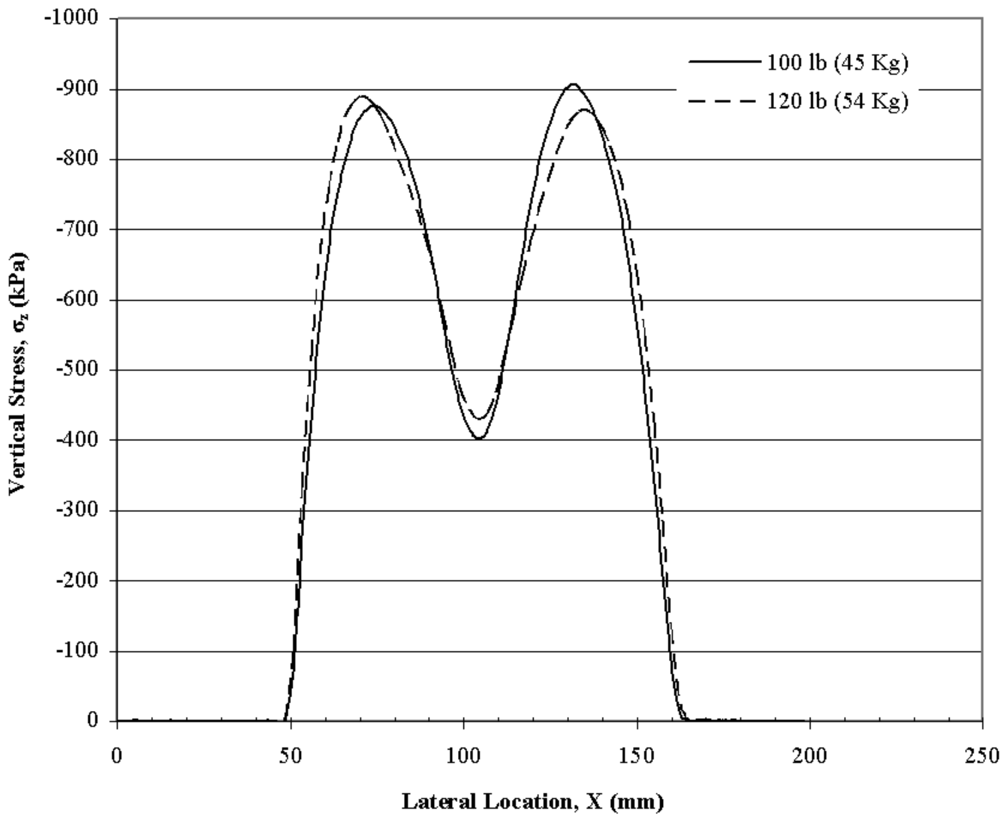

FIG. 3—*Vertical stress distribution under the pressurized hose.*

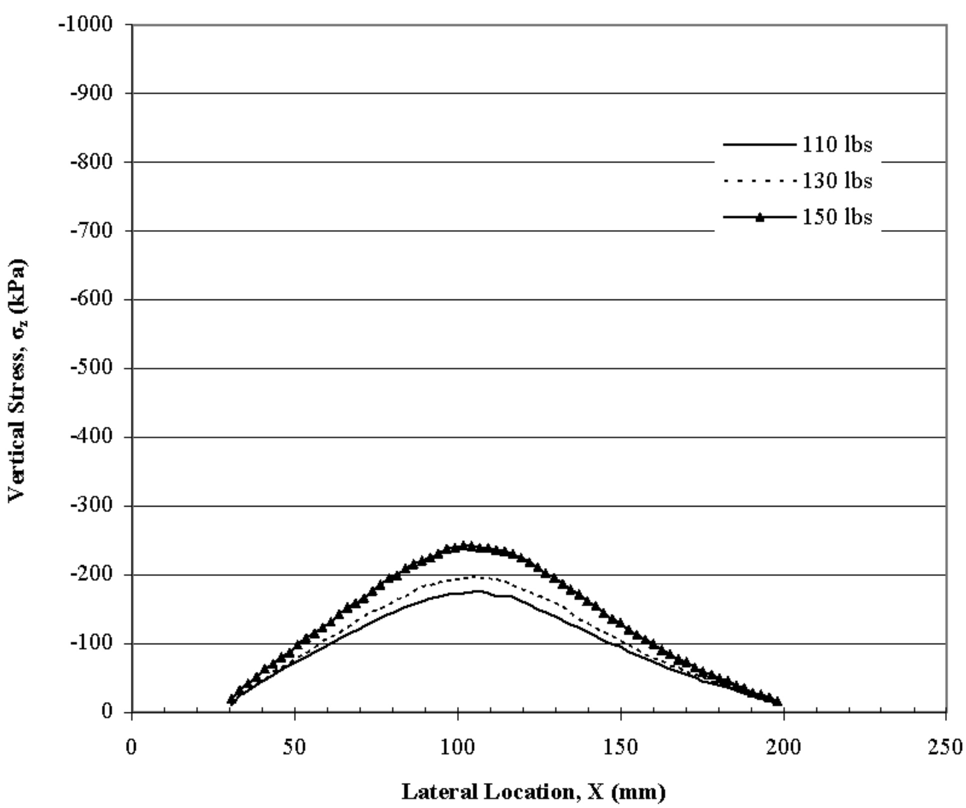

FIG. 4—*Vertical stress distribution under the loading strip.*

Figure 5 shows that the transverse stress distribution under the loading strip accurately captures the Poisson's effect found under individual tire ribs. The Poisson's effect states that, unless restrained, most materials expand laterally when loaded vertically. When individual ribs under a tire are loaded, they attempt to expand laterally, and the surface of the pavement tries to restrain the expansion, thus generating transverse stresses. Similar to the tire ribs but lower in magnitude, the loading strip induces lateral stresses that change sign (direction) at opposite sides of the loading strip (Fig. 5).

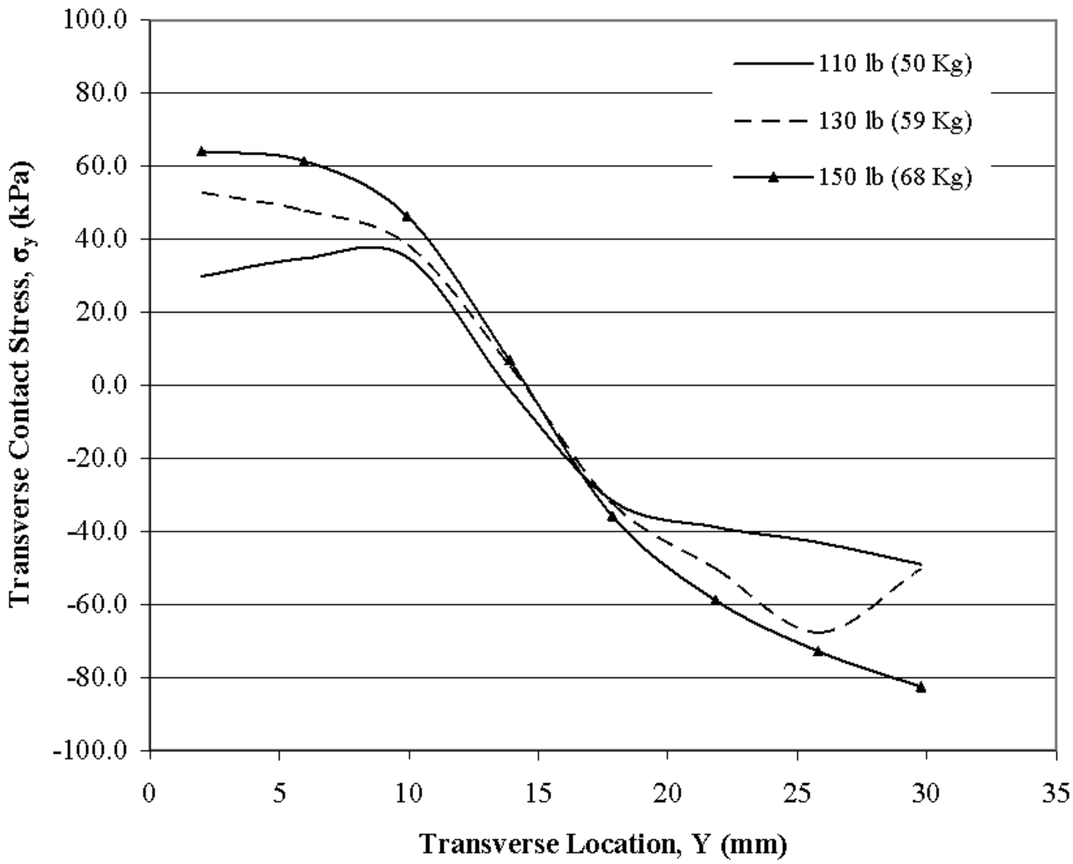

FIG. 5—*Lateral stress distribution under the loading strip.*

Stress Analyses

As mentioned earlier, experimental studies revealed that tire contact stresses are distributed in a highly non-uniform manner and differ significantly for various tire types [9,10,14]. These stresses include not only vertical normal stresses, but also transverse and longitudinal surface shear stresses. Other research suggests that a possible mechanism behind instability rutting is that radial tires, with their complex non-uniform loading, may be inflicting stress states in the HMA that are not predicted with traditional uniform vertical loading patterns [11,12]. Elastic layer and finite element analyses of asphalt pavements for three load cases – radial tire load, bias-ply tire load, and uniformly distributed vertical load – showed that radial-tire loads induce more severe stress states near the surface of the pavement.

Figure 6 shows the magnitude and direction of the maximum shear stress distribution along a vertical section under a modeled radial-tire load [12]. The arrows indicate the direction of the maximum shear stress closest to the horizontal, and the contour plot (shaded area) in the background specifies the magnitude of the shear stress (kPa). The direction of the shear stresses under the radial tire indicates the formation of shear planes that tend to "shove" the material away from the tire. Furthermore, the contour plot of the predicted maximum shear stress magnitude indicates that shear stresses peak in the same region that the shear planes develop.

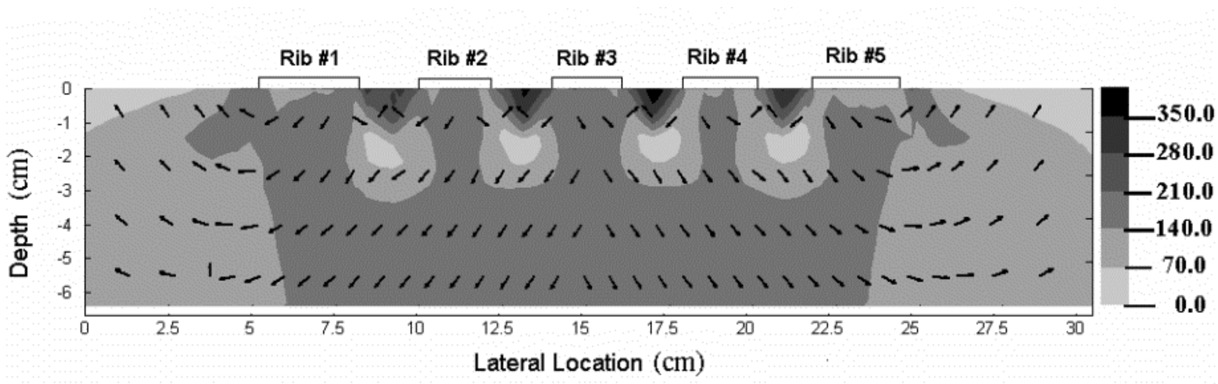

FIG. 6—*Maximum shear stress magnitude and direction under a modeled radial tire load [12].*

The measured contact stresses for the two APA loading mechanisms – pressurized hose and loading strip – were modeled with finite elements to evaluate the effects of the different loading conditions. The primary objective was to examine whether the loading strip could induce similar stress states in the modeled HMA specimen, as the radial tire induced in the modeled pavement.

The three-dimensional finite element model was constructed using the MSC/PATRAN pre-processor software to build the model geometry and to define the mesh and the HKS/ABAQUS software for the elastic analysis. An approximation method was used to convert and redistribute the measured contact stresses to nodal forces. The appropriate force for each element was determined by converting each uniform stress to an equivalent concentrated force. The forces were then converted to nodal forces with the help of shape functions and applied to the respective node [15].

Figure 7 shows the three-dimensional model for the APA mold and the HMA specimen. For practical purposes, only one of the two cylindrical-sample slots was used in the model. Furthermore, the model was separated into two main parts – the plastic mold ($E = 2758$ MPa, $\nu = 0.4$) and the asphalt concrete sample ($E = 690$ MPa, $\nu = 0.4$).

Figures 8 and 9 show the predicted magnitude and direction of the maximum shear stress (τ_{max}) distribution, along a vertical section, for the loading strip and pressurized hose loading conditions, respectively. The range of the τ_{max} magnitude under the loading strip (20–90 kPa) is lower than that predicted under the pressurized hose (60–500 kPa). This magnitude difference can be attributed to the higher vertical stresses measured under the pressurized hose because of the smaller initial contact area (Figs. 3 and 4).

The important finding of this analysis was the pattern of the τ_{max} distribution throughout the modeled specimen. Unlike the distribution under the pressurized hose, the modeled loading strip showed that the τ_{max} magnitude peaks near the surface of the specimen, under the loaded area. Furthermore, the magnitude contour plots for the loading strip condition indicate the existence of shear planes under the load, similar to those found under the modeled tire load, whereas the same is not true for the modeled pressurized hose load.

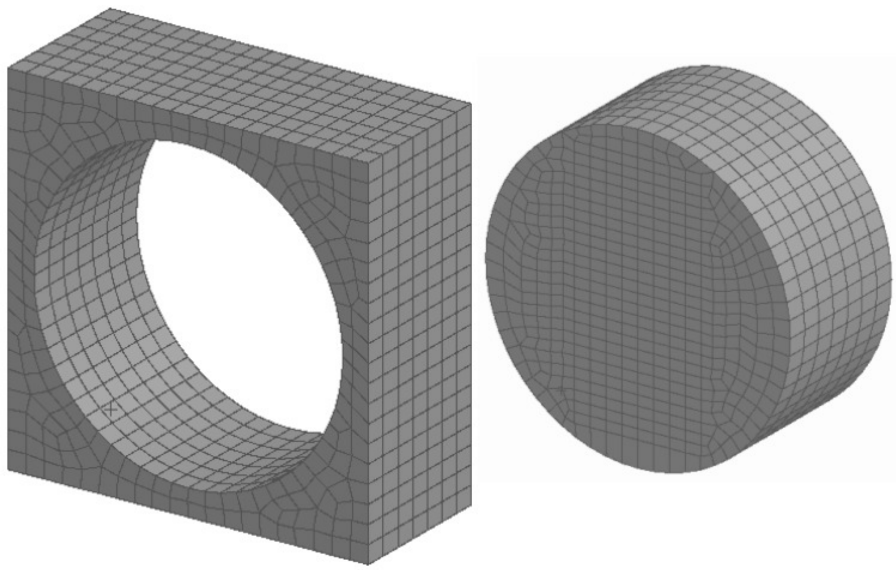

FIG. 7—*Three-dimensional finite element model for the APA mold and specimen.*

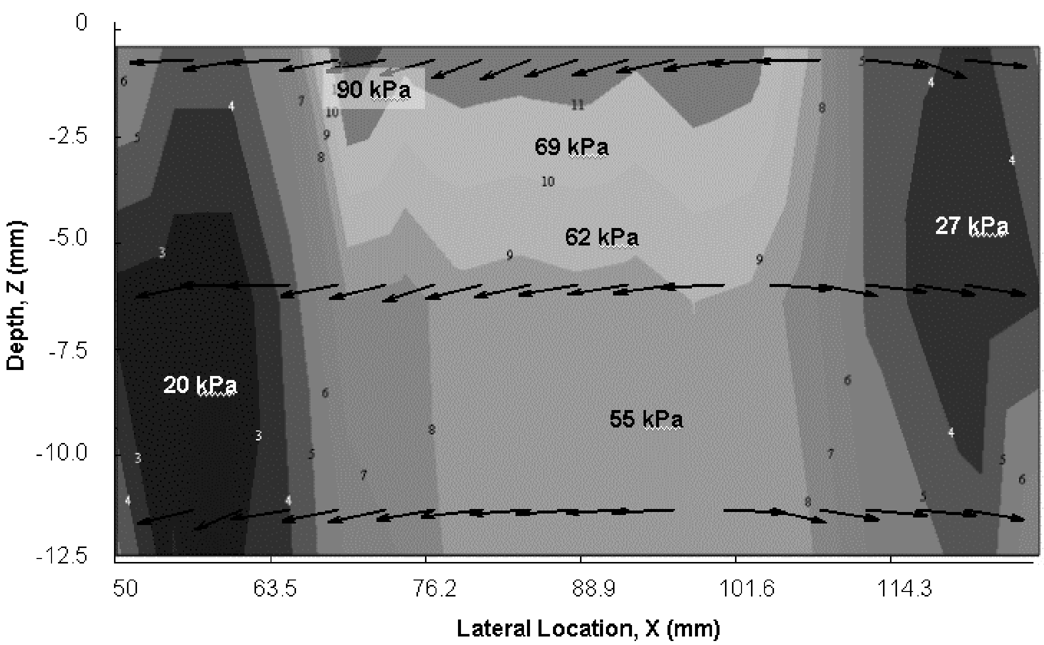

FIG. 8—*Maximum shear stress magnitude and direction under the modeled loading strip load.*

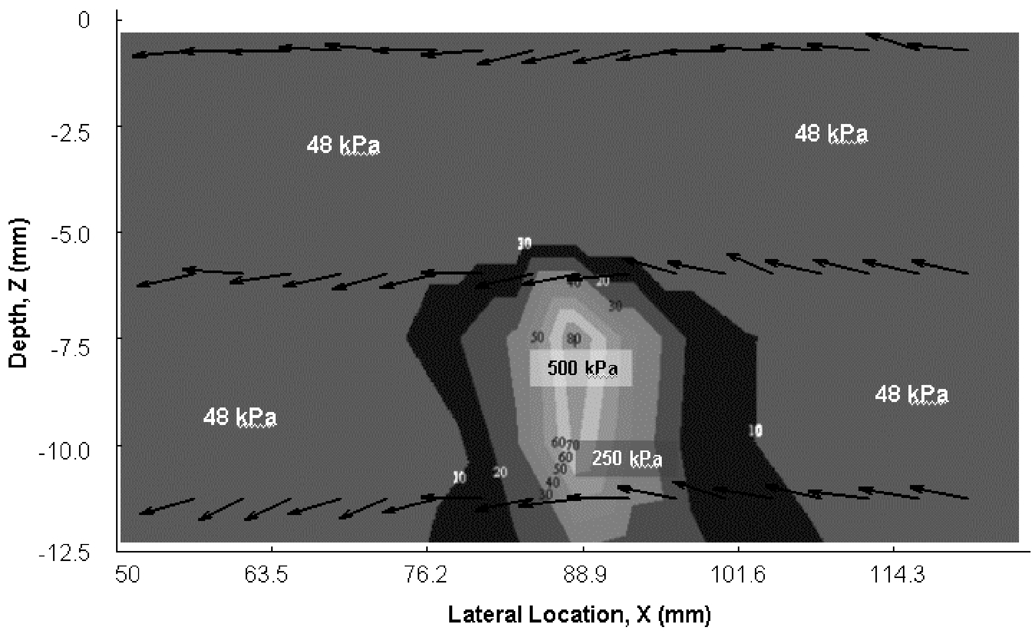

FIG. 9—*Maximum shear stress magnitude and direction under the modeled pressurized hose load.*

Materials and Methods

Materials

The selected mixtures for this study were placed in Florida in 1998 (Table 1), and the FDOT has been monitoring their field performance ever since. The Job Mix Formula (JMF) of the original FDOT mixtures had a Reclaimed Asphalt Pavement (RAP) component of 15–20 % that formed part of the aggregate constituent. However, the RAP material was no longer available at the time of this research, so the percentages of the other aggregates were adjusted to maintain the same gradation for each mix. Project 1 is a 9.5-mm nominal maximum-size coarse-graded mixture, and Project 7 is a 12.5-mm nominal maximum-size fine-graded mixture. More information about the mixtures properties can be found elsewhere [16].

TABLE 1—*Aggregate types and sources for the selected FDOT mixtures.*

Project No.	Mix No.	Material	FDOT Code	Pit No.	Producer	JMF %
1	97051A	Milled material	-	-	-	20
		# 89 Stone	51	GA 185	Martin Marrietta	45
		W-10 Screenings	20	GA 185	Martin Marrietta	25
		M-10 Screenings	21	GA 185	Martin Marrietta	10
7	980139A	Milled material	-	-	-	20
		S1A Stone	41	87-339	White Rock Quarries	20
		S1B Stone	51	87-339	White Rock Quarries	10
		Asphalt Screenings	20	87-339	White Rock Quarries	50

The field rut depths were measured using a transverse profiler at 30 locations of each project. Table 2 shows the average accumulated rut depths two years after the end of construction and opening of the pavements to traffic. The measured rut depths show that Project 1 experienced higher rutting (≈ 3.5 mm per million ESAL) relative to Project 7 (< 1 mm per million ESAL) within the same period.

TABLE 2—*Field rutting data.*

Project No.	Avg Field Rut Depth After Year 2 (mm)	Estimated ESAL at Year 2 (million)
1	5.1	1.48
7	2.5	2.99

New APA Measuring System

The APA test procedure was slightly modified to incorporate a new way of recording and analyzing the test results. Instead of using the roller dial gauge to measure a single (the lowest) point on the specimen, the new method uses a contour gauge that captures the entire surface profile of the sample. The aluminum plate openings (slits) were enlarged to a width of 5.5-in. (139.7 mm) to accommodate the contour gauge.

Figure 10 shows the contour gauge recording the surface profile at the middle location of the sample. The rods are pushed downward until they come in contact with the specimen, forcing the contour gauge to assume the shape of the specimen's surface. The recorded surface profile from each location on the measuring plate is traced on a card and then digitized for further analysis.

FIG. 10—*Contour gauge recording the surface profile of the specimen.*

The digitized data from the measured surface profiles are imported to a spreadsheet. Figure 11 illustrates the deformation profile of a specimen tested with the original pressurized hose. An interesting point on this graph is the way the deformation profile changes with the progress of the test. Apparently, the material does not only consolidate, but it also heaves to the sides of the loaded area. This is something that the traditional way of measuring the rut-depth results could not show.

The traditional way of calculating the rut depth for an APA specimen is to take two measurements – the lowest point at the beginning and the lowest point at the end of the test – and report the difference after 8000 cycles. For the purpose of this study, the traditional way of measuring rut depth will be identified as the Absolute Rut Depth (ARD). The Differential Rut Depth (DRD) is defined as the difference of the lowest point at the beginning of the test and the highest point recorded at the end of the test (Fig. 11).

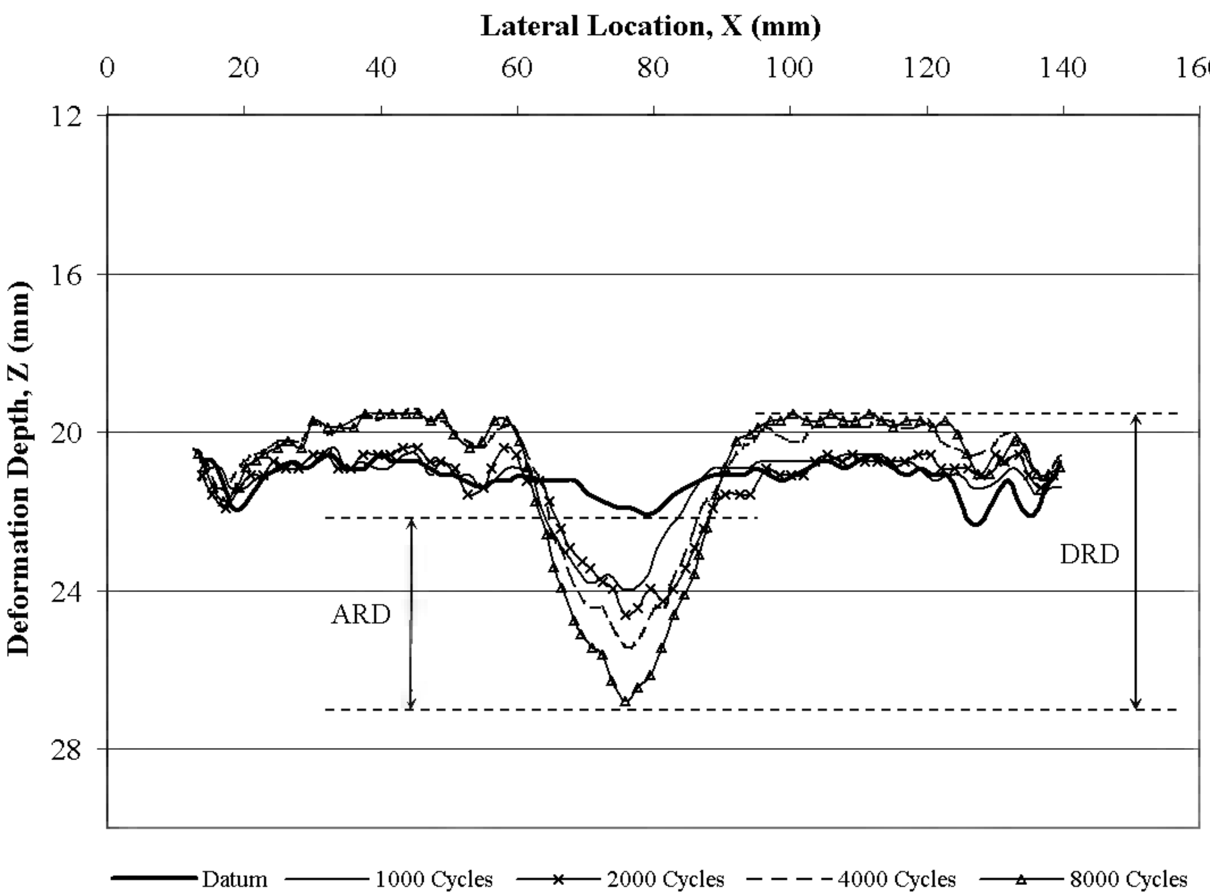

FIG. 11—*Deformation profile for a specimen tested with the APA pressurized hose.*

Area Change Parameter

In most cases, permanent deformation of asphalt mixtures in the field is a combination of two mechanisms – reduction of air voids (consolidation) and shear deformation (instability). Figure 11 proves that the same combination of failure mechanisms applies for HMA specimens tested in the APA. The objective here is to determine which of the two modes of deformation contributes the most in failing the material.

Figure 12 illustrates the theory behind the area change calculation. Assume the schematic in Fig. 12 represents an APA specimen that is experiencing excessive rutting. If there were a way to calculate the two shaded areas – A_1 and A_2 – it would be possible to determine if the permanent deformation was due primarily to shear instability or consolidation. When material fails due to shear deformation, the magnitude of A_1 and A_2 would be equal because the material is shoved to the side. With the same logic, if the material fails primarily due to consolidation, the magnitude of A_1 would be less than A_2.

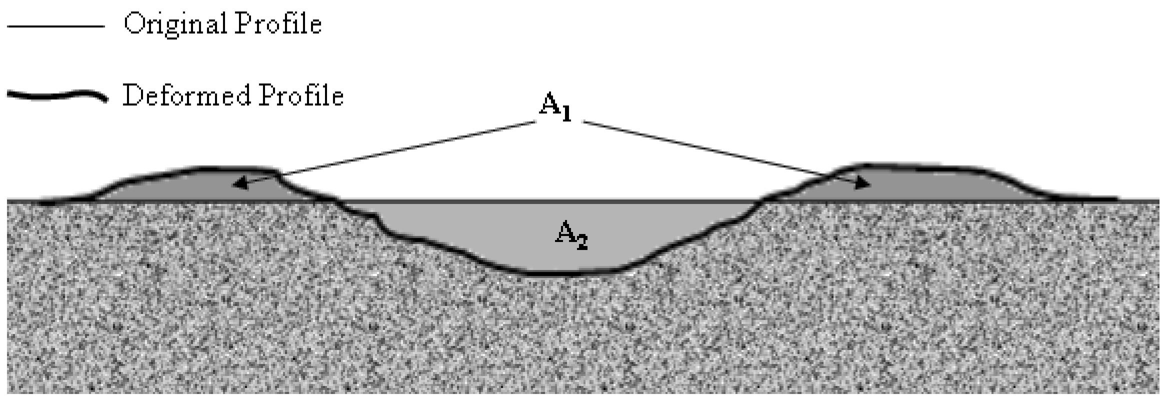

FIG. 12—*Area change interpretation.*

To analyze the APA test results, the data were transferred to MathCAD, and the LOESS function [17] was used to fit a polynomial to the original surface-profile data. The polynomial is then integrated over a certain interval to calculate the area under the curve. Based on the discussion above, the failure mode is primarily consolidation if the initial area (A_i) is less than the final area (A_f). If the A_i is greater or equal to A_f, then that clearly identifies the presence of shear instability.

A simple way to determine the effect of the area change was to calculate the percent area change (ΔA). A positive ΔA means that the mixture is experiencing instability rutting, whereas a negative ΔA indicates that the mixture is deforming primarily due to consolidation. Therefore:

$$\%\ \text{Area Change} = \frac{A_i - A_f}{A_i} \times 100 \tag{1}$$

$$\text{If }\%\ \text{Area Change} > 0 \rightarrow \text{Primarily Instability}$$

$$\text{If }\%\ \text{Area Change} \leq 0 \rightarrow \text{Primarily Consolidation}$$

APA Test Results

Two mixtures – Project 1 and Project 7 – were tested with the modified and original APA loading devices. The new method for measuring deformations, recording the entire surface profile, was used in both tests. Tests run with the loading strip were performed at two temperatures – 64°C and 70°C – whereas tests with the pressurized hose were run at 64°C. Also, the mixtures were prepared and tested at two air void content levels – 4 %AV and 7 %AV – to evaluate the effects of compaction on the test's ability to predict permanent deformation.

Absolute Rut Depth

Absolute rut depth is the measured difference between the lowest point of the initial surface profile and the lowest point of the final surface profile. This is the traditional way of measuring the specimen's performance in the APA. Various agencies suggest that the criterion for good field-rutting performance is to keep ARD less than 8 mm [18].

Figure 13 compares the absolute rut depth results between Project 1 and Project 7 for the three test methods – new APA 64°C, new APA 70°C, and the original APA 64°C – at two air void contents – 4 %AV and 7 %AV.

For the 4 %AV tests, results from the new and original APA tests at 64°C did not show any significant difference in performance between the two mixtures. However, the new APA tests at 70°C showed that the ARD for Project 1 increased, whereas the ARD for Project 7 remained at the same level compared to the results from the new APA 64°C. In the case of 7 %AV, results from all three tests showed significant difference between the performances for the two mixtures.

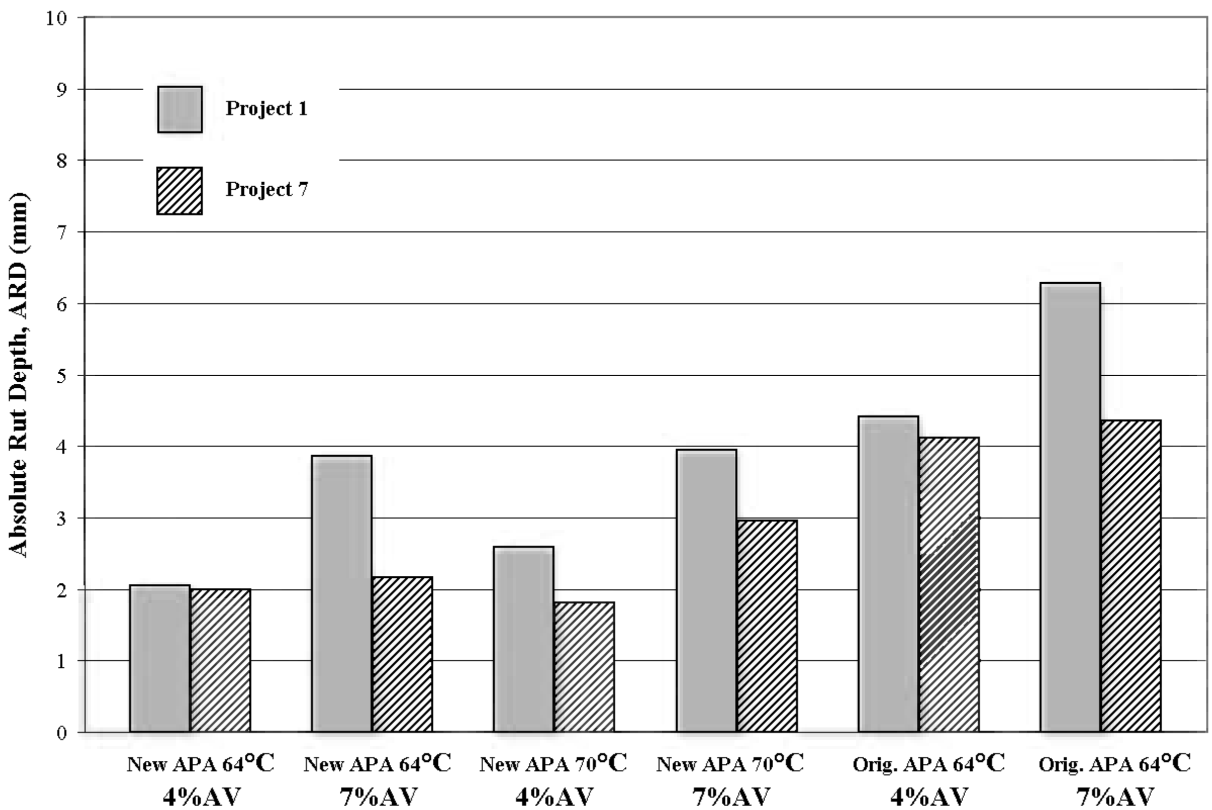

FIG. 13—*Absolute rut depth measurements for Project 1 and 7 tested with the two loading devices at 4 % and 7 % air void content.*

Differential Rut Depth

The differential rut depth is defined as the difference of the lowest point at the beginning of the test and the highest point recorded at the end of the test. The function of this parameter is to incorporate the instability characteristics of the material into the rutting prediction. Unlike the ARD, the DRD includes the dilated portion of the deformed material into the measurement.

Figure 14 compares the differential rut depth results between Project 1 and Project 7 for the three test methods at two air void contents. Similar to the ARD results, the new and original APA tests at 64°C did not show any significant difference in performance between the two mixtures for the 4 %AV specimen. Once again, for the 4 %AV, the new APA tests at 70°C showed that the DRD for Project 1 increased, whereas the DRD for Project 7 remained at the same level compared to the results from the new APA 64°C. Since the binder is the same for both projects, the difference in DRD suggests that the new APA might be able to account for the effect of aggregate structure in the mixture's ability to resist rutting, something other studies [7,18] showed that the APA was not able to do. Once again, the 7 %AV results from all three tests showed significant difference between the performances for the two mixtures.

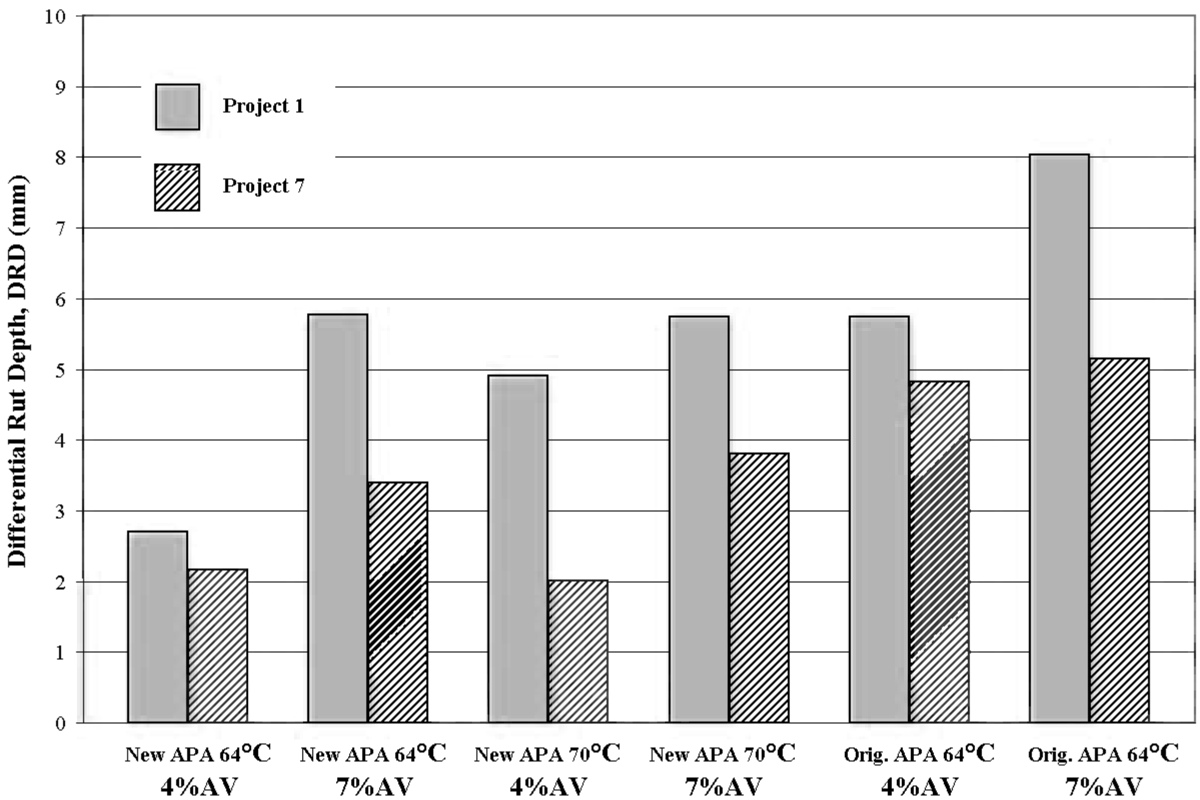

FIG. 14—*Differential rut depth measurements for Project 1 and 7 tested with the two loading devices at 4 % and 7 % air void content.*

Rut-Depth Findings

The key rut-depth findings are the following:

- Based on absolute rut depth measurements at 4 %AV, none of the tests were able to distinguish the better performing mixture between Project 1 and Project 7.
- Absolute rut depth results at 7 %AV for all test methods – new APA 64°C, new APA 70°C, and the original APA – showed that Project 7 performed better.
- The differential rut depth measurements at 4 %AV did not show any difference in the results at 64°C (original and new APA). There was, however, difference in the DRD

results for the new APA 70°C.
- All test methods showed a difference for the DRD at 7 %AV.

Results from the two Superpave™ projects tested at 7 %AV showed that the new and original APA test methods were able to differentiate the two mixtures according to their field performance. The issue, however, is whether the performance prediction based on rut depth measurement is adequate to describe the mixture's ability to resist permanent deformation. It is known that resistance to consolidation is not necessarily related to resistance to shear instability. Tests performed at 7 %AV cannot conclusively determine whether the mixture is failing primarily due to instability or because of excessive consolidation. The same mixture that fails at 7 %AV might demonstrate adequate performance at a higher density level.

At 4 %AV, it is easy to assume that most of the measured rutting will be associated with instability. However, rut depth results at 4 %AV from the new and original APA at 64°C did not distinguish between the mixtures. Thus, there is a need to identify a measure or a parameter that is uniquely associated with mixture shear instability.

Area Change

As discussed earlier, calculating the area change between the initial and final surface profiles enables us to determine the predominant mode of permanent deformation – consolidation or instability – of HMA mixture. The failure mode is primarily consolidation if A_i is less than A_f (negative percent area change), whereas the failure mode is considered to be primarily consolidation if A_f is less than A_i (positive percent change).

Field observations, reported from the Superpave™ monitoring project, show that Project 1 is experiencing higher rutting than Project 7 and that the failure mode for the Project 1 rutted sections appears to be instability [19]. Figure 15 shows the percent area change for the two mixtures, at 4 %AV and 7 %AV, calculated for the new and original APA test methods. All three methods – new APA 64°C, new APA 70°C, and the original APA – predicted positive area change (instability) for Project 1 and negative area change (consolidation) for Project 7.

Discussion

The rut-depth findings showed that both devices were able to distinguish between the two mixtures according to their field performance. However, rut depth by itself is not adequate to determine whether the measured deformation is primarily due to consolidation or because of shear instability. The introduction of the area-change parameter provided a tool to quantify consolidation and shear instability.

Both loading devices were able to show the difference in the mode of failure (permanent deformation) for the two mixtures. Project 1 had a positive area change – primarily instability – and Project 7 had a negative area change – primarily consolidation. The two loading devices were able to distinguish between the two mixtures for resistance to shear instability even though the stress distributions under the two loading mechanisms were found to be very different. The loading strip was designed and constructed to simulate stresses – in particular the lateral stresses – found under a radial-tire rib. These lateral stresses were found to be a key factor in the mechanism of instability rutting.

Even though the measured stresses under the pressurized hose did not show the presence of lateral stresses, the hose was still able to determine that Project 1 failed primarily due to shear instability. The reason behind this phenomenon is the continuously-changing contact area between the hose and the HMA sample. At the beginning of the test, the contact area between the hose and the specimen was measured to be approximately 6–8 mm. Figure 16 shows the initial contact area at the hose-specimen interface. At this stage the stresses induced at the hose-specimen interface are primarily vertical stresses.

As the test progresses and the specimen consolidates under the vertical stress, the hose "sinks" into the specimen, and the contact area increases. Figure 16 shows a hypothetical contact area at some point beyond 4000 cycles. At this point, the specimen is experiencing high shear stresses from the walls of the pressurized hose.

Findings from this study showed that both loading devices – loading strip and pressurized hose – were able to distinguish the better performing mixture based on the area-change calculation. However, the mechanism that drives the material to instability failure is different for each loading device. Measurements showed that the loading strip induces lateral stresses on the surface of the specimen at the beginning of the test that remain constant throughout – since the contact area remains the same. In contrast, the pressurized hose does not induce these critical stress states (lateral stresses) until after the specimen is consolidated. Thus, for a material that has good resistance to consolidation, the pressurized hose would be less successful in evaluating the mixture's ability to resist shear instability. Likewise, for a material that has poor resistance to consolidation, the pressurized hose could "sink-in" and induce high shear stresses that could lead to the misinterpretation of the mixture's shear strength.

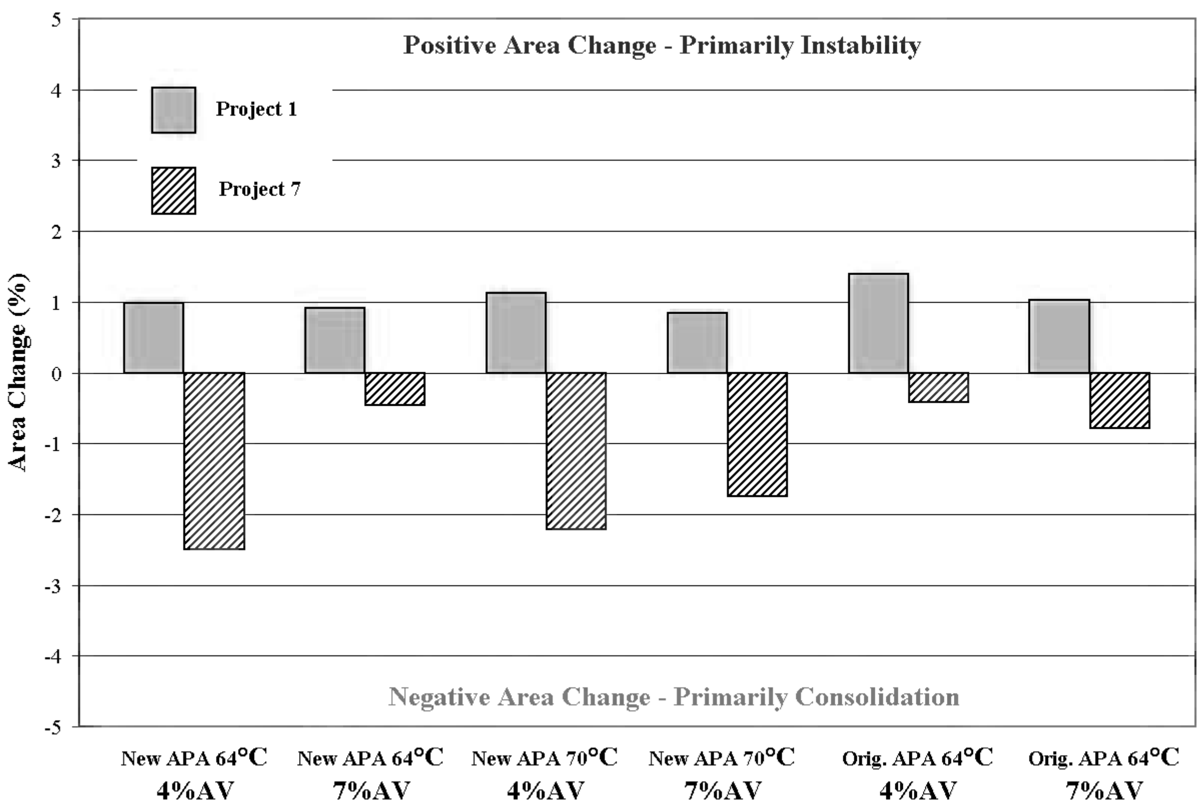

FIG. 15—*Area change measurements for Project 1 and 7 tested with the two loading devices at 4 % and 7 % air void content.*

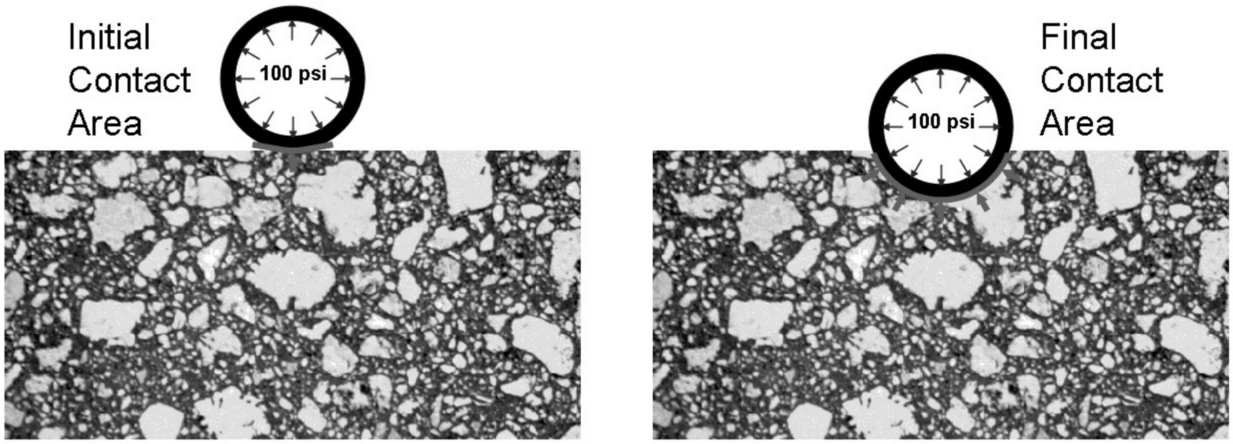

FIG. 16—*Schematic of the initial and final hose-specimen contact area.*

Conclusions and Recommendations

The following conclusions were drawn from this study:

- The new system (loading strip and profile measurement method) appears to have greater potential of evaluating a mixture's potential for instability rutting than the original (hose and single rut-depth measurement) configuration.
- It is possible to conduct more reliable interpretation of the original APA (pressurized hose) results by using the new system of measuring the entire surface profile of the specimen.
- The loading strip appears to be a better system in engineering terms, but the APA pressurized hose is more practical and widely available.

The following recommendations are based on the findings and conclusions from this study:

- The new data-measurement method should be implemented immediately with the existing equipment.
- Whenever possible, specimens should be tested at both 7 %AV and 4 %AV when evaluating the mixture's ability to resist instability rutting.
- At this point there is not enough evidence to support a move to higher temperature testing for a single-condition test (specimen tested at one temperature).

References

[1] Leahy, R. B., Harrigan, E. T., and Von Quintus, H., "Validation of Relationships Between Specification Properties and Performance," Report No. SHRP-A-409, Transportation Research Board, National Research Council, Washington, DC, 1994.
[2] Cooley, A. L., Kandhal P. S., and Buchanan S. M., "Loaded Wheel Testers in the United States: State of Practice," Transportation Research Circular, Number E-C016, July 2000, ISSN00978515.
[3] Federal Highway Administration, SUPERPAVE™ Support and Performance Models Management, "Preliminary Recommendations for the Simple Performance Test," FHWA

No. DTFH 61-94-R-00045, Research Report to the U.S. Department of Transportation, University of Maryland, College Park, MD, May 1998.

[4] Epps, J., Monismith, C. L., Seeds, S. B., Ashmore, S. C., and Mitchell, T. M., "WesTrack Full-Scale Test Track: Interim Findings," International Symposium on Asphalt Pavements (ISAP), August 1997, http://www.westrack.com/wt_04.htm, last accessed on 2/5/2003.

[5] Williams, R. C. and Prowell B. D., "Comparison of Laboratory Wheel-Tracking Test Results with WesTrack Performance," Transportation Research Record No. 1681, Transportation Research Board, Washington, DC, 1999, pp. 121–128.

[6] Kandhal, P. S. and Mallick R. B., "Evaluation of Asphalt Pavement Analyzer for HMA Design," Report No. 99-4, National Center for Asphalt Technology, June 1999.

[7] Romero, P. and Stuart K., "Evaluating Accelerated Rut Testers," Public Roads, Federal Highway Administration, U.S. Department of Transportation, Vol. 62, No. 1, July/August 1998, p. 50.

[8] Lai, J. S. and Lee, T. M., "Use of a Loaded-Wheel Testing Machine to Evaluate Rutting of Asphalt Mixes," Transportation Research Record No. 1269, Transportation Research Board, Washington, DC, 1990, pp. 115–184.

[9] De Beer, M., Fisher, C., and Jooste, F., "Determination of Pneumatic Tyre/Pavement Interface Contact Stresses Under Moving Loads and Some Effects on Pavements With Thin Asphalt Surfacing Layers," Proceedings of the Eighth International Conference on Asphalt Pavements, Seattle, Washington, 1997, pp. 179–226.

[10] Myers, L., Roque, R., Ruth, B., and Drakos, C., "Measurement of Contact Stresses for Different Truck Tire Types to Evaluate Their Influence on Near-Surface Cracking and Rutting," Transportation Research Record No. 1655, Transportation Research Board, Washington, DC, 1999, pp. 175–184.

[11] Drakos, C., Roque, R., and Birgisson, B., "Effects of Measured Tire Contact Stresses on Near Surface Rutting," Transportation Research Record No. 1764, Transportation Research Board, Washington, DC, 2001, pp. 59–69.

[12] Birgisson, B., Roque, R., Drakos, C., Novak, M., and Ruth, B., "Mechanisms of Instability Rutting in Hot Mix Asphalt Pavements," Canadian Technical Asphalt Association, Calgary, Canada, 2002.

[13] Roque, R., Myers, L. A., and Birgisson, B., "Evaluation of Measured Tire Contact Stresses for the Prediction of Pavement Response and Performance," Transportation Research Record No. 1716, Transportation Research Board, Washington, DC, 2000, pp. 73–81.

[14] Marshek, K. M., Chen, H. H., Conell, R .B., and Saraf, C. L., "Effect of Truck Tire Inflation Pressure and Axle Load on Flexible and Rigid Pavement Performance," Transportation Research Record No. 1070, Transportation Research Board, Washington, D.C., 1986, pp. 14–21.

[15] Cook, R., *Finite Element Modeling For Stress Analysis*, John Wiley and Sons, Inc., New York, 1995.

[16] Asiamah, S., "Relationship Between Laboratory Mix Properties and Rutting Resistance for Superpave Mixtures," Master's thesis, University of Florida, Gainesville, 2002.

[17] Cleveland, W. S., "Robust Locally Weighted Regression and Smoothing Scatterplots," *Journal of the American Statistical Association*, Vol. 74, 1979, pp. 829–836.

[18] Kandhal, P. S., and Cooley, Jr., L. A., "Evaluation of Permanent Deformation of Asphalt Mixtures Using Loaded Wheel Tester," Report No. 2002-08, National Center for Asphalt Technology, October 2002.

[19] Roque, R. and Villiers C., "Progress Report No.9: Comprehensive Monitoring of Field Performance of Superpave Project," UF Project No.: 49104504704-12, Department of Civil and Coastal Engineering, University of Florida, Gainesville, June 2003.

Journal of ASTM International, September 2005, Vol. 2, No. 8
Paper ID JAI12263
Available online at www.astm.org

Jaeseung Kim,[1] *Reynaldo Roque,*[1] *and Bjorn Birgisson*[1]

Obtaining Creep Compliance Parameters Accurately from Static or Cyclic Creep Tests

ABSTRACT: Obtaining creep compliance parameters that accurately represent the creep response of asphalt mixtures is critical for proper evaluation of the thermal cracking performance, as well as load induced cracking performance of asphalt pavements. A power law, which uses three parameters to describe the creep compliance curve, is commonly used for asphalt mixtures. However, the specific values of the parameters obtained can depend on both the testing and the data interpretation methods used. Different testing methods (for example, static versus cyclic creep) offer different advantages and disadvantages related to complexity in testing, as well as in the sensitivity of the data obtained from each test to the compliance parameters of interest. In general, cyclic creep tests provide greater sensitivity and accuracy at shorter loading times, while static creep tests are more accurate and reliable for the determination of the long-term creep response.

KEYWORDS: complex modulus, creep compliance, indirect tension test

Introduction

Background

Creep compliance is a fundamental property that describes the relationship between the time dependent strain and applied stress in viscoelastic materials. Accurate determination and representation of the creep compliance of asphalt mixture are essential to evaluate both the thermal and load induced cracking performance of pavements. It is well known that creep compliance directly controls the magnitude of thermal stress development in pavements subjected to given environmental conditions. More recently, it has been determined that the rate of load induced micro damage development in asphalt mixture is directly related to the amount of dissipated creep strain energy induced by applied load stresses. Although creep compliance includes elastic and delayed elastic as well as dissipated creep (viscous) response, it is possible to theoretically isolate these responses by using a function that accurately describes the creep compliance and whose parameters meaningfully represent the different types of responses. A power law function, which uses three parameters to describe the creep compliance curve, has been used successfully in this regard. However, the specific values of the parameters obtained can depend on both the testing and the data interpretation methods used to determine the function parameters. This may lead to errors in predicting the relative amount of elastic, delayed elastic, and dissipated creep response of mixtures subjected to load or temperature changes, which in turn leads to erroneous evaluation of cracking performance.

Manuscript received 30 April 2004; accepted for publication 4 March 2005; published September 2005. Presented at ASTM Symposium on Performance of Hot Mix Asphalt (HMA), including Fundamental and Empirical Procedures on 9 December 2003 in Tampa, FL.
[1] Graduate Research Assistant, Professor, and Associate Professor, respectively, Department of Civil and Coastal Engineering, University of Florida.

Consequently, there is a need to evaluate the effects of testing and data interpretation methods on the determination of creep compliance power law parameters. More specifically, it would be useful to identify and standardize testing and data interpretation methods to determine creep compliance parameters consistently and accurately from mechanical tests typically performed on asphalt mixture. Determination of parameters associated with the tensile response of asphalt mixtures at intermediate temperatures (0–20°C) are of particular interest since load induced micro damage and fracture are generally considered to be tensile failure mechanisms that predominantly occur in the intermediate temperature range.

Objectives

The overall objective of this study was to identify, evaluate, and standardize testing and data interpretation methods to determine tensile creep compliance power law parameters consistently and accurately from mechanical tests typically performed on asphalt mixture at intermediate temperatures (0–20°C). Creep compliance can be determined from either static creep tests or from cyclic tests performed at multiple loading frequencies. Static creep tests using the Superpave indirect tensile test (IDT) have been used successfully to determine tensile creep compliance master curves at low temperatures (< 0°C) to predict thermal cracking performance of asphalt pavement using models developed during the SHRP program. These models are currently being incorporated into the latest version of the AASHTO design guide for asphalt pavement structures. More recent work by Roque has shown that the Superpave IDT can also be used to accurately determine tensile properties of asphalt mixtures, including creep compliance, at intermediate temperatures. However, the greater degree of time dependent response exhibited by asphalt mixture at intermediate temperatures poses some new challenges in terms of accurately isolating elastic, delayed elastic, and viscous response.

Complex modulus and phase angle values determined from cyclic tests performed at multiple frequencies can be related theoretically to the creep compliance of the mixture. Determination of creep compliance from complex modulus tests offers several potential advantages over static creep tests, including better definition of creep compliance at shorter load times, as well as the potential of being able to define the creep compliance function from tests requiring significantly less time. Unfortunately, testing procedures had not been developed for complex modulus testing of asphalt mixture using indirect tension at the time of this study.

Therefore, the specific objectives of the study were as follows:

- To identify or establish suitable testing methods, as well as data acquisition and data reduction procedures to obtain complex modulus and phase angle values from cyclic load tests performed at multiple loading frequencies using the Superpave IDT.
- To develop the appropriate analytical procedures to convert complex modulus and phase angle values at multiple frequencies to creep compliance power law parameters.
- To perform static creep tests and cyclic tests at multiple loading frequencies on several asphalt mixtures in the intermediate temperature range using the Superpave IDT.
- To evaluate the effects of testing and data interpretation methods on the determination of creep compliance power law parameters from both static and cyclic tests.
- Based on the evaluation, to identify appropriate testing and data interpretation methods to determine tensile creep compliance power law parameters consistently and accurately

from mechanical tests typically performed on asphalt mixture.

Scope

The study involved six dense-graded mixtures obtained from pavements in Florida. Nine 6-in. diameter cores were obtained from each of the six pavement sections that were part of a larger study to investigate top-down cracking performance of pavements in Florida.

Two-in. thick slices were taken from each core for Superpave IDT testing. A total of 54 specimens from the six sections was tested at each of three test temperatures: 0°, 10°, and 20°C. Complex modulus test were performed at five testing frequencies: 0.33, 0.5, 1.0, 4.0, and 8.0 hz, and also static creep compliance tests were performed on the same specimens.

Overview of Tests for Viscoelastic Response

Creep Compliance Test

A typical creep compliance test on asphalt mixture is commonly performed using a static constant load. Creep compliance is simply obtained as the time-dependent strain divided by the constant stress. The creep compliance test using the Superpave IDT [1,3,13] was used as the reference test for comparison to the creep compliance from complex modulus tests using the Superpave IDT.

Complex Modulus Test

Complex modulus tests have been performed mainly using unconfined uniaxial compression tests. The standard test procedure is described in ASTM D 3497, which recommends three test temperatures (41, 77, and 104°F) and three loading frequencies (1, 4, and 16 Hz). Sinusoidal loads are applied without rest periods for a period of 30–45 s starting at the lowest temperature and highest frequency, and proceeding to the highest temperature and the lowest frequency. The complex modulus test is based on principles of linear viscoelasticity. Therefore, the test should be performed at small strain levels where principles of stress and strain superposition are thought to apply for asphalt mixtures. Witczak et al. [15] recommended a cyclic strain amplitude of between 75 and 200 micro strain, depending on temperature, for complex modulus tests performed in uniaxial compression. Damage accumulated during cyclic testing can also have a negative effect on complex modulus test results. Kim et al. [8] conducted tests at multiple frequencies, temperatures, and test durations to evaluate the effect of accumulated strain on complex modulus. They recommended a maximum of 70 micro strain to relieve the effects of accumulated strain in compression test.

The following equations, which are based on the theory of linear visco-elasticity, can be used to obtain creep compliance from complex modulus tests performed at multiple frequencies:

$$D(t) = \frac{2}{\pi}\int_0^\infty \frac{D'(\omega)}{\omega} \cdot \sin(\omega t) \cdot d\omega \quad (1)$$

$$D(t) = \frac{2}{\pi}\int_0^\infty \frac{D''(\omega)}{\omega} \cdot \cos(\omega t) \cdot d\omega \quad (2)$$

$$D'(\omega) = \frac{1}{|E^*|} \cdot \cos(\phi) \quad (3)$$

$$D''(\omega) = \frac{1}{|E^*|} \cdot \sin(\phi) \tag{4}$$

where D(t) = static creep compliance, |E*| = dynamic modulus, ϕ = phase angle, ϖ = frequency, and t = time.

Meanwhile, general viscoelastic books had introduced for the way to convert the complex modulus aided by to the creep compliance (Eqs 1–4). These equations, which were theoretically derived using the appropriate Laplace and Fourier transformations, indicate that creep compliances from static and cyclic load tests will be the same if the frequency and time domains are matched for the different modes of testing. Direct comparisons between creep compliance from static and dynamic tests have not been widely reported, especially for asphalt mixture. Zhang et al. [16] showed a generally good correlation between creep compliance of asphalt mixture from static and cyclic loading using the indirect tension test (IDT). The tests were performed over wide frequency ranges: 0.03, 0.1, 0.5, 1, 5, 10, 20, 30, 40, 50, and 60 hz at room temperature.

Indirect Tension Test (IDT) for Complex Modulus

Complex modulus tests using IDT also have been very limited. Buttlar and Roque [3] and Roque et al. [13] developed testing procedures and data reduction methods to obtain the following properties from the Superpave IDT: resilient modulus, creep compliance, tensile strength, and strain and fracture energy to failure. Kim [9] used the Superpave IDT to perform tensile complex modulus tests on asphalt mixtures at the University of Florida. He extended the test methods and data reduction procedures developed by Buttlar and Roque [3] and Roque et al. [13] to obtain dynamic modulus and phase angle from Superpave IDT tests. The tests were performed at room temperature for 1000 loading cycles on one mixture at four frequencies: 0.33, 1.0, 4.0, and 8.0 Hz. Kim observed significant changes in complex modulus during the first 20–30 cycles of loading, after which the results stabilized. For all frequencies evaluated, the dynamic modulus remained constant between 100 and 1000 cycles of loading, which indicates that a certain number of cycles must be applied before steady state conditions are reached.

Material and Methods

Materials

Six dense-graded mixtures were tested. Nine test specimens were obtained for each mixture from field cores taken from test sections associated with the evaluation of top-down cracking in Florida. Four test sections were from I-75: two in Charlotte County and two in Lee County. The other two sections were from SR 80 located in Lee County in southwest Florida. A total of 54 field specimens was prepared for the Superpave IDT. In addition, extraction and binder recovery was performed to determine binder and mixture properties. The averages of extracted binder and mixture properties obtained from the same specimens are presented in Table 1, and mixture gradations are shown in Fig. 1.

Testing Equipment

The basics of the test equipment and data acquisition system have been specified by Buttlar and Roque [3], Roque et al. [13], and AASHTO TP-9 [1]. Additional information on the specific testing system used in this study is as follows:

- An environmental chamber was used to control specimen temperature. The chamber is capable of maintaining temperatures between –30°C and 30°C with an accuracy of +0.1°C.
- The load control and data acquisition system used was accomplished with the MTS Teststar IIm system. A data acquisition program was written specifically for complex modulus tests.
- Vertical and horizontal deformation measurements were obtained using extensometers designed by MTS specifically for use with the Superpave IDT. A gage length of 1.5 in. was used for all specimens.

TABLE 1—*Material properties.*

Name	Air Void (%)	Gmb	Gmm	Effective AC (%)	Viscosity at 60°C (Poise)
I75-1U	2.53	2.242	2.369	4.92	7773
I75-1C	4.13	2.274	2.349	4.83	10844
I75-2U	5.32	2.241	2.386	3.90	12001
I75-3C	5.81	2.190	2.380	4.41	13812
SR 80-2U	6.13	2.213	2.338	3.84	64408
SR 80-1C	4.24	2.197	2.359	4.32	34635

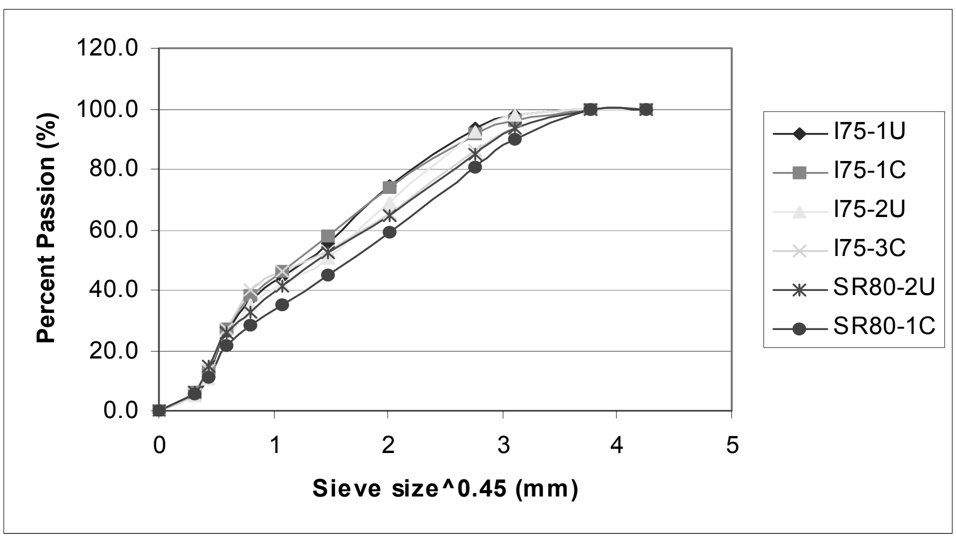

FIG. 1—*Gradation.*

Testing Procedure

Static Tests

Resilient modulus, complex modulus, creep compliance, and strength tests were performed on the same specimens using the Superpave IDT. A total of 54 specimens from six mixtures was tested at three temperatures: 0, 10, and 20°C. Specific testing procedures for the resilient modulus, creep compliance, and strength tests were specified by Roque and Buttlar [11], Buttlar and Roque [3], and Roque et al. [13].

Dynamic Tests Using Superpave IDT

A continuous sinusoidal load was applied to the specimen. The load was selected to maintain a horizontal strain amplitude of between 35 and 65 micro-strain. It was determined that the relative ratios between noise and true signal measured by the extensometers resulted in insignificant errors related to data interpretation within this strain range. Since prior work by Kim [9] showed the dynamic modulus values did not change between 100 and 1000 load cycles, testing was limited to 100 load cycles. This reduced the potential for micro-damage to affect the test results due to accumulated creep strain. In fact, the accumulated creep strain at the end of testing, for tests performed at all temperatures and loading frequencies, was limited to between 65 and 130 micro strain. This is well below the maximum recommended strain to stay within the linear viscoelastic limit of asphalt mixtures, which was conservatively determined to be in the order of 500 micro strain in earlier work performed with the Superpave IDT [3]. In addition, a 10-min rest period was allowed between tests to further minimize the potential effect of accumulated creep strain.

Test specimens were obtained from 6-in. diameter field cores from which 1-in. thick slices were taken using a water-cooled masonry saw that produces smooth and parallel faces. Three specimens were tested at each of three test temperatures for each mixture. Each specimen was tested at the following five frequencies: 0.33, 0.5, 1.0, 4.0, and 8.0 Hz. In all cases, the highest frequency test was performed first as recommended by ASTM D 3497. Additional details on the testing procedures used are as follows:

- After cutting, all specimens were allowed to dry in a constant humidity chamber for a period of two days.
- Four brass gage points (5/16-in. diameter by 1/8-in. thick) were affixed with epoxy to each specimen face.
- Extensometers were mounted on the specimen. Horizontal and vertical deformations were measured on each side of the specimen.
- The test specimen was placed into the load frame. A seating load of 8–15 lb was applied to the test specimen to ensure proper contact of the loading heads.
- The specimen was loaded by applying a repeated and continuous sinusoidal load, where strain amplitude was adjusted between 35 and 65 micro strain.
- When the applied load was determined, 100 total cycles were applied to the specimen, and the computer software recorded the test data.
- As mentioned earlier, a 10-min rest period was allowed between tests at different frequencies.

Development of Data Analysis Procedure

Creep Compliance Test

The aim of this study was to compare creep compliance obtained from static and cyclic load tests. An additional goal was to compare the power law parameters resulting from compliances obtained from each mode of loading. The following power law relationship was used to represent the time dependent creep compliance:

$$D(t) = D_0+D_1t^m$$

Since tests were performed at three temperatures, a single set of power law parameters was determined by fitting a master compliance curve obtained by shifting compliance data obtained at multiple temperatures to a single reference temperature. The procedure described by Buttlar et al. [4] was used to generate the power model for the master curve. Consequently, master curves were developed for each of the six mixtures tested.

Complex Modulus Test

Data Fitting Algorithm—A data analysis system was developed for determination of complex modulus from the Superpave IDT. The following equations were used to obtain the deformation amplitude and phase angle from measured sinusoidal load and deformation response:

$$\begin{aligned} g(t) &= X_1 \cdot \sin(\omega \cdot t + \phi_1) \\ &= X_1 \cdot \cos(\phi_1) \cdot \sin(\omega \cdot t) + X_1 \cdot \sin(\phi_1) \cdot \cos(\omega \cdot t) \end{aligned} \tag{5}$$

$$\begin{aligned} f(t) &= X_2 \cdot \sin(\omega \cdot t + \phi_2) + a \cdot t + b \\ &= X_2 \cdot \cos(\phi_2) \cdot \sin(\omega \cdot t) + X_2 \cdot \sin(\phi_2) \cdot \cos(\omega \cdot t) + a \cdot t + b \end{aligned} \tag{6}$$

$$g(t) = A_1 \cdot \sin(\omega \cdot t) + B_1 \cdot \cos(\omega \cdot t) \tag{7}$$

$$f(t) = A_2 \cdot \sin(\omega \cdot t) + B_2 \cdot \cos(\omega \cdot t) + a \cdot t + b \tag{8}$$

$$\phi = \tan^{-1}\left(\frac{B_2}{A_2}\right) - \tan^{-1}\left(\frac{B_1}{A_1}\right) \tag{9}$$

$$X_1 = \sqrt{A_1^{\,2} + B_1^{\,2}} \tag{10}$$

$$X_2 = \sqrt{A_2^{\,2} + B_2^{\,2}} \tag{11}$$

where $g(t)$ = loading function, $f(t)$ = deformation function, $X1$ = amplitude of deformation, $X2$ = amplitude of load, and a, b, A_1, B_1, A_2, B_2 = regression coefficients.

The loading curve can be represented as a sin curve, which by use of appropriate trigonometric functions, results in the second Eq 5. Similarly, the deformation curve can be assumed as a sin curve with a linear slope, which by a similar process, can be represented by the second Eq 6. Equations 7 and 8, where Xcos(f) and Xsin(f) are simplified by using symbols A and B, which simplifies the regression that must be performed to fit the test data. The regression coefficients are then used to determine phase angle and load and deformation amplitudes using Eqs 9–11.

Complex modulus test data have many irregular data points (noise), so accurate values of phase angle and magnitude cannot be expected from interpretation of just one or two loading cycles. Conversely, the use of too many cycles may induce error from nonlinearity in the deformation curve. It was determined that five loading cycles, recorded immediately before the 100$^{\text{th}}$ loading cycle, resulted in consistent and accurate determination of phase angle and strain amplitude.

Analysis of Superpave IDT Data—The Superpave IDT, which was developed by Roque and Buttlar as part of the strategic highway research program (SHRP), uses two main data analysis principles: true strains must be determined by eliminating the bulging effect that occurs due to the three-dimensional geometry of specimens, and Poisson's ratio must be accurately determined from vertical and horizontal measurements. This basic analysis concept was modified and adopted for use with the complex modulus test. The procedure requires three data sets obtained from three specimens for proper interpretation. The horizontal deformation carries the symbol,

ΔH, while the vertical deformation carries the symbol, ΔV. The horizontal phase angle carries the symbol, ΔPA. Herein, the deformations and phase angle were computed using Eqs 9 and 11. In addition, the following equations are required for proper data interpretation using the Superpave IDT.

- Normalization factors: since different specimens may have different thickness, diameter, or load, the deformations need to be normalized.

$$C_{NORM\,i} = \frac{t_i}{t_{AVG}} \cdot \frac{D_i}{D_{AVG}} \cdot \frac{P_{AVG}}{P_i} \tag{12}$$

$$H_{NORM\,j} = \Delta H_j \cdot C_{NORM\,i} \tag{13}$$

$$V_{NORM\,j} = \Delta V_j \cdot C_{NORM\,i} \tag{14}$$

where: t_i = thickness of each specimen (i = 1~3),
D_i = diameter of each specimen (i = 1~3),
P_i = loading amplitude of each specimen (i = 1~3),
T_{AVG} = average thickness of three specimens,
D_{AVG} = average diameter of three specimens ,
P_{AVG} = average loading amplitude of three specimens ,
ΔH_j = horizontal deformations for three specimens (j = 1~6),
ΔV_j = vertical deformations for three specimens (j = 1~6),
$H_{NORM\,j}$ = normalized horizontal deformations (j = 1~6), and
$V_{NORM\,j}$ = normalized vertical deformations (j = 1~6).

- Trimmed mean deformation and trimmed mean phase angle: the six normalized horizontal and vertical deformations and the six horizontal phase angles from three replicate specimens are ranked. To get the trimmed mean deformation and the trimmed mean phase angle, the highest and lowest deformation and the highest and lowest phase angle are deleted, and then the remaining four deformations and four phase angles are averaged.

$$\Delta H_{TRIM} = \frac{\sum \Delta H_{NORM\,j}}{2n-2} \tag{15}$$

$$\Delta V_{TRIM} = \frac{\sum \Delta V_{NORM\,j}}{2n-2} \tag{16}$$

$$\Delta PA_{TRIM} = \frac{\sum \Delta PA_j}{2n-2} \tag{17}$$

where: n = the number of specimens for each temperature (n = 3),
ΔH_{TRIM} = timed mean horizontal deformation,
ΔV_{TRIM} = timed mean vertical deformation, and
ΔPA_{TRIM} = timed mean horizontal phase angle.

- Poisson's Ratio: Buttlar and Roque [11] developed the following equations to calculate Poisson's ratio from Superpave IDT test data:

$$\nu = -0.100 + 1.480\left(\frac{\Delta H_{TRIM}}{\Delta V_{TRIM}}\right)^2 - 0.778\left(\frac{t_{AVG}}{D_{AVG}}\right)^2 \cdot \left(\frac{\Delta H_{TRIM}}{\Delta V_{TRIM}}\right)^2 \tag{18}$$

where: ν = Poisson's ratio.

- Correction Factors: Buttlar and Roque [3] developed the following equations to account for three-dimensional stress states in diametrically loaded specimen of finite thickness.

$$C_{BX} = 1.030 - 0.189 \cdot \left(\frac{t_{AVG}}{D_{AVG}}\right) - 0.081 \cdot \nu + 0.089 \cdot \left(\frac{t_{AVG}}{D_{AVG}}\right)^2 \tag{19}$$

$$C_{BY} = 0.994 - 0.128 \cdot \nu \tag{20}$$

$$C_{EX} = 1.07 \tag{21}$$

$$C_{EY} = 0.98 \tag{22}$$

$$C_{SX} = 0.9480 - 0.01114 \cdot \left(\frac{t_{AVG}}{D_{AVG}}\right) - 0.2693 \cdot \nu + 1.4360\left(\frac{t_{AVG}}{D_{AVG}}\right) \cdot \nu \tag{23}$$

$$C_{SY} = 0.901 + 0.138 \cdot \nu + 0.287 \cdot \left(\frac{t_{AVG}}{D_{AVG}}\right) - 0.251 \cdot \nu \cdot \left(\frac{t_{AVG}}{D_{AVG}}\right)^2 - 0.264 \cdot \left(\frac{t_{AVG}}{D_{AVG}}\right)^2 \tag{24}$$

- Horizontal Moduli, |E*|, E' and E": The following equations were developed to obtain |E*|, E', and E":

$$\left|E^*\right| = \left(\frac{1}{\frac{\Delta H_{TRIM}}{GL} \cdot C_{BX} \cdot C_{EX}}\right) \cdot \left(\frac{2 \cdot P_{AVG}}{\pi \cdot D_{AVG} \cdot t_{AVG}} \cdot C_{SX} - \nu \cdot \frac{6P_{AVG}}{\pi \cdot D_{AVG} \cdot t_{AVG}} \cdot C_{SY}\right) \tag{25}$$

$$E' = \left|E^*\right| \cdot \cos(\Delta PA_{TRIM}) \tag{26}$$

$$E'' = \left|E^*\right| \cdot \sin(\Delta PA_{TRIM}) \tag{27}$$

where GL = Gage Length, |E*| = dynamic modulus, E' = storage modulus, and E" = loss modulus.

The overall process used to calculate the complex modulus using the Superpave IDT is shown in Fig. 2. Figure 2 also explains basic concepts used in the data analysis program (ITLT_dynamic), which was specifically developed for the complex modulus test using the process described. The program has been thoroughly evaluated using hundreds of trial data sets, and it was found to be accurate, fast, and reliable. All complex modulus test results presented in this study were obtained using this data analysis program.

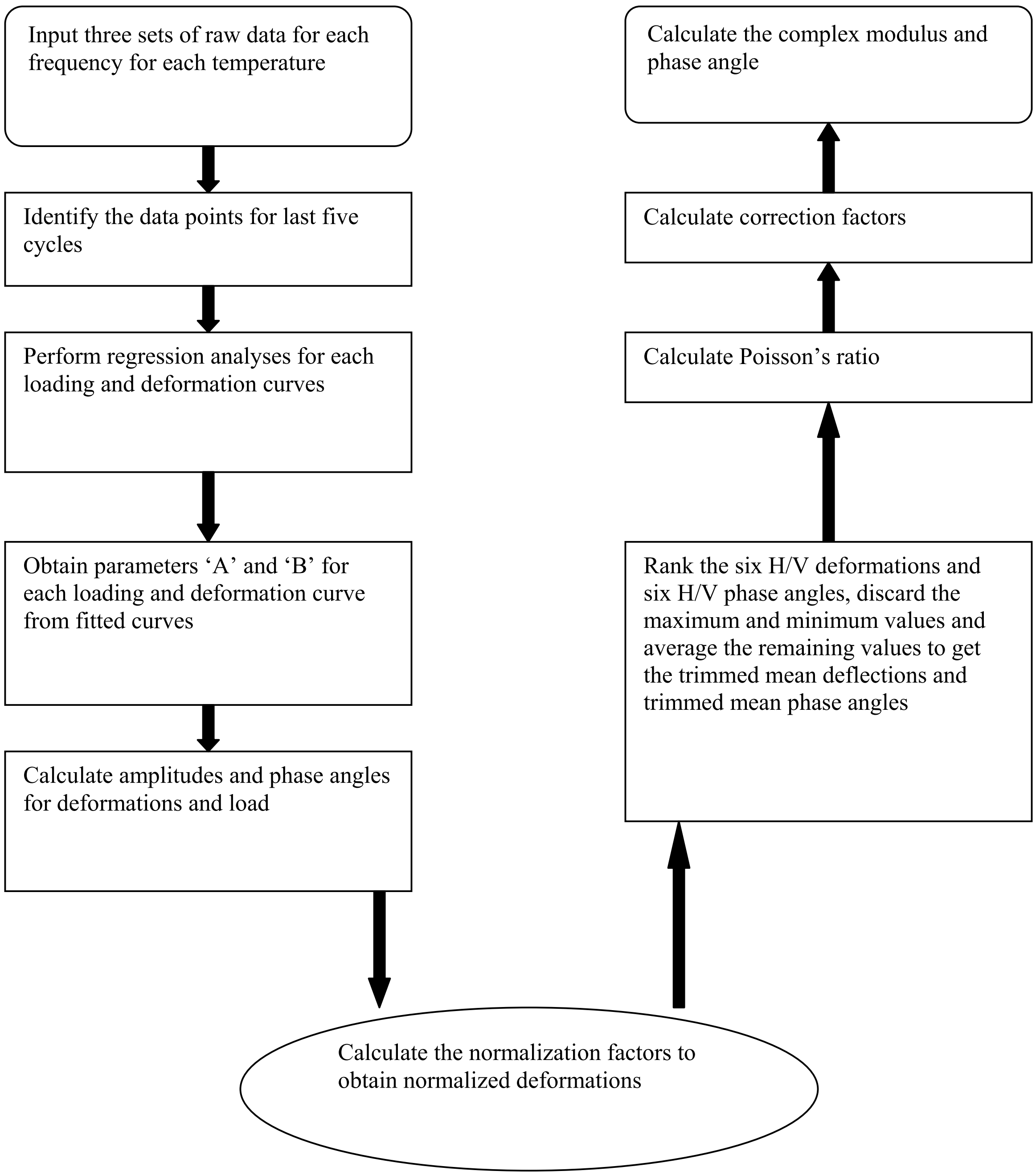

FIG. 2—*Complex modulus data analysis procedure.*

Creep Compliance from Complex Modulus Test

Conversion Process—Creep compliance data are generally expressed using a well-known power function (Eq 28). Equation 29 presents the Fourier Transform version of the power law [6]. This function was developed by Zhang et al. [16] to directly obtain the power model parameters (D_0, D_1, and 'm') from the real part of complex compliance where the following two-step regression algorithm to find the power model parameters (D_0, D_1, and 'm') was used: (a) guess initial unknown 'm' value (i.e., it should be between 0 and 1); and (b) find D_0 and D_1using linear regression (i.e., once the m- value is determined, Eq 29 becomes a linear function having two unknown values). Repeat this process until the guessed 'm' value has least square errors, where x-axis data are time and y-axis data are D'(ϖ) from the complex modulus test.

$$D(t) = D_0 + D_1 \cdot t^m \tag{28}$$

$$D'(\omega) = D_1 \cdot \frac{\Gamma(m+1)}{\omega^m} \cdot \cos(\frac{m \cdot \pi}{2}) + D_0 \tag{29}$$

$$D'(\omega) = \frac{1}{|E^*|} \cdot \cos(\phi) \tag{30}$$

where: D_0,D_1,m: power model parameters,
t: time,
ϖ: frequency,
Γ: Gamma function,
D'(ϖ): the real part of complex compliance,
|E*|: dynamic modulus, and
ϕ: phase angle.

Master Curve—The master curve describes the viscoelastic response of asphaltic materials as a function of time, or frequency, and temperature. Once determined, the master curve allows for the determination of compliance at any temperature and loading time or frequency. This is particularly useful for determination of creep compliance at longer loading times at lower temperatures, which can be determined through the master curve concept by using data obtained from short loading time tests at higher temperatures.

In order to generate a reasonable master curve, the shifting of the master curve needs to be carefully considered to fit the test data properly. One of the most well-known methods to generate the mater curve employs the WLF [14] equation, which has been used successfully to represent the compliance of asphalt binder [5]. The sigmoidal function, which involves a non-linear regression [10,8], has been used successfully to generate master curves for complex moduli from uniaxial or triaxial tests performed over a wide range of temperatures. These researchers recommended the use of the real component of the complex modulus to determine master curves. The IDT is usually performed at relatively low in-service temperatures (below 30°C), so it may be possible to use a simpler and more practical function to generate the master curve for D'(ϖ) (the real part of complex compliance) from complex modulus data. Buttlar et al. [4] developed an approach to construct the creep compliance master curve from Superpave IDT data. The approach involved fitting a second-degree polynomial function to the log compliance - log time data at each temperature in order to minimize the effects of irregular creep compliance data, and to obtain sufficient overlap in data between different temperatures to allow for accurate shifting (i.e., if the creep compliance data do not have sufficient overlap, then it can be extended using the polynomial function obtained). The authors have found that a second-degree polynomial function accurately fits measured compliance data obtained at a single temperature, which is the only time the function is used in the process. The data represented by the polynomial functions are then shifted to obtain shift factors, and a regression analysis is performed to determine the creep compliance power law parameters resulting in the best fit. Buttlar et al. [4] developed a computer program (MASTER) that automatically performs this analysis and generates a master curve. The general approach is presented in Figs. 3–5. The program was used to generate one master curve for D'(ϖ) using the following shifting and fitting regression algorism: (a) define the region 1 and region 2 (Fig. 3), (b) shift curve 2 by using a initial shift factor selected from region 1, (c) shift curve 3 over the region 2 for the shift factor selected from region 1, (d) fit the combined data from curve 1, the shifted curve 2, and the shifted curve 3 as a second-degree polynomial function, and (e) store regression coefficients and least square errors. Go back to the regression process (b), select another shift factor from region 1, and repeat the overall regression process (c–e) until minimum least square errors are achieved. Figure 4 shows a master curve using the shifting and fitting regression algorithm, and Fig. 5 shows shift factors where reference temperature was 0°C.

Overall Procedure to Obtain Creep Compliance from Complex Modulus—The 54 total field samples from six mixtures were tested using the Superpave IDT at three temperatures: 0, 10, and 20°C. The complex modulus test was performed right before the creep compliance test for five frequencies, 0.33, 0.5, 1, 4, and 8 hz. Six master curves were generated from the complex modulus data obtained, and then each master curve was converted to the creep compliance using the conversion procedure described above.

Results

Complex Modulus Test

The complex modulus test was performed with the Superpave IDT on a total of 54 field specimens from six state road sections to evaluate the testing and analysis system developed and described above. Dynamic properties such as |E*|, phase angle, E' and E" were successfully calculated with data analysis program developed (ITLT_dynamic).

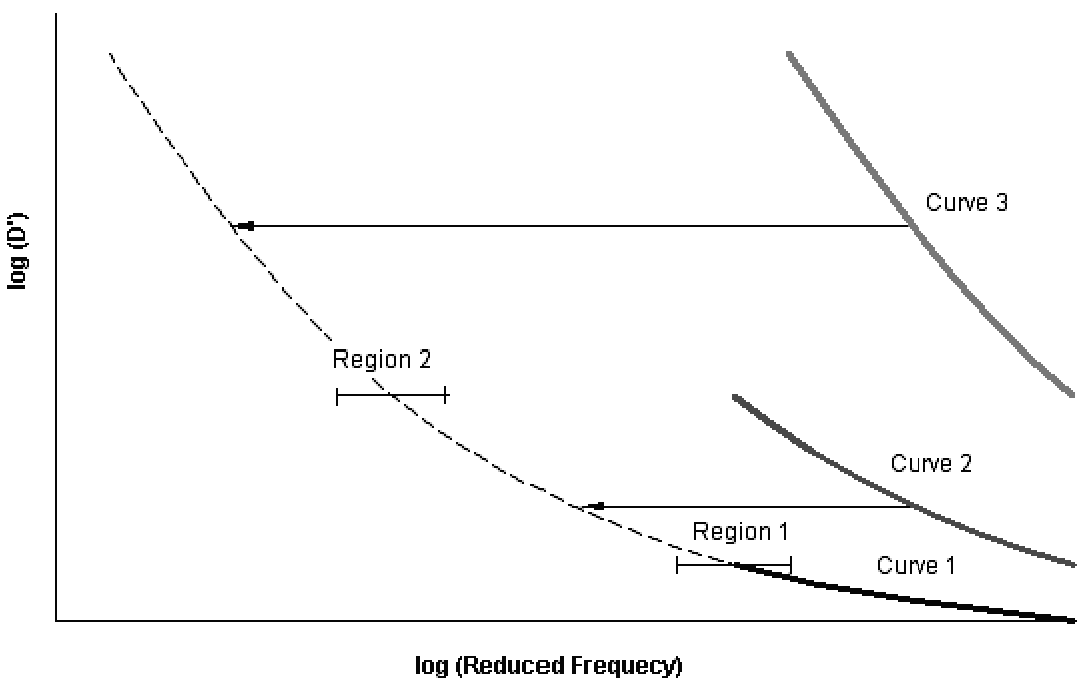

FIG. 3—*Shifting procedure.*

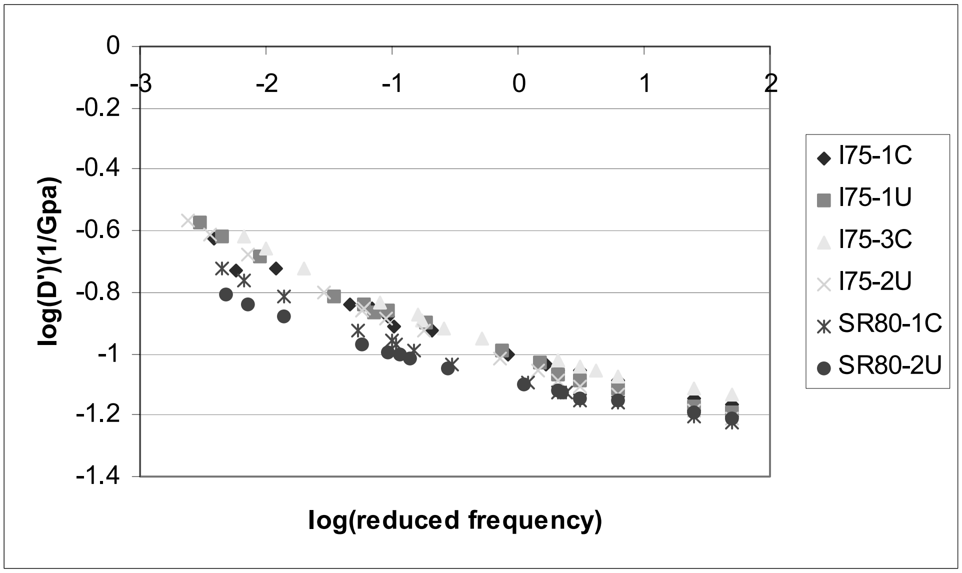

FIG. 4—*Master curve of D'(ϖ).*

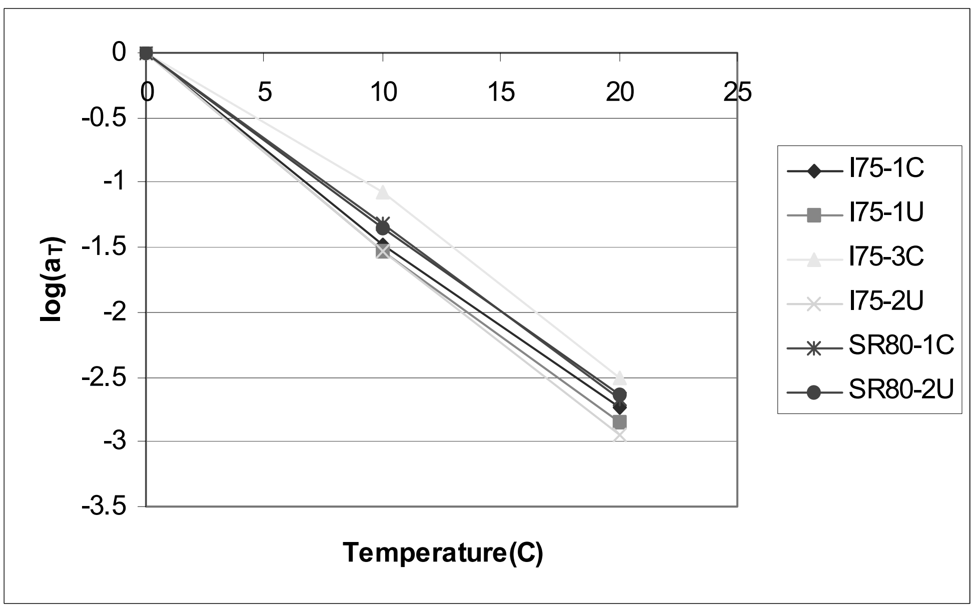

FIG. 5—*Shifting factors.*

Figure 6 shows the relationship between dynamic modulus and phase angle for all mixtures, test temperatures, and frequencies involved this study. In general, the dynamic modulus showed an increasing trend as temperature decreased or frequency increased. Conversely, the phase angles showed a decreasing trend as temperature decreased or frequency increased. These are obviously reasonable and expected trends, since asphalt mixture becomes stiffer and more elastic as test temperature decreases or frequency increases. Conversely, asphalt stiffness decreases and viscous response increases as temperature increases or frequency decreases.

As shown in Table 2, Poisson's ratios determined from complex modulus tests for the range of mixtures, frequencies, and temperatures involved in this study were within the range generally accepted as being reasonable for asphalt mixture. The authors' extensive experience with the

Superpave IDT has indicated that obtaining reasonable values of Poisson's ratio is an excellent indicator of the quality of the test data obtained. This indicates that the complex modulus values obtained from the Superpave IDT are probably also reasonable. However, it should be noted that as in all dynamic testing, the proper application of a sinusoidal loading waveform is also critical.

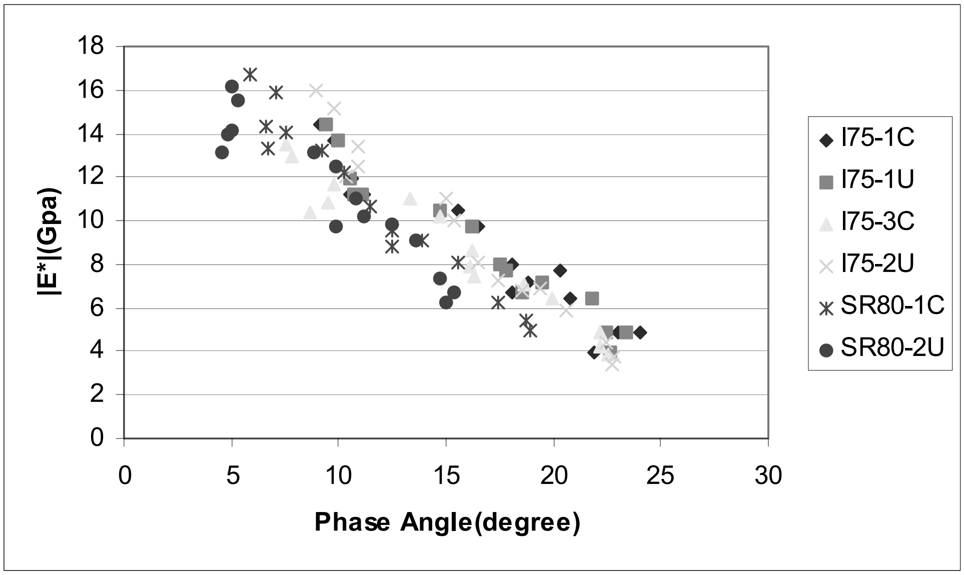

FIG. 6—*Dynamic modulus and phase angle.*

TABLE 2—*Poisson's ratios.*

Temperature (8°C)	Frequencies (hz)	Sections					
		I75-1C	I75-1U	I75-3C	I75-2U	SR80-1C	SR80-2U
		Poisson's Ratio					
0	0.333	0.33	0.35	0.30	0.32	0.36	0.22
	0.5	0.29	0.34	0.30	0.31	0.33	0.23
	1	0.29	0.34	0.30	0.30	0.33	0.23
	4	0.30	0.31	0.33	0.30	0.34	0.25
	8	0.29	0.31	0.30	0.29	0.33	0.25
10	0.333	0.38	0.37	0.42	0.38	0.38	0.31
	0.5	0.40	0.35	0.41	0.37	0.41	0.31
	1	0.37	0.32	0.40	0.35	0.40	0.31
	4	0.37	0.32	0.37	0.35	0.39	0.31
	8	0.34	0.32	0.36	0.35	0.40	0.29
20	0.333	0.44	0.42	0.38	0.38	0.33	0.40
	0.5	0.49	0.41	0.36	0.39	0.33	0.41
	1	0.41	0.41	0.35	0.36	0.33	0.38
	4	0.43	0.39	0.35	0.36	0.35	0.39
	8	0.40	0.39	0.32	0.38	0.35	0.37
Average		0.37	0.37	0.36	0.35	0.35	0.36

Comparison Between Creep Compliances from Static and Cyclic Tests

Based on the regression algorithm using conversion equation (29) discussed earlier, the master curves of D'(ϖ)s from each data set (six sections) were converted to power model parameters (D_0, D_1, and 'm') for comparison with conventional creep compliance parameters from static tests using the Superpave IDT. The creep compliance test was performed based on procedures described by Buttlar and Roque [3], and AASHTO TP-9 [1] for 100-s duration. The same conditions (testing equipment, specimens, and temperatures) were used to limit the potential differences between static and dynamic results.

Table 3 shows that power model parameters from static and dynamic tests were different. Figure 7 illustrates the key differences between the creep compliance relationships as determined from the two different testing modes. In general, the dynamic test data underestimate the long-term creep response, which is reflected in the lower m-value for the dynamic test. Conversely, the static test data appear to overestimate the short-term response, which is reflected in the higher D_0 value for the static test.

TABLE 3—*Power model parameters from two tests.*

Name	Static Creep Test			Cyclic Creep Test		
	D_0 (1/Gpa)	D_1 (1/Gpa)	m	D_0 (1/Gpa)	D_1 (1/Gpa)	m
I75-1C	6.57E-02	2.25E-02	0.454	5.09E-02	5.43E-02	0.237
I75-1U	8.75E-02	2.31E-02	0.490	4.67E-02	5.80E-02	0.256
I75-3C	9.04E-02	1.34E-02	0.531	5.96E-02	5.31E-02	0.285
I75-2U	7.29E-02	1.58E-02	0.479	4.67E-02	5.33E-02	0.268
SR80-1C	6.31E-02	7.30E-03	0.488	4.94E-02	3.84E-02	0.276
SR80-2U	6.57E-02	9.14E-03	0.402	5.05E-02	3.45E-02	0.238

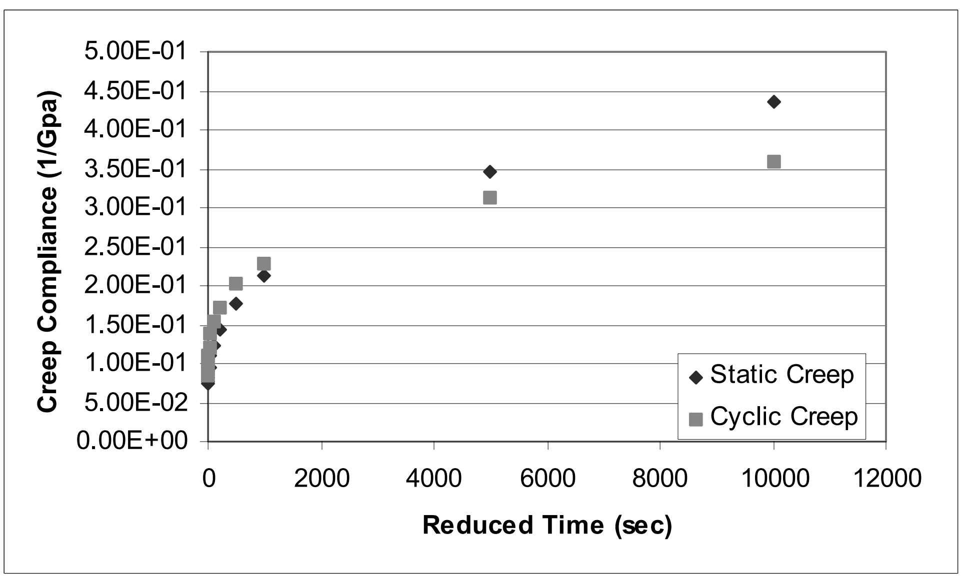

FIG. 7—*General trend of creep compliances.*

Upon further reflection, these results are reasonable and consistent with the sensitivity of each type of test to different response times. Static or constant stress creep tests are generally run for longer time periods, and their static nature makes the determination of the long-term creep response more accurate and reliable. However, it is difficult to accurately apply the load quickly enough in static creep tests to obtain reliable response measurements for definition of short-term response. The reverse is true for dynamic tests, which allow for very accurate application of short-term loads and measurement of associated response, but for which it is very difficult to apply low enough frequencies to obtain reliable response at longer loading times. One would lose the advantage of performing cyclic tests if one were to use frequencies that are low enough to obtain long-term response accurately (i.e., one may as well run a static test, which is simpler and generally more reliable).

Based on the observations presented above, it appears that the power model parameter D_0, which is primarily dependent on the mixture's short-term response, can be more accurately determined from dynamic tests. Conversely, the parameters D_1 and m-value, which are primarily dependent on the mixture's long-term response, can be more accurately determined from static creep tests.

Comparison Between Power Model Parameters from Static and Cyclic Tests

Figures 8–10 compare power model parameters from static and dynamic tests. The parameters D_1 and m-value are important to predict thermal stress or load-induced fatigue cracking in asphalt mixture [17,7]. The comparisons indicate that although the values are quite different, the general trend of the parameters is very similar between the two test methods. In other words, the parameters from one test method are well correlated with those of the other. This implies that either test method would result in similar comparisons between any one of the parameters obtained from two different mixtures. However, prior work by Roque et al. [12] has shown that mixture performance cannot be evaluated properly on the basis of any single parameter. Instead, the effects of the parameters must be considered together in the context of a fracture model that appropriately accounts for their relative effects. Consequently, the magnitude of the parameters, and not just their relative ranking, is also important for proper evaluation. The challenge is to identify an approach to determine accurately the power law parameters using static creep tests, dynamic creep tests, or a combination of both.

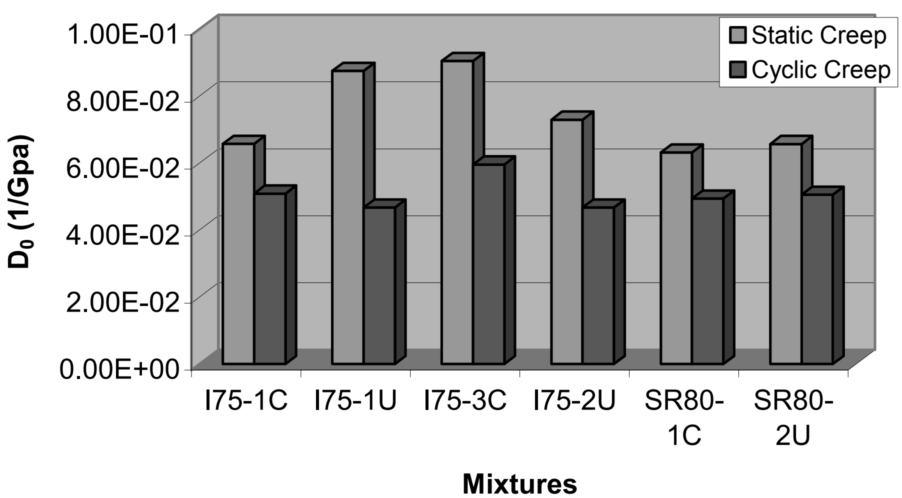

FIG. 8—*Power model parameter, D_0.*

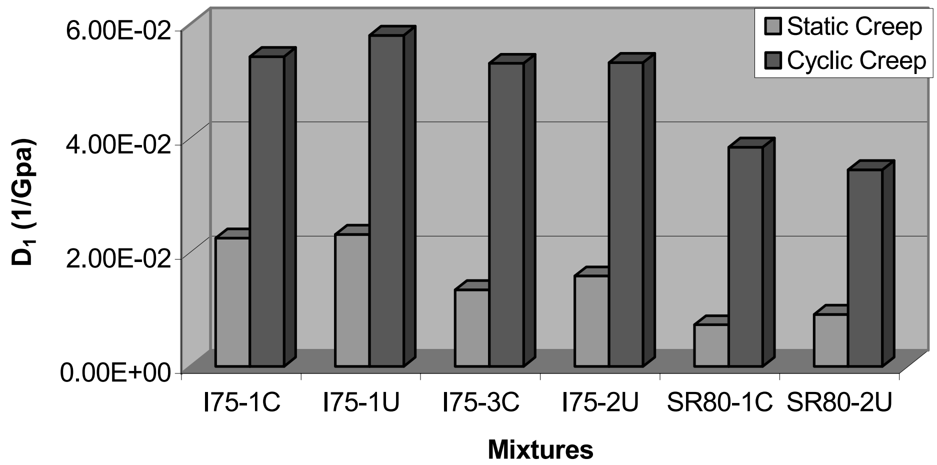

FIG. 9—*Power model parameter,* D_1.

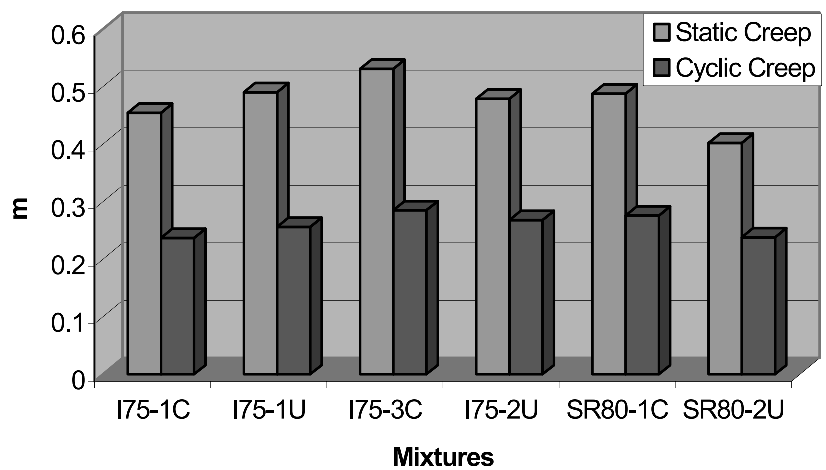

FIG. 10—*Power model parameter, m.*

Obtaining Creep Compliance Accurately and Efficiently

The discussion above indicates that it may be difficult, if not impossible, to obtain long-term creep response accurately from dynamic tests performed in the typical range of frequencies (0.1 Hz or higher), and that it may be difficult or impossible to obtain short-term responses accurately from static creep test data. In other words, static creep tests are better suited for determination of power law parameters D_1 and m-value, whereas D_0 can be obtained more reliably from dynamic tests. The effects can be observed in the simple rheological model presented in Fig. 11, which indicates that D_0 represents the purely elastic or time-independent behavior of the mixture. Consequently, one can isolate this response by performing tests at higher frequencies, such that the time-dependent components do not contribute much to the response of the material. In fact, if one could test at a high enough frequency, approaching the point where the load is applied in zero time (obviously impossible), then one could approach the true D_0 of the material. In practice, an estimate of this value can be obtained by extrapolating dynamic modulus data obtained at different frequencies to predict the dynamic modulus of the material at zero phase angle, which corresponds to the purely elastic behavior of the material. Thus, an accurate estimate of D_0 can be obtained by taking the inverse of the dynamic modulus at zero phase angle (E_0) through extrapolation of the data shown in Fig. 6.

One would expect that the D_0-values obtained in this manner should be very similar to those obtained from interpretation of complex compliance data. Figure 12 shows that for all mixtures tested, the values were almost identical, indicating that D_0-values obtained from dynamic modulus tests appear to be accurate.

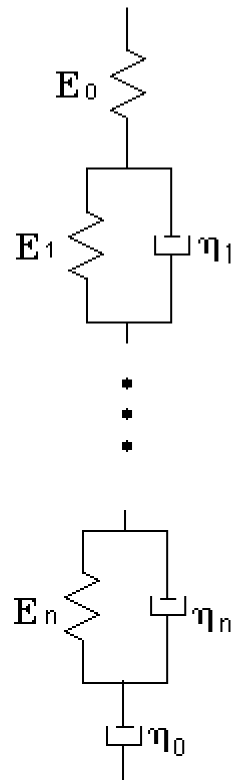

FIG. 11—*Rhelogical viscoelastic model.*

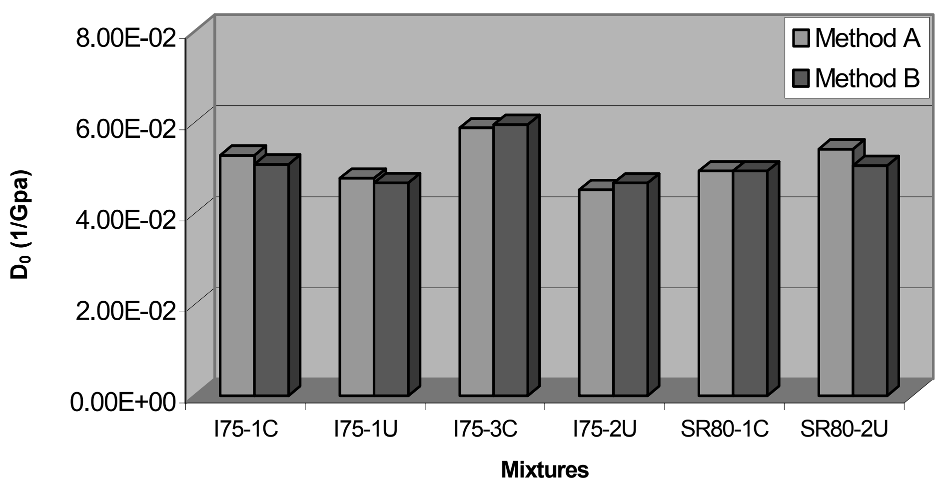

FIG. 12—*Comparison between D_0-values.*

Note that the power model parameters, D_0, D_1, and m-value, determined from creep compliance data are interrelated. Once any of the parameters is changed, the values of the other parameters are inevitably affected. Consequently, the values of D_1 and m-value obtained from static creep tests should be corrected to account for the fact that D_0 determined from the static data alone is inaccurate. A more accurate approach would be to obtain D_0 from dynamic test data, then use the static creep data to determine D_1 and m-value only. Figures 13 and 14 show a comparison of D_1 and m-values determined by these two different approaches (method A is based on static creep data only; method B is based on D_0 from dynamic tests and D_1 and m-value from static creep data). As shown in the figures, method B results in a lower D_1 and slightly higher m-value for all mixtures evaluated.

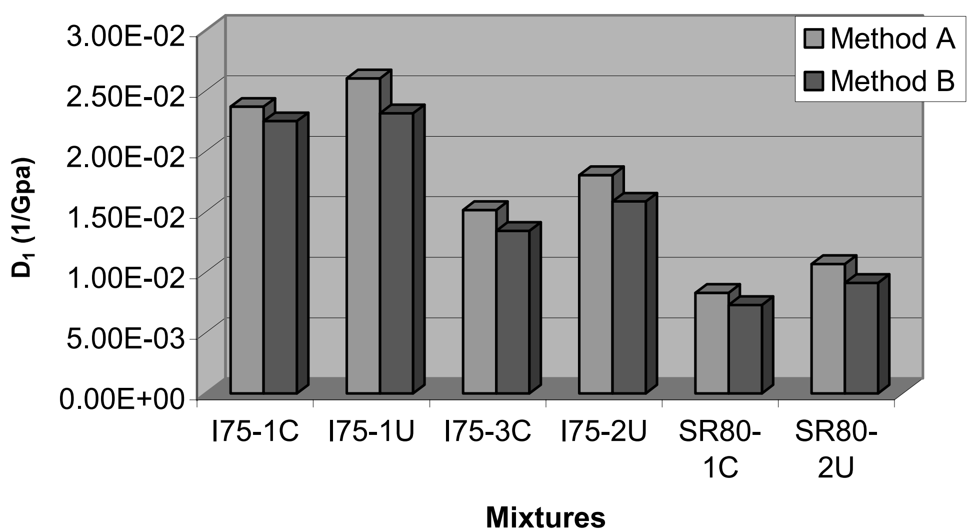

FIG. 13—*Corrected power model parameter, D_1.*

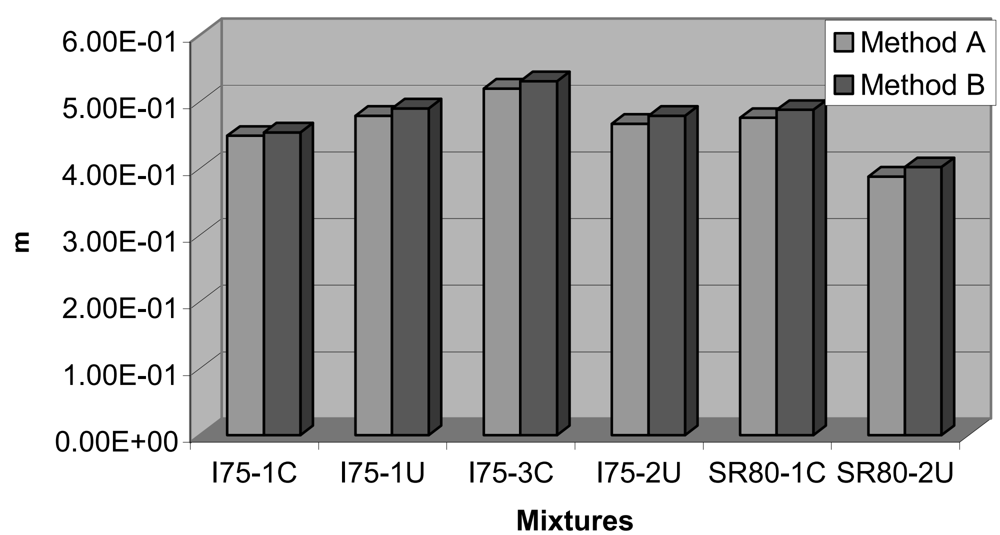

FIG. 14—*Corrected power model parameter, m.*

Summary and Conclusions

Test methods, data acquisition, and data reduction procedures were established for determination of complex modulus and phase angle from cyclic load tests with the Superpave IDT. Tests performed at multiple frequencies on six different asphalt mixtures obtained from field test sections indicated that dynamic modulus and phase angle values were within reasonable and expected ranges and exhibited appropriate trends. Analytical procedures were developed to convert complex modulus and phase angle values at multiple frequencies to creep compliance as a function of time.

Static creep tests were performed on the same mixtures using the Superpave IDT to compare creep compliance and creep compliance power law parameters to those derived from the cyclic test data. Significantly different power law parameters were obtained, and it was determined that static tests resulted in more accurate determination of the parameters that describe the longer-term creep response (D_1 and m-value), while dynamic tests resulted in more accurate determination of D_0, which describes the short-term elastic response.

An approach was developed and proposed to determine creep compliance parameters accurately by combining the results of dynamic and static tests. Cyclic tests performed at a minimum of two loading frequencies are first used to define D_0 as the inverse of the extrapolated dynamic modulus at zero phase angle (E_0). D_1 and m-value are then obtained from the static creep data, using this pre-determined value of D_0.

This work implies that for the normal range of testing frequencies used in laboratory dynamic testing of asphalt mixture, it may not be possible to accurately define the long-term creep response of the mixture. Use of creep data obtained in this fashion may result in serious errors in prediction of dissipated creep strain and damage in asphalt mixture.

References

[1] AASHTO, *AASHTO Provisional Standards*: TP-9, Washington, DC, American Association of State Highway and Transportation Officials, 1996.

[2] ASTM Standard D 3497, *Annual Book of ASTM Standard*s, Vol. 4.20, ASTM International, West Conshohocken, PA, 1997.

[3] Buttlar, W. G. and Roque, R., "Development and Evaluation of the Strategic Highway Research Program Measurement and Analysis System for Indirect Tensile Testing at Low Temperatures," *Transportation Research Record*, No. 1454, 1994, pp. 163–171.

[4] Buttlar, W. G., Roque, R., and Reid, B., "Automated Procedure for Generation of Creep Compliance Master Curve for Asphalt Mixtures," *Transportation Research Record*, No. 1630, 1998, pp. 28–36.

[5] Christensen, D. W. and Anderson, D. A., "Interpretation of Dynamic Mechanical Test Data for Paving Grade Asphalt Cements," *Journal of the Association of Asphalt Paving Technologists*, Vol. 61, 1992, pp. 67–116.

[6] Findley, W. N., Lai, J. S., and Onaran, K., *Creep and Relaxation of Nonlinear Viscoelastic Materials*, New York, Dover Publications, Inc., 1976.

[7] Hiltunen, D. R. and Roque, R., "A Mechanics-Based Prediction Model for Thermal Cracking of Asphaltic Concrete Pavements," *Journal of the Association of Asphalt Paving Technologists*, Vol. 63, 1994, pp. 81–117.

[8] Kim, Y. R., Chehab, G., Schapery, R. A., Witczak, M., and Bonaquist, R., "Time-Temperature Superposition Principle for Asphalt Concrete Mixtures with Growing Damage

in Tension State," *Preprint for Journal of the Association of Asphalt Paving Technologists*, 2002.

[9] Kim, J. S., *Complex Modulus from Indirect Tension Testing*, Master's Thesis, University of Florida, Gainesville, Florida, 2002.

[10] Pellinen, T. K. and Witczak, M. W., "Stress Dependent Master Curve Construction for Dynamic (Complex) Modulus," *Preprint for Journal of the Association of Asphalt Paving Technologists*, 2002.

[11] Roque, R. and Buttlar, W. G., "The Development of a Measurement and Analysis System to Accurately Determine Asphalt Concrete Properties Using the Indirect Tensile Mode," *Journal of the Association of Asphalt Paving Technologists*, Vol. 61, 1992, pp. 304–332.

[12] Roque, R., Birgisson, B., Drakos, C., and Dietrich, B., "Development and Field Evaluation of Energy-Based Criteria for Top-Down Cracking Performance of Hot Mix Asphalt," *Preprint for the 2004 Annual Meeting of Journal of the Association of Asphalt Paving Technologists*, 2004.

[13] Roque, R., Buttlar, W. G., Ruth, B. E., Tia, M., Dickison, S. W., and Reid, B., *Evaluation of SHRP Indirect Tension Tester to Mitigate Cracking in Asphalt Concrete Pavements and Overlays*, FL-DOT-MO-0510755, University of Florida, Gainesville, Florida, 1997.

[14] Williams, M. L., Landel, R. F., and Ferry, J. D., "The Temperature Dependence of Relaxation Mechanisms in Amorphous Polymers and Other Glass-forming Liquids," *The Journal of the American Chemical Society*, Vol. 77, 1955, pp. 3701–3706.

[15] Witczak, M. W., Bonaquist, R., Von Quintus, H., and Kaloush, K. "Specimen Geometry and Aggregate Size Effects in Uniaxial Compression and Constant Height Shear Tests," *Journal of the Association of Asphalt Paving Technologists*, Vol. 70, 2000, pp. 403–441.

[16] Zhang, W., Drescher, A., and Newcomb, D. E., "Viscoelastic Behavior of Asphalt Concrete in Diametral Compression," *Journal of Transportation Engineering*, Vol. 123, 1997, pp. 495–502.

[17] Zhang, Z., Roque, R., Birgisson, B., and Sangpetngam, B., "Identification and Verification of a Suitable Crack Growth Law," *Journal of the Association of Asphalt Paving Technologists*, Vol. 70, 2001, pp. 206–241.

Journal of ASTM International, November/December 2005, Vol. 2, No. 10
Paper ID JAI12276
Available online at www.astm.org

Linbing Wang,[1] *Laureano R. Hoyos,*[2] *Louay Mohammad,*[3] *and Chris Abadie*[4]

Characterization of Asphalt Concrete by Multi-Stage True Triaxial Testing

ABSTRACT: The feasibility of an existing servo-controlled true triaxial (cubical) apparatus for evaluating the mechanical response of nominal 4-in. cubical specimens of asphalt concrete (AC) under multi-axial stress states has been investigated. The apparatus allows the testing of specimens along a wide range of stress paths and stress levels that are not achievable in a conventional uniaxial or cylindrical apparatus. A multi-stage testing scheme can be followed by simultaneous control of the major, intermediate, and minor principal stresses directly applied to the specimens. Two cubical AC specimens cut from two WesTrack block samples were subjected to a series of multi-stage stress paths that included triaxial compression (TC), triaxial extension (TE), simple shear (SS), conventional triaxial compression (CTC), conventional triaxial extension (CTE), and cyclic conventional triaxial extension (CCTE). Experimental data were analyzed to assess volumetric creeping properties, resilient response, plastic deformation response, Poisson's ratio, loss angle, and dilatancy of asphalt concrete under general stress states. Test results highlight the potential of the cubical cell for mechanical characterization of asphalt concrete in a broad range of applications involving true triaxial stress states. Analysis of test results indicates all of the following: (a) Modulus of AC shows significant anisotropy in different orientations; (b) Volumetric creeping of AC is considerably significant at relatively high pressures; (c) AC shows significant dilatancy; and (d) Cubical Device can distinguish mixes of different performance.

KEYWORDS: cubical apparatus, stress states, triaxial testing, anisotropy

Introduction

Simple Performance Test (SPT) of bituminous materials has captured the attention of most researchers in recent years [6,8,12,16]. The NCHRP Project 9-29 "Simple Performance Tester for SuperPave Mix Design" aimed to identify the simple performance testers for SuperPave mix design. Among those considered are dynamic modulus test, creep test, and repeated load test. Most of these tests involve conventional triaxial testing on cylindrical or gyratory specimens and are usually conducted on three different specimens. During conventional triaxial testing, there are only two varying parameters, namely the vertical and the horizontal stresses. Therefore, the effect of more complex stress states cannot be evaluated using these conventional triaxial cells.

Asphalt concrete is a bonded granular material and, as such, its internal structure is anisotropic, which could be attributed to the anisotropy of particle shape, particle orientation,

Manuscript received 31 December 2003; accepted for publication 18 May 2005; published November 2005.
Presented at ASTM Symposium on Performance of Hot Mix Asphalt (HMA), including Fundamental and Empirical Procedures on 9 December 2003 in Tampa, FL.
[1] Assistant Professor, Department of Civil and Environmental Engineering, Louisiana State University and Southern University, Baton Rouge, LA 70803.
[2] Assistant Professor, Department of Civil Engineering, University of Texas at Arlington, Arlington, TX 76019.
[3] Associate Professor Department of Civil and Environmental Engineering, Louisiana State University and Southern University, Baton Rouge, LA 70803.
[4] Materials Research Administrator, Louisiana Transportation Research Center, Baton Rouge, LA 70803.

particle arrangement, and different compaction methods. The degree of anisotropy could influence material response [17]. For instance, if the axial and lateral moduli of a gyratory specimen are significantly different, the deformational characteristics obtained from an Indirect Tensile Test may be quite different from those obtained in an unconfined uniaxial test. In a conventional triaxial test, only transverse anisotropy can be evaluated. However, the material could be in a general anisotropy.

In a true triaxial (cubical) cell, specimens are cubical in shape, and the three principal stresses could be controlled independently. This flexibility facilitates the evaluation of general anisotropy and stress path dependent properties of the materials being tested. True triaxial testing can also be used to evaluate the fundamental stress-strain response of materials under general stress states. The technique has been extensively used in characterizing the constitutive relations of geological materials. The multi-stage nature of a true triaxial test allows the application of a sequence of different stress paths on the same specimen.

In the present work, the feasibility of an existing servo-controlled true triaxial (cubical) testing apparatus for evaluating the mechanical response of nominal 4-in. cubical specimens of asphalt concrete (AC) under multi-axial stress states is investigated. Two cubical AC specimens cut from two WesTrack block samples were subjected to a series of multi-stage stress paths that included triaxial compression (TC), triaxial extension (TE), simple shear (SS), conventional triaxial compression (CTC), conventional triaxial extension (CTE), and cyclic conventional triaxial extension (CCTE). Experimental data were analyzed to assess volumetric creeping properties, resilient response, plastic deformation response, the loss angle, the shear modulus, and dilatancy of asphalt concrete under general stress states.

Cubical Test System

General

Even though different types of true triaxial devices have been developed worldwide, they can be classified into three general categories: (1) Rigid boundary type [1,7], (2) Flexible boundary type [9,14], and (3) Mixed boundary type [5,10]. The advantages and disadvantages of each type have been discussed by Sture [15] and Arthur [2], among many others. The original development of the flexible boundary type of device used in this work was presented by Atkinson [3] for multi-axial testing of rock materials. A detailed description of the original components was presented by Atkinson [3], Sture [15], and NeSmith [11]. The stress-controlled, computer-driven apparatus consists of six main components or modules: (1) a frame, (2) six wall assemblies, (3) a deformation measuring system, (4) a stress application and control system, (5) six rigid membranes, and (6) a data acquisition and processing control system (DA/PCS). Figure 1 illustrates the device. A more detailed, illustrated description of these components can be also found in Wang et al. [17].

Multi-Stage Testing Program

In order to investigate the feasibility of the cubical cell in evaluating the mechanical properties of asphalt concrete under multi-axial stress states, a multi-stage loading procedure was adopted. Multi-stage loading allows the running of different tests, such as triaxial compression, triaxial extension, and repeated loading tests, on the same specimen, thus eliminating the need for multiple specimens. This is especially useful when low-level stresses are involved, causing little or no damage on the specimens. If numerical simulation can be used to account for specimen deformation during testing, the results can be better interpreted. Detailed description of the testing procedure can be found in Wang et al. [17].

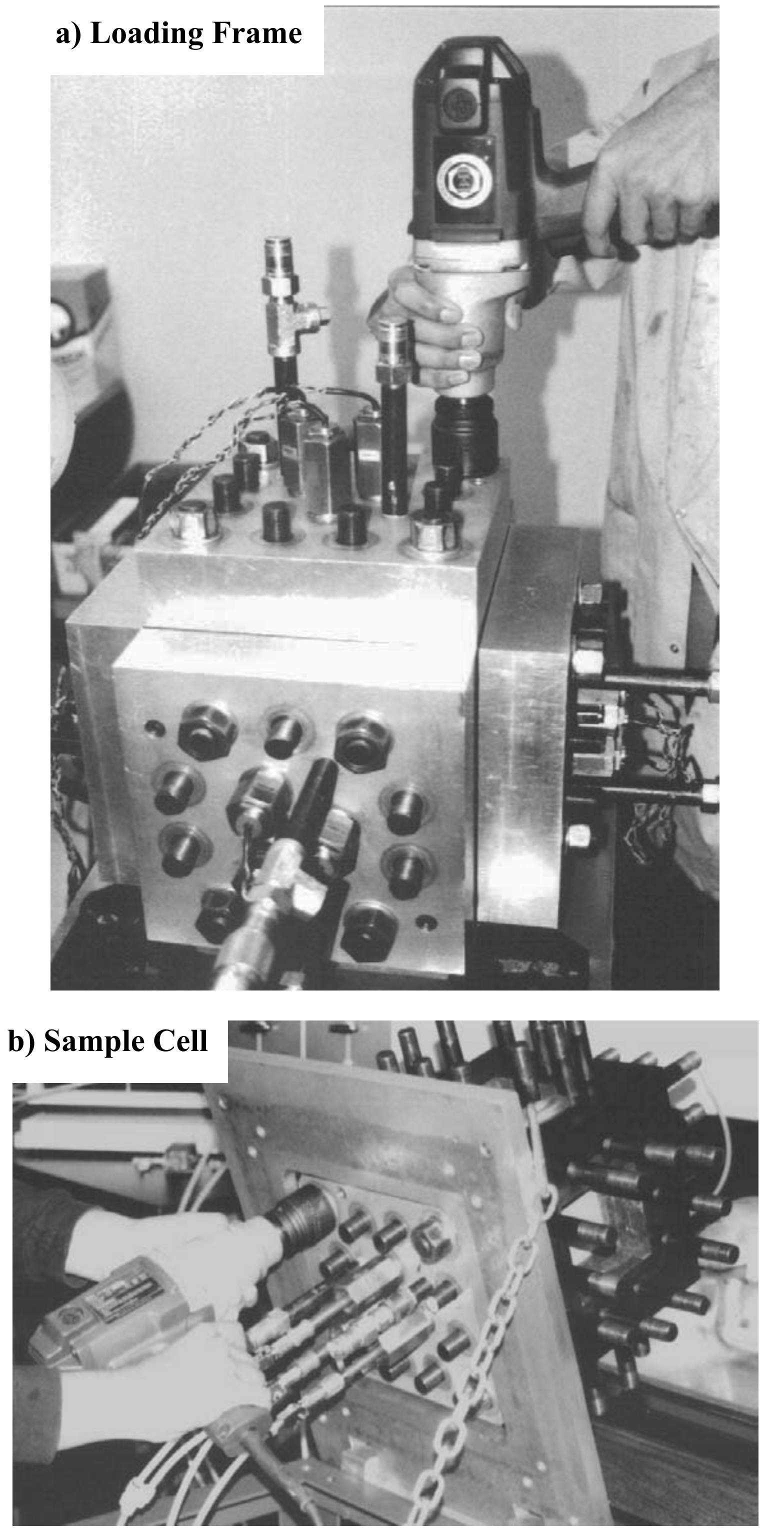

FIG. 1—*Illustration of the Cubicle Cell System.*

Two cubical specimens of nominal 4-in. lateral length were cut from two block samples cored from the WesTrack project [4], one from its coarse mix section, the other from its fine mix section. Both the coarse mix and the fine mix have targeted asphalt content of 5.7 % and air void content of 8 %. The loading sequence applied on the specimens was as follows: Isotropic Compression (IC) to 172.5 KPa (25 psi) in each direction followed by Triaxial Compression (TC), Triaxial Extension (TE), Simple Shear (SS), Conventional Triaxial Compression (CTC), Conventional Triaxial Extension (CTE), and cyclic CTE tests (CCTE). The tests were performed at room temperature of 25°C. At this temperature, asphalt concrete is much harder than at 40°C and requires larger stresses to induce deformation.

Analysis of Test Results

Anisotropic Properties

Figure 2 shows the strain responses in x, y, and z directions during the isotropic compression for stresses varying from 0.0–1.725 MPa (0.0–250 psi). It can be noted that the strain responses in all three principal directions are significantly different, with the slope of the stress-strain response in the z direction being the smallest (i.e., the largest modulus), evidencing the anisotropic properties of AC. As a bonded granular material, the granular skeleton of asphalt concrete demonstrates anisotropic properties and therefore the mixture properties. Anisotropic properties of asphalt concrete have rarely been studied. The general anisotropy usually cannot be evaluated using the conventional triaxial test. However, anisotropic properties of asphalt concrete have important implications in pavement stress-strain analysis and pavement design [17].

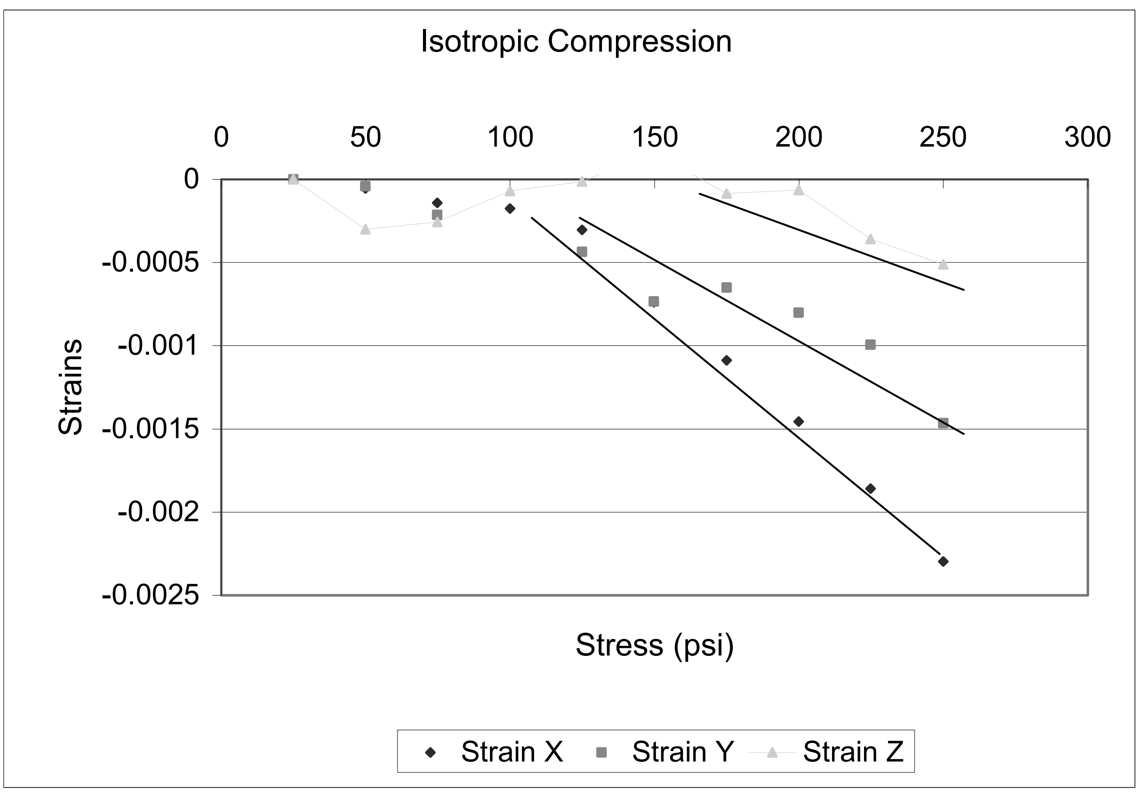

FIG. 2—*Stress-strain relation during isotropic compression.*

Volumetric Creeping and Dilatancy

Figure 3 shows the volumetric straining during the entire loading process. It should be noted that volumetric creeping (p = constant) is quite significant at relative high stress level such as 1.725 MPa (250 psi). During this process (TC, TE, SS tests), *p* is constant, and the compressive volumetric strain is due to the creeping effect. Historically, the volumetric creeping of asphalt concrete is usually considered negligible (SHRP-A-415).

It should also be noted that the volume of the specimen increases during shearing at constant mean stress (Fig. 4), representing dilatancy properties (volume change due to shearing) of asphalt concrete. The volumetric swelling is also quite significant. Nevertheless, the dilatancy presents only a perturbation to the general trend of compressive volume change. The dilatancy has significant implication; it means that the granular skeleton becomes loose during the shearing.

Shear Modulus

Shear modulus is an important parameter for estimating the shear deformation of asphalt concrete that is very much related to the rutting potential of asphalt concrete. Shear modulus can be calculated from several tests including the SS test, the CTC test, the CTE test, and the CCTE test.

One of the SS tests, for example, follows the $\Delta\sigma_x = 0, \Delta\sigma_y = \Delta\sigma, \Delta\sigma_z = -\Delta\sigma$ stress path; the shear stress is $\Delta\tau_{yz} = \frac{\Delta\sigma_y - \Delta\sigma_z}{2} = \Delta\sigma$. The shear strain corresponding to the maximum shear stress plane is $\Delta\varepsilon_{yz} = \frac{\Delta\varepsilon_y - \Delta\varepsilon_z}{2}$. The shear modulus is $G = \frac{\Delta\tau_{yz}}{\Delta\varepsilon_{yz}}$. Results for one of the SS tests are presented in Fig. 4. From this figure, the shear modulus can be obtained (the shear stress increases from 0–100 psi and decreases from 100 psi to 0 for the SS test).

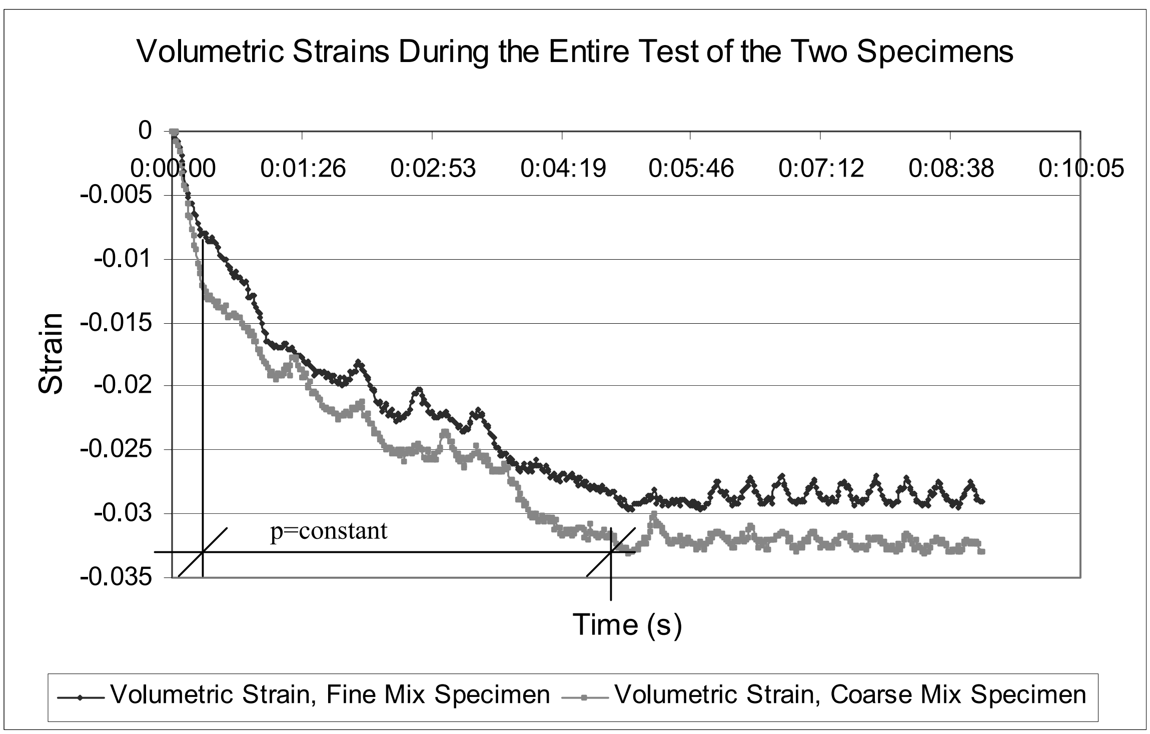

FIG. 3—*Volumetric strain during the entire test.*

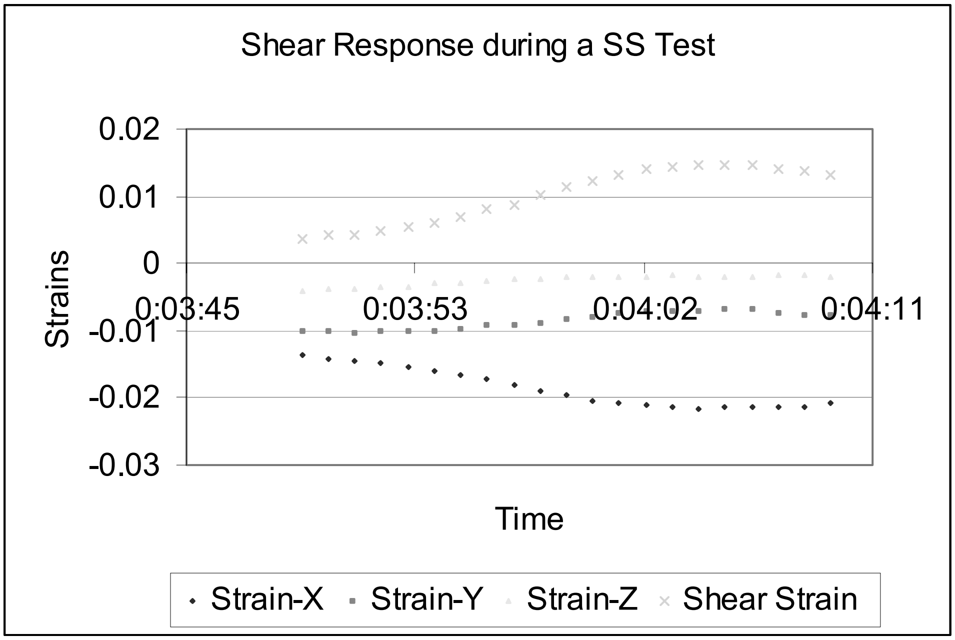

FIG. 4—*Shear response during a SS test.*

The cyclic conventional triaxial extension test (CCTE) follows this stress path: $\Delta\sigma_y = 0, \Delta\sigma_x = 0, \Delta\sigma_z = -\Delta\sigma$ and $\Delta\sigma_y = 0, \Delta\sigma_x = 0, \Delta\sigma_z = \Delta\sigma$. It was repeated for 8 cycles. Figure 5 presents the octahedral shear strain response during those 8 cycles. During the test, the magnitude of cyclic stress is $\Delta\sigma$=1.38 MPa (200 psi). Correspondingly, the maximum shear stress is 0.69 MPa (100 psi). The maximum resilient shear strain is 0.0015 (Fig. 5). Therefore, the shear modulus G is equal to 920 MPa (133 333 psi).

Loss Angle

Loss angle is an important parameter in testing viscoelastic materials. For an ideal elastic material, the loss angle is equal to zero; for an ideal viscous fluid, the loss angle is 90º. Depending on the temperature, the loss angle of asphalt concrete varies. The CCTE test results also give the information for determining the loss angle. From Fig. 5 it can be noted that the stress peak and the strain response peak are not in pace. As the period is 20 s for the loading cycle, the time difference between the peak stress and peak strain is 4 s as read from Fig. 5. Therefore, the loss angle is $\delta = \frac{2\pi}{20}4 = 72^\circ$.

Strain Hardening

Figure 5 also presents the accumulative irrecoverable straining process represented by the line tangent to the minimum points of the cyclic loading process. It can be noted that after few cycles, the irrecoverable strain approaches constant, or the incremental irrecoverable strain approaches zero. In other words, the material demonstrates strain-hardening phenomena. Apparently, the permanent strain versus number of loading cycles can be utilized to calibrate a rutting model, for example the strain hardening parameter.

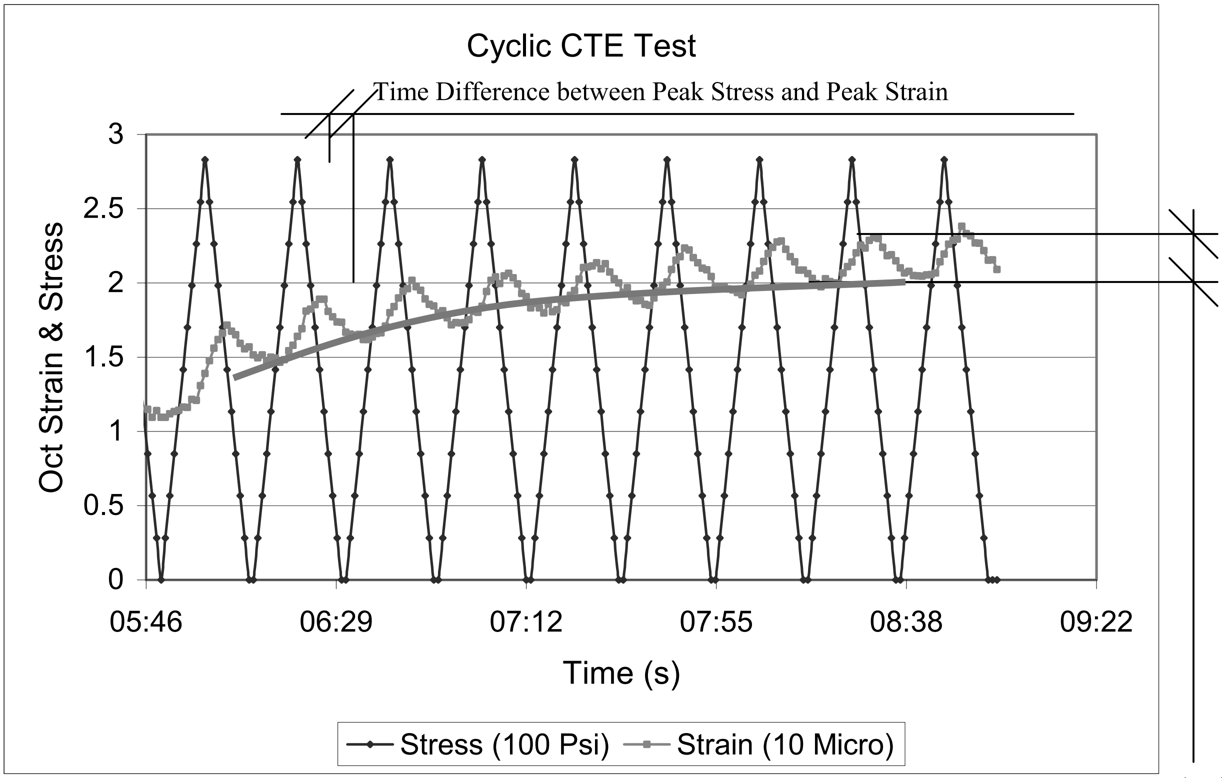

FIG. 5—*Cyclic CTE test to obtain shear modulus, loss angle, and plastic modulus.*

Resilient Modulus

The resilient modulus is defined as $E^* = \dfrac{\Delta\sigma}{\Delta\varepsilon_e}$, where $\Delta\varepsilon_e$ is the elastic strain due to the application of the cyclic loading. Using the deformation properties in the CCTE test (see Fig. 6), the resilient modulus of the mix can be calculated.

Poisson's Ratio

Poisson's ratio is also an important parameter affecting pavement analysis. With the same elastic modulus, different Poisson's ratios will result in different stress distributions. Poisson's ratio may also be a good indicator of the stability of a mix; larger Poisson's ratio may represent a weaker mix. The cubical device monitors the deformations of the specimen in three orientations at the same time. The deformations in the three orthogonal orientations can be used to calculate the Poisson's ratio. Figure 7 presents the deformation in the X, Y, and Z directions during a conventional triaxial compression test (CTC, $\Delta\sigma_y = 0, \Delta\sigma_x = \Delta\sigma, \Delta\sigma_z = 0$). During this test, two Poisson's ratios may be defined: $\nu_{zx} = \dfrac{\Delta\varepsilon_z}{\Delta\varepsilon_x}$ and $\nu_{xy} = \dfrac{\Delta\varepsilon_y}{\Delta\varepsilon_x}$. Other Poisson's ratios can also be calculated from other CTC tests. It should be noted that the elastic strains were used for the calculation of the Poisson's ratio. In this example $\nu_{zx} = 0.23$ and $\nu_{xy} = 0.153$.

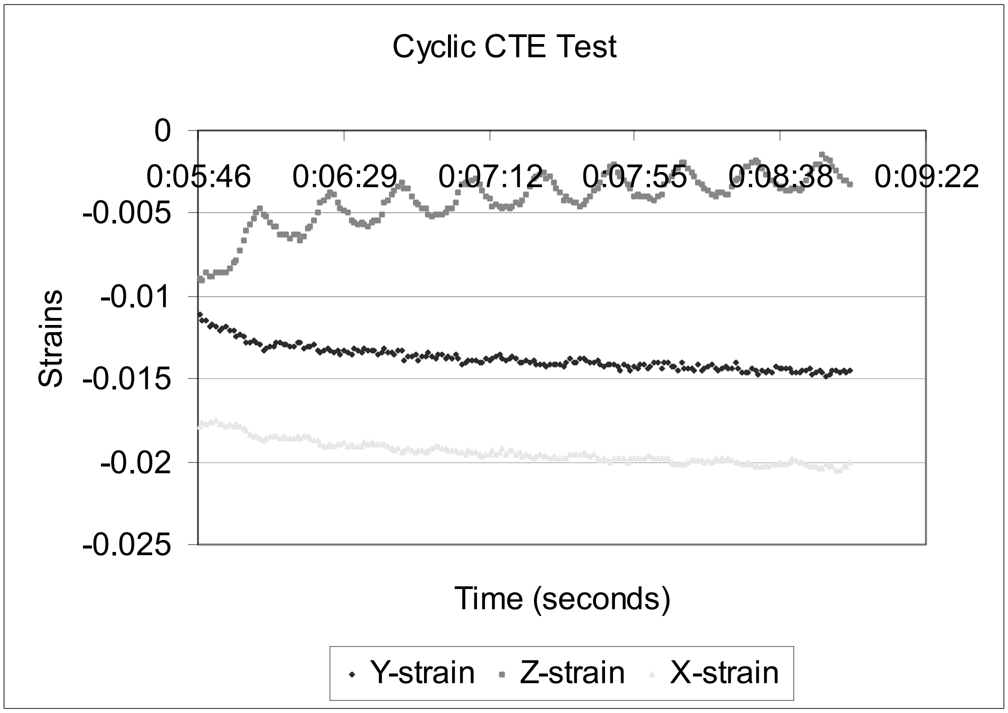

FIG. 6—*Strain responses in X, Y, and Z directions during a CCTE test.*

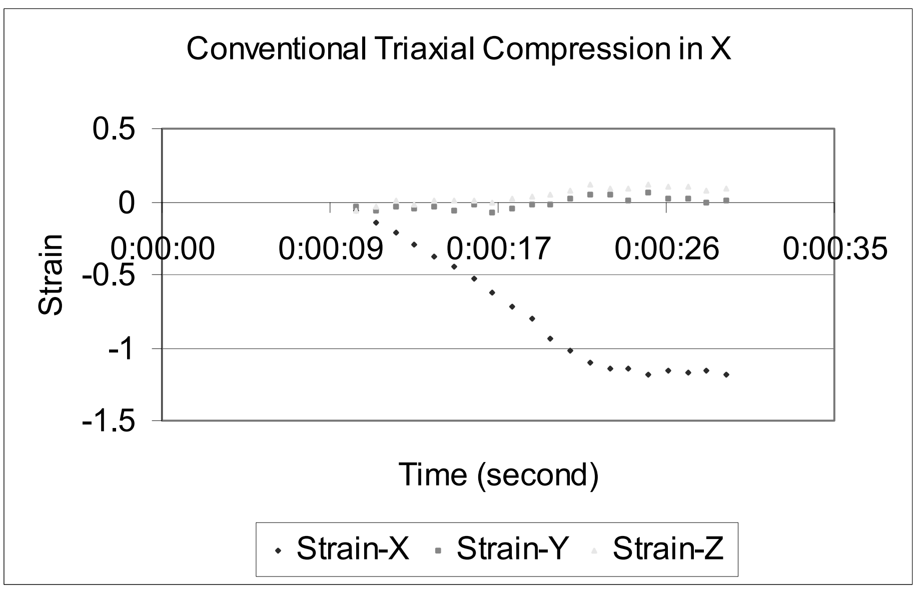

FIG. 7—*Computation of the Poisson's ratio from a CTC test.*

Comparison of the Deformation Characteristics of the Two Mixes in the WesTrack Project

Two of the three mixes, the fine mix and the coarse mix, in the WesTrack project [4] were studied in this project. One specimen for each of the mixes was tested using the same procedure. Figure 3 also presents the comparison of the volumetric deformation characteristics of the two mixes. It is apparent that the coarse mix has much larger volumetric deformation than the fine mix. In other words, the coarse mix has a weaker resistance against volumetric straining than the fine mix. Figure 8 presents the vertical strain response for the two mixes. It can be seen that the vertical elastic strains for the coarse mix are larger than those of the fine mix, indicating smaller elastic modulus of the coarse mix. The results for both tests are consistent with the field performance of the two mixes: the coarse mix is weaker than the fine mix in rutting [4].

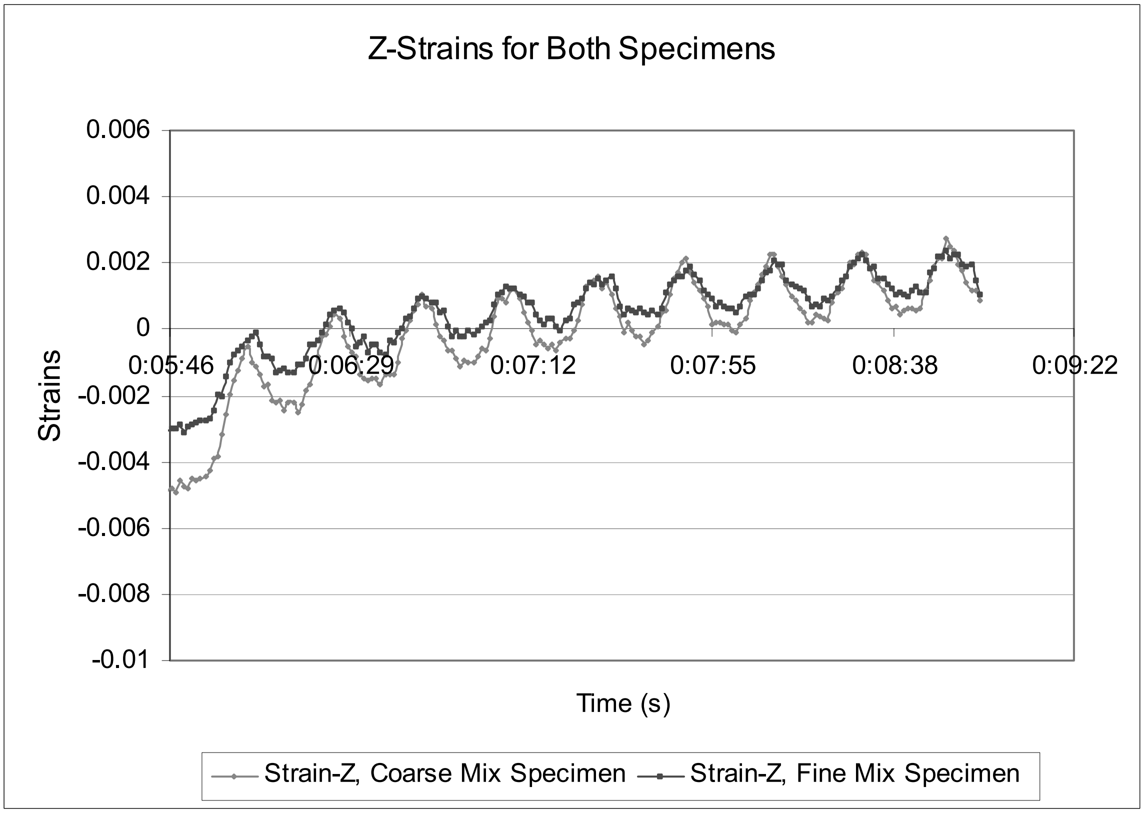

FIG. 8—*Comparison of the vertical deformation properties of the fine and coarse mixes.*

Summary and Conclusions

This paper demonstrates the potential of using multi-stage cubical cell tests to evaluate asphalt concrete properties including anisotropic modulus, volumetric creeping and dilatancy, shear modulus, loss angle, and permanent deformation using a single specimen but following a sequence of loading processes. The test results of the fine mix and coarse mix of the WesTrack project indicate that the multistage test successfully ranked the performance of the two mixes consistently with field observations. With an appropriately designed loading process, multistage cubical cell tests shall have promising perspectives for serving as a simple performance test and calibrating constitutive models of asphalt concrete. Further work to use the multistage cubical cell test for comparing the fundamental properties of asphalt concrete of different known performances is important for justifying its practical applications.

References

[1] Airey, D. W. and Wood, D. M., "The Cambridge True Triaxial Apparatus," *Advanced Triaxial Testing of Soil and Rock, STP 977*, ASTM International, West Conshohocken, PA,

1988, pp. 796–805.

[2] Arthur, J. R. F., "Cubical Devices: Versatility and Constraints," *Advanced Triaxial Testing of Soil and Rock, STP 977*, ASTM International, West Conshohocken, PA, 1988, pp. 743–765.

[3] Atkinson, R. H., "A Cubical Test Cell For Multiaxial Testing of Materials," Ph.D. Dissertation, University of Colorado at Boulder, Boulder, CO, 1972.

[4] Epps, J., Monismith, C. L., Alavi, S. H., Mitchell, T. M., "WesTrack Full-Scale Test Track: Interim Findings," http://www.westrack.com/wt_04.htm, 1997.

[5] Green, G. E., "Strength and Deformation of Sand Measured in an Independent Stress Control Cell," *Stress-Strain Behavior of Soils, Proc., Roscoe Memorial Symposium*, G. T. Foulis and Co. Ltd., Cambridge, England, 1971, pp. 285–323.

[6] Goodman, S. N., Hassan, Y., and Abd El Halim, "Shear Properties as Viable Measures for Characterization of Permanent Deformation of Asphalt Concrete Mixtures," TRB CD, 2002.

[7] Hambley, E. C., "A New Triaxial Apparatus," *Geotechnique*, Vol. 19, No.2, 1969, pp. 307–309.

[8] Kaloush, K. E. and Witczak, M. W., "Simple Performance Test for Permanent Deformation of Asphalt Mixtures," TRB CD, 2002.

[9] Ko, H. Y. and Scott, R. F., "A New Soil Testing Apparatus," *Geotechnique*, Vol. 17, No. 1, 1967, pp. 40–57.

[10] Lade, P. V. and Duncan, J. M., "Cubical Triaxial Tests on Cohesionless Soil," *ASCE J. Soil Mech*, Found. Div., Vol. 99, SM10, 1973, pp. 793–812.

[11] NeSmith, W. M., "Development of a Computer Controlled Multiaxial Cubical Testing Apparatus," M.Sc. Thesis, Georgia Institute of Technology, Atlanta, GA, 1997.

[12] Pellinen, T. K. and Witczak, M. W., "Use of Stiffness of Hot-Mix Asphalt as a Simple Performance Test," TRB CD, 2002.

[13] SHRP-A-415, "Permanent Deformation Response of Asphalt Aggregate Mixes," *Strategic Highway Research Program*, National Research Council, 1994.

[14] Sture, S. and Desai, C. S., "A Fluid Cushion Truly Triaxial or Multiaxial Testing Device," *Geotech. Test. J.*, Vol. 2, No. 1, 1979, ASTM International, West Conshohocken, PA, pp. 20–33.

[15] Sture, S., "Development of Multiaxial Cubical Test Device With Pore-Water Pressure Monitoring Facilities," Report No. VPI-E-79.18, Dept. Civil Eng., Virginia Polytechnic Institute and State University, Blacksburg, VA, 1979.

[16] Wen, H. F. and Kim, R. Y., "A Simple Performance Test for Fatigue Cracking of Asphalt Concrete Based on Viscoelastic Analysis of Indirect Tensile Testing and Its Validation Using Westrack Asphalt Mixtures," TRR 1789, 2002, pp. 66–72.

[17] Wang, L. B., Hoyos, L. R., Wang, X., Voyiadjis, G., and Abadie, C., "Anisotropic Properties of Asphalt Concrete: Characterization and Implications in Pavement Analysis and Design," *ASCE Journal of Materials in Civil Engineering*, 2005, in press.

www.astm.org

ISBN 0-8031-3495-9
ISBN 978-0-8031-3495-9
Stock #: STP1469